LBL-25295
UC-413

Nuclear Science Division 1986/87

ANNUAL REPORT

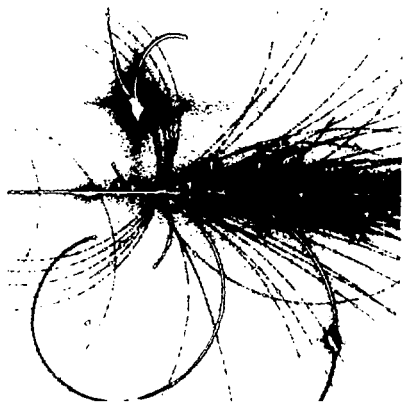

Lawrence Berkeley Laboratory
University of California

September 1988

Prepared for the U.S. Department of Energy under Contract DE-AC03-76SF00098

DISCLAIMER

Printed in the United States of America
Available from
National Technical Information Service
U.S. Department of Commerce
5285 Port Royal Road
Springfield, VA 22161
Price Code: A09

LBL--25295

DE89 008841

Nuclear Science Division

Annual Report for the Period

October 1, 1986 – September 30, 1987

Division Head
T.J.M. Symons

Assistant Division Head
Janis Dairiki

Editor
Jeannette Mahoney

Editorial Committee
D.M. Moltz, W.D. Myers, H-G. Ritter

Lawrence Berkeley Laboratory
1 Cyclotron Road
Berkeley, California, 94720, USA

This work was supported by the Director, Office of Energy Research, Office of High Energy and Nuclear Physics, Division of Nuclear Physics and by the Office of Basic Energy Sciences, Division of Nuclear Sciences, of the U.S. Department of Energy under Contract No. DE-AC03-76SF00098

Cover: One view of an event detected in the CERN NA35 streamer chamber as photographed by an image-intensified Charge-Coupled Device (CCD) camera developed by a group in the Nuclear Science Division at LBL. These cameras provide a digital picture made up of 1024 × 1024 picture elements (pixels) digitised to eight bits. In this event a 200 GeV/nucleon oxygen nucleus in the beam interacts with a neon nucleus in the gas of the chamber. Tracks of various curvatures are left by charged particles as they traverse the gas inside the chamber which is located in the field of a magnet.

Introduction

This report summarizes the activities of the Nuclear Science Division during the period October 1, 1986 to September 30, 1987.

A highlight of the experimental program during this time was the completion of the first round of heavy-ion running at CERN with ultrarelativistic oxygen and sulfur beams. Very rapid progress in being made in the analysis of these important experiments and preliminary results are presented in this report. During this period, the Bevalac also continued to produce significant new physics results, while demand for beam time remained high. An important new community of users has arrived on the scene, eager to exploit the unique low-energy heavy-beam capabilities of the Bevalac. Another major highlight of the program has been the performance of the Dilepton Spectrometer which has entered into production running. Dileptons have been observed in the p + Be and Ca + Ca reactions at several bombarding energies. New data on pion production with heavy beams measured in the streamer chamber continue to shed light on the question of nuclear compressibility, while posing some new questions concerning the role of Coulomb forces on the observed pion spectra. In another quite different area, the pioneering research with radioactive beams is continuing and is proving to be one of the fastest growing programs at the Bevalac. Exotic secondary beams (e.g., 8He, 11Li, and 14Be) have been produced for fundamental nuclear physics studies.

In order to further enhance the scientific research program and ensure the continued vitality of the facility, the Laboratory has proposed an upgrade of the existing Bevalac. Specifically, the Upgrade would replace the Bevatron with a modern, strong-focusing synchrotron to provide higher intensity and higher quality beams to continue the forefront research program.

The significant enhancement of the heavy ion capability at the 88-Inch Cyclotron as a result of the development of the ECR source has led to a renaissance of the cyclotron. This was clearly demonstrated in the review of the facility in March 1987 by the DOE Facilities Review Panel. The Panel report stated that "The quality of the present research and the near-term potential for significant discoveries were rated by the panel among the highest in this group of facilities." The facility has also benefited from innovative detector development. One of the most sophisticated detector systems in use at the 88-Inch Cyclotron is the High Energy Resolution Array (HERA) which has been instrumental in the observation and measurement of superdeformed bands at high nuclear spin. The newly established program in nuclear astrophysics in also beginning to bear fruit; several results are presented in this report.

One measure of a research program is the recognition accorded to its researchers. The Division was honored when Miklos Gyulassy was named the recipient of the 1987 E.O. Lawrence Award for his leadership in developing the theory of relativisitic heavy ion collisions, and for his studies of pion interferometry. Three NSD scientists received von Humboldt Awards during this period and three additional Division members were elected Fellows of the American Physical Society.

Nuclear Science Division members organized several major scientific meetings including the Workshop on Nuclear Structure at Moderate and High Spin, the Bevalac TPC Meeting and the Second Workshop on Experiments and Detectors for RHIC. Along with the planned Gamma-ray Detector Workshop in October and the 8th High Energy Heavy Ion Study to be held at LBL in November 1987, these meetings serve as focus points and guide posts for future exciting possibilities.

T.J.M. Symons

PART I: PROGRAMS

PART II: EXPERIMENT

PART III: THEORY

PART IV: INSTRUMENTATION AND METHODS

PART V: APPENDICES

PART I: PROGRAMS

Exotic Nuclei and Decay Modes

Group Leader
Joseph Cerny

F. Blonnigen
J. S. Hoffman*
M. A. C. Hotchkis
T. F. Lang†
D. M. Moltz
J. E. Reiff†
J. D. Robertson

**Undergraduate Student*
†Graduate Students

Studies of nuclei very far from the valley of stability provide tests of theoretical models that predict the existence, masses, and shapes of exotic nuclei. In addition, these studies have revealed new modes of radioactive decay as well as spectroscopic information on nuclides with unusually large proton to neutron ratios. Several techniques for studying these nuclei, which are produced in low yield reactions, are currently being used at the 88-Inch Cyclotron.

In the past, the $T_z = -2$ nuclei ^{22}Al and ^{26}P were discovered via their beta-delayed proton emission. Subsequently, these nuclei were shown to exhibit beta-delayed two-proton radioactivity. Then, the first $T_z = -5/2$ nucleus, ^{35}Ca, was discovered via its beta-delayed two-proton emission. The experimental technique used in these discoveries involved a minimal length helium jet to transport these short lived nuclides ($t_{1/2} < 75$ ms) from the target region to a slowly rotating collection wheel in front of two semiconductor telescopes.

To search for and characterize the decay modes of much shorter lived exotic nuclei (100 μs < $t_{1/2}$ < 10 ms), we have constructed a fast, variable speed (30–5000 PPM) rotating wheel apparatus. This wheel, with its twelve aluminum catcher foils around the circumference, stops nuclei recoiling from the target and carries them in front of detector telescopes so that their decay may be observed. Using this method, we have seen evidence for the beta-delayed two-proton decay of the $T_z = -5/2$ nucleus ^{31}Ar.

The third experimental tool used to study exotic nuclei is the on-line mass separator RAMA (an acronym for recoil atom mass analyzer). RAMA consists of a helium jet which transports recoil nuclei produced in the target chamber to an ion source. The ions are extracted from the source, magnetically analyzed, and collected at a detector station. Currently a second, highly shielded detector station is under construction. The low background environment at the new detector station will permit the study of p–γ, β–γ, and γ–γ coincidences. Initially we plan to use this setup to investigate the decays of the $T_z = -3/2$ nuclei ^{23}Al and ^{27}P.

Nuclear Astrophysics and Fundamental Symmetries

Group Leader
E.B. Norman

K.T. Lesko
R.M. Larimer
S. Kuhn

E. Horch,*
University of Chicago
Chicago, Illinois

**Undergraduate Student*

We are involved in a number of experiments in two distinct, but not unrelated, areas: 1) nuclear astrophysics and 2) tests of fundamental symmetries. In the area of astrophysics specific studies include:

1. Positions and decay modes of excited states in ^{148}Pm and their relevance for determining the s-process neutron density.
2. Level scheme of ^{180}Ta and the survivability of ^{180}Ta in stars.
3. Measurements of γ-ray production cross sections from proton and alpha-particle induced reactions required for γ-ray astronomy.
4. Searches for the β^- decay of ^{54}Mn and the β^+ decay to ^{56}Ni.

Under the heading of fundamental symmetries, we are involved in several different tests of conservation laws. Specific studies include:

1. Measurement of the beta decay asymmetry parameter for ^{35}Ar.
2. Search for the isospin formidden Fermi decay of ^{56}Ni.
3. Search for neutrino oscillations (LAMPF E645)
4. Searches for massive, long-lived, negatively charged elementary particles.

Members of the group preparing for measurements of γ-ray production cross sections using germanium detectors. Left to right: Stephanie Crane, Kevin Lesko, Ruth-Mary Larimer, Dawn Meekhof, Eric Norman, and Hugh Bussell.

XBC 867-5659

Nuclear Structure Studies at High Angular Momentum

Group Leaders:
R.M. Diamond
F.S. Stephens

M.A. Deleplanque
J.C. Bacelar
A.O. Macchiavelli
E.M. Beck*

J.E. Draper,
C. Duyar,*
University of California at Davis

J. Burde,
The Hebrew University, Jerusalem, Israel

**Graduate students*

The group's experiments center on the use of the Berkeley High Energy-Resolution Array, HERA. A stand for it was built early in the year at the SuperHILAC making possible experiments there with the full array, as was already possible at the 88-Inch Cyclotron. Completion of the 40 bismuth germanate sectors of the small central ball has been delayed for a few months, but the prototypes have been tested and the ball should be in operation by the end of 1987.

Studies of superdeformed (SD) bands have been a major emphasis in the program at the 88-Inch Cyclotron during the past year. After the discovery of such a band in ^{135}Nd, two more were found in ^{134,136}Nd, and papers published on these results. These bands resemble the strongly deformed band known previously in ^{132}Ce and are less deformed than the famous 2:1 example in ^{152}Dy. A paper has also been published on our study of the latter case, which confirms the Daresbury work, but results in a different ratio of excited SD states (ridges) to the lowest discrete band. Producing the SD bands in ^{152}Dy is still a third way, by means of the nearly symmetric reaction ^{76}Ge+^{80}Se→^{152}Dy+4n, has indicated that the origin of this difference in the yields of SD bands is not a special entrance channel effect, but is the result of the different angular momentum and excitation energy brought to the nucleus by the three reactions. Finally, other regions of the Periodic Table are also under investigation to learn about the systematics of the SD bands.

Decay scheme studies have continued this past year and led to papers on **New Structures at High Spin in** ^{159}Er and **High-Spin Spectroscopy of** ^{168}Hf. In the former paper, the effects of occupying specific orbitals are discussed, and in the latter, the second backbend is observed, putting an end to the region with a surprisingly constant moment of inertia. It remains to determine the B(E2) values in this very high spin region.

Continuum γ-ray studies are represented by publication of a paper on **Three-Photon Correlations.** This treats the damping of rotational cascades at moderate excitation energies (2–8 MeV above yrast) and suggests that the resulting spread in γ-ray transition energies is closer to 300 keV than to the 90–100 keV originally suggested both experimentally and theoretically. This work involved the first use of the triple γ-ray events (double-gating) in continuum studies, and indicates their importance (and that of higher folds) in such studies.

A collaborative experiment with researchers from the Universities of Rochester, Tennessee, and California studied one- and two-particle transfer reactions with very heavy ions (from the SuperHILAC) in which the transfer can occur from (Coulomb) excited states of moderate spin, rather than from the ground state as is usually investigated. From such experiments it is hoped to learn how the pairing correlations change (are reduced) with increase in spin, as well as about the level structure in certain (e.g., actinide) nuclei that are difficult to make any other way.

In a collaboration with a Stanford University group, an experiment with 14 Compton-suppressed HERA detectors was run for more than 150 hours at the SuperHILAC to look for back-to-back, coincident, equal-energy γ rays from a 6 MeV uranium

beam on ^{232}Th targets. Such γ rays are a possible alternate decay mode of the neutral particle suggested to explain the coincident e^+, e^- peaks observed in such reactions at G.S.I. A narrow line of 1062±1 keV was observed in the summed-energy, two-photon spectrum, with a statistical significance of 6σ. This energy does not correspond to any of the known e^+, e^- energies, but is lower and would not have been observed with the positron detectors. It remains for future work to determine how and where these photons actually originate and whether they are indeed related to the e^+, e^- emission.

Heavy-ion Reactions at Low and Intermediate Energies

Group Leaders:
R.G. Stokstad
Y.D. Chan

A. Harmon
J. Pouliot

E. Chavez,*
A. Dacal,
M.E. Ortiz,
Instituto de Fisica
Universidad Nacional
Autónoma
de México

E. Plagnol
Institute de Physique
Nucléaire
Orsay, France

**Graduate Student*

During this past year our group continued its development of plastic scintillator detectors of the phoswich design. These developments were in two directions. The first involved position-sensitive detectors that cover a large solid angle without requiring a corresponding large number of phototubes and electronics. The other direction was to develop arrays of individual phoswich elements that provide high geometrical efficiency through close packing, identification of elements up to Ne, and of course the multi-hit capability that comes with high granularity. Two such arrays have been constructed: one for use at the 88-Inch Cyclotron and the other for an experiment at the Bevalac.

At the 88-Inch Cyclotron we made heavy use of the intense (10 ena on target) and stable beam of fully stripped ^{16}O at 32.5 MeV/nucleon to perform a series of experiments in which nucleon transfer to and from the projectile was studied. At these bombarding energies, nucleon pickup by the projectile produces a highly excited fragment that then decays by particle emission. We were able to show that this process can result in the sequential emission of more than one particle. The stripping of nucleons from the projectile also produces fragments that subsequently decay. It is thus essential to measure coincidences between projectile-like fragments and the accompanying protons and alpha particles if one is to be able to follow the evolution of nucleon transfer reactions as the bombarding energy is raised through the Fermi energy.

Central collisions of projectiles with heavy targets have been investigated by adding a pair of position sensitive parallel-plate avalanche counters to determine the linear momentum transfer associated with the production of fast light particles and other charged fragments observed in the plastic scintillators. It has been possible with this apparatus to determine the spectrum of linear momentum transfer as a function of the multiplicity of the fast, forward-going light particles.

The array of 34 truncated pyramid phoswich detectors was used to study both central and peripheral collisions in a reverse kinematics mode by bombarding targets of Be and C with beams of 32.5 MeV/nucleon ^{12}C, ^{14}N, and ^{16}O. Charged particle multiplicities up to six were observed. In some of the events we expect to be able to account for all of the momentum and energy brought into the collision by the projectile. In particular, the multi-fragmentation of the projectile is of interest.

A forward-angle phoswich hodoscope, also consisting of 34 elements, has been constructed to observe the projectile-like and intermediate mass fragments produced in collisions of 100 MeV/nucleon niobium ions with a gold target. This experiment, which includes an array of nine large solid angle gas-plastic detectors (the "pagoda"), is in collaboration with physicists from LLNL, LASL, and ANL.

The recent installation of two large NaI spectrometers at the 88-Inch Cyclotron has made it possible to study the production of high-energy photons in heavy ion collisions. Our group has decided to pursue the special region of mass and bombarding energy in which nuclear bremsstrahlung, as this process is loosely named, becomes observable. Test experiments with 25 MeV/nucleon ^4He on ^4He have shown the feasibility of observing energetic photons above the additional background arising from the use of a gas cell target. This opens the possibility for a series of experiments on such

systems as $^{3}He+^{3}He$ and $^{16}O+^{16}O$. These experiments are in collaboration with physicists from TUNL and NBS.

Finally, the measurements of intermediate mass fragments and evaporation residues produced in the reverse kinematics reactions of $^{40}Ar+^{12}C$ (in collaboration with the Moretto/Wozniak group) were completed.

Heavy Element Radiochemistry

The group uses all three of the LBL accelerators to produce and characterize new elements and isotopes, to perform atom-at-a-time studies of the chemical and nuclear properties of the heavy actinide and transactinide elements, to study nuclear reaction mechanisms, and to educate students in modern nuclear and radiochemistry. Our studies of nuclear and chemical properties are complementary and proceed hand in hand. Current research is focused in the following areas:

1. Synthesis and identification of new actinide and transactinide isotopes.
2. Atom-at-a-time studies of the chemical and nuclear properties of the heavy elements, especially of element 103 which completes the actinide series, and of the transactinide elements 104 and 105.
3. Studies of the spontaneous fission (SF) of the transcalifornium elements where sudden and unpredicted changes in SF half lives and properties have been found to occur. Searches for beta-delayed fission in both neutron-rich and neutron-deficient actinide isotopes have also been initiated.
4. Systematic studies of the production cross sections for actinides from both transfer and compound nucleus reactions using heavy actinide targets and a variety of projectiles including $^{16,18}O$, $^{20,22}Ne$, and $^{40,44,48}Ca$ in order to understand the mechanisms involved and choose the best target-projectile-energy combinations for our studies of nuclear and chemical properties.
5. Characterization of the mechanisms operating in intermediate energy (10-100 MeV/nucleon) and relativistic (≥250 MeV/nucleon) heavy ion reactions through studies of the target fragment yields, energies, angular distributions, etc.

Research on target fragmentation at the Bevalac has involved single particle inclusive survey measurements of the angular, mass and charge distributions of the target fragments from the interaction of heavy relativistic ions with heavy targets.

In the past year we have performed experiments with 3-minute ^{260}Lr, produced at the 88-Inch Cyclotron via the $^{249}Bk(^{18}O,\alpha,3n)$ reaction, to deduce the ionic radius of Lr(III). Collaborative studies with GSI and the University of Mainz were conducted using their automated system, to obtain more data on the ionic radius of Lr, and to determine the hydration enthalpies of Md(III) and Lr(III). We are also developing new radiochemical separation techniques and have performed the first aqueous chemistry studies of hahnium (element 105) using 35-second ^{262}Ha produced in the $^{249}Bk(^{18}O,5n)$ reaction.

Collaborative studies using ^{254}Es targets are continuing and illustrate the feasibility and promise of the proposed Large Einsteinium Activation Program (LEAP). Members of our group have participated in experiments with LLNL in which the new longer-lived isotopes of Lr, 39-minute ^{261}Lr and 216-minute ^{262}Lr were produced by transfer reactions between ^{22}Ne projectiles and ^{254}Es targets. They are produced in sufficient quantity to permit studies of their SF and chemical properties. Their half lives are even longer than originally predicted in the LEAP proposal, confirming the extra stability toward SF of isotopes containing an odd number of protons and/or neutrons. It now seems quite probable that longer-lived isotopes of element 105 should exist and might be produced from ^{254}Es targets.

Group Leaders:
D.C. Hoffman
G.T. Seaborg

D.A. Bennett*
R.B. Chadwick*
R.M. Chasteler
C.M. Gannett
K.E. Gregorich
H.L. Hall*
R.A. Henderson*
D.M. Lee
J.D. Leyba*
M.J. Nurmia
P.A. Wilmarth*

K. Aleklett,
Studsvik Science Research Laboratory

PH.R. von Gunten,
A. Türler,*
University of Bern, Switzerland

G. Herrmann,
University of Mainz, Germany

W.D. Loveland,
C. Casey,*
Oregon State University

H. Nakahara,
Y. Hatsukawa,*
Tokyo Metropolitan University

**Graduate students*

New Element and Isotope Synthesis

Group Leaders:
A. Ghiorso
J.M. Nitschke

R.M. Chasteler*
R.B. Firestone
L.P. Somerville
K. Vierinen
P.A. Wilmarth*
S. Yashita

P. Möller,
Lund University, Sweden

J. Gilat,
Soreq Nuclear Research Center, Israel

K.S. Toth,
J. Ellis-Akovali,
Oak Ridge National Laboratory

F.T. Avignone III,
University of South Carolina, Columbia, South Carolina

**Graduate students*

During the spring running period, a number of tests with heavy recoils were made with SASSY2, which showed that the instrument should perform as expected and that the extensive realignment had been successful. A number of short bombardments were made which resulted in the discovery of a new neutron deficient isotope of astatine; however, it became apparent that there would probably be difficulty in tuning the instrument to the high magnetic fields needed for the heaviest elements because of saturation in the quadrupole. No stronger quadrupole with an 8-inch aperture was available so it was decided to modify the existing one by reducing its aperture by 20%. Fortunately, it was possible to replace the pole tips without disturbing the alignment and this formidable task was accomplished during the summer shutdown.

A major improvement in the handling of the data from SASSY2 was made by incorporating another hard disk so that it will be possible to determine α–α correlations on-line as each experiment proceeds. This capability will be extremely valuable for low cross section experiments, such as that directed at element 110.

The other major research tool of the New Element and Isotope Synthesis Group is the On-line Apparatus for SuperHILAC Isotope Separation (OASIS). Due to a unique design of the ion source that permits operating temperatures near 3000K, heavy ion reaction products can be mass separated and analyzed in a fraction of a second.

A total of 26 new β-delayed proton precursors and several new β-delayed γ emitters have thus far been identified with OASIS. They are located in the region of $56<Z<72$ and $N<82$ and include spherical, transitional, and well deformed nuclei. Beside obtaining proton spectra and half-lives we have, in several cases, determined spins and parities from final state feedings, measured proton branching ratios, (Q_{EC}–S_p) energy differences, and identified new levels in the proton decay daughters. We have also observed mixed β-delayed proton decay from precursor ground states and isomers. Statistical model calculations have been carried out using GT β-strength functions obtained from RPA calculations with Nilsson-model wave functions. We have found that the correct functional form of the β-strength function is very critical in reproducing the observed proton spectra. Deviations from the statistical description and difficulties in the calculation of β-strength functions are encountered near magic numbers due to low level densities and rapidly changing deformations.

For the N=81 precursors ^{151}Yb, ^{149}Er, and ^{147}Dy pronounced structure in the proton spectra is observed. Contrary to studies of lighter nuclei no individual levels in the intermediate nuclei can be identified that decay by proton as well as γ-decay. The nature of the observed peaks can, however, be understood in a new framework of an "intermediate structure" based on two-particle, one-hole "doorway states." In the case of N=81 even-odd precursors these states are created via β/EC decay of zero-particle, one-hole configurations. They show a width that is intermediate between direct reaction widths and compound nucleus widths, and that depends on the strength of the residual interaction, a sum of two-body potentials coupling the compound state to the outgoing proton wave function. In this framework the emission of a proton is analogous to the second step in "compound elastic scattering." We are presently studying the results of Nilsson model calculations of the β-strength to doorway states in comparison to the

experiments, and the influence of dynamic vs. static ground state deformations on GT strength distribution.

For nuclei in the same general region we have extended our detailed γ-ray analysis to more deformed nuclei. From the resulting decay schemes absolute branching ratios for β-delayed proton emission have been extracted. These ratios are crucial for delimiting parameter values in the statistical model used to extract β-strength information from the experimental proton spectra. In the future, nuclear structure effects (e.g., the predicted breakdown of the Z=64 proton shell gap around N=77) near the proton drip line will be explored.

Isotopes Project

Group Leaders:
E. Browne
R.B. Firestone

V.S. Shirley
B. Singh

The Isotopes Project is a member of the U.S. Nuclear Data Network (USNDN) with responsibility for evaluating nuclear structure and decay data for mass chains with A=167–194. Evaluations for mass chains with A=168, 173, 178, 179, 182, 186, and 194 were submitted for publication in *Nuclear Data Sheets* in 1987. This represents about 30% of the total number of evaluations submitted by members of the USNDN and the International Network for Nuclear Structure Data Evaluation this year. In addition, the evaluations for mass chains with A=180 and 183, completed last year, were published in *Nuclear Data Sheets*. As of August 1987, sales of books produced by the Isotopes Project totaled 9587 for the *Table of Isotopes*, published in 1978, and 1508 for the *Table of Radioactive Isotopes*, published in 1986.

The Isotopes Project provides access to the LBL/ENSDF database, which contains numerical information from the *Table of Radioactive Isotopes*, from the ENSDF file of nuclear data, and from *The 1983 Atomic Mass Table* of Wapstra *et al.* Computer guest accounts are now available for remote users of the database. These accounts also provide access to the Physics Program Library (PPL) and to the databases of the National Nuclear Data Center at Brookhaven National Laboratory. The PPL program library contains interactive computer codes for calculating commonly used quantities such as log *ft* values and internal conversion coefficients. Computer access can be obtained by telephone or through the HEPnet, MILNET and TYMNET computer networks. In addition, the Isotopes Project performs database searches on request.

The Isotopes Project contributes to the development of methodology for nuclear data evaluation. Topics pursued in 1987 include the normalization of decay scheme intensity data and the adoption of transition energies and branching ratios. Computer codes have been developed to implement our methodology and are being distributed to other evaluation centers.

The Isotopes Project maintains an extensive collection of nuclear physics references and reprints It subscribes to major nuclear physics journals and acts as a specialized library and local resource at LBL.

Complex Fragments and Highly Excited Compound Nuclei

Group Leaders:
L.G. Moretto
G.J. Wozniak
D.R. Bowman*
D.N. Delis*
R.J. Charity
L. Vinet

R.J. McDonald,
M.A. McMahan,
Accelerator & Fusion Research Division, LBL

H. Han,
K. Jing,
Institute of Atomic Energy, Beijing People's Republic of China

W.L. Kehoe*,
B. Libby,
A.C. Mignerey,
Department of Chemistry, University of Maryland, College Park, Maryland, 20742

A. Moroni,
I. Iori,
INFN and Department of Physics, University of Milano, Via Celoria 6 20133 Milano, Italy

N. Colonna,
G. Guarino,
A. Pantaleo,
L. Fiore,
INFN, 70100, Bari, Italy

A. Gobbi,
K. Hildenbrand,
Gesellschaft für Schwerionenforschung, 6100 Darmstadt, West Germany

**Graduate students*

Our recent work has been directed towards elucidating the mechanisms of compound nucleus decay and complex particle emission both at low and high energy.

The recent observation of complex fragment emission in intermediate energy nuclear reactions has been interpreted as evidence for the onset of new reaction mechanisms. At low bombarding energies, virtually the only observed decay modes of excited nuclei are light particle emission, and fission for the heavier elements. This simple and allegedly well understood picture seems to change dramatically as the bombarding energy is raised into the intermediate-energy region (10–100 MeV/nucleon), where previously unobserved decay products with masses between alpha particles and fission fragments are produced in easily detectable amounts.

Preliminary experiments at various energies and projectile-target combinations produced mass distributions apparently following a power law, in general accordance with widely contrasting theoretical predictions such as those based upon cold fragmentation, liquid-vapor equilibrium, and the thermal fragmentation of a participant region. The possibility that these fragments might have their origin in statistical emission by an equilibrated compound nucleus seemed a more likely possibility to us. Since all of the more exotic mechanisms have predicted thresholds somewhere above 10 MeV/nucleon bombarding energy, we decided to search for complex fragment emission from a compound nucleus at very small incident energies, below 50 MeV total center-of-mass energy, using the ^{3}He + Ag reaction. Although the cross sections were very low (sub microbarn), the angular distributions and kinetic energy distributions for fragments from Li to Na were consistent with compound nucleus decay. To certify this as a bona fide compound nucleus process, we have measured the excitation functions associated with individual fragments in the reaction ^{3}He + Ag from just above the barriers up to 130 MeV of total excitation energy. The rapid rise of the excitation functions with energy quantitatively confirms the compound nucleus hypothesis and allows one to obtain the individual conditional-barrier heights. Strong finite-range effects predicted by modern versions of the liquid drop model are verified in detail.

To investigate the mechanism responsible for complex fragment emission at higher energies, we have found it profitable to utilize reverse kinematics reactions with heavy projectiles (^{139}La, ^{93}Nb, ^{63}Cu, ^{40}Ar) and light targets (^{9}Be, ^{12}C, ^{27}Al) at energies ranging from 8 to 50 MeV/nucleon at the SuperHILAC, the 88-Inch Cyclotron, the UNILAC, and the Bevalac. The latter accelerator has allowed us to greatly extend the energy domain over which we could study complex fragment formation. The use of reverse kinematics (projectile much heavier than target) presents many advantages in this kind experiment. The use of light target nuclei limits the range of impact parameters available and hence the number of sources. The kinematic focusing allows for coverage of a very large angular range in the center-of-mass with a small laboratory acceptance angle, thus enhancing greatly the detection efficiency for both singles and coincidences. Furthermore, the large velocity of the center-of-mass allows one to detect and identify the atomic number of the entire range of products. It is important to have access to products with masses between that of the projectile and the target because in this region a much cleaner differentiation of the mass distributions associated with the different mechanisms is expected.

For asymmetric entrance-channel reactions up to 50 MeV/nucleon, we have verified that the binary decay of the equilibrated compound nucleus can account for the major production of complex fragments. At low bombarding energies near the Coulomb barrier, the compound nuclei are produced in complete fusion reactions whereas, at higher energies they are produced in incomplete fusion reactions. In both reactions, highly excited compound nuclei are formed that move forward with high velocity. The two kinematic solutions associated with the isotropic decay in the center of mass with Coulomb-like energies are readily observed and provide a direct measure of the momentum transfer and of the Coulomb splitting. Coincidence measurements verify the binary mechanism and confirm that the sum of the charges is nearly independent of the asymmetry of the decay and close to the Z value of the incomplete fusion product after evaporation is accounted for. These compound nuclei are characterized by a temperature and a mean excitation energy per nucleon approaching the mean nucleon binding energy. It is expected that a great deal can be learned about the stability of nuclei at high excitation energy, in particular about the effect of high temperature on size and surface energy as well as about the modes of decay.

In this series of experiments we have demonstrated the pervasive nature of complex fragment emission from compound nuclei. Clearly, any other novel mechanism of production has to deal with the coexisting compound nucleus mechanism as background. In fact, the expected onset of multifragmentation at even higher excitation energy may very well be dominated by a series of sequential binary decays.

In order to study the onset and the nature of multifragmentation, we are building a detection system consisting of an array of 49 (7×7) telescopes. Each telescope consists of a 0.3 mm Si detector, a 5 mm Li-drifted detector and a 7.5 cm plastic scintillator. The first and second detectors are position sensitive along the x and y directions, respectively. This system has multihit capabilities and should be able to characterize a multifragmentation event completely if the reaction is studied in reverse kinematics. Our immediate goals with this detector system are to follow the binary decay process from 50 MeV/nucleon up to its disappearance and to study the excitation function of multifragmentation events.

As mentioned above sequential binary decay is expected to provide a sizable background to more exotic multifragmentation processes, if they exist. We have called the fragmenting of a system by a compound nuclear sequential binary decay, nuclear comminution. This process can be quantitatively assessed in terms of the complex fragment decay probability. We have shown that this mechanism predicts mass distribution with a characteristic power law dependence in the light mass region. As a consequence such a power law cannot be considered diagnostic of liquid-vapor equilibrium.

Relativistic Nuclear Collisions: Nucleus-Nucleus Collisions

Group Leader
P.B. Price

S. Barwick
T. Coan*
J. Drach
G. Gerbier
D. Ifft*
D. Lowder*
M. Salamon
M. Solarz
A. Westphal*
W. Williams*

**Graduate Students*

All this group's offices and equipment are located in Birge Hall on the UCB campus, which makes it easy to attract new students but restricts to some extent interaction with Nuclear Science Division staff. Current research falls into the following six principal areas:

1. Systematics of radioactive decay via emission of heavy ions such as ^{14}C, ^{24}Ne, ^{28}Mg, and ^{34}Si (DOE support);

2. Search for highly ionizing particles in e^+e^- annihilation (TRISTAN experiment and LEP [OPAL] experiment, supported by NSF) and in $\bar{p}p$ annihilation (Fermilab experiment, NSF support);

3. Cosmic-ray astrophysics (NASA and NSF support):
   a. Construction of an experiment to detect anti-iron nuclei in cosmic rays at a level 3×10^{-7} of iron (in collaboration with Indiana University and the University of Michigan);
   b. Measurements of the energy spectrum of antiprotons at $E < 1$ GeV with a balloon-borne magnetic spectrometer;

4. Development of new types of glass detectors and an automated measurement system for experiments to resolve isotopes of relativistic nuclei up to lead (NASA support);

5. Ultrarelativistic nucleus-nucleus collisions (DOE support):
   a. 200 GeV/nucleon collisions of ^{16}O and ^{32}S at CERN,
   b. 15 GeV/nucleon collisions of ^{16}O and ^{32}S at Brookhaven,
   c. Detector response as a function of Lorentz factor,
   d. Planning for heavier projectiles.

Relativistic Nuclear Collisions: Pion and Correlation Studies

Group Leaders:
K.M. Crowe
J.O. Rasmussen

J.A. Bistirlich
R.R. Bossingham*
A.D. Chacon*
M. Justice*
S. Ljungfelt*
C.A. Meyer
M.A. Stoyer*
K. Wyatt*

R. Van Dantzig,
F.W.N. DeBoer,
NIKHF-K,
Amsterdam,
The Netherlands

P. Kammel,
Austrian Academy
of Science,
Vienna, Austria

C. Petitjean,
Swiss Institute
for Nuclear Research,
Villigen, Switzerland

*Graduate students

The Bevalac research of our group centers on the study of charged pions and correlated pairs of particles produced in relativistic heavy-ion collisions. We have utilized (Janus), a large (4 meter flight path) dipole-dipole magnetic spectrometer and combinations of fast scintillators and wire chambers in a series of pion interferometry studies. The Hanbury-Brown/Twiss effect, which has been used in astronomy to measure the radii of stars, may also be used to probe nuclear matter. Thus pion interferometry experiments allow measurements of the radius, lifetime, and coherence of the pion-emitting source.

In practice, we measure the momenta ($\vec{p}_1$ and $\vec{p}_2$) of coincident like-charged pions in our spectrometer and, using the two pion yields thus obtained, form the correlation function C ($\vec{p}_1$,$\vec{p}_2$). This experimental correlation function is then fitted to a model, which assumes a Gaussian space-time distribution for the sources, and the source parameters are extracted (see figure). Thus far we have used this technique to measure source parameters for the systems 1.8 GeV/nucleon ^{40}Ar on KCl, 1.8 GeV/nucleon ^{20}Ne + NaF, 1.7 GeV/nucleon ^{56}Fe on Fe, and 1.5 GeV/nucleon ^{93}Nb on ^{9C}Nb. The Fe data show an oblate source, in agreement with intranuclear cascade model calculations (see LBL-19420 and LBL-18709).

A new two-pion experiment (1.3 GeV/nucleon ^{139}La on La) has been approved, in which a multiplicity array will be incorporated to provide impact parameter definition. The correlation of the source dimensions with impact parameter is of basic interest in interpreting the two-pion data. We will measure projectile spectator multiplicities with a 50 detector scintillator wall subtending a 5 cone with respect to the beam. A prototype 9-element has been tested, with encouraging results.

A search for "pineuts" (bound clusters of neutrons and negative pions) was conducted in January 1987 using the Janus spectrometer. The experiment was sensitive to particles with lifetimes of the order of 10 ns or longer. Positive particle data was taken as a reference; these data show good time-of-flight and momentum resolution. The negative particle data are currently being analyzed.

Our group has also been involved in developing heavy ion one- and two-neutron transfer reactions as a probe for studying high spin states. Recent experiments include syntax error file -, between lines 655 and 655 ^{235}U (^{58}Ni,^{59}Ni) ^{234}U at E = 325 MeV at Oak Ridge National Laboratory in May, 1986, and ^{235}U (^{206}Pb,^{207}Pb) ^{234}U and ^{233}U (^{206}Pb,^{207}Pb) ^{232}U at E_{LAB} 1300 MeV at the SuperHILAC in May, 1987. Such reactions provide a unique tool for work in the actinide region as they appear to involve mainly "cold" neutron transfer mechanisms, thus eliminating fission competition. Theoretical work is also progressing in understanding these reactions.

Several members of our group have been involved in muon catalyzed fusion ($d+t+\mu^- \rightarrow \alpha+n+\mu^-$) experiments at Swiss Institute for Nuclear Research (SIN). Systematic investigations made over a wide range of hydrogen isotope concentrations and densities have resulted in detailed information concerning the complicated reaction kinetics (see Phys. Rev. Lett. 58, 329). Our latest run in March/April of 1987 included an improved target setup, developed at LBL, specifically designed for studying the

fusion cycle in solid hydrogen. Currently a new target, capable of containing deuterium/tritium mixtures in the unexplored region above 1000K, is being constructed in collaboration with Lawrence Livermore National Laboratory.

Our research group is presently working on development and construction of the Jet Drift Chamber (JDC) to be used as early as summer 1988 in the Crystal Barrel experiment at CERN's Low Energy Antiproton Ring (LEAR). The JDC is a 20-inch diameter, 18-inch long cylinder with 30 pie-shaped sectors comprised of multi-layers of precision-positioned sense, guard and field wires, strung axially. The charge deposited on the sense wire (by passage of a charged particle in a gas medium and 1 kV/cm electric field) will be processed by a differential amplifier based on the Fujitsu-MB43468 chip. We have successfully tested our JDC prototype and two types of prototype amplifiers at SIN using pions and protons to give us a good understanding of the background noise, dynamic range and compatibility with flash-type analog to digital converters.

The main issue of the proposed experiment, PS 197, is the search for phenomena related to Quantum Chromodynamics (QCD). A striking prediction of this theory is the existence of new boson resonances with constituent gluons: glueballs and hybrids. Experimental detection of these hadronic states would be a milestone in the understanding of low energy QCD.

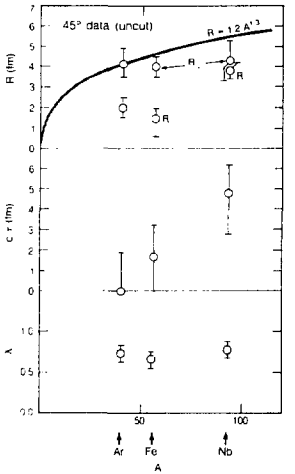

Fig. 1. See text.

XBL 8710-9336

Relativistic Nuclear Collisions: HISS

Technical Director
H. Wieman

F.S. Bieser
P.J. Lindstrom
W.F.J. Müller
J. Wolf

H.J. Crawford,
I. Flores,
UCSSL

F.P. Brady,
J. Romero,
C. Tull,*
W. Christie,
U.C. Davis,
D.L. Olson,
U.C. Riverside

**Graduate student*

The HISS facility consists of a large solid angle magnetic spectrometer designed to measure multi-particle final states produced in relativistic heavy ion collisions. The heart of the facility is a 7 Tm, superconducting magnet surrounded by a variety of detectors which can be arranged in different ways to suit the needs of specific experiments. In addition to the local group listed here, users from RIKEN, KEK, Osaka, Michigan State University, Kent State University, U.C. Riverside and GSI-Darmstadt are active at the facility.

During the period under review, three major experiments ran at the HISS facility. The RIKEN-KEK-OSAKA-LBL collaboration took data on the fragmentation of secondary beams such as ^{11}Li and ^{8}He. These experiments follow on from earlier experiments studying interaction cross sections and interesting results have already been obtained regarding the momentum distributions of nucleons in these nuclei. The second experiment was to measure complex fragment emission at midrapidity. This is of great interest as a means of measuring the entropy of the final state. Finally, a new experiment was done measuring pion-correlation in Ar and X induced reactions. Both of these latter experiments used the new 2 time 1.5 m drift chamber to measure multiparticle completions.

During the year, considerable progress was made on the development of the MUSIC II detector which measures the change and position of highly charged ions. Initial tests of the detector have been successful and an electronic readout system is now being developed for the detector. Finally, initial design was done for a new time-of-flight array that will augment the system presently available at the HISS facility.

Relativistic Nuclear Collisions: The Plastic Ball

Group Leaders:
A.M. Poskanzer
H.-G. Ritter

A. Franz,
P. Kristiansson,
LBL

H.H. Gutbrod,
H.-R. Schmidt,
T. Siemiarczuk,
GSI

H.-A. Gustafsson,
Lund University
Sweden

K.-H. Kampert,
H. Löhner,
University of Münster
West Germany

B. Jacak,
Los Alamos National Laboratory

The work of the group centers on the use of the Plastic Ball and other detectors to study central collisions of nuclei at bombarding energies ranging from 200 MeV/nucleon to 200 GeV/nucleon, with the aim of learning about nuclear matter at high temperature and density. Much of the work of the group in the past decade has been in collaboration with GSI (Gesellschaft für Schwerionenforschung, Darmstadt, West Germany).

In the past year a major experiment was performed at the CERN Laboratory's Super Proton Synchrotron (SPS) using 60 and 200 GeV/nucleon ^{16}O, and 200 GeV/nucleon ^{32}S beams. This is an expanded collaboration involving the University of Münster, Lund University and Oak Ridge National Laboratory. The experiment, called WA80, consists of five detector systems: The Plastic Ball, Multiplicity Arrays, a Lead Glass Spectrometer, a Wall Calorimeter, and a Zero-Degree Calorimeter. The goal is to study the systematics in this new energy range and to search for signatures of the quark-gluon plasma. Excellent data were obtained with both the ^{16}O and ^{32}S beams, and several papers have been submitted for publication based on the ^{16}O results.

The Bevalac Plastic Ball data are still being published. Papers have been produced on entropy, correlations, and fragment production. For fragment production the systems studied were 200 MeV/nucleon Au on Au and Fe targets. The goal is to learn about multifragmentation or the liquid-gas phase change. This work is a collaboration with the Harris group and a group from LANL.

Fig. 1 The CERN SPS WA80 group after the oxygen experiment. XBB 8711-9834

Relativistic Nuclear Collisions: DLS

Group Leaders:
H.G. Pugh
G. Roche
L.S. Schroeder

R.L. Fulton
G. Krebs
E. Lallier
H.S. Matis
J. Miller
C. Naudet
P. Seidl
Z.F. Wang
A. Yegneswaran*

S. Christo,
P.N. Kirk,
Louisiana State University, Baton Rouge, LA

T. Hallman,
L. Madansky,
Johns Hopkins University Baltimore, MD

D. Miller,
Northwestern University, Evanston, IL

J. Bystricky,
J. Carroll,
J. Gordon,*
G. Igo,
University of California at Los Angeles

G. Landaud,
Université de Clermont-Ferrand Aubière, France

**Graduate student*

The construction of the Dilepton Spectrometer (DLS) was completed and the whole system successfully tested with an Ne beam in November 1986. The DLS is a large aperture two-arm magnetic detector constructed and operated by a consortium involving the Lawrence Berkeley Laboratory, Johns Hopkins University, Louisiana State University, Northwestern University, UCLA and Clermont-Ferrand. It is instrumented with segmented gas Cerenkov arrays in front and back of the magnets to discriminate $e^{\pm}$'s from $\pi^{\pm}$'s and protons, scintillation hodoscopes (front and back) for fast charged particle triggering, and drift chambers in front and back for tracking. A multiplicity detector will be constructed in 1988. The system is installed in the BEVALAC beam-30 cave.

The goal of DLS collaboration is to measure the e^+e^- mass spectrum between 100-800 MeV and p_T distribution up to 700 MeV/c. The program includes both proton-nucleus and nucleus-nucleus collisions. In proton-nucleus interactions, it aims to establish the existence of direct lepton (electron) pairs at BEVALAC energies and help clarifying the mechanism(s) of their production. In nucleus-nucleus collisions, dileptons are excellent probes of the hot, compressed phase of the nuclear medium and should tell us a great deal about the fundamental processes going on at this stage of the collision and provide another means for obtaining additional information on the nuclear equation of state.

In December 1986, data were taken in p + Be at 4.9 GeV and the existence of a direct electron pair signal established by mid-February of 1987. The strength of the signal, expresses as usual in terms of e/π ratio, is estimated in between 5×10^{-5} and 5×10^{-4}, which is consistent with the high energy typical number of a few 10^{-4}. A second of the DLS was done in May 1987. Two reactions were studied: p + Be at 2.1 GeV and Ca + Ca at 1.95 GeV/nucleon. Here again direct electron pairs were observed at about the same rate. The analysis of these data is in progress.

Relativistic Nuclear Collisions: Radioactive Beam Study and Light Particle Emission Study

Group leaders
L.S. Schroeder
K. Matsuta

J.R. Alonso
G. Krebs
K. Sugimoto
T.J.M. Symons

O. Hashimoto,
Y. Shida,
INS, University of Tokyo, Japan

M. Izumi,
T. Minamisono,
Y. Nojiri,
N. Takahashi,
K. Takeyama,
Laboratory of Nuclear Studies, Osaka University, Japan

T. Kobayashi,
National Laboratory for High Energy Physics Tsukuba, Ibarak, Japan

S. Nagamiya,
University of Columbia

I. Tanihata,
RIKEN
Wako, Saitama, Japan

S. Shimoura,
E. Ekuni,
Kyoto University
Kyoto, Japan

Our group has been studying high-energy heavy-ion reactions at the Bevalac in a collaboration between the Institute for Nuclear Study (INS), the University of Tokyo, Osaka University, and LBL. The experimental program of the group emphasizes two types of measurements, one measures the interaction cross section (E690H and E852H) and magnetic moments (E732H) using beams of radioactive nuclei, and the other measures light particle emissions ($\pi^{\pm}$, p, d) from heavy-ion collisions (E593H,E733H).

In experiments E690H and E852H, interaction cross sections between two nuclei were measured using beams of ^{3,4,6,8}He, ^{6,7,8,9,11}Li, ^{8,10,11,12,13,14}Be and ^{12,13,14,15}B at 790 MeV/nucleon. Beams of radioactive nuclei were produced through the projectile fragmentation of 800 MeV/nucleon ^{11}B, ^{20}Ne, ^{22}Ne and ^{18}O. Separation of the nuclei were made using a magnetic analyzing system of the Bevalac beam line(B-42). After the separation of the secondary beam, interaction cross sections were measured using the HISS spectrometer. Root-mean-square matter radii of He, Li, Be and B isotopes were deduced from the interaction cross sections using a Glauber-type calculation. Appreciable differences of radii among isobars (^{6}He-^{6}Li, ^{8}He-^{8}Li, and ^{9}Li-^{9}Be) were observed for the first time. The nucleus ^{11}Li showed a remarkably large radius suggesting a large deformation or a long tail in the matter distribution. The experiment is being extended to all sd-shell nuclei.

A new experiment E732H has been planned to determine nuclear moments of unstable nuclei in the $f_{7/2}$ shell. For this purpose an NMR method will be applied to short-lived β emitting nuclei produced through projectile fragmentation. Test runs have already begun in Bevalac beam line B-44 to confirm the separability of isotopes and polarization production using a tilted foil technique. In the test run, ^{20}F, ^{21}F and ^{39}Ca nuclei were successfully collected and the nuclear lifetimes were obtained by detecting β rays and NMR on ^{39}Ca was detected to show a significant amount of polarization in the beam. The technique will be applied for determination of magnetic moments of ^{37}Ca and ^{43}Ti.

Experiment E593H measured pion spectra at 0° in coincidence with heavy fragments emitted at the same angle for studying Coulomb distortion effects on pion spectra. The experiment was performed at HISS using a La beam of 800 MeV/nucleon, and the data analysis is in progress. A prominent peak has been observed in the π^- spectrum at around the projectile velocity. The peak position shifts to lower momentum for smaller impact parameter, and this shift is thought to be due to larger friction in collisions of smaller impact parameter. The distribution of the projectile fragment sum charge has been measured in the La + C reaction. The results indicate that a transverse growth of the cascade has a large effect in the reaction.

The projectile- and target-mass dependence of light particle production in heavy ion collisions has been studied by measurements of pions and light nuclear fragments (p, d, t, ^{3}He, and ^{4}He) in La + La collisions at 800 MeV/nucleon (E733H). A magnetic spectrometer was used for detection of these particles and a set of 120 multiplicity counters was used for event selection. We have measured (a) energy spectra, (b) angular distributions, (c) the pion to nucleon yield ratio, and (d) the coalescence relation for

the formation of composite fragments in both low- and high-multiplicity events. By comparing these results with the previous data for lighter mass collisions, we have found that both pion yield and pion kinetic energy are greatly influenced by final state interactions.

Streamer Chamber Experiments

The Streamer Chamber allows the study of charged particles as well as K^0 and Λ^0 over most of the 4π solid angle in high energy heavy ion collisions. Using it, and a forward angle 384-element scintillator array, we have made measurements of π^- multiplicities and spectrum shapes as a function of beam energy and of participant number (i.e., impact parameter). We have studied Λ^0 production in near-central collisions, and we have reconstructed and measured all the tracks in a large sample of events, to extract such quantities as flow and transverse momentum distributions. Our results indicate that the nuclear matter equation of state is stiffer than had been supposed.

Several improvements to the Streamer Chamber facility are underway to extend these studies to the heaviest projectiles (which is desirable to minimize surface effects and to emphasize bulk properties of the "fireball"); to provide enhanced particle identification (and hence more complete evaluation of individual events); and to permit greater efficiency in data analysis.

High-gain image intensifiers and CCD cameras have been installed, together with a fully digitized data acquisition and analysis system, developed and tested on the NA35 experiment at CERN. A test run was completed at the Bevalac in Spring of 1987. The Streamer Chamber was successfully operated at lower pulse voltages near the avalanche mode with complete elimination of "flares," improved track definition, and linearity of response (which is important for particle identification by dE/dx measurement). On-line monitoring of the chamber performance and on-line studies of event topologies (with, for example, on-line availability of track multiplicities) were performed. The complete digitization of the data acquisition and analysis system will permit rapid automatic scanning and preselection of events, and a major enhancement in the speed of (operator-assisted) total event reconstruction.

The CCD camera system uses three cameras, each with 1024 x 1024 pixels. The information in the pixels is digitized to 9 bits and transferred in parallel to an on-line image processing system based on a VAXstation II computer (Micro VAX II). Attached to this is a 10 million-instruction-per-second integer coprocessor, the Mercury Computer System 3216, and peripherals. Data are stored on a high density digital VHS cassette tape recording system.

Group Leaders:
J.W. Harris
H.G. Pugh
L.S. Schroeder

J.P. Brannigan,
S.I. Chase,*
I.W. Muskovich,
G. Odyniec,
G. Rai,
W. Rauch,
L. Teitelbaum,*
L.M. Tinay,
M. Tincknell,
J.-M. Walker,
LBL

R.E. Renfordt,
R. Stock,
S. Wenig,*
University of Frankfurt,
W. Germany

H. Ströbele,
Gesellschaft für Schwerionenforschung,
Darmstadt,
W. Germany

J.P. Sullivan,
K. Wolf,
Texas A&M University,
College Station,
Texas 77843

**Graduate students*

Ultrarelativistic Nuclear Collisions

Group Leaders:
J.W. Harris
H.G. Pugh
L.S. Schroeder

S.I. Chase*
G. Odyniec
G. Rai
W. Rauch
L. Teitelbaum*
L.M. Tinay
M. Tincknell
J.-M. Walker

**Graduate student*

The NA35 experiment at the CERN Super Proton Synchrotron is a collaboration of about 60 physicists from 14 institutions: Athens – Bari – Berkeley – CERN – Cracow – Darmstadt (GSI) – Frankfurt – Freiburg – Heidelberg – Marburg – Munich (MPI) – Warsaw – Zagreb. This experiment (and, in fact, the entire heavy ion program at CERN) developed from a proposal submitted by the GSI-LBL collaboration at the Bevalac, with R. Stock as spokesman. The proposal, approved as experiment PS190, was subsequently split into two parts: NA35, using a streamer chamber, and led by R. Stock; and WA80, using the Plastic Ball, and led by H.H. Gutbrod. The experiments were made possible by the joint construction by GSI, LBL, and CERN, of a new heavy ion injector for the CERN complex of accelerators. LBL's Accelerator and Fusion Research Division constructed a radio-frequency quadrupole linac (RFQ) as part of this injector.

The NA35 experiment had its first run, using a beam of 200 GeV/nucleon (3.2 TeV) ^{16}O ions, during September and December, 1986. A paper based on that run has been published in Physics Letters. A successful second run with a 200 GeV/nucleon (6.4 TeV) ^{32}S beam was completed during September and October, 1987.

The objective of the NA35 experiment is to explore the prediction of strong interaction lattice gauge theory that the hadronic state of matter is transformed, at sufficiently high energy density, into a new phase consisting of deconfined quarks and gluons. Such extreme conditions, with an energy density of several GeV/fm^3 (more than ten times that of ground state nuclear matter) could be reached in central nucleus-nucleus collisions by converting the initial c.m. energy into internal excitation of a "fireball" formed at rapidities intermediate between those of target and projectile, provided sufficient beam energy and sufficient "stopping power" in the nuclear interaction. In the initial phase of the study, the emphasis has been to find out if such conditions are reached in ^{16}O-nucleus collisions at 200 GeV/nucleon. The first indications are favorable.

The NA35 set up consists of a 2 × 1.2 × 0.72 m^3 **Streamer Chamber** in the 1.5 Tesla field of a superconducting "vertex" magnet. Three cameras, each equipped with two-stage magnetically focused image intensifiers, view the Streamer Chamber, and record events on 70 mm film. In addition, three Charge-Coupled Device (CCD) electronic cameras, equipped with image intensifiers, record data for on-line supervision and digital storage of events for later analysis. Downstream, a highly segmented **Photon Position Detector** (PPD) measures most of the energy of photons and π^0 particles. Directly behind the PPD is a **Ring Calorimeter** of thickness sufficient to absorb all the energy of hadronic showers produced in the interaction. These two detectors cover the mid-rapidity region $2.5°<\theta<12°$. The internal aperture of the Ring Calorimeter is filled by the **Intermediate Calorimeter**, covering the angular range $0.3°<\theta<2.5°$. The energy flux in the projectile fragmentation domain $\theta<0.3°$ is measured by a **Veto Calorimeter.**

LBL contributions to the experimental hardware include the Intermediate Calorimeter and high voltage power supplies for the Ring Calorimeter. A major feature of the experiment, provided by LBL, is the CCD **Streamer Chamber Supervision and Data Acquisition System.** This system uses three CCD cameras with 1024 × 1024 pixels

each. The CCD pixels are digitized to 9 bits and transferred in parallel to an on-line image processing system based on a VAXstation II computer (Micro-VAX II). Attached to this is a 10 million-instruction-per-second integer coprocessor, the Mercury Computer Systems 3216, and peripherals, including a VHS digital recording system for data storage. The system provides quantitative on-line analysis of streamer chamber performance and event topology to optimize the use of beam time. It provides, for example, a measure of the multiplicity of charged particles produced in each event, which can be correlated on line with such measured quantities as transverse energy in the PPD and Ring Calorimeter, or the energy in the Veto Calorimeter. In the ^{32}S experiment the CCD system was used extensively for data acquisition.

LBL's contribution to the data analysis is focused on the scanning and measuring tables developed for use in Bevalac Streamer Chamber experiments. The secondary particle multiplicities are substantially higher than those in Bevalac collisions. Nevertheless, events with up to 371 charged particle tracks have been successfully measured. Each such event, on its own, contains a substantial amount of information and warrants careful study. Emphasis is presently being placed on specific attributes of the events such as the production of strange particles and antiparticles.

Nuclear Theory

Group Leaders:
N.K. Glendenning
M. Gyulassy
W.D. Myers
J. Randrup*
W.J. Świątecki

F.R. Klinkhamer
D. Hahn
M. Redlich

G. Faï
Kent State University
Ohio

P. Möller,
Lund University
Sweden

F. Brut,
Institut des
Sciences Nucléaires
University of
Grenoble, France

L. Wilets,
University of Washington
Seattle

**Scientific Director*
of the Theory Program

The nuclear theory program covers many of the major topics in nuclear physics, partly reflecting but also extending beyond the already rather broad range of our experimental program.

Non-perturbative aspects of field theories are becoming increasingly relevant to nuclear physics. The areas of research include the structure of the interactions in superstring theory, the quark-confinement mechanism, and topological solutions to effective meson field theories. The internal nucleon structure is being investigated with soliton models and the effect on matter properties is being examined, as well as the deconfinement of quarks in the sense of color conductivity.

Matter at high energy density as may arise in high-energy collisions and neutron stars. Using relativistic hadronic field theory, the existence of phase transitions, abnormal matter and hyperons in neutrons stars have been studied. Current studies include pion production in a hot nuclear fireball model, constraints on the equation of state from nuclear and astrophysical evidence, and vacuum renormalization effects in neutron stars.

Nuclear collisions at ultra-relativistic energies. Studies of nuclear stopping power and the space-time development of hadronization seek to determine the energy densities achieved. A QCD transport theory has been developed for the description of chromodynamic plasmas far from equilibrium. A Monte-Carlo code extending the Lund string model to nuclear collisions has been developed and applied to preliminary BNL and CERN data. Microscopic studies of the transition from plasma to hadronic matter and possible experimental signatures for the quark-gluon phase are being studied.

Nuclear collisions at intermediate energies. Cascade, fluid dynamic, and statistical models are employed in order to elucidate the complicated reaction dynamics. The microcanonical description of interacting fragments at subsaturation densities is being developed and has been used to study the effect of fragment interactions, particularly the repulsions resulting from the Coulomb force and the nuclear incompressibility. The proper treatment of highly excited fragments is also being investigated. A self-consistent momentum-dependent Vlasov equation has been derived from quantum hadrodynamics for application to Bevalac energies. A new method for determining the azimuthal orientation of the reaction plane has been proposed.

Nuclear dynamics at moderate energies. Extensive studies have been completed illustrating the relation between the order-to-chaos transition in nucleonic motions and the solid-to-fluid transition of an idealized nucleus undergoing shape oscillations of various multipolarities (P2 to P6). A series of lectures and collaborations has been initiated, aiming at bringing together nuclear physicists and workers in the rapidly growing field of non-linear dynamics. The evolution of the dynamics of nuclear collisions with increasing energy has been studied on the basis of the nucleon-exchange transport model, which has been extended to allow a tracing of the further fate of the transferred nucleons. These are followed as they cascade through the recipient nucleus and the resulting yield of promptly emitted neutrons has been calculated and compares with with a variety of data. The production of photons in the associated neutron-proton collisions is currently being studied.

Macroscopic nuclear properties. The predictive power of the Droplet Model is being steadily improved. Recent advances include a finite-range correction term and the surface contributions to nuclear moments. For fission of the heaviest elements, it was found that qualitatively different fission paths exist and yield bimodal fission-fragment energy distributions.

88-Inch Cyclotron Operations

D.J. Clark
D.R. Elo
L.R. Glasgow
R.S. Lam
R.M. Larimer
S.A. Lundgren
C.M. Lyneis
R.A. Peterson
J.W. Roberts
R.G. Stokstad

The 88-Inch Cyclotron continued operation as a reliable source of light and heavy ions, benefiting greatly from the ECR source, which was installed in 1985. The operation now requires less operating manpower than with the PIG sources, since the ECR source needs essentially no maintenance between the weekly shutdown maintenence shifts.

The 88-Inch Cyclotron is a national facility and is used extensively by outside groups from many institutions in the U.S. and abroad. Table I shows the numbers of users from LBL and elsewhere. Allocation of beam time is done on the basis of recommendations by a Program Advisory Committee, which considers proposals for individual nuclear science experiments on a four-month cycle. The scheduling of experiments is done on a weekly basis, although experiments involving users who must make travel arrangements are scheduled further in advance. The members of the PAC during the period covered by this report were Charles Goodman (IUCF), Jørgen Randrup (LBL), John Rasmussen (LBL), Robert Vandenbosch (U. Washington), Leo Riedinger (University of Tennessee) and Joseph Natowitz (Texas A&M). Marshall Blann and Władisław Świątecki served at the August 1987 meeting. Table II shows the ratio of requested to available beam time for recent allocation cycles. Note the increase in the demand for time. The distribution of beam time among various categories (nuclear science, beam development, inside use, outside use, etc.) is shown there. Recharge use is the category in which the users of the cyclotron pay for the time on an (operating) cost-recovery basis. Since the funds provided by the DOE to operate the cyclotron for nuclear science have become increasingly inadequate, even for a 14-1/2 shift per week schedule, the recharge use has become a correspondingly important item in the total operations budget. Without this source of income, the operation for nuclear science would have to be curtailed even more, since operation at less than our present rate would be less cost effective. The members of the Users Executive Committee were Kenneth Hulet (LLNL) and, from LBL, Yuen-dat Chan, Marie-Agnes Deleplanque, and Eric Norman.

The cyclotron plays a significant educational role. In FY87 eight graduate students from the University of California at Berkeley employed this facility in their research toward the PhD degree. In addition 15 graduate students from other universities participated in research at the cyclotron.

The cyclotron was operated 14-1/2 eight hour shifts per week. In addition one shift was used for maintenance at the beginning of each week and one half shift at the end for shutdown over the weekend. The distribution of cyclotron time is shown in Table III. The light ion beams of protons, deuterons, ^{3}He and α-particles are available using either the ECR source or the standard internal filament source. The polarized ion source operates reliably and provides beams of polarized protons and deuterons. Heavy ions (A>4) occupied 66% of the scheduled time, using only the ECR source. A beam list is shown in Table IV.

The following improvements were made to the cyclotron facility:

A. ECR Source

1. The upgrade to the first stage of the ECR source was in the design and fabrication stage.

2. A high temperature oven was designed for the second stage of the ECR source. Fabrication was started. It will provide beams such as copper and nickel.

3. A beam attenuator using metal meshes on air cylinders was built and installed on the ECR beam line. It provides a fast (two seconds) method of beam intensity control by the operator.

4. A beam pulser power supply was built to drive existing steering plates in the ECR beam line. Rise and fall times are 5 ms.

5. Ventilation and smoke detection capability was improved in the ECR control and power supply racks.

B. Cyclotron

The trim coil regulation improvement project is 80% complete. The purpose is to regulate the currents to 1/1000, particularly against line voltage fluctuations due to Bevatron pulsing. This will provide much more stable cyclotron beams.

C. Experimental Area

1. A new beamline was installed in Cave 1 for outside users.

2. Beamline 5B was dismantled for equipment for Cave 4C.

3. Cave 0 hood work area was finished.

4. A second sodium iodide detector was installed in Cave 4C.

5. A beam sweeper power supply was built and installed in Cave 3 to drive a sweeping magnet with a triangular wave shape.

6. A new intercom system was installed for the use of experimental groups.

D. Building

1. Emergency lighting and power was improved in deficient areas.

2. Desktop publishing and calculating power were improved by the addition of several Macintosh personal computers, a laser printer and an Appletalk inter-office network.

Table I

Distribution of Cyclotron Users in FY87

LBL, U.C. Berkeley Staff			22
Graduate Students			23
	U.C. Berkeley	8	
	Other Institutions	15	
Post-doctoral Scientists			18
	LBL	11	
	Other Institutions	7	
Outside User Staff			110
	Universities	15	
	Other Institutions	33	
	Industry	62	
Total			173

Table II

Cyclotron Time Allocation Summary for Five Scheduling Periods

		Jan–April 86	May–Sept 86	Oct 86–Feb 87	Mar 87–June 87	July 87–Oct 87
Total Requests						
Total Allocations		1.40	1.53	2.01	1.49	1.62
Nuc. Sci. Requests						
Nuc. Sci. Allocations		1.63	1.72	1.91	1.82	1.88
Allocated Time	(%)					
Recharge		16	13	17	19	18
Beam Dev.		6	4	5	7	5
Discretionary		6	8	7	10	6
Nuclear Science		72	75	71	64	71
Nuc. Sci outside						
Nuc. Sci.	(%)	23	32	55	32	32
Nuc. Sci LBL						
Nuc. Sci.	(%)	77	68	45	68	68
LBL Alloc.						
Total Alloc.	(%)	55	51	42	43	49

Table III

Cyclotron Time Distribution for FY87

		Hours	%
Operating Time			
Machine Studies		208	5.6
Cyclotron, ECR Tuning		329	5.7
Beam Optics		371	6.5
On Target		4218	73.7
Nuclear Science	3602		
Other	616		
Wait for Experimenter		16	.3
		5142	**89.8**
Maintenance Time			
Scheduled Maint.		560	9.8
Weekly	314		
Summer	246		
Unscheduled Maint.		16	.3
Power outages, etc.		6	.1
		582	**10.2**
Total		**5724**	**100.0**
Holiday		388	
Budgetary Shutdown		2648	
Total Time		8760	

Ion	Charge State (e^5A)	External Beam (MeV/u)	E/A Range/Max (e^5A)	Ion State (MeV/u)	Charge Beam	External Max	E/A
p	1	100-10	.2-55	^{32}S	7	3.5	7
		8	2.0	9			
p (pol.)	1	.7-.4	6-50	9	1.0	11	
	10	.4	14				
d	1	100-10	.3-32	11	.1	17	
	12	.02	20				
d (pol.)	1	.7-.4	5-32	13	.003	23	
	14	.001	27				
^3He	2	100-10	1-47				
	^{35}Cl	9	.4	9			
^4He	2	100-10	1-32	10	.1	11	
	11	.02	14				
^{12}C	4	2.0	16	12	.005	16	
	5	.06	24				
	6	.001	32				
^{14}N	5	3.0	18	^{39}K	9	4	7
	6	.15	26	10	2	9	
	7	.005	32	11	1	11	
	12	.02	13				
^{16}O	6	3.0	20				
	7	.1	27	^{40}Ar	9	3.0	7
	8	.03	32	10	1.5	9	
	11	.6	11				
^{19}F	7	.6	20	12	.4	13	
	13	.09	15				
^{20}Ne	6	2.0	13	14	.015	17	
	7	.4	17	15	.002	20	
	8	.1	22				
	9	.015	28	^{40}Ca	9	1.5	7
	10	1.0	9				
^{24}Mg	6	1.5	9	11	.8	11	
	7	.7	12	12	.4	13	
	8	.2	16	13	.06	15	
	9	.1	20	14	.006	17	
	10	.03	24	15	.002	20	
	11	.001	29				
	^{44}Ca	12	.6	8.9			
^{28}Si	6	2.0	6				
	7	1.0	9	^{48}Ca	13	.05	8.6
	8	.6	11				
	9	.1	14	^{84}Kr	17	.2	6
	10	.04	18	19	.08	7	
	11	.007	22	20	.04	8	
	12	.002	26				
	^{129}Xe	23	.01	4			
	27	.01	6				

PART II: EXPERIMENT

Polarization Observables in the $^2H(d,\gamma)^4He$ Reaction

H.R. Weller, R.M. Whitton,* E. Hayward,† W.R. Dodge,† S. Kuhn, R.-M. Larimer*

Our work at the 88-Inch Cyclotron is part of our experimental program to study polarization observables and the cross section of the $^2H(d,\gamma)^4He$ reaction over a wide range of projectile energies, from 300 keV to 50 MeV. These observables are used to deduce the details of the reaction mechanism and especially the influence of the D-state of ^4He, which manifests itself in the presence of a non-zero tensor analyzing power A_{yy}. The results at the higher energies of the 88-Inch Cyclotron reflect the properties of the D-state wave function at smaller distances and thus provide a crucial test for the several theoretical models of that wave function.

Our experimental setup at the 88-Inch consists of a dedicated beam line in Cave 4C with two movable, actively and passively shielded large NaI γ-spectrometers, a liquid nitrogen cooled gas target, an α- particle recoil detector using plastic scintillators and a heavily shielded beam dump.

So far we have sampled a complete data set of vector analyzing power (A_y) and tensor analyzing power (A_{yy}) distributions at 20 MeV, 30 MeV and 50 MeV. Our data show that A_{yy} increases with energy, as expected from the increasing influence of the D-state of ^4He, while the vector analyzing power A_y is fairly small at high energies, indicating that the problems arising from non-E2 radiation at lower energies are not present in our LBL data. Our next run, in January 1988, will be dedicated to measuring another tensor analyzing power component, namely A_{xx}, at 50 MeV beam energy.

Footnotes and References

*Physics Dept. Duke University, Durham, NC 27706

†National Bureau of Standards, Gaithersburg ML 20899

Beta-Delayed Two-Proton Emission*

D.M. Moltz, J.E. Reiff, J.D. Robertson, T.F. Lang and J. Cerny

Beta-delayed particle emission has made the study of light proton rich nuclei much easier. In fact, as experiments have proceeded further from beta stability, detection of these decay modes has become the probe of choice. A recent review[1] of all proton rich light nuclei covered the advantages of utilizing beta-delayed particle emission to elicit relevant physics. However, as experiments proceed toward the proton drip-line, other decay modes (beta-delayed two-proton, proton and two-proton emission) are expected to dominate. Beta-delayed two-proton emission was discovered in the decay of ^{22}Al, an isotope first observed via its beta-delayed single proton decay channel.[2] Ground state proton emission has not been observed below A = 100 and ground state two-proton emission has never been observed.

After the initial discovery of beta-delayed two-proton emission, it was subsequently seen in the decay of ^{26}P[2] and utilized to discover the first $T_z = -5/2$ nuclide, ^{35}Ca.[3] This decay process may proceed via several mechanisms, but the two most probable mechanisms are sequential emission (dependent upon the intermediate nuclear state configuration in the first proton daughter) and ^2He emission (more dependent upon the properties of ^2He). Initial experiments probing the decay mechanism have succeeded only in limiting the ^2He admixture to <15% for ^{22}Al decay. ^{26}P decay to the ground state of ^{24}Mg must be sequential because of spin-parity limitations. Mechanism studies on $T_z = -5/2$ nuclides are made extremely difficult by the very small production cross sections; none have thus been performed.

Since the phenomenon of beta-delayed two-proton emission occurs only near the proton drip-line, production cross sections are necessarily small in traditional compound nucleus reactions. The production

rates of these nuclei can be significantly increased by utilizing projectile fragmentation reactions combined with a fragment separator. The existence of other stable $T_z = -5/2$ nuclides and the first known $T_z = -3$ nuclide (^{22}Si)[4] has been determined utilizing this technique. Subsequently, the beta-delayed single-proton emissions of ^{31}Ar and ^{27}S have been observed.[5] More recently, the beta-delayed two-proton emission of ^{31}Ar has been studied[6] by utilizing a fast rotating wheel technique (all prior studies were performed with the helium-jet technique). Beta-delayed two-proton emission has proven to be a powerful new spectroscopic tool. As can be seen in Fig. 1, many more light proton-rich nuclei should exhibit this decay mode. The study of these nuclei and the decay mode itself will require a large effort.

Footnotes and References

*Condensed from reports LBL-22998 and LBL-24035.

1. J. Äystö and J. Cerny, to be published in v. 8 of Treatise on Heavy Ion Science, D.A. Bromley, ed., (1987).

2. M.D. Cable *et al.*, Phys. Rev. C **30**, 1276 (1984).

3. J. Äystö *et al.*, Phys. Rev. Lett. **55**, 1384 (1985).

4. M. Langevin *et al.*, Nucl. Phys. **A455**, 149 (1986).

5. V. Borrel *et al.*, Orsay Report Number IPNODRE 87-18.

6. J.E. Reiff *et al.*, contribution to this report.

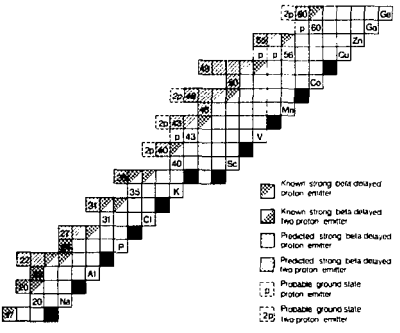

Fig. 1. Proton rich portion of the chart of the nuclides from Z = 10-32 depicting known and predicted beta-delayed and direct particle decaying nuclides.

XBL 8612-5973

The Beta-Delayed Two-Proton Decay of ^{31}Ar

J.E. Reiff, D.M. Moltz, J.D. Robertson, T.F. Lang, and J. Cerny

As experiment defines the proton drip line in the light nuclei, current interest centers on investigating those nuclides with $T_z = -5/2$. Four such nuclei with $Z \leq 20$ are predicted by the updated Kelson-Garvey charge symmetry approach[1,2] to be bound with respect to ground state proton emission: ^{23}Si, ^{27}S, ^{31}Ar, and ^{35}Ca. While ^{35}Ca was discovered via its beta-delayed two-proton emission,[3] the other three nuclides have been detected in fragmentation reactions using the LISE spectrometer at GANIL.[4] The beta-delayed proton decay of ^{31}Ar has also been observed at GANIL.[5] We wish to report the beta-delayed two-proton decay of ^{31}Ar.

^{31}Ar nuclei were produced by bombarding a 2 μg/cm^2 ZnS target on a 1.5 μg/cm^2 Al backing with a pulsed 135 MeV ^{3}He beam of 1–2 μA intensity from the 88-Inch Cyclotron. The ^{31}Ar recoils were stopped in one of twelve 500 μg/cm^2 Al foils on a variable speed rotating catcher wheel located behind the target. Both the wheel and the target were inclined at an angle of 20° with respect to the beam. The 12-inch diameter wheel, rotating at 130 RPM, transported the activity in front of two, two-element Si detector telescopes which straddled the wheel. The space between the beam and the telescopes corresponded to the distance traveled by the wheel in one half a pulse cycle. Data was acquired only when the beam was off. To minimize the long

term effect of radiation damage, the detectors were cooled to –40°C.

The two-proton sum coincidence spectrum collected during the bombardment of the ZnS target for 240 mC is shown in Fig. 1. The peaks are necessarily broad due to the kinematics and the large solid angle subtended by the detectors. The two ^{22}Al peaks at 4.4 MeV and 6.0 MeV show up very clearly. The group at ~7.6 MeV is assigned to the decay of ^{31}Ar. This decay energy is the highest expected from any of these $T_z = -5/2$ nuclides and is in close agreement with the predicted value of 7.8 MeV obtained by combining the mass of ^{31}Ar from the Kelson-Garvey mass formula and the mass of the isobaric analog state in ^{31}Cl predicted from the formula of Antony, Britt, and Pape.[6]

Footnotes and References

1. I. Kelson and G.T. Garvey, Phys. Lett. **23**, 689 (1966).

2. A.H. Wapstra and G. Audi, The 1983 Atomic Mass Table, Nucl. Phys. A **432**, 1 (1985).

3. J.Äystö, D.M. Moltz, X.J. Xu, J.E. Reiff, and J. Cerny, Phys. Rev. Lett. **55**, 1384 (1985).

4. M. Langevin, A.C. Mueller, D. Guillemand-Mueller, M.G. Saint-Laurent, R. Anne, M. Bernas, J. Galin, D. Guerreau, J.C. Jacmart, S.D. Hoath, F. Naulin, F.Pougheon, E. Quinious, and C. Détraz, Nucl. Phys. **A455**, 149 (1986).

5. V. Borrel, J.C. Jacmart, F. Pougheon, A. Richard, R. Anne, D. Bazin, H. Delagrange, C. Détraz, D. Guillemaud-Mueller, A.C. Mueller, E. Roeckl, M.G. Saint-Laurent, J.P. Dufour, F. Hubert, and M.S. Pravikoff, Institut de Physique Nucléaire Report Number IPNO DRE 87-18.

6. M.S. Antony, J. Britt, and A. Pape, At. Data Nucl. Data Tables, **34**, 279 (1986).

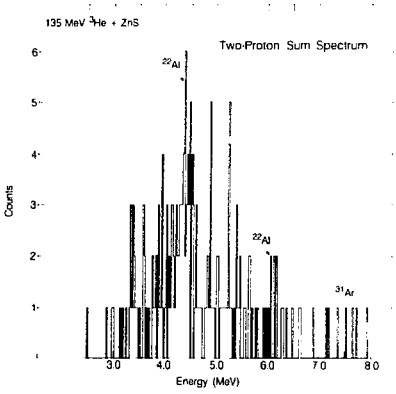

Fig. 1. Beta-delayed two-proton spectrum from the decay of ^{31}Ar. Also present are the beta-delayed two-proton sum peaks from the decay of ^{22}Al.

XBL 8712-8203

Projectile-Breakup and Transfer-Reemission Reactions in the ^{12}C+^{20}Ne System*

K. Siwek-Wilczynska,† J. Wilczynski,‡ C.R. Albiston, Y. Chan, E. Chavez,§ S.B. Gazes, H.R. Schmidt and R.G. Stokstad

The ^{12}C(^{20}Ne,α^{16}O$_{g.s.}$), ^{12}C(^{20}Ne,α^{20}Ne)^{8}Be$_{g.s.}$, and ^{12}C(^{20}Ne,α^{12}C)^{16}O* reactions at E(^{20}Ne)=157 MeV were studied by using position-sensitive telescopes. It was established that α-^{16}O coincidences in the first reaction result not only from sequential breakup of the projectile, but also from the transfer-reemission process ^{12}C(^{20}Ne,^{16}O$_{g.s.}$) ^{16}O* $\rightarrow \alpha +$ ^{12}C$_{g.s.}$. Distributions of the excitation energy in the primary reaction products were deduced by calculating respective branching ratios with a Hauser-Feshbach statistical-decay code. It was found that excitation energy is generated in mass transfer reac-

tions quite asymmetrically: it is mostly concentrated in the nucleus that acquires mass, while the "donor" nucleus, on the average, remains cold. These results clearly support the basic concept "spectator" models of heavy-ion reactions.

*Condensed from Phys. Rev. C **35**, 1316 (1987).

†Permanent address: Institute of Experimental Physics, Warsaw University, 00-681 Warsaw, Poland

‡Permanent address: Institute for Nuclear Studies, 05-400 Swierk/Warsaw, Poland

§Permanent address: Instituto de Física, Universidad Nacional Autónoma de México, .México, DF.

^{12}C Decay of ^{24}Mg Following Nuclear Inelastic Scattering*

J. Wilczynski,† K. Siwek-Wilczynska,† Y. Chan, E. Chavez,§ S.B. Gazes, and R.G. Stokstad

The decay of ^{24}Mg into two ground-state ^{12}C nuclei following inelastic scattering of 15 MeV/nucleon ^{24}Mg by a ^{12}C target was studied. Three states at excitation energies in ^{24}Mg of 21.9, 23.6 and 24.8 MeV were observed. Their spins, J^{π}=2 and most likely, 0^+ (2^+) and 0^+, respectively, have been inferred from the ^{12}C-^{12}C angular correlations.

*Condensed from Phys. Lett. **B181**, 229 (1986).

†Permanent address: Institute for Nuclear Studies, PL-05-400 Swierk/Warsaw, Poland

‡Permanent address: Institute of Experimental Physics, Warsaw University, PL-00-681 Warsaw, Poland

§Permanent address: Instituto de Física UNAM, A.P. 20364, México, D.F., 0100 México

Neutron Pickup and Four-body Processes in Reactions of ^{16}O+^{197}Au at 26.5 and 32.5 MeV/nucleon*

*S.B. Gazes,† Y.D. Chan, E. Chavez,‡ A. Dacal,‡ M.E. Ortiz,‡ K. Siwek-Wilczynska,§ J. Wilczynski,** and R.G. Stokstad*

Projectile breakup in reactions of 424 MeV and 520 MeV ^{16}O + ^{197}Au was studied via coincidence measurements of projectile-like fragments and light particles. The quasi-elastic breakup of the projectile showed features consistent with a sequential-decay mechanism. Significantly, the Q_3 spectrum for the $^{12}C - \alpha$ channel was found to have important contributions from four-body final states. The bombarding-energy dependence and particle-particle correlations of this latter component indicate a process whereby the projectile picks up a neutron and subsequently decays by successive neutron and charged-particle emission. This process shows a yield comparable to the quasi-elastic part of the $^{12}C - \alpha$ channel and points to an important mechanism for multi-fragmentation of the projectile in intermediate-energy heavy-ion reactions.

Footnotes and References

*To be submitted to Physics Letters.

†Present address: Department of Physics, University of Rochester, Rochester, NY 14627

‡Permanent address: Instituto de Física, UNAM, 01000 DF México

§Permanent address: Institute of Experimental Physics, Warsaw University 00-681

**Permanent address: Institute for Nuclear Studies, 05-400 Swierk-Otwock, Poland

Energetic Particle Emission and Linear Momentum Transfer in Central Collisions Induced by 32.5 MeV/nucleon $^{16}O+ {}^{238}U$, ^{197}Au*

Y. Chan, E. Chavez, A. Dacal, S.B. Gazes, A. Harmon, M.E. Ortiz E. Plagnol, J. Pouliot, R.G. Stokstad

An experiment has been performed to study the relative importance of the nucleonic degrees of freedom versus the effective nucleus-nucleus interaction in incomplete-fusion processes induced by 32.5 MeV/nucleon ^{16}O beam on heavy targets.

Kinematic properties of the emitted energetic fragments were measured with phoswich detectors. Their correlation with fusion-like products, such as the linear momentum transferred to the target nucleus (LMT), was deduced from the fission fragment folding angle using multi-wire proportional counters.

The most probable LMT was found to be only about 75% of the beam for both the ^{238}U and ^{197}Au targets. The correlation between the energetic fragment species (Z_{FRAG}) and the fission opening angle Θ_{12} is shown in Fig. 1. There are three regions of interest :

(A) Binary transfer, the strongly correlated region (Z=5,6,7).

(B) Preequilibrium emission and/or massive transfer (Z=1,2 fragments).

(C) Mutual projectile and target excitation, fission accompanied by sequential-breakup. The small LMT implies that both projectile remnants escape from the target field.

Generally speaking, the binary massive transfer mechanism appears to be able to account for many of the observed features of the reaction. Even though there are indications that a higher fast particle multiplicity is required to account for the missing momentum in case of large LMT, favoring the interpretation of prompt nucleon emission, the observed experimental proton spectra are softer than those predicted by preequilibrium emission models. All these probably imply that collisions in this energy domain is dominated by nuclear mean field dynamics.

Footnotes and References

*Condensed from LBL report LBL-23381

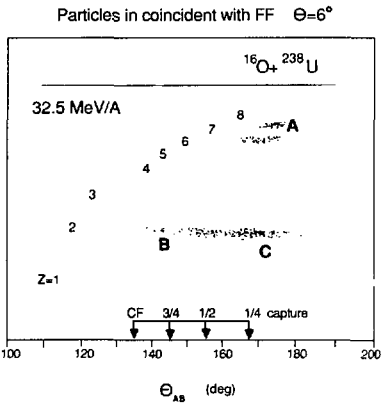

Fig. 1. Correlation between the Z of the detected energetic fragment and fission fragment folding angles.

XBL 8712-5137

The Beta Decay Asymmetry Parameter for ^{35}Ar: An Anomaly Resolved*

J.D. Garnett,† E.D. Commins,† K.T. Lesko, and E.B. Norman

The observed[1] beta decay asymmetry in the decay of polarized ^{35}Ar has led to a persistent puzzle in weak interaction physics. If the experimental value of the ground-state ⇒ ground-state asymmetry, λ_0, is taken, the value of the Cabibbo angle deduced for ^{35}Ar decay is consistent with zero. This disagrees with the value of $\Theta_c = 0.23\pm0.01$ radians obtained from other nuclear and particle decay experiments. We have completed our reinvestigation of the beta decay asymmetry of ^{35}Ar. Analysis of these data yield a value of $A_0=0.49\pm0.10$ which leads to a value for the quark mixing angle $\Theta_c=0.28\pm0.08$ rad in agreement with the accepted value of 0.23 ± 0.01 and in strong disagreement with the anomalous result.[1]

Footnotes and References

*Condensed from Phys. Rev. Lett. **60**, 499 (1988).

†Physics Department, University of California, Berkeley, CA 94720

1. F.P. Calaprice, E.D. Commins, and D.A. Dobson, Phys. Rev. **137**, B1453 (1965).

Measurements of Cross Sections Relevant to γ-ray Line Astronomy*

K.T. Lesko, E.B. Norman, R.-M. Larimer, S. Kuhn, D.M. Meekhof, S.G. Crane, and H.G. Bussell

To interpret spectra obtained from the expanding field of γ-ray line astronomy, cross sections for the production of nuclear γ-rays must be known. The recent discovery of jets of matter moving at nearly relativistic velocities in SS-443 has increased the realm of energies which needs to be considered in γ-ray production sites to much higher values.

To this end we have measured γ-ray production cross sections for the γ-ray lines which are most strongly excited in the proton bombardments of C, N, O, Mg, Al, Si, and Fe targets of natural isotopic composition. High resolution germanium detectors were used to collect γ-ray spectra at proton bombarding energies of 8.9, 20, 30, 33, 40 and 50 MeV. The analysis of this work has been completed and it has been submitted to Physical Review C.

The bombardments at 33 MeV were chosen to correspond with the center of mass energy of the jets in SS-433. We have also bombarded a sample of meteorite to more closely simulate actual γ-rays production in extraterrestrial sites. These measurements of particular interest to astrophysics are nearing completion and will be submitted to Astrophysical Journal.

Footnotes and References

*Condensed from Phys. Rev. C 37, 1808 (1988).

The s-Process Branch at ^{148}Pm*

E.B. Norman, K.T. Lesko, S.G. Crane, R.-M. Larimer, R.M. Diamond, F.S. Stephens, M.A. Deleplanque, J.C. Bacelar, E.M. Beck, and A.E. Champagne†

We have continued our studies of the level scheme of ^{148}Pm in order to exploit the s-process branching that occurs at this nucleus to determine the s-process neutron density. Using the Princeton University cyclotron and Q3D spectrograph, we have employed the ^{149}Sm(d,^{3}He) reaction to determine the energies of approximately 25 excited states in ^{148}Pm.

At LBL we have studied the γ-ray transitions in

^{148}Pm using the ^{148}Nd(p,n) reaction. Gamma-ray singles and $\gamma-\gamma$ coincidence data have been acquired with the High Energy Resolution Array. We are in the process of analyzing these data to develop a partial level scheme. In particular we are seeking a low lying level ($\leq$1 MeV excitation energy) which decays to both the ground state and the long lived isomeric state at 137.2 keV excitation. We have identified several levels under 600 keV which appear, in the preliminary analysis, to decay to both states.

The existence of these levels will assure that the ground state ($t_{1/2}$ = 5.37 d) and isomer ($t_{1/2}$= 41.3 d) will be in thermal equilibrium at temperatures $\geq 1 \times 10^9$K. This equilibration will raise neutron density estimates by a factor of 3 over those calculated for these environments assuming that equilibrium is not achieved. Further analysis of these data is underway.

Footnotes and References

*Condensed from Phys Rev. C. **37**, 860 (1988).

†*Physics Department, Princeton University, Princeton NJ 08544*

Search for Supermassive Cahn-Glashow Particles in Lead

E.B. Norman, K.T. Lesko, R.M. Larimer, R.B. Chadwick, and D.C. Hoffman

It has been suggested that massive long-lived, negatively-charged elementary particles (X^-) may have been produced in the Big Bang and have survived to the present day in concentrations small enough to have escaped detection.[1] As a result of nucleosynthesis in stars, such particles may be concentrated in certain elements such as lead. A radiochemical search has been made for X^- particles in lead by utilizing the fact that a PbX^- bound state system would have essentially the nuclear properties of lead but the chemical properties of thallium. We have looked for evidence of PbX^- by searching for gamma rays emitted following the beta decay of $^{206}BiX^-$ produced by $^{nat}PbX^-$(p,yn) reactions. Preliminary analysis of the measured gamma spectra allows an upper limit to be placed on the possible concentration of X^- particles in lead of $< 1 \times 10^{-11}$ per nucleon.

Footnotes and References

R.N. Cahn and S.L. Glashow, Science **213**, 607 (1981).

Gamma-Ray Transitions in ^{180}Ta

E.B. Norman, K.T. Lesko, R.M. Larimer, R.M. Diamond, F.S. Stephens, M.A. Deleplanque, J.C. Bacelar, and E.M. Beck

As described in last year's annual report, we are studying the question of whether $^{180}Ta^m$ can survive in the high-temperature environments found in stars in which the s- and r-process nucleosynthesis occurs. To answer this question, the positions and gamma-ray decay properties of levels in ^{180}Ta below about 1 MeV must be known. While there are about 50 such levels now known, there is no published data on any gamma-ray transitions. We are continuing our analysis of the data taken with the High Energy Resolution Array. So far, a large number of gamma rays have been placed into two major families--those which ultimately feed $^{180}Ta^g$ and those which ultimately feed $^{180}Ta^m$. No "cross over" transition has yet been found, but many observed gamma rays have yet to be placed in the level scheme.

Cosmic-Ray Lifetime of ^{56}Ni*

E.B. Norman, K.T. Lesko, R.M. Larimer, and E. Horch

A major product of charged-particle induced nucleosynthesis in stars is the doubly-magic nucleus ^{56}Ni. In the laboratory, this isotope decays via electron capture with a half-life of 6.1 days. In the absence of atomic electrons, however, ^{56}Ni would be stable were it not for the possibility of beta-plus decay. The most likely beta-plus decay branch is that to the $J^{\pi} = 3^{+}$ level at 158 keV in ^{56}Co, and the partial half-life for this branch has been estimated to be $(0.1\text{–}6) \times 10^{6}$ years.[1]

Soon after the supernova explosion that produces the ^{56}Ni takes place, temperatures are low enough that electrons are bound to nuclei and neutral atoms can exist. Thus, the half-life of ^{56}Ni would be its laboratory value. However, it is thought that supernovae may be sites of cosmic-ray production and acceleration. If ^{56}Ni produced in such explosions were accelerated to high energies then it would be quickly stripped of its electrons. Thus, the cosmic-ray lifetime of ^{56}Ni would be determined by its beta-plus decay half-life. Future observations of ^{56}Ni in the cosmic rays could be used to determine the time interval between nucleosynthesis and cosmic-ray acceleration if this half-life were known.

We plan to measure the beta-plus decay lifetime of ^{56}Ni using a four-fold coincidence technique. ^{56}Ni is produced by bombarding iron foils with a beam of ^{3}He ions provided by LBL's 88-Inch Cyclotron, and is then chemically separated from the target. To detect ^{56}Ni beta-plus decay, the activity is placed at the center of a large sodium iodide annular detector that is split into two optically isolated halves. Located inside the annulus on one side of the source is a germanium gamma-ray detector, and on the other side of the source is a silicon surface-barrier detector. This system is being used to search for events in which a positron is detected in the silicon detector, a 511-keV annihilation gamma ray is recorded in each half of the annulus, and a 158-keV gamma ray is recorded in the germanium detector. In a series of preliminary tests of this scheme, a large number of such four-fold coincident events have been observed. If these were naively assumed to be due to the sought-for decay, the inferred branching ratio would be on the order of 10^{-3} which is much greater than the expected value of 10^{-7} to 10^{-6}. The origin of these events is now being investigated.

Footnotes and References

*Condensed from LBL-23037.

1. L. Wilson, LBL-7723

Cosmic-Ray Lifetime of ^{54}Mn*

E.B. Norman, K.T. Lesko, R.M. Larimer, and E. Horch

Measurements of the elemental and isotopic composition and energy spectra of the cosmic-ray nuclei just below iron have indicated the presence of the radioactive nucleus ^{54}Mn in the cosmic rays.[1] In the laboratory, ^{54}Mn decays via electron capture with a half-life of 312 days. As a high-energy cosmic ray, ^{54}Mn would be stripped of its atomic electrons through interactions with the interstellar medium. Thus cosmic-ray ^{54}Mn would be stable were it not for the possibility of both beta-minus and beta-plus decay. Such decays are energetically allowed, although hindered because of the large spin changes required. The most likely decay of a bare ^{54}Mn nucleus is the beta-minus decay to the ground state of ^{54}Fe, and the partial half-life for this branch has been estimated to be $(0.06\text{–}10) \times 10^{6}$ years.[2] The measured fluxes of cosmic-ray ^{54}Mn could be used to determine the mean age of cosmic-ray secondary nuclei if this half-life were known.

We have recently begun a project to measure the

beta-minus decay lifetime of ^{54}Mn. A source of ^{54}Mn is mounted in close geometry to a silicon surface-barrier detector telescope. This assembly is then placed at the center of a large annular sodium iodide detector. The well of the annulus is then filled with two sidecap sodium iodide detectors. Searches are then made for events in the silicon detector telescope that are in anticoincidence with signals in the sodium iodide array. Such events will include the sought-for beta-minus particles. In a series of preliminary experiments of this kind, we found that electrons produced by the 2.5×10^{-3} internal conversion decay branch of ^{54}Mn are a problem for our measurement. Such electrons can backscatter off the silicon detectors and thus deposit only a fraction of their total energy. This produces a large background that a present hides the sought-for beta particles. However, from analysis of the data taken thus far, we can set an upper limit on the beta-minus decay branching ratio of ^{54}Mn of 5×10^{-4}. Further improvements of our system will soon be made in order for the beta-minus decay lifetime of ^{54}Mn to be measured.

Footnotes and References

*Condensed from LBL-23037.

1. G. Tarlé *et al.*, Astrophys. J. **230**, 607 (1979).

2. L. Wilson, LBL-7723

Observations of Chernobyl Fallout in Imported Food Products

E.B. Norman and B.G. Harvey

Prompted by reports of Chernobyl fallout still appearing in European food products, we have conducted a small scale survey of imported foods currently available on the shelves of local stores. We have used a 109 cm^3 high-purity germanium detector shielded with 10 cm of lead to count approximately 50 different food products from 21 different European countries. In approximately one third of the samples counted, we find evidence of ^{134}Cs and ^{137}Cs activities. These two long-lived isotopes are responsible for essentially all of the remaining contamination from Chernobyl. We also counted 5 American food products with null results. Examples of the spectra obtained are shown in Fig. 1. The ratio of these two Cs activities, when corrected for the time since the reactor accident, agrees well with the value measured in the prompt fallout material in Europe. This indicates that the source of the ^{134,137}Cs that we now observe was in fact the Chernobyl reactor accident. The combined ^{134,137}Cs activities we observe range from 0.1 to 5 pico-Curies per gram which are well below the ceiling of 10 pico-Curies per gram set by the U.S. Department of Agriculture. Nevertheless, it is interesting to see that the effects of this tragic accident are still with us.

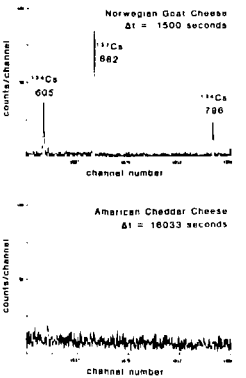

Fig. 1. Top panel shows a portion of the gamma-ray spectrum observed from 25 minutes counting a 104-gram sample of Norwegian goat cheese. Lower panel shows the same region of the spectrum observed form 267 minutes counting a 198 gram sample of American cheddar cheese. XBL-8711-4615

Superdeformed Band at High Spin in Z = 66 and 68 Isotopes*

M. J. A. deVoigt,† J.C. Bacelar,† E.M. Beck,‡ M.A. Deleplanque, R.M. Diamond, J.E. Draper,§ H.J. Riezebos,† and F.S. Stephens

The nucleus ^{152}Dy, with sharp superdeformed (SD) ridges above 800 keV in the γ-γ energy correlation matrix, stands out from three neighboring nuclei which exhibit less pronounced structures. A valley appears in ^{150}Dy, but little ridge, while ^{154}Er shows a ridge and little valley at the higher transition energies. Neither feature, is apparent in the matrix for ^{156}Er. In ^{152}Dy, as made by us with ^{40}Ar on ^{116}Cd, the ridges are composed mainly of unresolved (excited) SD bands, and not just the discrete band discovered at Daresbury with the reaction ^{48}Ca+^{106}Pd. The moment of inertia, however, determined from the ridge separation, $J^{(2)} = 85 \pm 4$ MeV^{-1} $\hbar^2$, is the same, and the discrete band can be observed by summing the spectra obtained from double gates on that band. By comparing the intensities of the double-gated spectra corresponding to different ridges with the corresponding number of combinations possible, we obtained the first unambiguous evidence that there is little or no decay out of the discrete SD band over a spin region of $\sim 35\hbar$, down to the state fed by the 602 keV transition.

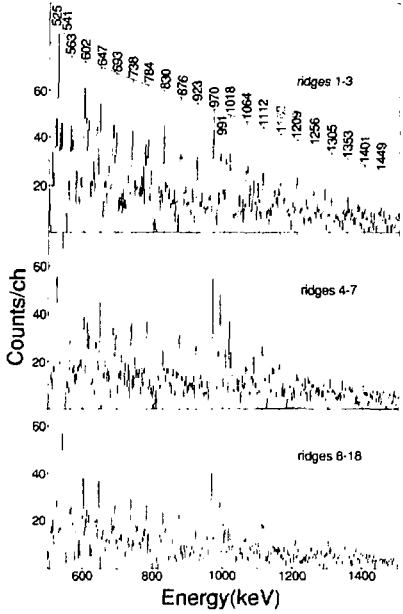

Fig. 1. Comparison of spectra of the third γ-ray in coincidence with all possible combinations of two SD discrete-line transitions. The upper spectrum is a sum of combinations within the first three ridges (gates on any two consecutive transitions, or on those separated by one or two other transitions). The middle spectrum represents the sum of the 4th to the 7th ridges, and the lower one the sum of the 8th to 18th ridges. The three spectra are normalized in intensity to the number of possible double-gate combinations. A background has been subtracted by using the full projection of the total (ungated) matrix.

XBL 8610-4174

Footnotes and References

*Condensed from Phys. Rev. Lett. **59**, 270 (1987).

†K.V.I., Rijksuniversiteit, NL-9747 AA Groningen, The Netherlands

‡Institut f. Strahlen- u. Kernphysik, University of Bonn D-5300 Bonn, Federal Republic of Germany

§University of California, Davis, California 95616

New Structures at High Spin in ^{159}Er*

M.A. Deleplanque, J.C. Bacelar, E.M. Beck, R.M. Diamond, J.E. Draper, R.J. McDonald, and F.S. Stephens

The ^{159}Er nucleus is located in a "critical" region of nuclei between less collective ones (like ^{158}Er) which have terminating bands, and the heavier (like ^{164}Er) more collective ones. In these "intermediate" nuclei, it is possible that the orbital in which the odd nucleon is located influences the shape evolution of the nucleus at high spins.

The nucleus ^{159}Er was produced in the reaction ^{124}Sn (^{40}Ar,5n) at 180 MeV at the 88-Inch Cyclotron. Three bands were extended to higher spins, and three new bands were found (see Fig. 1). We observe a rich variety of behaviors at high spins in this nucleus. There are indications that the yrast ("A") band is terminating (i.e., becomes oblate shaped), whereas the "E" (probably originating from the 3/2[521] $h_{9/2}$ Nilsson orbital, signature +1/2) band seems to remain more collective (triaxial) and makes use of the high-j orbitals in the next empty shell to generate angular momentum. The "F" (same as E, signature −1/2) band also probably remains collective at the same frequencies as the "E" band but does not backbend (yet), probably because it retains its prolate shape. Finally, we begin to see higher-K bands (the band with cascade and cross-over transitions in Fig. 1) as in heavier (more collective and prolate) nuclei. Our results indicate that the individual orbitals (and in particular the odd neutron) influence rather strongly the shape and collectivity of this "transitional" nucleus.

Footnotes and References

*Condensed from Phys. Lett. **193B**, 422 (1987)

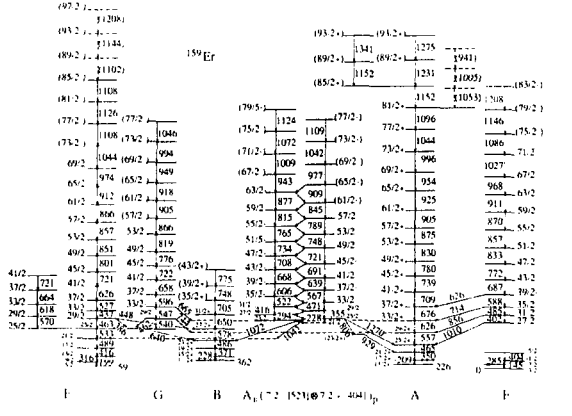

Fig. 1. Level scheme of ^{159}Er. For clarity, the (known) Δl=1 transitions between E and F, and between A and B are not shown.

XBL 871-145

Superdeformed Band in ^{135}Nd*

E.M. Beck,† F.S. Stephens, J.C. Bacelar, M.A. Deleplanque, R.M. Diamond, J.E. Draper,‡ C. Duyar,‡ and R.J. McDonald

A superdeformed (SD) band (β=0.4-0.5) was found in ^{135}Nd, the first one in an odd-mass nucleus. It consists of 13 transitions with an average moment of inertia $\Im^{(2)} \approx 59\hbar^2$ MeV^{-1}, and gathers at its bottom ~10% of the reaction events leading to ^{135}Nd. Of the 3 known SD bands (^{132}Ce, ^{152}Dy, ^{135}Nd), it is the most strongly populated and the one observed to the lowest spins. This band in ^{135}Nd has a $\Im^{(2)}$ similar to that in ^{132}Ce, i.e., smaller than a value corresponding to a 2:1 axial ratio.

Footnotes and References

*Condensed from Phys. Rev. Lett. 58, 2182 (1987).

†Institut f. Str ien- u. Kernphysik, University of Bonn, D-5300 Bonn, Federal Republic of Germany

‡University of California, Davis, California 95616

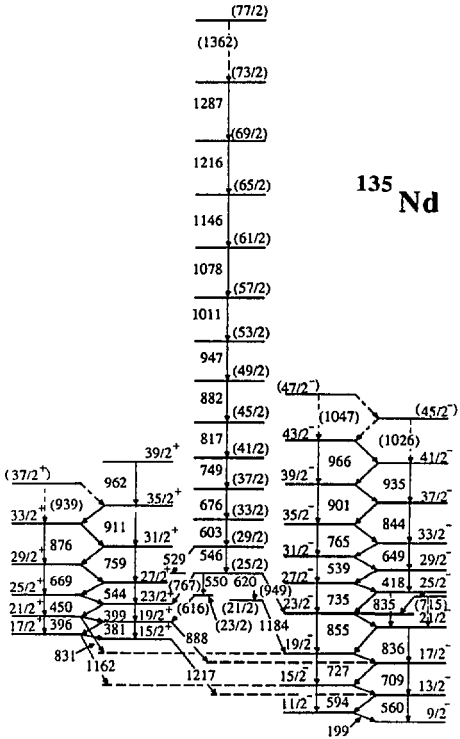

Fig. 1. Level scheme of ^{135}Nd from the present work. Transition energies are given in keV. XBL 8612-5058

Superdeformed Bands in Nd Nuclei*

E.M. Beck,† R.J. McDonald, A.O. Macchiavelli, J. C Bacelar,‡ M.A. Deleplanque, R.M. Diamond, J.E. Draper,§ and F.S. Stephens

Superdeformed bands were found in ^{134,136}Nd. Their dynamic moments of inertia are about as large as those of the previously known bands in ^{132}Ce and ^{135}Nd, corresponding to $\beta \sim 0.5$. A high probability for staying in the band is determined for the discrete members of the bands in ^{134,136}Nd, in contrast to the unresolved members of the superdeformed bands in the ridges of the two-dimensional (continuum) arrays.

Footnotes and References

*Condensed from Phys. Lett. **B195**, 531 (1987).

†Institut f. Strahlen- u. Kernphysik, University of Bonn, D-5300 Bonn, Federal Republic of Germany

‡K.V.I. Rijksuniversiteit, 9747 AA Groningen, The Netherlands

§University of California, Davis, California 95616

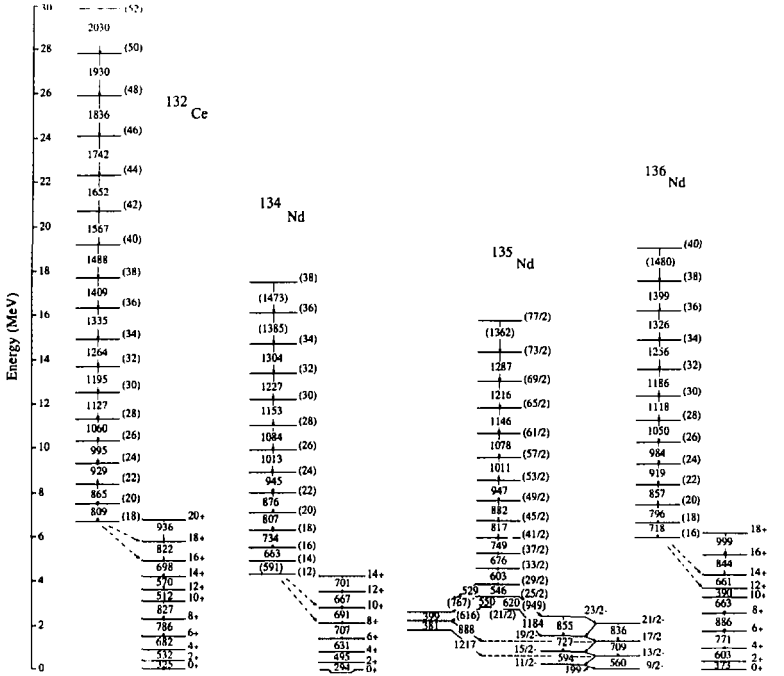

Fig. 1. Superdeformed bands and some yrast transitions in ^{132}Ce, ^{134}Nd, ^{135}Nd and ^{136}Nd. The dashed arrows indicate unobserved linking transitions. XBL 873-700

High-Spin Spectroscopy of ^{168}Hf*

E.M. Beck,† M.A. Deleplanque, R.M. Diamond, R.J. McDonald, F.S. Stephens, J.C. Bacelar,† and J.E. Draper§

The nucleus ^{168}Hf was studied up to spin 38^+ in the yrast band and to spins 41^- and 38^- in the lowest two negative-parity bands. The onset of a proton alignment, $h_{9/2}$ or $i_{13/2}$, was observed in these bands for the highest transitions, ending a region of remarkably constant moment of inertia. A new band with even spins and negative parity was found, and the interaction strength between the ground-state band and the AB band was measured.

Footnotes and References

*Condensed from Z. Phys. **A327**, 397 (1987).

†Institut f. Strahlen- u. Kernphysik, University of Bonn, D-5300 Bonn, Federal Republic of Germany

‡K.V.I., Rijksuniversiteit, NL-9747 AA Groningen, The Netherlands

§University of California, Davis, California 95616

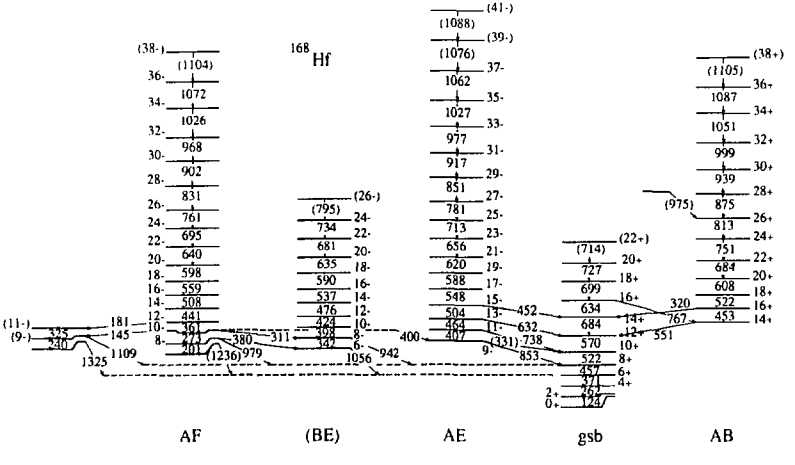

Fig. 1. Level scheme of ^{168}Hf as obtained in the present work. Bands are identified by their configuration at low spins. XBL 873-884

Search for Entrance-Channel Effects in the Production of Superdeformed Nuclei*

A.O. Macchiavelli,† M.A. Deleplanque, R.M. Diamond, R.J. McDonald, F.S. Stephens, and J.E. Draper‡

In order to look for the influence of the entrance channel in the feeding of the Superdeformed band (SD) in ^{152}Dy we have studied the nearly symmetric reaction ^{74}Ge+^{82}Se→ ^{152}Dy+4n and compared it with the two other reactions that have produced this SD band with different projectile target combinations.[1,2] The ^{74}Ge beam was provided by the SuperHILAC accelerator at an energy of 4.6 MeV/nucleon. Fourteen Compton-Suppressed Ge detectors from the HERA array were used.

The yields of the SD band from this reaction and those from the other two previously published are shown in Table I. We conclude from our results that there is no evidence for entrance-channel effects in the yields of these three reactions. It appears that all yields can be explained by the expected maximum angular momentum for fusion ℓ_{max} and excitation energy E* at which the compound nucleus is formed. The lower yield for the ^{40}Ar reaction is due to insufficient angular momentum (and/or too high E*) and the similar yield for the ^{48}Ca and ^{74}Ge reactions results from the similar (lower) excitation energies and ℓ_{max} at (or above) the fission limit.

Footnotes and References

*Condensed from Phys. Rev. **C36** (1987).

†Permanent Address C.N.E.A. Buenos Aires, Argentina

‡Permanent Address University of California, Davis

1. P.J. Twin *et al.*, Phys. Rev. Lett. **57**, 811 (1986).

2. M.J.A. de Voigt *et al.*, Phys. Rev. Lett. **59**, 270 (1987).

Table I

SD band intensities in ^{152}Dy; excitation energies E* and maximum angular momentum from the Bass Model for the compound nucleus.

Reaction	E_{lab}	E*	ℓ_{max}	I_{SD}	I_{Ridge}
	MeV		$\hbar$	%	
^{40}Ca + ^{108}Pd	200	75.5	70	~2	~2
^{40}Ar + ^{116}Cd	173	75.4	60	~0.5	~5±2
^{74}Ge + ^{82}Se	299	76.6	75	2.0±0.4	6±3

Three-Photon Correlations in Rotational Nuclei*

F.S. Stephens, J.C. Bacelar,† E.M. Beck,‡ M.A. Deleplanque, R.M. Diamond, and J.E. Draper§

Warm nuclei (0.2<T<0.7 MeV) with high spins are produced following the evaporation of particles in heavy-ion fusion reactions. The subsequent gamma-ray decay initially follows so many pathways that the spectrum cannot be resolved. However, the rotational behavior can still be studied through the average gamma-ray properties. Thus, studies of the average lifetimes, directional correlations, and correlations of gamma-ray energy with spin, have shown rather convincingly that the behavior is rotational. However more detailed studies[1,2] found that the correlations between the gamma-ray energies are much weaker than expected for good rotational behavior, leading to the suggestion of some damping.[3] More recently[4,5] attempts have begun to characterize the damping in greater detail. The present work represents a step in this direction, where we examine the correlations between three gamma-ray energies at high resolution. The first result seems to be a rather clear indication that the main damping widths are larger than was first thought,[1,2] in better agreement with other types of recent studies.[4,5] The full

spectrum appears to be a mixture of these rather strongly damped cascades and some essentially undamped ones.

Footnotes and References

*Condensed from Phys. Rev. Lett. **58**, 2186 (1987).

†Permanent address: Kernfysisch Versneller Instituut, Rijksuniversiteit, 9747 AA Groningen, The Netherlands

‡Present address: Institut f. Strahlen- u. Kernphysik, University of Bonn, D5300 Bonn, West Germany

§Permanent address: University of California, Davis, CA 95616.

1. J.E. Draper *et al.*, Phys. Rev. Lett. **56**, 309 (1986).

2. J.C. Bacelar *et al.*, Phys. Rev. Lett. **55**, 1858 (1985).

3. B. Lauritzen *et al.*, Nucl. Phys. **A457**, 61 (1986).

4. F.S. Stephens *et al.*, Phys. Rev. Lett. **57**, 2912 (1986).

5. F.S. Stephens *et al.*, to be published.

Absolute Electron Capture, Positron, and β-delayed Proton Branching Ratios

R.B. Firestone, J.M. Nitschke, P.A. Wilmarth, and K. Vierinen

As part of the decay studies at the SuperHILAC with the OASIS on-line mass separator facility we have determined absolute decay branching ratios. These ratios are important for interpreting the decay schemes of nuclei far from stability where substantial γ-ray intensity is too weak to observe. Electron capture branchings are determined from measured absolute K_α and K_β x-ray intensities, corrected for internal conversion, fluorescence yield, and the theoretical K/total ratio. Positron branchings are determined from the 511.0-keV annihilation intensity which is analyzed into components by half-life or by a multilinear analysis of the form

$$I_{\beta^+}(tot) = I_{\beta^+}(1)I_\gamma(1) + I^+_\beta(2)I_\gamma(2) + \ldots + I_\beta(i)I_\gamma(i)$$

where $I_\beta(i)$ and $I_\gamma(i)$ are the positron intensity and the intensity of a specific γ ray associated with an isotope. The absolute intensity of β-delayed protons are measured directly in an E-ΔE detector telescope and if more than one proton emitter is present, the intensity is divided by half-life. A summary of absolute branching ratios is given in the following table.

Table I:

Absolute Decay Branching Ratios Determined with OASIS

Isotope	$\%\epsilon$	$\%\beta^+$	$(\epsilon+\beta^+)p$
^{142}Pm	77±3	23±3	
^{142}Sm	<5	>95	
^{142}Eu	90±2	10±2	
^{142}Gd	48±5	52±5	
^{142}Tb	96.8±0.4	3.2±0.4	$\sim 3\times10^{-5}$
^{142}Dy	90±4	10±4	$(8\pm4)\times10^{-3}$
^{149g}Ho	57±19	43±19	
^{149m}Ho	60±6	40±6	
^{149g}Er	-	-	0.11±0.03
^{149m}Er†	44±4	53±4	$(1.5\pm0.3)\times10^{-3}$
^{149}Tm	~60	~40	$\sim 6\times10^{-4}$

†^{149m}Er also decays by a 3.0±0.3% IT decay branch

Decay of $^{149}Er^{g+m}$ by Positron Emission, Electron Capture, and Delayed Proton Decay

R.B. Firestone, J.M. Nitschke, P.A. Wilmarth, K. Vierinen, J. Gilat, and K.S. Toth†*

In this study the decay of $^{149}Er^{g+m}$ by positron emission, electron capture, and β-delayed proton emission was investigated. γ rays associated with $^{149}Er^{m}$ decay were placed in a decay scheme on the basis of $\gamma\gamma$- and xγ-coincidence information and half-life. We assigned 123 γ rays deexciting 87 levels in ^{149}Ho from 8.9±0.2 sec $^{149}Er^{m}$ decay. A 3.0±0.3% IT decay branch and a 0.15±0.03% β-delayed proton decay branch were assigned to $^{149}Er^{m}$ decay. 3 γ rays could be associated with $^{149}Er^{g}$ decay and an 11±3% β-delayed proton decay branch was measured. $(Q_\epsilon - S_p) = 7.0^{+0.5}_{-0.4}$ MeV for $^{149}Er^{g}$ decay and $S_p = 1.4^{+1.0}_{-0.6}$ for ^{149}Ho were determined from measured ϵ/β^+ ratios. The β-delayed proton spectrum from $^{149}Er^{g}$ consisted of a highly structured component corresponding to levels between 4–5 MeV in ^{149}Ho and a structureless component corresponding to levels at higher excitations. The β-strength function for $^{149}Er^{g+m}$ decay can be explained in terms of simple single-particle shell model structures, weak coupling to the ^{148}Dy core, and decay across the shell closure to the $\nu h_{9/2}$ orbital.

Footnotes and References

*Soreq Nuclear Research Center, Yavne 70600, Israel

†Oak Ridge National Laboratory, Oak Ridge, Tennessee 37831

Determination of Q_ϵ for $^{149}Er^{g+m}$ Decay

R.B. Firestone, J.M. Nitschke, P.A. Wilmarth, and K. Vierinen

The decays of $^{149}Er^{g+m}$ were investigated at the SuperHILAC with the OASIS on-line mass separator facility and are described in another report. The Q_ϵ values for these decays have been determined in two ways. From the intensity of x-rays and annihilation in coincidence with the 4699.6-keV transition, assuming negligible feeding from higher-lying levels, we determine that ϵ/β^+=0.68±0.34 to the 4.7-MeV level deexcited by that transition. This corresponds to $Q_\epsilon = 4.4^{+0.9}_{-0.4}$ MeV to the 4.7-MeV level implying $Q_\epsilon = 9.1^{+0.9}_{-0.4}$ MeV. The value of $(Q_\epsilon - S_p)$ can be calculated from the ratio of intensities in the total and positron- coincident proton spectra. This ratio is proportional to $\epsilon + \beta^+/\beta^+$. The 2688-, 2890-, 3138-, and 3947-keV proton groups were analyzed by a χ^2 analysis where $\chi^2 = \sum_i \frac{(aR_{exp}-R_{th})^2}{\Delta R^2_{exp}}$ where R_{exp} and R_{th} are the experimental and theoretical $\epsilon + \beta^+/\beta^+$ ratios for each proton group and a is the absolute efficiency for positron detection. For various values of $(Q_\epsilon - S_p)$, a is a free parameter chosen to minimize χ^2_i. The χ^2 minimization of the decay energy is shown in Fig. 1 where we determine that $(Q_\epsilon - S_p) = 7.0^{+0.5}_{-0.4}$ MeV. From Wapstra *et al.*[1] systematics, $S_p = 1.17$±0.21 MeV implying $Q_\epsilon = 8.2$±0.5 MeV. This value can be reconciled with the first value if we assume that the protons are associated with $^{149}Er^{g}$ decay and the 4699.6-keV γ-ray with $^{149}Er^{m}$ decay. From these two measurements and the $^{149}Er^{m}$ excitation energy of 0.74 MeV we determine that $S_p = 1.4^{0.6}_{1.0}$ MeV which is consistent with the value from systematics. We have adopted the systematic value for $Q_\epsilon - S_p$ and we assume that Q_ϵ=8.2 MeV.

1. $Q_\epsilon - S_p$ for ^{149g}Er decay. XBL 8711-4999

Decay of Neutron Deficient Eu, Sm and Pm Isotopes Near the Proton Drip Line

K. Vierinen, J.M. Nitschke, P.A. Wilmarth, R.B. Firestone, and J. Gilat†*

The radioactive decays of $^{134-136}$Eu, $^{134-136}$Sm, $^{134-136}$Pm and ^{135}Nd were studied *via* β-delayed proton and γ-ray emission. The measurements were performed at the OASIS on-line mass separator with heavy-ion beams from the SuperHILAC. The compound nucleus reactions were ^{92}Mo(^{46}Ti,xpyn) with bombarding energies in the range of E = 192–212 MeV. On-line mass separation and x-ray coincidences were used for isotope identification. In Fig. 1 Pm and Nd K x-ray coincident γ-ray spectra are presented that were measured with a planar Hyperpure Ge x-ray detector (Fig. 1a) and a high efficiency (52.3%) n-type Ge γ-ray detector (Fig. 1b and c).

Half-lives of 0.5 ±0.2 s and 1.5 ± 0.2 s were measured for the new isotopes ^{134}Eu and ^{135}Eu respectively. In the decay of ^{136}Eu we found two half-life components of 3.3 ±0.5 s and ~4.0 s. Beta delayed proton emission was observed in the decays of ^{134}Eu, ^{135}Sm and ^{136}Eu, with proton energy ranges of 1.5 MeV < E_p < 6.0 MeV in all cases. The ^{134}Eu and ^{136}Eu are the first Eu isotopes observed to decay by β-delayed proton emission. Proton branching ratios of $(8.7\pm2.5)\times10^{-4}$ for ^{136}Eu and $(1.6\pm0.5)\times10^{-4}$ for ^{135}Sm were determined. In the decay of ^{135}Sm, beta delayed proton emission to the 0^+ ground and to the 2^+ excited states in ^{134}Nd was observed.

The ^{135}Eu activity was identified by Sm K_α x-rays following its electron capture decay; in addition a 120.8-keV γ ray could be associated with this decay. Twenty-six γ rays in ^{136}Sm were assigned to the decay of ^{136}Eu, and γ-ray emission following the β-decay of ^{134}Sm (19 γ rays) and ^{135}Sm (23 γ rays) was observed for the first time. In the case of the ^{136}Sm decay 40 β-delayed γ rays were identified. Fast allowed Gamow-Teller $0^+ \rightarrow 1^+$ β transitions were assigned to the 119 keV level in ^{134}Pm and 114.5 keV level in ^{136}Pm in ground state β decays of ^{134}Sm and ^{136}Sm respectively. The low spin β decays of ^{136}Pm and ^{135}Nd were studied for the first time without a strong interference from the high spin isomer, because these isotopes were not produced in the reaction directly but were fed by low spin β-decay parents. Partial level schemes were constructed for $^{134-136}$Pm, $^{134-136}$Nd and ^{136}Sm.

Footnotes and References

*On leave from University of Helsinki, SF00180, Finland

†On leave from Screq Nuclear Research Center, Yavne 70600, Israel

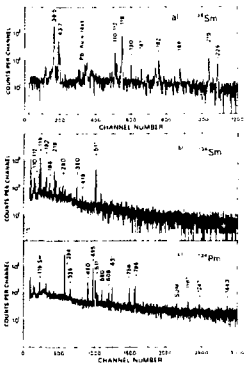

Fig. 1. Gamma spectra measured in coincidence with Pm and Nd K x-rays. Gated background spectra were subtracted. The low energy γ-spectrum of the x-ray detector coincident with Pm K x-rays in the 52.3% Ge detector is shown in a). The high energy γ-ray spectra of the 52.3% Ge detector in coincidence with Pm and Nd x-rays are presented in b) and c), respectively. The energies of the marked peaks are given in keV. XBL 8711-4820

Studies of the Level Systematics of Even-Even Neutron Deficient Sm, Nd, and Ce Isotopes

K. Vierinen, J.M. Nitschke, P.A. Wilmarth, R.B. Firestone, and J. Gilat†*

Beta decay studies of neutron deficient Eu, Pm and Pr nuclei with A= 128–136 have been performed using the OASIS[1] on-line mass separator facility at the SuperHILAC. The level structure of the even Nd, Sm and Ce isotopes was investigated. The low lying members of the γ-vibrational and ground state rotational bands were identified and their energy dependence as a function of neutron number was followed (Fig. 1). The analyses of β-delayed γ-ray data of masses A=134 and A=136 have been completed and we are continuing our studies of the A=132, 130 and 128 mass chains. In Fig. 1 the level systematics of Sm and Nd isotopes is presented. The energy differences of the second 2^+ and the first 4^+ levels in Nd and Sm isotopes and the excitation energies of these levels decrease systematically as a function of increasing deformation and with decreasing neutron number. In ^{132}Nd the second 2^+ level was reported[2] to lie about 213 keV above the 4^+ state (Fig. 1). This signifies a possible strong deformation change between neutron numbers 74 and 72; an effect that was not observed in even-even Sm and Ce isotopes.

The Sm, Nd and Ce nuclei have spherical shape near the line of β-stability, and in going to more neutron deficient isotopes their shape transforms first to triaxial and then to axially symmetric prolate with a quadrupole parameter of $\epsilon_2 \geq 0.3$. Besides large deformation and triaxiality nuclei near A$\sim$130 also show superdeformation.

Footnotes and References

*On leave from University of Helsinki, SF00180, Finland

†On leave from Soreq Nuclear Research Certer, Yavne 70600, Israel

1. J.M. Nitschke, Nucl. Instr. and Meth. **206**, 301 (1983).

2. M. Kortelahti *et al.*, Z. Phys. Short Note, **A327**, 231 (1987).

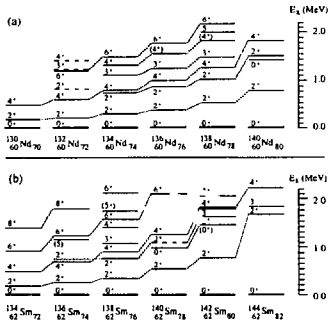

Fig. 1. Level systematics of even-even Nd (a) and Sm (b) isotopes. The level structure information was collected from the literature and from this work.

XBL 8711-4819

Observation of ^{149}Tm Decay to ^{149}Er Levels and β-Delayed Proton Emission

K.S. Toth, J. Gilat,† J.M. Nitschke, P.A. Wilmarth, K. Vierinen,‡ and F.T. Avignone III §*

With the use of the OASIS on-line isotope separator,[1] ^{149}Tm ($T_{1/2}$ = 0.9 ± 0.2 s) was identified in ^{58}Ni bombardments of ^{94}Mo. Seven γ rays were observed to follow the isotope's (β^+ + electron

capture) decay, including the 111.3-keV transition known from $^{149}Er^{m}$ isomeric decay to be the $d_{3/2}$ (111.3 keV) → $s_{1/2}$ (0.0 kev) γ ray in ^{149}Er. In addition to the previously known levels at 111.3 ($d_{3/2}$) and 741.5 ($h_{11/2}$) keV in ^{149}Er, our data established three other excited states at 907.4 ($d_{5/2}$), 1066.2 ($f_{7/2}$), and 1482.9 ($9/2^-$, $11/2^-$) keV.

Fig. 1 shows systematics of levels below 1.5 MeV in the three known N = 81 even-Z isotones with Z ≥ 64, i.e., ^{145}Gd, ^{147}Dy, and ^{149}Er. One sees the smooth trends with proton number of the $s_{1/2}$, $d_{3/2}$, $h_{11/2}$, $d_{5/2}$, $f_{7/2}$, and $g_{7/2}$ neutron hole states. Note that due to a low production cross section for ^{149}Tm (calculated[2] to be 1.5 mb) we were unable to observe γ rays deexciting the $g_{7/2}$ state in ^{149}Er.

Coincidences observed between Er K x rays and protons in the A = 149 mass chain show that ^{149}Tm is a β-delayed proton precursor. By using the total ^{149}Tm β decay intensity derived from our data we estimate the β-delayed-proton branch of ^{149}Tm to be about 2×10^{-3} with an uncertainty factor of two.

Footnotes and References

*Oak Ridge National Lahoratory Oak Ridge, TN 37831

†On leave from Soreq Nuclear Research Center, Yavne 70600, Israel

‡On leave from University of Helsinki, SF 00180, Finland

§University of South Carolina, Columbia, SC 29208.

1. J.M. Nitschke, Nucl. Instr. Methods Phys. Res. **206**, 341 (1983)

2. W.G. Winn, H.H. Guthrod, and M. Blann, Nucl. Phys. **A188**, 423 (1982); also, M. Blann and J. Bisplinghoff, US DOE Report UCID-19614 (1982)

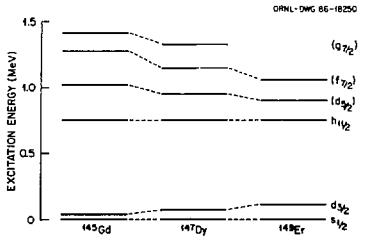

Fig. 1. See text. XBL 8710-4486

Delayed Proton Emission of N=81 Odd-Odd Precursors: ^{148}Ho, ^{150}Tm, and ^{152}Lu

J.M. Nitschke, P.A. Wilmarth, J. Gilat, K.S. Toth,† and F.T. Avignone III‡*

Beta-delayed proton decay was observed in ^{148}Ho, ^{150}Tm, and ^{152}Lu for the first time. Unlike neighboring even-Z N=81 isotones, the proton spectra appear structureless and statistical in nature. Upper limit proton branching ratios for the three isotopes, based on the intensity of γ-ray transitions in the intermediate nuclei, are: $(8\pm1) \times 10^{-4}$, $(1.4 \pm 0.1) \times 10^{-2}$, and $(1.5 \pm 0.7) \times 10^{-1}$, respectively. The onset of proton emission in all three cases occurs at a proton to γ width ratio of about 10^{-4}. Protons were found to be in coincidence with x rays, γ rays, and positrons. Coincident K x rays served to identify the Z of the precursor, while the γ rays gave quantitative information about proton decay to excited states in the daughter nuclei. By comparing the γ intensities with statistical model calculations it was concluded that ^{148}Ho and ^{150}Tm both have isomers with probable spin values of 1^+ and 6^-. Statistical model calculations with "standard" prescriptions for level densities and γ widths reproduced the ^{148}Ho but not the ^{150}Tm and ^{152}Lu branching ratios. For the latter two isotopes, a reduction of the level density parameter to 70% of the "back shifted" Fermi level density was necessary to achieve agreement. To reproduce the shape of the proton spectrum it was necessary to assume Gaussian shaped GT β strength functions

centered near 8 MeV excitation energy. In the course of these experiments β-delayed proton emission in ^{148}Er was also identified. Fig. 1 shows an example of the observed statistical proton spectra at mass 148.

Footnotes and References

*On leave from Soreq Nuclear Research Center, Yavne 70600, Israel

†Oak Ridge National Laboratory, Oak Ridge, TN 37831

‡University of South Carolina, Columbus, SC 29208

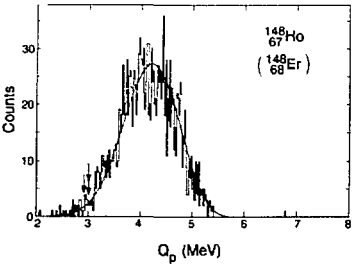

Fig. 1. Proton spectrum from Ho and Er decay observed with the ΔE-E particle telescope at mass 148. The proton energy Q_p is calculated as the sum of the experimental energy and the recoil energy. A single arrow marks the energy at which $\Gamma_p = 10^{-5}$eV, a double arrow indicates where $\Gamma_p/\Gamma_\gamma = 10^{-4}$. The smooth curve is the result of a statistical model calculation for the ^{148}Ho high-spin isomer only normalized to the total number of observed protons.
XBL 876-9708

Beta Decay Properties of ^{148}Er, ^{148}Ho and ^{148}Dy

K.S. Toth, D.C. Sousa,† J.M. Nitschke, and P.A. Wilmarth*

The decay properties of ^{148}Er, ^{148}Ho, and ^{148}Dy, produced in ^{58}Ni bombardments of ^{94}Mo, were investigated following mass separation with the OASIS on-line facility. New γ rays were observed for all three nuclides. In addition, coincidences between protons and x and γ rays establish ^{148}Er and ^{148}Ho to be β-delayed-proton precursors; their proton branching ratios are estimated to be ~1.5 x 10^{-3} and (8 ± 1) x 10^{-4}, respectively.

It was determined that much of ^{148}Er β decay populates the ^{148}Ho low-spin isomer directly. With a Q_{EC} of ~ 7 MeV, estimated from decay energies listed in ref. 1., we calculate a log*ft* of ~ 4.7 for this β transition. This log*ft* establishes the J^π of the ^{148}Ho low-spin isomer to be 1^+ since a $0^+ \rightarrow 0^+$ transition is either isospin forbidden, with a log*ft* value ≥ 6.5, or superallowed, with a log*ft* in the range of 3.48 to 3.50.

Transitions assigned to ^{148}Ho decay are predominantly from the decay of the high-spin isomer. The proposed decay scheme (shown in Fig. 1) is constructed on the basis of singles and coincidence γ-ray data and of available in-beam results (see, e.g., ref. 2). The presence of the 94.5- and 101.5-keV γ rays in our data shows that the yrast 8^+ level (ref. 2) is fed, directly or indirectly, by the ^{148}Ho high-spin isomer. On the other hand, we did not see, either in singles or in coincidence, the 85.7-keV transition which proceeds from the 10^+ level[2] at 2920 keV to the 8^+ level. These observed and unobserved level feedings together with the log*ft* value of ~ 5.3 (a Q_{EC} of 9.6 ± 0.3 MeV[1] was used) calculated for the intense β-decay transition to the 5^- state at 2349.4 keV favor a 6^- assignment for the ^{148}Ho parent. We propose seven new levels in ^{148}Er at 2969.3, 2994.7, 3115.0, 3188.5, 3278.9, 3322.6, and 4289.4 keV. While no spin assignments are given for these states spin values of ≥ 4 and ≤ 7 would seem to

be most consistent with the suggested decay scheme. The nuclide ^{148}Dy was first characterized[3] by the one intense 620.2-keV γ ray that follows its β decay. In agreement with the earlier investigation, a gate set on this γ ray revealed no coincident transitions in our data; however, the spectrum in coincidence with Tb K x rays showed three other transitions, i.e., 178.5, 950.6, and 1247.3 keV. Their intensities, however, sum to $\sim$ 2.5% of the 620.2-keV γ-ray intensity so that the corresponding log*ft* value to the 620.2-keV level remains at $\sim$ 3.9 indicating that the β transition is allowed and, as noted in ref. 3, connects the 0^+ parent with a 1^+ excited state at 620.2 keV in ^{148}Tb.

Footnotes and References

*Oak Ridge National Laboratory, Oak Ridge, TN 37831

†Eastern Kentucky University, Richmond, KY 40475

1. A.H. WapsDra and G. Audi, Nucl. Phys. **A432**, (1985).

2. P.J. Daly *et al.*, Z. Phys. **A298**, 173 (1980).

3. K. S., Toth *et al.*, Phys. Rev. C **11**, 1370 (1975).

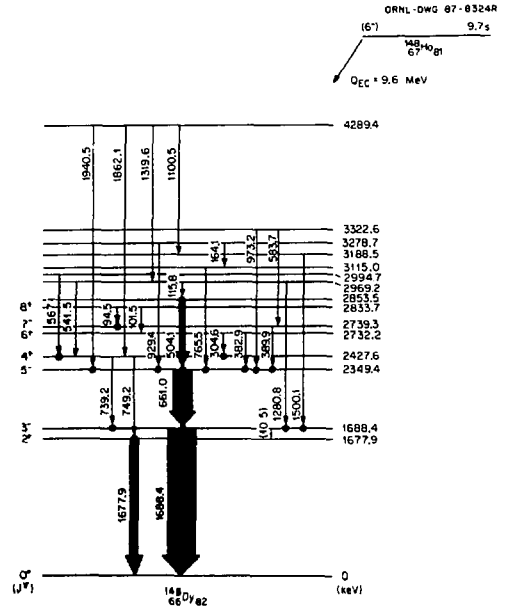

Fig. 1. See text.

XBL 8710-4485

Decay Studies of Neutron Deficient Rare Earth Isotopes with OASIS

J. Gilat, J.M. Nitschke, P.A. Wilmarth, K. Vierinen, and R.B. Firestone*

The on-line mass separator facility OASIS is being used for a systematic study of highly neutron deficient rare earth isotopes produced in heavy ion induced compound nucleus reactions at the Berkeley SuperHILAC. The mass-separated reaction products are deposited on a programmable moving tape system and viewed with a shielded array of particle, x-ray and γ-ray detectors, in both singles and coincidence modes. Results of several γ-ray studies are summarized in Table I. Underlined entries denote new isotopes observed in our work. Literature values of half-lives not determined in our measurements are given in brackets. Columns 4 and 5 denote, respectively, the total number of γ transitions assigned to each decay and the observation of β-delayed proton emission.

Level schemes incorporating most of the observed γ transitions have been constructed. The implications of the data for the predicted region of prolate deformation below N=78 is being studied. As an example, the low lying levels in ^{141}Gd established by the IT decay of the newly discovered $11/2^-$ isomer at 378 keV follow closely the systematics of analogous levels in other N=77 isotones.[1,2] This indicates that the Z=64 shell has little effect on the spectroscopy of these neutron levels. However, the B(E3) transition rate for the 120 keV $11/2^-$ to $5/2^+$ transition is only $\sim 9 \times 10^{-4}$ Weisskopf Units, i.e., about 5–10 times slower than the rate observed for the other three isotones.

Table I

Summary of γ Decay Studies of Neutron Deficient Rare Earth Isotopes

Reaction	Isotope	T(s)	γ-rays	Protons
^{36}Ar	^{124}Pr	1.2(2)	1	+
+	^{124}Ce	~6	4	
^{92}Mo	^{124}La	30(2)	15	
	^{125}Ce	10(1)	25	+
	^{125}La	70(3)	30	
^{40}Ti	^{134}Eu	0.5(2)		+
+	^{134}Sm	~10	23	
^{92}Mo	^{134}Pm	[24]	26	
	^{135}Eu	1.5(2)	1	
	^{135}Sm	10(1)	25	+
	^{135}Pm	[49]	45	
	^{136m}Eu	~5		(+)
	^{136g}Eu	3.2(5)	18	(+)
	^{136}Sm	[44]	40	
	^{140m}Tb	2.4(2)	3	+
	^{140}Gd	15.8(4)	35	
	^{140m}Eu	0.125(5)	2	
	^{140g}Eu	1.51(4)	18	
^{54}Fe,^{52}Cr	^{141}Dy	0.9(2)		+
+	^{141}Tb	3.5(2)	30	
^{92}Mo	^{141m}Gd	24.5(9)	35	
	^{141g}Gd	~20	7	+
	^{141m}Eu	2.7(3)	10	
	^{142}Dy	2.3(3)	1	+
	^{142m}Tb	0.30(1)	4	
	^{142g}Tb	0.60(2)	7	+
	^{142}Gd	70.2(6)	30	
^{58}Ni,^{56}Fe	^{144}Ho	0.7(1)		+
+	^{144}Dy	9.1(5)	21	+
^{92}Mo	^{144m}Tb	4.1(1)	15	
	^{144g}Tb	[~1.5]	4	

Footnotes and References

*On leave from the Soreq Nuclear Research Center, Yavne 70600, Israel

1. C.M. Lederer and V.S. Shirley, eds. **Table of Isotopes** 7th ed. (Wiley, New York, 1978).

2. J. Deslauriers, S. Guijrathi, S.K. Mark and S.P. Sud, Z. Phys. **A325**, 421 (1986).

Synergistic Extraction Studies of Actinides and Lanthanides

R.B. Chadwick, G.D. Jarvinen, B.F. Smit,* D.M. Lee, and D.C. Hoffman*

Our group, in collaboration with Los Alamos National Laboratory, is studying a newly "engineered" chemical, 4-benzoyl-2, 4-dihydro-5-methyl- 2-phenyl-3H-pyrazol-3-thione (BMPPT), to determine its be-

havior as a selective extractant for the actinides and lanthanides. The structure of BMPPT is shown in Fig. 1. This ligand in synergistic combination with tri-octylphosphine oxide (TOPO) has been observed to give a selectivity of Am(III) over Eu(III) ($K_{d_{Am}}$) =7.5, Am/Eu=68, pH 3.0, 0.01M (TOPO), 0.30M (BMPPT).[1] The slope of the BMPPT dependency was found to be 2.8 and the slope of the TOPO dependency was 2.0 for Am(III). This suggests that the major reactant species is $Am(TOPO)_2$ $(BMPPT)_3$. We are presently extending our studies of this system to the other actinides and lanthanides in an effort to develop new methods of separating these elements.

Footnotes and References

*Los Alamos National Laboratory, Los Alamos, New Mexico

1. B.F. Smith, G.D. Jarvinen, G.G. Miller, R.R. Ryan, and J.J. Peterson, submitted to Solvent Extraction and Ion Exchange.

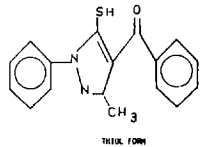

Fig. 1. Structure of 4-benzoyl-2, 4-dihydro-5-methyl-2-phenyl-3H-pyrazol- 3-thione (BMPPT).

XBL-8711-4845

Beta-Delayed Proton Decay in the Lanthanide Region

J.M. Nitschke, P.A. Wilmarth, J. Gilat, P. Möller,† and K.S. Toth‡*

A total of 26 new β-delayed proton precursors has been identified with the OASIS on-line mass separator facility at the SuperHILAC. They are located in the region of $56 < Z < 72$ and $N < 82$ and include spherical, transitional, and well deformed nuclei. Besides obtaining proton spectra and half-lives we have, in several cases, determined spins and parities from final state feedings, measured proton branching ratios, $(Q_{EC} - S_p)$ energy differences, and identified new levels in the proton decay daughters. We have also observed mixed β-delayed proton decay from precursor ground states and isomers. A summary of the results is given in Table I. ^{119}Ba, ^{120}Nd, ^{131}Nd, ^{133}Sm, and ^{135}Sm were also studied but not listed in Table I, which shows the isotope, measured half-life, calculated half-life, decay mode (βp and $\beta\gamma$ denote β-delayed proton and γ emission, respectively), mean energy and energy range of protons, number of γ rays observed, experimental spin, calculated spin, and whether x rays and/or γ rays were observed in coincidence with protons.

For the N=81 precursors ^{151}Yb, ^{149}Er, and ^{147}Dy, pronounced structure in the proton spectra is observed. Contrary to studies of lighter nuclei no individual levels in the intermediate nuclei could be identified that decay by proton as well as γ-decay. The nature of the observed peaks can be interpreted in a new framework of an "intermediate structure" based on two-particle, one-hole "doorway states." In the case of N=81 even-odd precursors these states are created via β/EC decay of zero-particle, one-hole configurations. They show a width that is intermediate between direct reaction widths and compound nucleus widths, and that depends on the strength of the residual interaction, a sum of two-body potentials coupling the compound state to the outgoing proton wave function. In this framework the emission of a proton is analogous to the second step in "compound elastic scattering."

Footnotes and References

*On leave from Soreq Nuclear Research Center, Yavne 70600, Israel

†On leave from Lund University, Sweden

‡Oak Ridge National Laboratory, Oak Ridge, Tennessee 37831

TABLE I. New isotopes and decay branches observed at OASIS

ISOTOPE	$T_{1/2}$(exp)	$T_{1/2}$(calc)	MODE	ENERGY	N_γ	J^π(exp)	J^π(calc)	PHOTONS
^{120}La	2.8(2)	1.8[a]	βp	3.7[2.1-5.6]	–	–	–	x
^{122}La	8.7(7)	5.5[a]	βp	3.4[2.0-4.6]	–	–	–	x
^{123}Ce	3.8(2)	2.6	βp[b]	3.6[2.0-5.8]	–	5/2	$5/2^+$	x,γ
^{125}Ce	10(1)	10	βp	3.3[1.7-5.1]	25	5/2	$1/2^+$	x,γ
^{124}Pr	1.2(2)	0.6[a]	βp	3.7[2.2-6.0]	1	–	–	x,γ
^{126}Pr	3.2(6)	2.0[a]	βp	3.8[2.1-5.0]	–	–	–	–
^{128}Pr	3.2(5)	7.7[a]	βp	3.2[1.9-5.0]	–	–	–	x
^{127}Nd	1.8(4)	1.7	βp	3.7[2.2-6.0]	–	–	$1/2^+$	x,γ
^{130}Pm	2.2(6)	1.7[a]	βp	3.9[2.1-5.8]	–	–	–	x
^{132}Pm	5.0(8)	3.7[a]	βp[b]	3.6[2.2-5.0]	–	–	–	x
^{131}Sm	1.2(2)	1.6	βp	3.7[1.8-6.6]	–	–	$7/2^-$	x,γ
^{134}Eu	0.5(2)	1.3[a]	βp	3.8[1.8-6.0]	–	–	–	x
^{135}Eu	1.5(2)	2.1	$\beta\gamma$	n.a.	1	–	$1/2^-$	n.a.
^{136}Eu	3.2(5)	1.8[a]	βp	3.9[2.0-6.0]	28	–	–	x
^{137}Gd	7(3)	1.2	βp	3.8[2.2-6.6]	–	–	$9/2^-$	–
^{139}Gd	5(1)	4.5	βp	3.8[2.1-5.5]	–	–	$7/2^+$	–
^{140}Gd	15.8(4)	15.3	$\beta\gamma$	n.a.	35	0^+	0^+	n.a.
^{141m}Gd	24.5(9)	n.a.	$\beta\gamma$	n.a.	35	$11/2^-$	n.a.	n.a.
^{141g}Gd	~20	16.3	βp	3.6[2.2-4.9]	10	$1/2^+$	$1/2^+$	x,γ
^{140m}Tb	2.4(2)	n.a.	βp	4.2[2.2-6.6]	3	–	n.a.	x
^{141}Tb	3.5(2)	3.4	$\beta\gamma$	n.a.	35	–	$1/2^-$	n.a.
^{142m}Tb	0.3(1)	n.a.	$\beta\gamma$	n.a.	4	–	n.a.	n.a.
^{142g}Tb	0.6(2)	3.5[a]	βp	3.9[2.5-5.2][c]	7	–	–	x,γ
^{141}Dy	0.9(2)	1.4	βp	4.0[2.4-6.1]	–	–	$7/2^+$	x,γ
^{142}Dy	2.3(3)	2.7	βp	3.9[2.5-5.2][c]	1	0^+	0^+	x,γ
^{143}Dy	3.8(6)	2.9	βp	4.2[2.5-6.5]	–	–	$3/2^-$	x,γ
^{144}Dy	9.1(5)	9.7	βp	3.2[2.6-4.5]	21	0^+	0^+	x
^{144}Ho	0.7(1)	1.3[a]	βp	4.2[2.2-7.0]	–	–	–	x
^{146}Ho	3.1(5)	2.9[a]	βp[b]	4.1[2.4-6.3]	9	≥ 6	–	x
^{148m}Ho[d]	9.7(3)	n.a.	βp[b]	4.1[2.2-5.4][c]	39	6^-	n.a.	x,γ
^{148}Er	4.4(2)	n.a.	βp[b]	4.1[2.2-5.4][c]	5	0^+	0^+	x,γ
^{149}Tm	0.9(2)	n.a.	βp	n.a.	7	$11/2^-$	$11/2^-$	x
^{150m}Tm[d]	2.2(2)	n.a.	βp[b]	4.7[2.2-7.5]	12	6^-	n.a.	x,γ
^{151m}Yb	1.6(1)	n.a.	βp	4.0[2.5-6.0]	1	$11/2^-$	n.a.	x,γ
^{151g}Yb	1.6(1)	0.9	βp	4.8[2.3-7.5]	–	$1/2^+$	$11/2^-$	x,γ
^{152m}Lu[d]	0.7(1)	n.a.	βp	4.6[2.3-7.9]	3	4^-,5^-,6^-	n.a.	x

[a]The ground state to ground state transition in odd-odd to even-even decay is not included,

[b]new delayed-proton branch in known isotope,

[c]mixture of all delayed protons in this mass chain,

[d]relative position of low- and high-spin isomers unknown.

Lawrencium Chemistry: No Evidence for Oxidation States Lower than 3+ in Aqueous Solution*

U.W. Scherer,† J.V. Kratz,† M. Schädel,† W. Brüchle,† K.E. Gregorich, R.A. Henderson, D.M. Lee, M.J. Nurmia, and D.C. Hoffman

Relativistic effects on the atomic electron orbits become increasingly important as one moves toward the end of the periodic table. In the case of Lr, (element 103), the heaviest of the actinides, relativistic calculations[1,2] indicate that the electronic ground state of the atom should be $(Rn)5f^{14}\ 7s^27p$ as opposed to $(Rn)5f^{14}6d7s^2$, which is the configuration analogous to Lu, the heaviest lanthanide. One other postulated effect is the relativistic stabilization of the 7s shell, allowing a Lr^{1+} ion to exist. In experiments performed at the LBL 88-Inch Cyclotron, we have attempted to produce this lower oxidation state using V^{2+}, Cr^{2+}, Zn^0, and hydroxylamine-hydrochloride as reductants.

We bombarded a ^{249}Bk target with ^{18}O ions to produce 3-min ^{260}Lr and other heavy actinide isotopes. The recoiling atoms were deposited by our He/KCl aerosol jet on a quartz frit in the collection site of the Automated Rapid Chemistry Apparatus 3 (ARCA), containing two chromatographic columns. The KCl aerosols were dissolved with 0.3 M HCl solution containing 0.01 M reductant. For the experiment using Zn as the reductant, 0.03 M HCl was pumped through a Zn(Hg) amalgam column heated to 80°C. In the experiment using hydroxylamine as the reductant, a column containing inert Celite with sorbed HDEHP heated to 100°C was used. The solution was pumped to the first of two HDEHP columns, also at 80°C. On the first HDEHP column, the reduced activities and No^{2+} were removed from the column with 0.2 M HCl and pumped onto the second HDEHP column. In between the two columns H_2O_2 was added to re-oxidize any reduced elements. The No^{2+} was removed from the second column using 0.2 M HCl. Finally, the re-oxidized elements were removed using 4.0 M HCl. Individual fractions were collected on Ta disks, flamed, and measured with our alpha and spontaneous fission spectrometry system at the 88-Inch Cyclotron.

The bulk of these experiments was performed using V^{2+} and Cr^{2+} ions as the reductants. In neither case were any Lr atoms detected in the reduced fraction. Md was reduced by both the V^{2+} and Cr^{2+} ions, consistent with its reduction potential of $E^0 = -0.2$ V. Based on the most conservative estimates of the reductant concentration from off-line experiments, we can set a limit on the reduction potential for Lr of $E^0 = -0.44$ V. This potential is for reducing Lr^{3+} to either Lr^{2+} or Lr^{1+}, as the chemistry performed cannot distinguish between these two oxidation states.

Footnotes and References

*Condensed from a paper submitted to Inorganic Chemica Acta

†Institut für Kernchemie, Universität Mainz, D-6500 Mainz, Germany

‡Gesellschaft für Schwerionenforschung mbH, D-6100 Darmstadt, Germany

1. L.J. Brewer, J. Opt. Soc. Am. **61**, 1101 (1971).

2. J.-P. Desclaux, B. Fricke, J. Physique **41**, 943 (1980).

3. M. Schädel, W. Brüchle, B. Haefner, Preprint GSI-87-29, submitted to Nucl. Instr. and Methods.

Spontaneous Fission*

D.C. Hoffman and L.P. Sommerville†

A review of experimental information about spontaneous fission properties determined since the last reviews[1,2] has been prepared. A survey of recently obtained results on half lives (including a compre-

hensive table of assigned spontaneous fission activities with their half lives and partial SF half lives or branches), fragment mass and kinetic-energy distributions, neutron emission, and gamma-ray emission is given. Particular emphasis is given to new results for the heaviest isotopes and a table of spontaneous fission properties of trans-Bk isotopes and graphical representations of the mass-yield and total kinetic-energy distributions for these isotopes are presented.

Footnotes and References

*Condensed from LBL-23475, to be published as Chapter I of Volume III of "Charged Particle Emission from Nuclei", CRC Press, Inc., Boca Raton, FL.

†Physics Department, San Jose State University, San Jose, California

1. Hoffman, D.C., and Hoffman, M.M., Post-Fission Phenomena, Ann. Rev. of Nucl Sci., **24**, 151 (1974).

2. Hoffman, D., Fission Properties of Very Heavy Actinides, in Proc. of the Int. Symp. on the Phys. and Chem. of Fission, Vol. II, Julich, West Germany, May 1418, 1979, Int. At. Energy Agency, Vienna, Austria, 275, (1980).

Heavy Actinide Production from the Interactions of ^{44}Ca with ^{248}Cm

J.D. Leyba, D.A. Bennett, R.B. Chadwick, R.M. Chasteler, C.M. Gannett, H.L. Hall, R.A. Henderson, K.E. Gregorich, M.J. Nurmia, D.C. Hoffman, A. Turler, and H. R. von Gunten*,†*

Our group is interested in new, neutron-rich isotopes produced via transfer reactions involving actinide targets and heavy-ion projectiles. By studying these transfer reactions, we hope to determine the best possible conditions for the production of specific nuclides. In addition, such studies of various target-projectile-energy combinations should aid in our understanding of the reaction mechanisms involved.

Cross sections for isotopes of Bk, Cf, Es, and Fm produced from the interaction of ^{44}Ca with ^{248}Cm were measured at energies from just below the Coulomb barrier to about 85 Mev above the barrier. The largest cross sections occurred for transfers involving the fewest nucleons. A rapid decrease in the cross sections was observed as the number of nucleons transferred increased.

In a previous study[1] which used the projectile pair ^{40}Ca and ^{48}Ca with ^{248}Cm, it was shown that the maxima of the isotopic distributions for Bk, Cf, Es, and Fm from the ^{48}Ca interaction were shifted by two to three mass numbers relative to ^{40}Ca. In the present study, the measured isotopic distributions (Fig. 1) were comparable in both shape and width to those obtained from ^{40}Ca and ^{48}Ca with ^{248}Cm. That is, the distributions are symmetric about the maxima and have a full-width at half maximum of about 2.5 mass numbers. These similarities suggest that the final isotopic distributions are somewhat independent of the projectile. Typical excitation functions for two Fm isotopes are shown in Fig. 2 for ^{40}Ca, ^{44}Ca, and ^{48}Ca interactions with ^{248}Cm. In each case, the measured excitation functions are consistent with calculated excitation energies assuming binary reactions and based upon the ingoing and outgoing Coulomb barriers and the ground state Q values. In general, the reactions with ^{40}Ca are rather exoergic while those with ^{48}Ca are endoergic.

The maxima of the Bk isotopic distributions for ^{40}Ca and ^{44}Ca occur at the same mass number, about two mass numbers lower than the ^{48}Ca maximum. However, the maximum of the Cf isotopic distribution for ^{44}Ca occurs at the same mass number as the maximum for ^{48}Ca, which is about two mass numbers higher than the maximum for ^{40}Ca. Furthermore, the maximum of the Es isotopic distribution for ^{44}Ca lies between the maxima for ^{40}Ca and ^{48}Ca as does the maximum of the Fm isotopic distribution for ^{44}Ca. Various theoretical treatments are being considered in an attempt to model the data.

*Universität Bern, Switzerland

†Eidg. Institut für Reaktorforschung, Wurenlingen, Switzerland

1. D.C. Hoffman, *et al.*, Phys. Rev. C **31**, 1763 (1985).

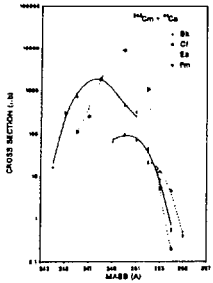

Fig. 1. Isotopic distributions from the interaction of ^{44}Ca with ^{248}Cm. XBL 8711-4842

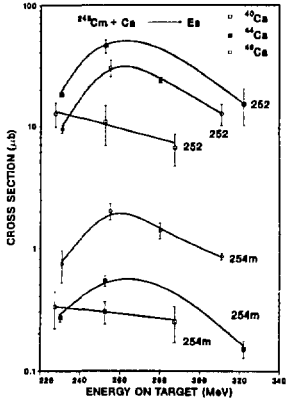

Fig. 2. Excitation functions for ^{252}Es and ^{254}Es^{m} from the interactions of ^{40}Ca, ^{44}Ca, and ^{48}Ca with ^{248}Cm. Data for ^{40}Ca and ^{48}Ca from ref. 1. XBL 8711-5025

The Hydration Enthalpies of Md^{3+} and Lr^{3+}

W. Brüchle, M. Schädel,* W. Scherer,† J.V. Kratz,† K.E. Gregorich, D.M. Lee, M.J. Nurmia, R.M. Chasteler, H.L. Hall, R.A. Henderson, and D.C. Hoffman*

In the only other study on the chemistry of Lr, Silva[1] showed that Lr is indeed the last member of the actinide series with characteristic trivalent oxidation state in aqueous solution. Our experiments are primarily aimed at learning more about Lr on the basis of its thermodynamic properties, and, in this case, on determining the enthalpy of hydration based on its elution position from a cation column. The linear relationship between the crystal ionic radius of actinides and lanthanides and the log of the distribution coefficient[2] allows us to infer a value for the ionic radius of Lr^{3+} by measuring its elution position from a cation exchange column. The enthalpy of hydration can then be calculated from this value. We have also determined the enthalpy of hydration of Md^{3+} in the same experiment.

Lr and Md activities were produced by bombarding ^{249}Bk with ^{18}O ions at the 88-Inch Cyclotron. The recoiling atoms were transported to the collection site of the Automated Rapid Chemistry Apparatus (ARCA) system 3 via a He/KCl jet. The activity was washed from the glass collection frit with 0.05M alpha-hydroxyisobutyric acid, α-HIB, containing Tm, Er, and Ho tracers and sorbed on a column containing Aminex A6 cation exchange resin. The activities were then eluted from the column with 0.12M α-HIB solution adjusted to pH=4.58. Samples were collected from the column, evaporated, flamed, and the alpha and spontaneous fission activities were measured with surface barrier detectors. The rare-earth tracer activities were measured with Ge(Li) detectors after the completion of the alpha counting.

Lr was found to elute with Er, and Md just after the Ho peak. The position of the Lr elution position had not been expected. Initially, based on the spacings of the other actinides and lanthanides, we expected that Lr should elute very near Tm. From this, Lr is seen to have a somewhat larger ionic radius than expected.

From the elution positions we calculated the enthalpy of hydration to be 3689±13 kJ/mol for Lr^{3+} and 3654±12 kJ/mol for Md^{3+}. These values are independent of the values chosen for the ionic radii, which depend on the set of crystal ionic radii chosen for the lanthanide elements. There is considerable disagreement among the various sets of data for the ionic radii of the lanthanides, so we do not report a value for the ionic radius of Lr. However, as Lr was found to elute nearly with Er, we infer that its radius is nearly the same as the Er value, regardless of the values chosen for the lanthanides.

Footnotes and References

*Gesellschaft für Schwerionenforschung mbH, D-1600 Darmstadt, Germany

†Institut für Kernchemie, Universität Mainz, D-6500 Mainz, Germany

1. R.J. Silva, T. Sikkeland, M. Nurmia, and A. Ghiorso, Inorg. Nucl. Chem. Lent. **6**, 733 (1970).

2. Y. Marcus, A.S. Kertes **Ion Exchange and Solvent Extraction of Metal Complexes**, Wiley, Interscience, New York 1969, p. 287.

3. M. Schädel, W. Brüchle, B. Haefner, Preprint GSI-87-29, submitted to Nuc. Instr. and Methods.

Yields of Bk, Cf, Es and Fm Isotopes from the Reactions of 151 MeV ^{18}O Projectiles with ^{248}Cm

C.M. Gannett, D.M. Lee, K.E. Gregorich, M.J. Nurmia, R.A. Henderson, R.M. Chasteler, H.L. Hall, D.A. Bennett, and D.C. Hoffman

The bombardment of a 0.644 mg/cm^2 ^{248}Cm target with 151 MeV $^{18}O^{5+}$ projectiles was carried out at the LBL 88-Inch Cyclotron. Recoiling reaction products were stopped in a 1.5 mg/cm^2 gold foil. The foil was dissolved and Bk, Cf, Es, and Fm were radiochemically separated and counted for gamma, alpha and spontaneous fission activities. The resulting cross sections were compared to those we measured previously for the same reaction at lower projectile energies.

The isotopic distribution curves are shown in Fig. 1. Each is consistent with a full width half maximum (FWHM) of about 2.5 mass units, as has been seen for similar reactions[1-5] of light-heavy ion projectiles with actinide targets. Also, a difference in cross section of about two orders of magnitude occurs between the transfer of H and He fragments. This is comparable to the difference of one to three orders of magnitude which has been seen in virtually all other studies[1,3,4,5] of light-heavy ion reactions with heavy actinide targets. The only exceptions known so far are ^{16}O and ^{18}O on ^{249}Cf.[1,2]

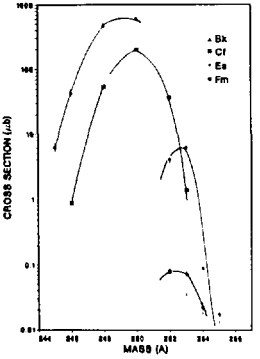

Fig. 1. Isotopic distribution curves for Bk, Cf, Es and Fm isotopes formed in the reactions of 151-MeV ^{18}O with ^{248}Cm. XBL 8711-4844

Generally, the high energy points for the excitation functions for ^{18}O plus ^{248}Cm lie on a smooth extrapolation of the corresponding lower energy points. As an example, the results for the Cf isotopes are shown in Fig. 2. Exceptions to this trend are ^{253}Es and ^{250}Bk, which are five to ten times higher than expected. These excitation functions drop off rather slowly with increasing projectile energy, indicating that such transfer reactions can result in heavy products with relatively low excitation energies.

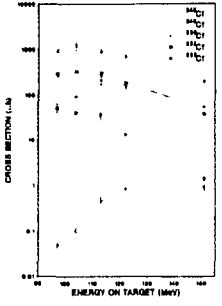

Fig. 2. Excitation functions for Cf isotopes formed in the reactions of ^{18}O with ^{248}Cm. XBL 8711-5009

Footnotes and References

1. D.M. Lee, K.J. Moody, M.J. Nurmia, G.T. Seaborg, H. R. von Gunten and D.C. Hoffman, Phys. Rev. C **27**, 2656–2665 (1983).

2. R.M. Chasteler, R.A. Henderson, D.M. Lee, K.E. Gregorich, M. J. Nurmia, R.B. Welch, and D.C. Hoffman, LBL-23681.

3. D.M. Lee, H. von Gunten, B. Jacak, M. Nurmia, K. Liu, C. Luo, G.T. Seaborg, and D.C. Hoffman, Phys. Rev. **C25**, 286–292 (1982).

4. D.C. Hoffman, N.M. Fowler, W.R. Daniels, H.R. von Gunten, D.M. Lee, K.J. Moody, K. Gregorich, R. Welch, G. T. Seaborg, W. Brüchle, M. Brügger, H. Gäggeler, M. Schädel, K. Sümmerer, G. Wirth, Th. Blaich, G. Herrmann, N. Hildebrand, J.V. Kratz, M. Lerch, and N. Trautmann, Phys. Rev. **C31**, 1763–1769 (1985).

5. M. Schädel, W. Brüchle, M. Brügger, H. Gäggeler, K.J. Moody, D. Schardt, K. Sümmerer, E.K. Hulet, A.D. Dugan, R.J. Dugan, J.H. Landrum, R.W. Lougheed, J.F. Wild, and G.D. O'Kelley, Phys. Rev. **C33**, 1547–1550 (1986).

Neutron Deficient Berkelium Isotopes

H.L. Hall, R.A. Henderson, R.B. Chasteler, D.A. Bennett, C.M. Gannett, R.B. Chadwick, J.D. Leyba, K.E. Gregorich, D.M. Lee, M.J. Nurmia, and D.C. Hoffman

The study of the neutron deficient Bk isotopes is of interest for several reasons. Delayed fission processes, which are important to astrophysical models of the *bf* r-process,[1] should become an observable decay mode as one moves away from the line of β-stability. EC-delayed fission also provides a method for indirectly investigating the shape of the fission barrier in this region.[2] Such data are needed to refine theoretical predictions of the fission characteristics of heavier nuclei.

However, delayed fission processes have have been reported in only a few systems. β-delayed fission has been reported to occur in $^{236,238}Pa$,[3] although a recent investigation failed to confirm the result for ^{238}Pa.[4] We have observed β-delayed fission in the decay of ^{250m}Es to ^{250}Fm.[5] EC-delayed fission has been reported in the light Am and Np isotopes, and ^{232}Am has been reported to have a delayed fission branch of 1.3%[6] of total decay. The neutron deficient region of the berkelium isotopes, $^{240,241,242,243}Bk$, should therefore prove an interesting study of t' e systematics of EC-delayed fission as one moves stepwise away from the line of β-stability.

We are studying the $^{241}Am(^4He,xn)^{245-x}Bk$ reac-

tion. The 4n channel leads to the as yet unknown isotope ^{241}Bk. ^{240}Bk is known and was discovered in Dubna;[7] ^{242}Bk was discovered here in Berkeley.[8] The reaction products are swept from our target chamber at the 88-Inch Cyclotron via a KCl/He jet aerosol to the experimental area about five meters above. The activity-laden aerosols are collected in a 1.1 mL vial, and are then subjected to chemical separations to yield a Bk sample suitable for gamma counting.

We have not yet observed any activity unequivocably attributable to the unknown ^{241}Bk, but we can report a better half-life for the ^{242}Bk isotope. That value is $t_{1/2}$ = (5.61 ± 0.3) minutes. Figs. 1 and 2 show the decay fits for the Cm K_{α_1} and K_{α_2} x-rays resulting from the EC decay of the Bk isotopes. The fits are with two components, one being the 5.61 minute ^{242}Bk and the other the 270 minute ^{243}Bk. We have observed no γ-rays attributable to ^{242}Bk.

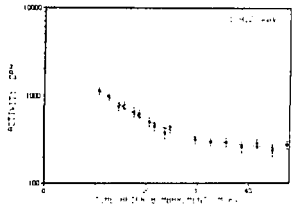

Fig. 1. Decay of the ^{242}Bk as observed in the Cm K_{α_1} x-rays. The short-lived component is ^{242}Bk with a $t_{1/2}$ of 5.61 minutes. The long-lived component is ^{243}Bk, $t_{1/2}$ = 270 minutes. XBL 8711-4963

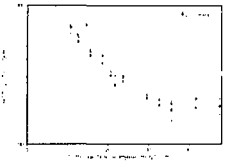

Fig. 2. Decay of the ^{242}Bk as observed in the Cm K_{α_2} x-rays. XBL 8711-4962

Footnotes and References

1. H.V. Klapdor, T. Oda, J. Metzinger, W. Hillebrandt, and F.K. Thielmann Z. Physik A **299**, 213–229 (1981).

2. H.V. Klapdor, C.-O. Wene, I.N. Isosimov, and Yu. W. Naumow, Z. Physik A **292**, 249–255 (1979).

3. Yu. P. Gangrskii, G.M. Marinescu, M.B. Miller, V.N. Samosyuk, and I.F. Kharisov, Sov. J. Nucl. Phys. **27(4)**, 475–478 (1978).

4. A. Baas-May, J.V. Kratz, and N. Trautmann, Z. Physik A **322**, 457–462 (1985).

5. H.L. Hall, R.A. Henderson, K.E. Gregorich, D.M. Lee, D.C. Hoffman, J.B. Wilhelmy, M.E. Bunker, J.W. Starner, M.M. Fowler, and P. Lysaight, to be published.

6. D. Habs, H. Klewe-Nebenius, V. Metag, B. Neumann and H.J. Sprecht, Z. Physik **A285**, 53–57 (1978).

7. Yu. Ts. Oganessian *et al.*, JINR-P7–10797 (1977).

8. K. Williams, Ph. D. Thesis, LBL (1978).

Excitation Functions for Production of Heavy Actinides from Interactions of ^{16}O with ^{249}Cf*

R.M. Chasteler, R.A. Henderson, D.M. Lee, K.E. Gregorich, M.J. Nurmia, R.B. Welch†, and D.C. Hoffman

Heavy actinides were produced by bombarding a 0.334 mg/cm^2 target of ^{249}Cf with ^{16}O ions at the LBL 88-Inch Cyclotron. Projectile energies of 90-, 96-, 106-, 115-, 122-, 139-, and 150-MeV (all quoted energies are the average energy in the target in the laboratory system) were used in order to obtain ex-

citation functions for the isotopes produced. Recoil products were caught on a gold catcher foil which was chemically processed to obtain seperated samples of Bk, Cf, Es, and Fm isotopes. These were alpha, gamma, and spontaneous fission counted for about six weeks. Decay analysis was performed in order to obtain initial activities from which cross sections were calculated. The excitation functions for the Fm isotopes are shown in Fig. 1. The shapes and magnitudes of the excitation functions are similar to those measured earlier for ^{18}O + ^{249}Cf and ^{16}O + ^{248}Cm reactions.[1] The mass-yield curves obtained for the Bk, Es, and Fm isotopes are shown in Fig. 2 with the mass-yield curves obtained for the ^{18}O + ^{249}Cf reaction.[1] In earlier work,[2] mass-yield shifts of 2-mass number were measured for $^{16,18}O$ and $^{20,22}Ne$ ion pairs on ^{248}Cm. In this study it can be seen that the Bk curves show this 2-mass number shift, but the Es and Fm curves show only a 1/2 and 1 mass-number shifts respectively. Recent studies[3] of reactions of $^{16,18}O$ and $^{20,22}Ne$ projectiles with ^{254}Es also show smaller shifts in their mass-yield curves.

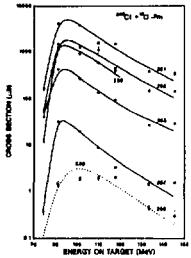

Fig. 1. Excitation functions for Fm isotopes produced in the bombardment of ^{249}Cf with ^{16}O. Points are connected only as a visual aid. XBL 871-185

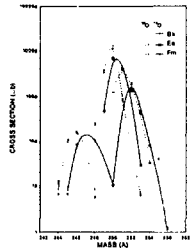

Fig. 2. Isotopic distributions measured for ^{16}O and ^{18}O bombardments of ^{249}Cf. Plotted points are the maxima of the excitation functions for each isotope. The data for ^{18}O reactions are from ref. 2.

XBL 871-189

Footnotes and References

*Condensed from LBL-23681 and Phys. Rev. C (in press).

†Present address: Institut für Anorganische Chemie, Freiestrasse 3, 3012 Bern,Switzerland.

1. D. Lee *et al.*, Phys. Rev. C **27**, 2656 (1983).

2. D. Lee *et al.*, Phys. Rev. C **25**, 286, (1982).

3. M. Schädel *et al.*, Phys. Rev. C **33**, 1547 (1986).

Discovery of ^{261}Lr and ^{262}Lr

D.C. Hoffman, D.M. Lee, C.M. Gannett, R.A. Henderson, R.W. Lougheed, E.K. Hulet,* J.F. Wild,* K.J. Moody,* and R.J. Dougan**

We have collaborated in studies of the Lr isotopes produced via transfer reactions in bombardments at the LBL 88-Inch Cyclotron of ^{254}Es targets with ^{22}Ne projectiles. Extensive radiochemical separations involving elutions of the individual actinides from cation exchange resin columns with ammonium alpha-hydroxyisobutyrate were performed to separate the Lr fraction. Two new isotopes, ^{261}Lr and ^{262}Lr, which appear to decay by spontaneous fission (SF) with half-lives of 39 minutes and 216 minutes, respectively, were identified. The assignments to Lr were ba[illegible]n the chemical separations and

the mass assignments were based on mass separation and cross-section measurements. These isotopes are produced in sufficient quantity via transfer reactions using Es targets (50 to 70 micrograms/cm^2) to permit more detailed studies of the SF properties. Their half-lives are even longer than originally predicted in the LEAP proposal,[1] confirming the extra stability toward SF of isotopes containing an odd number of protons and/or neutrons.

Footnotes and References

*Nuclear Chemistry Division, Lawrence Livermore National Laboratory, Livermore, CA

1. D.C. Hoffman, Nucl. Instr. Meth. Phys. Res. **A249**, 13 (1986).

Atom-at-a-Time Radiochemical Separations of the Heaviest Elements: Lawrencium Chemistry*

D.C. Hoffman, R.A. Henderson, K.E. Gregorich, D.A. Bennett, R.M. Chasteler, C.M. Gannett, H.L. Hall, D.M. Lee, M.J. Nurmia, S. Cai,† R. Agarwal, A.W. Charlop, Y.Y. Chu, G.T. Seaborg, and R.J. Silva‡

The 3-minute isotope ^{260}Lr, produced in reactions of ^{18}O projectiles with ^{249}Bk at the LBL 88-Inch Cyclotron was used to perform chemical experiments on lawrencium (element 103) to learn more about its chemical properties and to verify that the 3-minute activity was indeed properly assigned to lawrencium. The experiments involved extractions with thenoyl trifluoroacetate (TTA), ammonium alpha-hydroxyisobutyrate (HIB) elutions from cation exchange resin columns and reverse-phase chromatography using hydrogen di(2-ethylhexyl)orthophosphoric acid (HDEHP). The TTA extractions were conducted at 10 different pH values in about one hundred 6- to 10-minute collections and separations. About 27 events attributable to ^{260}Lr were detected and their extraction behavior allowed us to conclude that the chemistry of the 3-minute, 8.03-MeV alpha emitter is consistent with that of lawrencium in the trivalent oxidation state and is therefore, properly assigned to lawrencium. The half-life for these events was consistent with the value of 3.0±0.5 minutes reported earlier by Eskola *et al.*[1] From another series of TTA extractions conducted so as to avoid contamination from nobelium (element 102) activities, about 45 alpha events from ^{260}Lr were detected and a cross section for its production via the ^{249}Bk(^{18}O, α3n) reaction at 102 MeV was calculated to be 8.3±1.7 nb. In the HIB elutions, the lanthanide tracer pairs Yb-Er and Tm-Ho were used to bracket the elution position of Lr. We found that it eluted only slightly later than Er and the ionic radius was calculated to be 0.0005±0.0003 nm larger than that of Er. Only 7 events were detected in 18 such experiments which were performed manually. About 6 minutes were required for chemical processing. Additional experiments using an automated system have now been performed and are described in another contribution to this report.

Footnotes and References

*Condensed from an invited talk presented by D.C. Hoffman at the International Conference on Methods and Applications of Radioanalytical Chemistry, Kona, HI (April 5-10, 1987) and LBL-23367, to be published in J. Radioanal. & Nucl. Chem.

†Institute for Atomic Energy, Beijing, Peoples Republic of China.

‡Lawrence Livermore National Laboratory.

1. K. Eskola, P. Eskola, M. Nurmia, A. Ghiorso, Phys. Rev. C **4**, 632 (1971).

Preliminary Results on the Hydrolysis and Carbonate Complexation of Dioxoplutonium(V)

D.A. Bennett, H. Nitsche, R.J. Silva, D.C. Hoffman*

The pentavalent oxidation state of plutonium is thermodynamically unstable with respect to disproportionation. As can be seen in Eq. 1, the equilibrium of the disproportionation reaction is strongly pH dependent.

$$2PuO_2^+ + 4H^+ \Longleftrightarrow Pu^{4+} + PuO_2^{2+} + 2H_2O \quad (1)$$

Until recently, essentially all plutonium chemistry was performed under acidic conditions. Consequently, Pu(V) was considered unimportant and has not been extensively investigated. However, recent solubility studies have shown that Pu(V) is a dominant soluble species in near neutral solutions. These results indicate that Pu(V) may play a major role in the possible migration of plutonium from nuclear waste repositories through interaction with ground water. Therefore, the hydrolysis (Q) and carbonate complexation (β_{11}) constants of Pu(V) are important parameters for the thermodynamic data base for geochemical modeling of safe nuclear waste disposal.

The carbonate complexation reaction has been studied by measuring the changes in the electronic absorption spectrum as carbonate is added. As shown in Fig. 1, the band at 569 nm decreases and a peak emerges at 551 nm as the carbonate concentration increases. From these experiments, log β_{11} was calculated to be 4.4±0.7. Future studies will determine if the species formed is actually a carbonate or bicarbonate complex. The hydrolysis reaction has also been investigated. There is no change in the absorbence spectrum between pH 2.45 and 7.15. Above pH 7.15, precipitation complicates the experiments. This precipitation may be the result of CO_2 absorption by the NaOH solution. Future experiments will be conducted under inert atmosphere to test this hypothesis.

Currently, precipitates from both the carbonate complexation and hydrolysis reaction are being characterized by Fourier transform infrared spectroscopy and X-ray diffraction.

Footnotes and References

*Permanent address: Lawrence Livermore National Laboratory, Livermore, CA 94550.

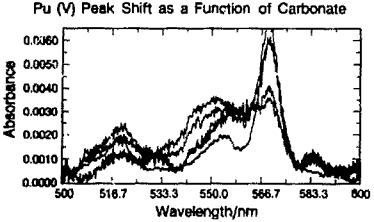

Fig. 1. See text. XBL 878-10319

Aqueous Chemistry of Element 105: Extraction*

K.E. Gregorich, R.A. Henderson, D.M. Lee, M.J. Nurmia, R.M. Chasteler, H.L. Hall, D.A. Bennett, C.M. Gannett, R.B. Chadwick, J.D. Leyba, G. Herrmann,† and D.C. Hoffman

The extraction of Ta and Nb, elements in group 5 of the periodic table, from acidic fluoride solutions into methyl isobutyl ketone (MIBK) is well known.[1] Tantalum extracts under a broader range of conditions than does niobium. If this periodic table trend were to continue, it could be expected that

element 105, in the eka-tantalum position, would extract under conditions in which tantalum is extracted. The 34-s isotope $^{262}105$ was produced via the $^{249}Bk(^{18}O,5n)$ reaction with a 100-MeV ^{18}O beam from the 88-Inch Cyclotron. The reaction products recoiling out of the target were transported via a He/KCl aerosol jet to a chemistry area where the KCl + reaction products were collected on an aluminum foil. At the end of a 90-second collection time, the foil was removed from the collection site and the activity and KCl were dissolved in 20 fl of 3.8 M HNO_3 / 1.1 M HF. This solution was added to a 1-ml centrifuge cone containing MIBK. The two phases were mixed ultrasonically and then separated by centrifuging. The MIBK phase was removed and dried on an Al disc. This disc was counted for the alpha and spontaneous events due to the decay of $^{262}105$. The chemical separation time was 50s and the procedure could be repeated every 105s. In on-line tracer experiments it was found that under these conditions, ^{172}Ta is extracted quantitatively. In 335 individual extraction experiments, no alpha particles with energies which could be assigned to the decay of $^{262}105$ or its 4.3-s daughter, ^{258}Lr, were seen. In addition, no fissions with lifetimes consistent with the $^{262}105$ half-life were seen. We calculate that if element 105 were extracted quantitatively, we should have seen 14 alpha particles and 14 fissions. Clearly, under these conditions, element 105 is not behaving like its lighter homolog, Ta. There are several possible reasons for this apparent non-tantalum like behavior, some of which may be expected of eka-tantalum. When moving down group 5 of the periodic table, the fluoride complexing strength and the tendency to hydrolyze, even in strong acid solution, increases. The fluoride complexing and/or the tendency to hydrolyze may be so much stronger in element 105 than in Ta that it forms unextractable species under conditions in which Ta is extracted. We cannot exclude the possibility that relativistic stabilization of the 7s electronic orbital could lead to 105^{3+}, which would not extract.

Footnotes and References

*Condensed from LBL-23834 (1987) (submitted to Radiochimica Acta).

†Visiting Miller Research Professor, Berkeley, Spring 1987 Institut für Kernchemie, Universität Mainz, D-6500 Mainz, Fed. Rep. of Germany.

1. P. Stevenson, H. Hicks, Anal. Chem. **25**, 1517 (1953).

Aqueous Chemistry of Element 105: Adsorption*

K.E. Gregorich, R.A. Henderson, D.M. Lee, M.J. Nurmia, R.M. Chasteler, H.L. Hall, D.A. Bennett, C.M. Gannett, R.B. Chadwick, J.D. Leyba, G. Herrmann,† and D.C. Hoffman

In the first determinations of aqueous phase chemical properties of element 105, we have made use of some chemical properties unique to the elements in group 5 of the periodic table. It has been shown that Nb adsorbs on glass surfaces from strong nitric acid solutions.[1] We have also found that Ta is adsorbed under similar conditions, while other elements are not adsorbed. We therefore expected that element 105 should behave as eka-tantalum and adsorb under these conditions. The 34-s isotope $^{262}105$ was produced via the $^{249}Bk(^{18}O,5n)$ reaction with a 101 MeV ^{18}O beam from the 88-Inch Cyclotron. The reaction products recoiling out of the target were transported via a He/KCl aerosol jet to a chemistry area where the KCl and reaction products were collected on a glass microscope cover slip. At the end of a one minute collection time, the cover slip was removed from the collection site and a 5-fl drop of 10 M HNO_3 was rapidly dried on the KCl deposit. This HNO_3 fuming process was repeated, and the KNO3 was removed (along with all non-group 5 activities) by rinsing the glass plate with dilute HNO_3.

Any aqueous phase remaining on the glass was removed by rinsing with acetone, and the glass cover slip was dried in a stream of hot air. This cover slip was then monitored for the alpha and spontaneous fission decay of adsorbed $^{262}105$ atoms. The chemical separation time was 51s and the procedure could be repeated every 75s. In 801 individual separations, 47 events due to the alpha or spontaneous fission of $^{262}105$ were observed, corresponding to a production cross section of 3.2 nb. This cross section is in agreement with $^{262}105$ cross sections from earlier work,[2,3] measured without chemical separation, indicating that under these conditions, element 105 is indeed behaving as eka-tantalum. 24 alpha decays were observed whose energies and lifetimes indicate that they are due to the decay of 34-s $^{262}105$ or its 4.3-s daughter, ^{258}Lr. The alpha particle spectrum for the first 30s of counting of the 801 samples is presented in Fig. 1. In five cases, both the parent and daughter alpha decays were seen from the same atom. We also observed 23 spontaneous fission decays with lifetimes similar to those for the $^{262}105$ alpha decay. This corresponds to a 49±13% fission branch. In one case, the alpha decay of $^{262}105$ was followed by a fission event, indicating that the daughter ^{258}Lr has an electron-capture decay branch to ^{258}No of about 11%.

Footnotes and References

*Condensed from LBL-23834, (submitted to Radiochimica Acta).

†Visiting Miller Research Professor, Berkeley, Spring 1987 *Institut für Kernchemie, Universität Mainz, D-6500 Mainz, Fed. Rep. of Germany.*

1. M. Weis, H. Denschlag, J. Inorg. Nucl. Chem. **43**, 437 (1981).

2. A. Ghiorso *et al.*, Phys. Rev. **C4**, 1850 (1971).

3. V.A. Druin, *et al.*, Sov. J. Nucl. Phys. **29**, 591 (1979).

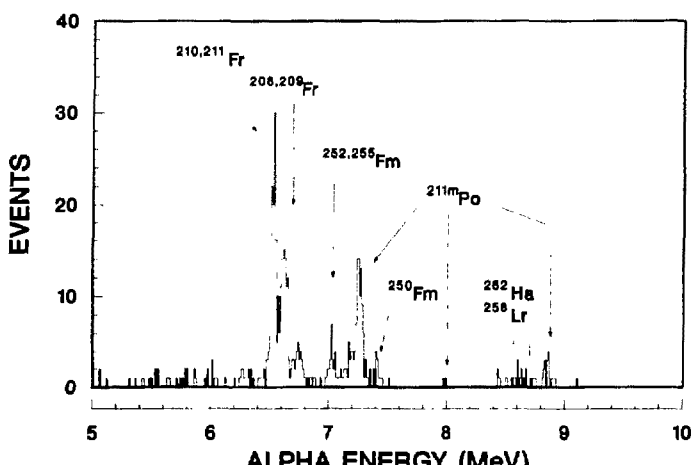

Fig. 1. A summed spectrum containing all of the alpha data from the first 30 s of counting from the 801 experiments involving the adsorption of ^{262}Ha on glass from concentrated nitric acid solutions. XBL 877-3315

Heavy Fragment Radioactivities*

P.B. Price†

This recently discovered mode of radioactive decay, like alpha decay and spontaneous fission, is believed to involve tunneling through the deformation-energy barrier between a very heavy nucleus and two separated fragments the sum of whose masses is less than the mass of the parent nucleus. In all known cases the heavier of the two fragments is close to doubly magic ^{208}Pb, and the lighter fragment has even Z. Four isotopes of Ra are known to emit ^{12}C nuclei; several isotopes of U as well as ^{230}Th and ^{231}Pa emit Ne nuclei; and ^{234}U exhibits four hadronic decay modes – alpha decay, spontaneous fission, Ne decay and Mg decay. No modes involving emission of ions heavier than Mg have yet been discovered. Table I compares measured branching ratio B (or an upper limit on B) with values predicted by several theoretical models. The bottom row gives figures of merit for the models.

Footnotes and References

*Condensed from Proceedings of Fifth International Conference on Nuclides Far from Stability, held at Rosseau Lake, Ontario, Canada, 1987.

†Also at Department of Physics, University of California at Berkeley

Table I: Nuclei with Measured Branching Ratios for Heavy Ion Decay

Decay	E_k (MeV)	Theoretical Predictions of –log B						Measured	
		Poe. I[1]	Poe. II[1]	SSI[2]	SSII[2]	PP[3]	BBB[4]	PSBR[5]	–log B	log(T1/2 sec)
^{221}Fr→ ^{14}C	29.28	12.5	11.9	11.1	13.6	14.0	-	12.5	>13.3	>15.77
^{221}Ra→ ^{14}C	30.34	11.9	12.3	11.1	13.3	13.2	10.4	12.6	>12.9	>14.35
^{222}Ra→ ^{14}C	30.97	11.0	9.6	8.8	9.7	11.7	9.1	10.5	9.43±0.06	11.02±0.06
^{223}Ra→ ^{14}C	29.85	8.7	8.9	8.2	9.7	9.6	7.3	9.6	9.21±0.05	15.2±0.05
^{224}Ra→ ^{14}C	28.63	11.9	10.4	10.2	11.0	12.5	11.1	11.3	10.37±0.12	15.9±0.12
^{225}Ac→ ^{14}C	28.57	12.2	11.6	11.8	13.7	13.1	–	12.7	>12.4	>18.34
^{226}Ra→ ^{14}C	26.46	11.7	10.2	10.5	10.2	12.2	11.8	11.1	10.6±0.2	21.33±0.2
^{230}Th→ ^{24}Ne	51.75	12.5	12.8	13.0	12.2	13.7	–	12.6	12.25±0.07	24.64±0.07
^{232}Th→ ^{26}Ne	55.37	10.8	11.0	10.4	10.4	12.0	–	11.6	>10.3	>27.94
^{232}Pa→ ^{24}Ne	54.14	10.0	12.2	11.0	11.4	11.4	12.5	11.7	11.22	23.23
^{232}U→ ^{24}Ne	55.86	10.9	11.3	10.3	10.4	12.4	13.3	11.3	11.7±0.1	21.06±0.1
^{233}U→ ^{24}Ne	54.27	10.3	12.0	10.4	11.7	11.7	12.6	10.8	12.±210.15	24.82±0.15
^{234}U→ ^{24}Ne	52.81	11.9	13.1	–	–	13.5	16.1	13.0	12.18±0.12	25.07±0.12
^{234}U→ ^{28}Mg	65.26	10.6	12.8	–	–	>13.5	21.0	12.4	12.66±0.25	25.55±0.25
^{237}Np→ ^{30}Mg	61.16	11.6	13.3	13.5	13.7	13.9	–	13.9	>13.4	>27.27
^{240}Pu→ ^{34}Si	78.07	13.3	14.8	15.6	15.2	16.2	–	15.1	>12.88	>24.25
^{241}Am→ ^{34}Si	80.60	12.4	14.3	14.3	16.1	15.4	13.1	14.9	>15.1(22);>14.1	>25.3;>24.2

1. Poenaru *et al.* 2. Shu and Świątecki 3. Pik-Pichak
4. Baranco, Broglia and Bertsch 5. Price, Stevenson, Barwick and Ravn

Search for Heavy-Ion Radioactivity from ^{241}Am*

K.J. Moody,† E.K.Hulet,† S-Ch. Wang,‡,§ P.B. Price,‡ and S.W. Barwick‡

Using phosphate glass detectors capable of withstanding a background dose of ~1014 alphas/cm^2, we have searched for rare decay modes of ^{241}Am involving emission of energetic heavy ions. Predictions of the branching ratio for ^{34}Si emission relative to alpha decay of ^{241}Am range from 4×10^{-13} to 4×10^{-15}. In a six-month exposure to 8 mg of ^{241}Am, with detectors subtending a solid angle of 2.51 ster, we detected no particles with $12 \leq Z \leq 16$, from which we infer an upper limit (2σ) of 7.4×10^{-16}.

Footnotes and References

*Condensed from a paper accepted for publication in Phys. Rev. C, Rapid Comm., 1987.

†University of California, Lawrence Livermore National Laboratory.

‡Also at Space Sciences Laboratory and Department of Physics, University of California at Berkeley.

§Also at Institute of High-Energy Physics, Academia Sinica, Beijing, China.

Table I.

Comparison of our Limit with Predictions

	log B(^{34}Si/α)
Measured limit (this work)	-15.1
Predictions of Models	
Model 1.Poenaru *et al.*	-12.4
Model 2.Poenaru *et al.*	-14.3
Model 3.Shi and Świątecki	-14.3
Model 4.Shi and Świątecki	-15.1
Model 5.Pik-Pichak	-15.4

Radioactive Decay of ^{234}U via Ne and Mg Emission*

S-Ch. Wang,†,‡, P.B. Price‡, S.W. Barwick‡, K.J. Moody, and E. K. Hulet

Using phosphate glass track detectors, we have identified three modes of radioactive decay of ^{234}U by barrier penetration (in addition to alpha decay): emission of a Ne ion, emission of a Mg ion, and spontaneous fission. Lifetimes are $(3.7^{+1.2}_{-0.9}) \times 10^{17}$ yr, $(1.1^{+1.3}_{-0.6}) \times 10^{28}$ yr and $(1.9 \pm 0.1) \times 10^{16}$ yr., respectively . This is the first example of a nuclide with four hadronic decay modes. Fig. 1 shows the measurements of etchpit sizes and ranges for Ne-decays and Mg-decays compared with curves obtained at the Superhilac using ion beams. Energies of emitted Ne and Mg ions inferred from measured ranges are consistent with Q values calculated for ^{24}Ne, ^{26}Ne, and ^{28}Mg.

Footnotes and References

*Condensed from a paper submitted to Phys. Rev. Lett., 1987.

†Also at Institute of High-Energy Physics, Academia Sinica, Beijing, China.

‡Also at Space Sciences Laboratory and Department of Physics, University of California at Berkeley.

§University of California, Lawrence Livermore National Laboratory.

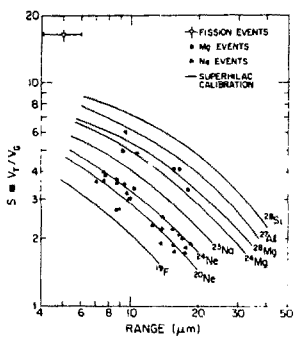

Fig. 1. See text. XBL 8710-4463

Population of High-Spin States in the Actinide Region by Heavy-Ion Transfer Reactions*

C.Y. Wu,† X.T. Liu,† J.P. Sorensen,†,‡ R.W. Kincaid,† M. W., Guidry,†,‡ D. Cline,§ W.J. Kernan,§ E. Vogt,§ T. Czosnyka,§ A.E. Kavka,§ M.A. Stoyer J.O. Rasmussen, and M.L. Halbert‡

Population of states with spin as high as 24^+ (26^+) in ^{234}U is observed in the one-neutron pickup reaction ^{235}U (^{58}Ni,^{59}Ni)^{234}U at E_{lab} = 325 MeV. The total γ-ray energy and multiplicity measured in this reaction channel indicate that transfer is populating mostly "cold" states, without appreciable fission competition. The prospect of studying high-spin states in the actinide region using even heavier projectiles is discussed, and we conclude that discrete states with spin higher than 30 may be accessible by these methods.

An obvious additional advantage of this method is that unstable nuclei which cannot be accessed by Coulomb excitation can be studied. Since the number of stable actinide nuclides which can be used for targets is severely limited, extension of the present methodology to include proton and multi-nucleon transfer would expand its use as a spectroscopic probe.

Footnotes and References

*Condensed from Physics Letters **B188**, 25 (1987).

†Department of Physics and Astronomy, University of Tennessee, Knoxville, TN 37996-1200, USA

‡Oak Ridge National Laboratory, Oak Ridge, TN 37830, USA

§Nuclear Structure Research Laboratory, University of Rochester, Rochester, NY 14627, USA

Hard Photons in Heavy Ion Collisions: Direct or Statistical

L.G. Moretto

High energy γ rays associated with intermediate-energy heavy-ion reactions were studied initially in order to observe the theoretically predicted "coherent bremsstrahlung"[1,2] associated with the collective deceleration of the two partners in the collision. However, the current interpretation of the data favors at the moment "incoherent nucleon-nucleon bremsstrahlung"[1,2] which is a process associated with the entrance channel. This interpretation is probably correct in many cases. However, there is the possibility, as yet unexplored, that some of the high energy γ rays could come from some excited compound nuclei present in the exit channel. In most experiments the exit channels are too poorly characterized to permit any serious analysis of this sort.

Fortunately in the experiment, ^{100}Mo + ^{100}Mo at 20 MeV/nucleon,[3] the exit channel has been well characterized. In this reaction the two nuclei undergo a deep inelastic collision. The dissipated energy which may amount to as much as 800 MeV (400 MeV for each fragment!) is disposed of mainly by sequential light particle emission. This emission is a true evaporation from the two deep inelastic fragments and has been studied in detail as a function of exit channel kinetic energy.[4]

The experiment measured γ rays up to 60 MeV of energy for 10 bins of total kinetic energy loss. The ungated γ rays look very much like those measured in other reactions and interpreted in terms of nucleon-nucleon bremsstrahlung. However, when these spectra are gated with different bins of total kinetic energy loss (TKEL), a very surprising picture emerges, suggesting an exit channel rather than an entrance channel origin.

In Fig. 1 three spectra are shown covering the total kinetic energy loss range of the experiment. Notice

how the high excitation energy bin is associated with the stiffest γ-ray tail while the low excitation energy bin is associated with the softest. In Fig. 2a this is shown better by plotting the slope parameters vs the TKEL. The square root-like dependence is very suggestive and one is tempted (and should be!) to interpret the slope parameter as a temperature. Similarly, the integrated multiplicites with two different lower bounds of 15 and 30 MeV γ-ray energies shown in Fig. 2b, when plotted vs the fragment excitation energy, reveal a dependence typical of compound nucleus decay.

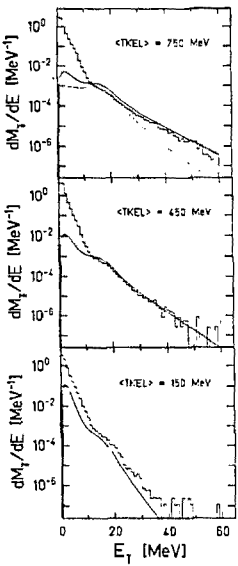

Fig. 1. Gamma ray spectra for three different bins in total kinetic enegy loss. The solid curves represent statistical model calculations. The dotted curve curve is obtained in the same way as the solid curve except for the elimination of the quasideuteron component in the γ-cross section. XBL 881-285

This evidence does not come totally unexpected. We *know* that there are two compound nuclei in the exit channel. We know that they decay as such by light particle emission and by complex fragment emission. Why should they not decay by γ-ray emission? *Perhaps* there are additional sources for the γ rays, like incoherent bremsstrahlung, etc., but we know *for sure* that *those compound nuclei must emit γ rays.* We can calculate the γ decay width in an "almost" model independent way from detailed balance and the inverse cross section:

$$P(\varepsilon_\gamma) = \frac{\Gamma(\varepsilon_\gamma)}{\hbar} \cong \frac{8\pi}{c^2h^3}\sigma(\varepsilon_\gamma)\varepsilon_\gamma^2\Theta^{-\varepsilon_\gamma/T}. \quad (1)$$

The inverse cross section is fairly well known experimentally. In the low energy region between 6 and 20 MeV, it is dominated by the giant dipole resonance, while above that the quasi deuteron mechanism prevails. The temperature T can be calculated from the excitation energy as $E_x = aT^2$. In the actual decay, γ emission competes with n, p and a particle emissions which can be calculated in a similar fashion. In this way we can generate the "first chance" γ ray emission probability vs excitation energy:

$$P_\gamma(\varepsilon_\gamma) = \frac{\Gamma(\varepsilon_\gamma)}{\Gamma_T} \cong \frac{\Gamma(\varepsilon_\gamma)}{\Gamma_n + \Gamma_p + \Gamma_\alpha + \cdots} \quad . \quad (2)$$

At this point one proceeds trivially to calculate the 2nd, 3rd etc. chance emission probability. The overall sum can be compared with experiment. In Fig. 1 we see that this calculation reproduces the spectra from 15 MeV γ-ray energy up to 60 MeV almost perfectly for all the energy bins, both qualitatively and quantitatively. The slope parameters can also be compared with the data. This is shown in Fig. 2a and again the fit is essentially perfect. The solid line in the figure represents the initial calculated temperature. The actual slope parameter is somewhat smaller due to the substantial presence of higher chance emission at the highest energies. Similarly the integrated γ-ray multiplicities are equally well reproduced by the calculation, as can be seen in Fig. 2b. The inescapable conclusion is that all of the γ rays observed experimentally actually come from

the statistical emission of the fragments. No room is left here for any other mechanism!

Somebody might object by saying, and perhaps by showing, that "other" theories fit the data almost as well and that there is no reason to choose one "theory" over another. The point is that our calculation is really no theory to speak about. We know that there are two compound nuclei in the exit channel, emitting light particles and complex fragments, because their decay products have been measured and their statistical properties verified. Therefore, we know that these compound nuclei must also emit γ rays. All we have done is to calculate, as it were, the "background" γ rays coming from compound nucleus decay. Any other "theory" can be tested only after this "background" has been substracted. In this case nothing is left and the matter is settled.

It would be interesting to check how much of the $\sigma^0, \sigma^{\pm}$ production in intermediate heavy ion reactions can be explained in terms of emission from the compound nuclei present in the exit channel. Unfortunately, this will have to wait for more complete experiments, although it is an easy guess that, in certain low energy reactions, the compound nucleus contribution may not be negligible and must be evaluated.

Footnotes and References

1. W. Cassing *et al.*, Phys. Lett. **181B**, 217 (1986).
2. H. Nifenecker *et al.*, Nucl. Phys. **A442**, 478 (1985).
3. N. Herrmann *et al.*, to be published in Phys. Rev. Lett.
4. K.D. Hildenbrand *et al.*, Proc. Int. Workshop on Gross Properties of Nuclei and Nuclear Reactions XIII, Hirschegg, 111 (1985).

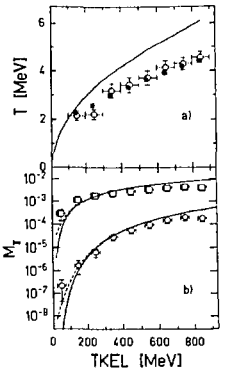

Fig. 2. a) "Temperatures" of Boltzman fits to measured (open circles) and calculated (stars) γ spectra. The solid line denotes the primary temperature of the fragments which has been calculated from the energy loss. b) Experimental and theoretical multiplicities of hard photons with energies ≥ 15 (squares) and 30 MeV (circles), respectively. The different lines are the result of a statistical model calculation and show the first chance contribution (dotted line), the sum over all generations (solid line) and the effect of the experimental binning of the excitation energy (dashed line). XBL 881-286

Compound Nucleus Interpretation of the Charge Distributions and their Energy Dependence in Intermediate Energy Reactions

R.J. Charity, M.A. McMahan, G.J. Wozniak, R.J. McDonald, L.G. Moretto, D. G. Sarantites, L.G. Sobotka,* G. Guarino,† A. Pantaleo,† L. Fiore,† A. Gobbi,† and K. D. Hildenbrand‡*

All the evidence available for intermediate-energy complex-fragment emission points rather convincingly towards a compound nucleus mechanism. However, the most compelling evidence for this mechanism lies primarily in the statistical competition between complex fragment emission and the major decay channels, like n, p, and ^{4}He emission. The simplest and most direct quantity testing this hy-

pothesis is the absolute cross section and its energy dependence.

Absolute cross sections as a function of Z value are shown in Fig. 1 for the reaction ^{93}Nb + ^{9}Be at energies up to 30 MeV/nucleon. In general, for a given system, the cross sections associated with the charge distributions increase in magnitude rapidly at low energies, and very slowly at high energy. However, the shape of the distributions is rather insensitive to the bombarding energy over the energy range explored, although one observes a flattening of the distributions with increasing bombarding energy. We have attempted to reproduce these effects quantitatively by means of a statistical calculation. Examples of these fits are shown in Fig. 2. The calculations are performed with an evaporation code GEMINI extended to incorporate complex-fragment emission. Angular-momentum dependent finite-range barriers are used.[1] All the fragments produced are allowed to decay in turn both by light particle emission or by complex fragment emission. In this way higher chance emission, as well as sequential binary emission, are accounted for. The cross section is integrated over ℓ waves up to a maximum ℓ value that provides the best fit to the experimental charge distributions. In the case of the ^{93}Nb + ^{9}Be, for bombarding energies up to 30 MeV/nucleon, the quality of the fits is exceptionally good and the fitted values of ℓ_{max} correspond very closely to those predicted by the Bass model[2] or by the extra push model.[3]

These calculations allow one to evaluate the contribution to the charge distributions of the pure evaporation residues arising solely from the emission of fragments with mass A $\leq$ 4. This contribution is shown in Fig. 2 by the dashed curves. One should note that for these asymmetric reactions below 20 MeV/nucleon, evaporation residues are predicted to be the dominant products of the compound nucleus decay. At higher bombarding energies, as incomplete fusion sets in, there is a slow decline in the complex fragment production cross section due to the relative decrease of the incomplete fusion cross section, and, more important, to the decline of the excitation energy and angular momentum. The maximum in

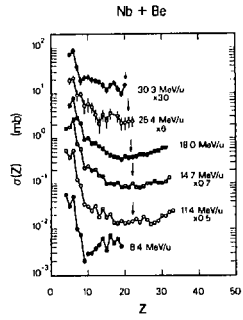

Fig. 1. Angle-integrated charge distributions of complex fragments associated with fusion-like reactions of ^{93}Nb and ^{9}Be at five bombarding energies. The arrows indicate the secondary Z-values at each bombarding energy associated with a primary symmetric division. XBL 8710-4389

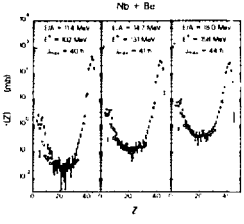

Fig. 2. Comparison of experimental and calculated charge distributions for the ^{93}Nb + ^{9}Be reaction at 11.4, 14.7, and 18.0 MeV/nucleon. The experimental data are indicated by the hollow circles and the values calculated with the code GEMINI are shown by the error bars. The dashed curve indicates the cross sections associated with classical evaporation residues which decay only by the emission of light particles ($Z \leq 2$). Note the value of the excitation energy (E*) corresponding to complete fusion and the value of J_{max} assumed to fit the data.

XBL 8710-4396

the cross section is achieved around 18 MeV/nucleon, just before the onset of incomplete fusion. Above this bombarding energy, it is possible to reproduce all the cross sections by means of compound nucleus decay of the incomplete fusion product.

This remarkable success in reproducing the absolute charge distributions over a bombarding energy range of 8.5 to 30 MeV/nucleon is also achieved for the $^{93}Nb + ^{12}C$ reaction which demonstrates that the compound nucleus mechanism characterized at the lowest energies dominates the picture at intermediate energies. It seems fair to say that, for atomic numbers between projectile and target, the compound nucleus mechanism accounts for all of the fragment emission, while for the remaining Z range it constitutes an important component, together with the quasi elastic and deep inelastic processes which are abundantly represented in this region.

Footnotes and References

*Chemistry Department, Washington University, St. Louis, MO, 63110, USA

†Istituto Nazionale di Fisica Nucleare INFN, Sezione di Bari, Italy

‡Gesellschaft für Schwerionenforschung, 6100 Darmstadt, West Germany

1. A.J. Sierk, Phys. Rev. **C33**, 2039 (1986).

2. R. Bass, Nucl. Phys. **A231** 45 (1974).

3. W.J. Świątecki, *Nucl. Phys.* **A376** 275 (1982).

Origin of Complex Fragments in the Reaction: 12.6 MeV/nucleon $^{63}Cu + ^{27}Al$

H. Han, K. Jing,* D.R. Bowman, R.J. Charity, L. Vinet,† L.G. Moretto, E. Plagnol,‡ and G.J. Wozniak*

Experiments carried out in the bombarding energy range 10–50 MeV/nucleon for reactions like La, Nb + Be, C, Al have shown that, for atomic numbers between those of the target and the projectile, complex fragments are produced almost exclusively by the decay of a compound nucleus formed either in complete or in incomplete fusion reactions. In the remaining Z range quasi and deep inelastic products dominate over compound nucleus decay products.

It is expected that compound nucleus decay should be important also for substantially lighter systems. In order to verify this expectation, we have studied the reaction $^{63}Cu + ^{27}Al$ at 12.6 MeV/nucleon in reverse kinematics. The use of reverse kinematics allows one to collect and identify fragments very efficiently due to the boost in kinetic energy of the fragments and to the rather small aperture of the kinematic cone.

The ^{63}Cu beam was provided by the 88-Inch Cyclotron by running the ECR source with a nitrogen support gas and sputtering Cu from inside the source. The fragments were detected with two quad telescopes each of which consisted of a gas ΔE detector and a solid state E detector. Both telescopes were position sensitive in the x and y coordinates.

Singles and coincidence data were taken. The large angular coverage allowed us to obtain complete plots of the cross section $\partial^2\sigma/\partial v_\parallel \partial v_\perp$ in the velocity plane $v_\parallel - v_\perp$ for each atomic number. These plots, a selection of which are shown in Fig. 1, are all characterized by a distinct Coulomb ring indicating that the process associated with fragment formation is binary. The binarity of the process has been checked also with the coincidence data. For atomic numbers below that of the target, one also sees at backward angles a lower than Coulomb velocity component attributed to quasi elastic processes. This component finds its counterpart in a forward angle higher than Coulomb velocity component asociated with the complementary fragments.

However, even if one restricts the observation to center of mass Coulomb-like velocities, one observes a backward peaking in the target-like fragments which slowly evolves into a forward peaking

for target-like fragments. Isotropy throughout the Coulomb ring is observed only for Z = 13 and 14.The systematic variations of these angular distributions suggest that a large amount of the cross section arises from deep inelastic reactions. Thus the Coulomb rings in Fig. 1 vividly illustrate a complete relaxation of the kinetic energy associated with an incomplete relaxation of the rotational modes. The downshift in atomic number of the projectile-like and target-like fragments is due to a substantial charge loss due to sequential evaporation after the deep inelastic collision. We conclude that the complex fragment production in this reaction is dominated by deep inelastic processes which seem to overwhelm the compound nucleus component.

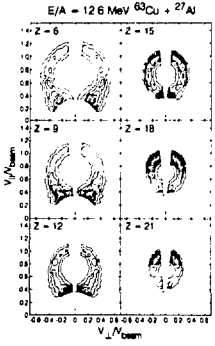

Fig. 1. Contours of the experimental cross section $\delta^2\sigma/\delta v_{\parallel}\delta v_{\perp}$ in the $v_{\parallel} - v_{\perp}$ plane for representative fragments detected in the reaction E/nucleon = 12.7 MeV ^{63}Cu + ^{27}Al. The beam direction is vertical towards the top of the figure. The dashed lines show the maximum and minimum angular thresholds and the low velocity thresholds of the detectors. The magnitude of the contour levels indicated are relative. XBL 881-8008

Footnotes and References

*Institute of Atomic Energy, Beijing, People's Republic of China

†CERN European Organization for Nuclear Research, CH-1211 Geneva 23, Switzerland

‡Institut de Physique Nucléaire, Orsay, FRANCE

Changes in Target Fragmentation Mechanism with Increasing Projectile Energy in Intermediate Energy Nuclear Collisions*

*W. Loveland,† K. Aleklett,‡ L. Sihver,† Z. Xu,† C. Casey,† D.J. Morrissey,§ J.O. Liljenzin,** M. De Saint-Simon,†† and G.T. Seaborg*

We have measured the target fragment production cross sections and angular distributions for the interaction of 16 MeV/nucleon ^{32}S, 32 MeV/nucleon ^{40}Ar and 44 MeV/nucleon ^{40}Ar with ^{197}Au. We have deduced the fragment isobaric yield distributions and moving frame angular distributions from these data. The fission cross sections decrease with increasing projectile energy (σ_f= 2190, 1770, 1150 mb, respectively) and the heavy residue cross sections (which are much larger than previous counter measurements) increase (σ_{HR}= 1380, 1790, 3720 mb). We have used the symmetry properties of the moving frame distributions to establish the relative time scale of the reaction mechanisms involved. The fission fragments associated with the peripheral collision peak in the folding angle distribution originate in a normal, slow fission process in which statistical equilibrium has been established. At the two lowest projectile energies, the fission fragments associated with the central collision peak in the folding angle distribution originate in part from fast, non-equilibrium processes. The fast non-equilibrium pro-

cess giving rise to these fragments has many of the characteristics of "fast fission" but the cross sections associated with these fragments are larger than one would expect from current theories of "fast fission."

At the highest projectile energies, there are no fission fragments associated with high momentum transfer events. The intermediate mass fragments originate primarily in events in which statistical equilibrium has not been established.

Footnotes and References

*Condensed from Phys. Rev. C (in press).

†Oregon State University, Corvallis OR 97331

‡Studsvik Neutron Research Laboratory, S-61182 Nykoping, Sweden

§Michigan State University, E. Lansing, MI 48824

**University of Oslo, Oslo, Norway

††Laboratoire Rene Bernas, F-91406 Orsay, France

Total Projectile Kinetic Energy Scaling in Energetic Nucleus-Nucleus Collisions*

W. Loveland,† Z. Xu,† C. Casey,† K. Aleklett,‡ J.O. Liljenzin,§ D. Lee, and G.T. Seaborg

The target fragment production cross sections have been measured for the reaction of 150 MeV per nucleon ^{139}La with ^{197}Au. From these cross sections, the fragment isobaric yields were deduced. The resulting isobaric yield distribution (Fig. 1) is very similar to those observed for reactions in which limiting fragmentation is occurring (such as the reaction of 8 GeV ^{20}Ne with ^{197}Au) and unlike that observed with projectiles of similar velocity. This result is another, albeit extreme, example of total projectile kinetic energy scaling. We find that this scaling is apparently a result of "conventional" physics in that it is predicted by the Yariv-Fraenkel[1] intranuclear cascade code.

We find a substantial cross section for the ^{197}Au (^{139}La, X) ^{160}Au reaction of 765±48 mb. We deduce a value of the electromagnetic dissociation cross section of 447 mb, a value substantially below the estimate of the Alder-Winther theory.[2]

Footnotes and References

*Condensed from Phys. Rev. C. (to be published).

†Oregon State University, Corvallis, OR 97331

‡Studsvik Neutron Research Laboratory, Nykoping, Sweden

§University of Oslo, Oslo, Norway

1. Y. Yariv and Z. Fraenkel, Phys. Rev. C**20**, 2227 (1979).

2. A. Winther and K. Alder, Nucl. Phys. **A319**, 518 (1979).

3. S.B. Kaufman and E.P. Steinberg, Phys. Rev. **C22**, 167 (1980).

4. D.J. Morrissey, W. Loveland, M. de Saint-Simon and G.T. Seaborg, Phys. Rev. **C21**, 1783 (1980).

5. W. Loveland, *et al.*, LBL-16280.

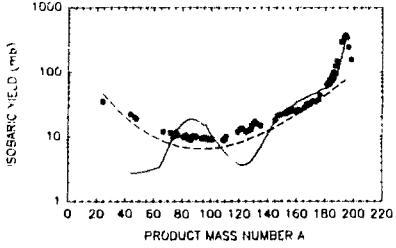

Fig. 1. Isobaric yield distributions for the fragmentation of ^{197}Au by (a) 150 MeV/nucleon ^{139}La, this work, solid points (b) 200 MeV protons,[3] dotted line (c) 8 GeV ^{20}Ne,[4] dashed line (d) 86 MeV/nucleon ^{12}C,[5] solid line.

XBL 8711-5008

Complex Fragment Emission and Associated Charged Particle Multiplicity in the Reactions 250 MeV/nucleon ^{20}Ne + Ag, Au

D.R. Bowman, W.L. Kehoe, R.J. Charity, H. Han,† K. Jing,† B. Libby,* R.J. McDonald, M.A. McMahan, A.C. Mignerey ,* L.G. Moretto, and G.J. Wozniak*

Recently a new generation of high energy light ion - nucleus experiments has been performed and some intreresting results have been presented concerning the production of complex fragments. A binary decay mechanism is required in order to account for much of the experimental data. In particular, Sangster *et al.*[1] found it necessary to include gaussian (presumably binary) components in their fits to the kinetic energy spectra of complex fragments in 1 – 6 GeV proton induced reactions. Additionally, evidence for the binary thermal fission of heavy targets (Ho and Au) following reactions with He of up to 800 MeV/nucleon has been presented.[2] In this latter study, contrary to the results from an earlier work at a somewhat higher energy,[3] binary coincidences were detected with trigger fragments of mass $10 \leq A \leq 140$.

To investigate both the decay mechanism of the excited target residue, and the process of momentum and energy deposition during the primary interaction, we have studied the emission of slow complex fragments following 250 MeV/nucleon ^{20}Ne + Ag, Au reactions. We have performed this experiment using very low threshold ($\sim$ 400 keV) ΔE - E telescopes with excellent angular ($\sim 0.2°$) and charge resolution ($Z \sim 17$). Charge, energy, and angular distributions have been measured for complex fragments from 25°to 110°in the lab, along with the associated charged particle multiplicity and sum energy in a 17 element Si array covering approximately 40 % of 49.

The preliminary results are similar to the large body of previous work in that the fragments of $4 \leq Z \leq 14$ appear to be emitted with Coulomb energies, and a representation of the invariant cross-section in the $V_{\parallel}$ - $V_{\perp}$ plane (Fig. 1) for $Z = 6$ fragments shows the striking circular distribution similar to that seen previously at much lower energies (E/nucleon $\leq$ 50 MeV),[4] suggestive of a very slowly moving source (0.6 ± 0.2 cm/ns) emitting fragments statistically in its own center-of-mass.

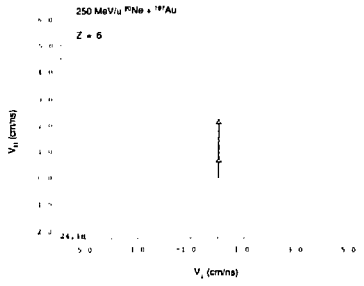

Fig. 1. Contours of the experimental cross section $\partial^2\sigma/\partial V_{\parallel}\partial V_{\perp}$ in the $V_{\parallel} - V_{\perp}$ plane for $Z = 6$ fragments detected in the reaction 250 MeV/nucleon ^{20}Ne + ^{197}Au. The beam direction is vertical. The experimentally determined source velocity (short arrow) and the velocity corresponding to full momentum transfer are shown for comparison.

XBL 8712-5358

Footnotes and References

*Department of Chemistry, University of Maryland, College Park, Maryland, 20742.

†Institute of Atomic Energy, Beijing, People's Republic of China

1 T.C Sangster *et al.*, Phys Lett **188B**, 29 (1987).

2. G. Klotz-Engmann *et al.*, Phys Lett **187B**, 245 (1987).

3. A.I Warwick *et al.*, Phys Rev **C27**, 1083 (1983).

4. D.R Bowman *et al.*, Phys Lett **189B**, 282 (1987); R.J. Charity *et al.*, LBL-22447, and accepted by Nucl. Phys.; R.J. Charity *et al.*, LBL-22448.

Fragment Flow in Nuclear Collisions

K.G.R. Doss, H.-A. Gustafsson, H. Gutbrod, J.W. Harris, B.V. Jacak, K.-H. Kampert, B. Kolb, A.M. Poskanzer, H.-G. Ritter, H.R. Schmidt, L. Teitelbaum, M. Tincknell, S. Weiss and H. Wieman

Collective nuclear flow in relativistic nucleus-nucleus collisions was initially predicted in theoretical nuclear fluid dynamics.[1] A sideways flow of light particles (Z=1,2) has since been observed[2,3] in collisions studied at the Bevalac. Several calculations predict a stronger collective flow effect for nuclear fragments than observed for light particles. Previous experiments identifying heavier fragments have only studied single fragment inclusive distributions or correlations other than fragment flow.

In this work the LBL/GSI Plastic Ball detector system was upgraded to measure light and intermediate mass fragments ($2 < Z < 10$) over a large solid angle in reactions of 200 MeV/nucleon Au + Au and Au + Fe. Computer-controlled high voltage modules were implemented allowing online gain-matching and extension of the energy loss spectra to neon fragments.

In order to study the flow of fragments, the transverse momentum analysis technique[4] was employed to determine the reaction plane of each event. In this metnod the vector difference of the transverse momentum components of particles going forward and those going backwards in the c.m. is used together with the beam axis to define the reaction plane. This difference corresponds to the collective transverse momentum transfer in the c.m. The transverse momentum $p_\perp$ of each particle is then projected onto the reaction plane, where the particle of interest has been excluded from determination of the plane (i.e., autocorrelations are removed), yielding the inplane transverse momentum p_x. For each particle the fraction of the particle's transverse momentum that lies in the reaction plane is calculated. Displayed in Fig. 1 is the mean value of the transverse momentum alignment $< p_x/p_\perp >$ in an intermediate multiplicity range for particles as as function of their rapidity for Z = 1,2,3 and 6. Positive and negative values of $< p_x/p_\perp >$ correspond to emission projected into the reaction plane, but on opposite sides. The forward-backward asymmetry is an artifact of experimental biases at low particle energies (near target rapidity) and spectator cuts in the projectile rapidity region. Since participant-spectator discrimination is not unique, the slopes of the curves at midrapidity in Fig. 1 best characterize the flow. Fig. 1 clearly shows that an increasingly larger part of the fragment's transverse momentum lies in the reaction plane as the fragment mass increases. The Z = 3,6 fragments are more aligned in the plane than the Z = 1,2 particles which are interpreted to flow collectively. Furthermore, the absolute value of the transverse momentum per nucleon projected into the reaction plane is observed to increase weakly with fragment mass.

The results provide conclusive evidence that the fragments exhibit stronger flow effects than light particles.

Footnotes and References

1. W. Scheid, H. Mueller and W. Greiner, Phys. Rev. Lett. **32**, 741 (1974).

2. H.-A. Gustafsson *et al.*, Phys. Rev. Lett. **52**, 1590 (1984).

3. R.E. Renfordt *et al.*, Phys. Rev. Lett. **53**, 763 (1984).

4. P. Danielewicz and G. Odyniec, Phys. Lett. **157B**, 146 (1985).

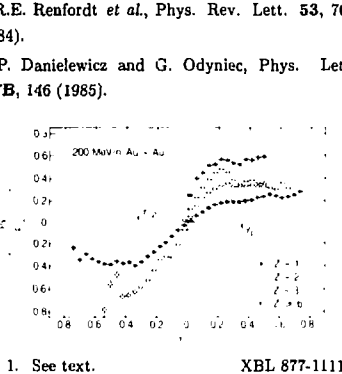

Fig. 1. See text. XBL 877-11115

Collectivity in Composite Fragment Emission from Relativistic Heavy Ion Collisions*

*R. Bock,† G. Claesson,† K. G.R. Doss, R.L. Ferguson,‡ I. Gavron,§ H. -A. Gustafsson,** H.H. Gutbrod,† J.W. Harris, B.V. Jacak,§ K. -H. Kampert,†† B. Kolb,† P. Kristiansson, F. Lefebvres, A.M. Poskanzer, H.G. Ritter, H.R. Schmidt,† T. Siemiarczuk,† L. Teitelbaum, M. Tincknell, S. Weiss, H. Wieman,† and J. Wilhelmy§*

Composite fragments of $2 < Z < 10$ have been measured in the Plastic Ball Spectrometer in 200 MeV per nucleon Au + Au and Au + Fe collisions. To answer the question whether or not the composite fragments produced in heavy ion reactions exhibit collectivity, the following variable

$$W_2 = \left|\sum_{i=1}^{n} \frac{\vec{p}_{ti}}{m_i}\right| \Big/ \sum_{i=1}^{n} \frac{|\vec{p}_{ti}|}{m_i}$$

was defined, where p_{ti} and m_i are the transverse momentum and the mass of the i^{th} composite fragment, respectively; n is the number of composite fragments in the event. W_2 measures the azimuthal alignment within the group of analyzed fragments in the event; it is equal to 1 when all particles considered are exactly aligned. We compare the experimental distribution of W_2 with a reference distribution, which we calculate on an event-by-event basis by randomizing the azimuthal angles while keeping the polar angles and lengths of momentum vectors of fragments unchanged. This ensures energy conservation and destroys possible azimuthal correlations. To demonstrate the difference between the experimental and randomized W_2 distributions, we define the correlation function:

$$R(W_2) = \frac{D(W_2) - B(W_2)}{D(W_2) + B(W_2)}$$

where $D(W_2)$ and $B(W_2)$ are the experimental and randomized W_2 distributions, respectively. They are normalized to the same area. In Fig. 1 a very distinct collective azimuthal alignment of composite fragments is observed for the Au + Au system, whereas for the Au + Fe case, the effect is very weak. Note that for the symmetric Au + Au collisions, the collective effect is observed within the group of composite fragments emitted into the forward hemisphere in the CMS.

Thus, we have demonstrated the existence of strong collective azimuthal alignment of composite fragments in the Au + Au reaction: the fragments tend to fly close together.

Footnotes and References

*Condensed from Modern Physics Letters A2, 721 (1987).

†Gesellschaft für Schwerionenforschung, Darmstadt, W. Germany

‡Oak Ridge National Laboratory, Oak Ridge, U.S.A.

§Los Alamos National Laboratory, Los Alamos, U.S.A.

**University of Lund, Lund, Sweden

††University of Münster, Münster, W. Germany

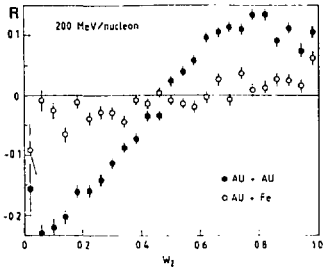

Fig. 1. The correlation function $R(W_2)$ for Au + Au (black points) and Au + Fe (open circles) at 200 MeV/nucleon. XBL 8711-4680

Transverse Energy Production in High Energy Nuclear Collisions and the Equation of State of Nuclear Matter*

K.G.R. Doss, H.A. Gustafsson,† H.H. Gutbrod,‡ K.H. Kampert,§ B. Kolb,† H. Löhner,§ B. Ludewigt, A.M. Poskanzer, H.G. Ritter and H.R. Schmidt‡

In nuclear collisions of Au+Au, Nb+Nb and Ca+Ca at bombarding energies between 150 and 800 MeV per nucleon, transverse energy and transverse momenta of light particles are studied event by event at $\vartheta = 90°$ in the center of mass system. At all energies a rise of the mean transverse energy per nucleon is observed with increasing charged particle multiplicity. Particularly large values of $E_\perp$ have been found for ^{3}He - fragments. The hydrodynamical picture is discussed for a possible separation of the collective flow and the thermal parts of the $E_\perp$ - spectrum. From this, evidence for a rather stiff equation of state is found.

Footnotes and References

*To be published in Phys. Rev. C.

†University of Lund, 522362 Lund, Sweden

‡Gesellschaft für Schwerionenforschung D-6100 Darmstadt, West Germany

§Institut für Kernphysik, D-4400 Münster, West Germany

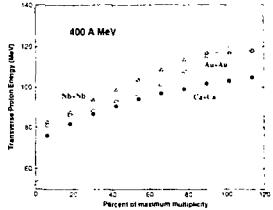

Fig. 1. Mean transverse proton energy as a function of normalized multiplicity at $\vartheta_{cm} = 90°$ for Au+Au, Nb+Nb and Ca+Ca at 400 MeV per nucleon.

XBL 8711-4681

Pion Spectra in Central La + La Collisions at 530, 740 and 1350 MeV/nucleon

G. Odyniec, J. Bartke, R. Brockmann, S.I. Chase, J.W. Harris, H.G. Pugh, G. Rai, W. Rauch, R. Renfordt,† A. Sandoval,* L.S. Schroeder, R. Stock,† H. Ströbele,* J.P. Sullivan,‡ L. Teitelbaum, M. Tincknell, and K.L. Wolf,‡*

Negative pion spectra were studied in central collisions of La + La at energies of 530, 740 and 1350 MeV/nucleon. The measurements were made using the Streamer Chamber at the Bevalac. A "super-central" trigger selected events with the least number of secondary charged particles passing through a scintillator downstream from the target (in the projectile fragmentation cone). In a geometrical model this corresponds to impact parameters b < 0.24 b max. For particles in a thermal distribution the CMS energy spectrum should follow a simple exponential law:

$$\frac{d^2N}{dEd\Omega} = \text{const.} * p * E * \exp(-E/T) \qquad (1)$$

where p is the momentum, E is the total energy of the particle and T is the temperature. The pion spectra at 90 degrees in the CMS are shown in Fig. 1 a,b,c for 530, 740 and 1350 MeV/nucleon, respectively. All spectra are corrected for electron contamination. Dashed lines correspond to a single component fit (1); the solid line in Fig.1c represents a two component fit. A single exponential law describes the data fairly well for 530 and 740 MeV/nucleon (Fig. 1a,b), however a slight enhancement in the high en-

ergy part of the spectrum is noticed. It is clear that a single exponential law is inadequate for the highest energy (Fig. 1c). The two component fit reproduces the data for 1350 MeV/nucleon very well. The parameters of the fits are shown in Table I. For 1350 MeV/nucleon the parameters of the one component fit and the two component fit are presented. R represents the fraction of the pion yield that falls in the first exponential defined by T (Fig. 1c). The χ^2 of the fits are also shown in Table I.

The interpretation of these results is not yet clear. In the Ar + KCl[1,2] reaction at 1.8 GeV/nucleon we found an indication of a second component. There the main (95±1 %) component with T=58±3 MeV could he understood in terms of cascade model calculations including Δ decay kinematics. A small (5±1 %) component with T = 110±10 MeV may be interpreted as a contribution of direct pions escaping from the early stages of hot, dense nuclear matter (fireball). In the present results the low energy part of the spectrum is again consistent with cascade calculations, but the higher component in the 1350 MeV/nucleon La + La system is much more prominent than for the 1.8 GeV/nucleon Ar + KCl.

Footnotes and References

*Gesellschaft für Schwerionenforschung, Darmstadt, Germany.

†Univ. of Frankfurt

‡Texas A&M

1. R. Brockmann *et al.*, Phys. Rev. Lett. **53**, 2012 (1984).

2. A. Sandoval *et al.*, 7th High Energy Heavy Ion Study, GSI Darmstadt, October 1984, GSI-85-10, 477 (1985).

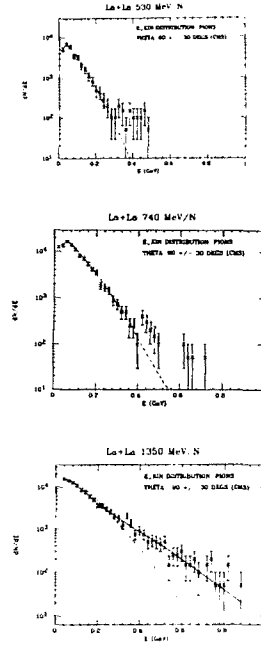

Fig. 1. Pion CMS energy spectra at 90+30 degrees for central La+La collisions at 530, 740 and 1350 MeV/nucleon. XBLs 8711-5002, 5003, 5004

Table I

$La + La \rightarrow \pi^- + X$

E/A [MeV/A]	$T(T_1)$ [MeV]	T_2 [MeV]	R [%]	χ^2 [N/ndf]
1350	58+1			3.4
	45+1	101+7	68+4	0.9
740	47+1			1.5
530	37+2			2.5

Multiplicity and Bombarding Energy Dependence of the Entropy in Relativistic Heavy-Ion Reactions*

*K.G.R. Doss, H.-A. Gustafsson,† H.H. Gutbrod,‡ D. Hahn, K.-H. Kampert,§ B. Kolb,‡ H. Löhner,§ A.M. Poskanzer, H.G. Ritter, H.R. Schmidt,† and H. Stöcker***

The yield ratios of light clusters (d,t,^{3}He,alpha) to protons were measured with the Plastic Ball spectrometer for the reactions Nb+Nb and Au+Au for incident beam energies of 150, 250, 400 and 650 MeV/nucleon. The ratios are analyzed in the framework of the Quantum Statistical Model and the specific entropy is extracted as a function of the participant proton multiplicity. A comparison of S/A at different bombarding energies gives no evidence for a significant amount of extra entropy at the lowest bombarding energy (150 MeV/nucleon) as would be expected from a phase transition. A comparison of S/A for the two colliding systems shows at all energies only little dependence on the system. A comparison with fireball and hydrodynamic mean field models gives further evidence for significant compression effects in relativistic heavy ion reactions and for a rather stiff equation of state.

†University of Lund, Lund, Sweden

‡Gesellschaft für Schwerionenforschung, Darmstadt, West Germany

§University of Münster, Münster, West Germany

**University of Frankfurt, Frankfurt, West Germany

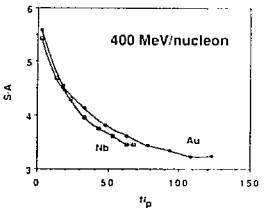

Fig. 1. Comparison of the mass dependence of S/A as a function of the participant proton multiplicity Np at 400 MeV/nucleon beam energy.

XBL 8711-4682

Footnotes and References

*Condensed from Phys. Lett. **B199**, 297 (1987).

Flow Analysis from Streamer Chamber Data

H. Ströbele, P. Danielewicz,‡ G. Odyniec, R. Bock,* R. Brockmann,* J. W. Harris, H. G. Pugh, W. Rauch, R. E. Renfordt,† A. Sandoval,* D. Schall,* S. Schroeder, and R. Stock†*

We studied reactions with Ar, La beams at 800 MeV/nucleon on KCl, La, and Pb targets with the Streamer Chamber. The standard trigger on the absence of leading fragments selected central collision events (b < 2.4 fm for Ar+KCl, b < 8.5 fm for La+La, and b < 5.5 fm for Ar+Pb). Protons are separated from deuterons by visual inspection of track density in the low momentum range or from kinematical considerations assuming fireball emission of the particles[1,2]. The flow analysis was carried out with the method described in ref. 3. The results on the mean transverse momenta in the reaction plane for deuterons are given in Fig. 1. The average forward in-plane transverse momenta per nucleon are seen to increase with the mass of the colliding system, from about 50 MeV/c for Ar+KCl, through 70 MeV/c for La+La, to 140 MeV/c for Ar+Pb. For the flow defined as a slope of <px/A>, with respect to the normalized rapidity y-ycm, we find 100 MeV/c for the Ar+KCl reaction, and 140 MeV/c for the La+La reaction. For the variation with bombarding energy, we observe that the average momenta in the Ar+KCl reaction rise from 50 MeV/c at 0.8 GeV/nucleon, through 70 MeV/c at

1.2 GeV/nucleon,[4] to 95 MeV/c at 1.8 GeV/nucleon. At the last bombarding energy the average momenta <px/nucleon> were determined from all identified nuclear fragments, as the kinematic conditions for particle separation were more favorable, and the number of deuterons was lower than in the reaction at 0.8 GeV/nucleon. In the asymmetric Ar+Pb reaction at 0.8 GeV/nucleon, it is seen in Fig. 1 that the results for <px/nucleon> agree well with the predictions of VUU calculations[5,6] with a stiff equation of state.

Footnotes and References

*Gesellschaft für Schwerionenforschung, 6100 Darmstadt, West Germany

†Institut für Hochenergiephysik, Universität Heidelberg, 6900 Heidelberg, West Germany

‡Fachbereich Physik, Universität Frankfurt, 6000 Frankfurt, West Germany

§Institute of Theoretical Physics, Warsaw University, ul. Hoza 69, 00-681 Warsaw, Poland

1. H. Stroebele, Nucl. Instr. and Meth. 221, 523 (1984).

2. P. Danielewicz *et al.*, IFT/42/87, University of Warsaw preprint.

3. P. Danielewicz and G. Odyniec, Phys. Lett. **157B**, 146 (1985).

4. D. Beavis *et al.*, Phys. Rev. C **33**, 1113 (1986).

5. J.J. Molitoris, D. Hahn, and H. Stoecker, Nucl. Phys. **A447**, 13c (1985).

6. J.J. Molitoris and H. Stoecker, Phys. Lett. **162B**, 47 (1985).

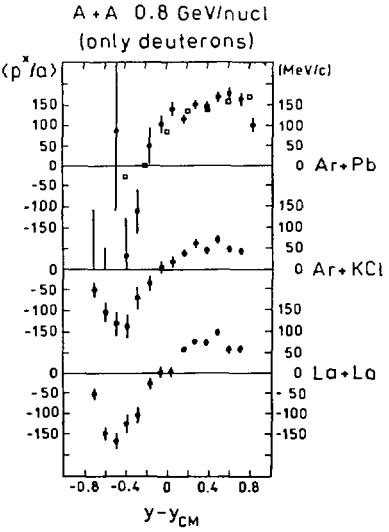

Fig. 1. Mean transverse momenta per nucleon in the reaction plane as a function of rapidity. Open squares for the Ar + Pb reaction indicate a prediction of the VUU calculation (refs. 4 and 5).

XBL 8711-4989

Systematics of Subthreshold Pion Production With Heavy Beams*

J. Miller, W. Benenson,† G. Claesson, G. Krebs, G. Landaud,‡
G. Roche, L. Schroeder, J. van der Plicht,† and J. Winfield†

Bevalac experiment 738H measured the cross-section for production of charged pions and light fragments at several beam energies below the $NN \rightarrow NN\pi$ threshold and center of mass angles between 30 and 90 degrees. During the past year we have continued the analysis of this experiment. In particular, we made detailed studies of the mass and charge dependences of the pion spectra.

The mass dependence of the differential yield, $d\sigma/d\Omega$, for negative pions at $\theta_{cm} = 90°$ is shown in Fig. 1. (The figure includes data from several experiments done on the same spectrometer.) The steep increase in the relative yield from $^{139}La + ^{139}La$ vs $^{20}Ne + NaF$ below threshold is

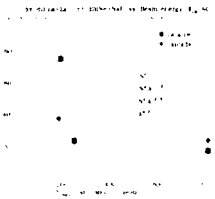

Fig. 1. Ratio of $d\sigma/d\Omega$ at $\theta_{cm} = 90°$ for π^- from ^{139}La + ^{139}La and ^{20}Ne + NaF collisions above and below threshold for three different beam energies. The results of an intranuclear cascade simulation[2] for the same systems are included for comparison. Data are from refs. 1, 3, 4 and 5. XBL 8711-4987

only partially accounted for by a collision model.

Fig. 2 illustrates the charge dependence of the pion spectra. We have studied this phenomenon in the framework of both Coulomb distortion and fragmentation models, neither of which entirely accounts for the magnitude and pion energy dependence of the effect.

It appears that a complete understanding of these dependences will require systematic studies over a range of system masses and beam energies below threshold.

Footnotes and References

*Condensed from LBL-23094.

†Michigan State University Cyclotron Laboratory

‡Université de Clermont II

1. J. Miller *et al.*, Phys. Rev. Lett. **58**, 2408 and **59**, 519 (1987).

2. J. Cugnon, Nucl. Phys. **A387**, 191 (1982).

3. S. Nagamiya *et al.*, Phys. Rev. **C24**, 971 (1981).

4. S. Nagamiya *et al.*, Phys. Rev. Lett. **48**, 1780 (1982).

5. S. Hayashi, Master's thesis, University of Tokyo (1986).

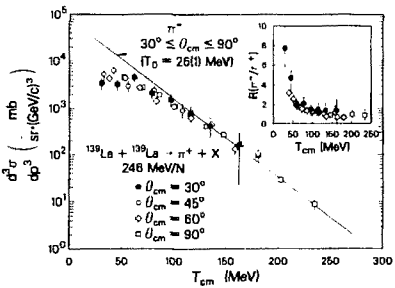

Fig. 2. Energy spectra for the reaction 246 MeV per nucleon ^{139}La + ^{139}La → π^+ + X at $\theta_{cm} = 30° - 90°$ superimposed on a fit to the π^- data from the same reaction. The inset shows the ratio of π^- to π^+ yields as a function of pion energy. XCG 872-6772A

NMR on β-emitting ^{39}Ca Produced through Projectile Fragmentation in High-Energy Heavy-Ion Collisions*

Y. Nojiri,† K. Matsuta,† T. Minamisono,† K. Sugimoto,† K. Takeyama,† K. Omata,‡ Y. Shida,‡ I. Tanihata,§ T. Kobayashi,•• S. Nagamiya,†† K. Ekuni,†† S. Shimoura,†† J.R. Alonso, G.F. Krebs, and T. J.M. Symons

A new experimental method has been developed for studies of magnetic moments of mirror nuclei in the $f_{7/2}$ region.

The method including the tilted foil technique[1] to polarize the nucleus has been developed using ^{39}Ca (I^π=3/2$^+$, $T_{1/2}$=0.86 sec), for which the magnetic moment has been previously measured.[2] A secondary beam of ^{39}Ca ion was produced through projectile fragmentation of ^{40}Ca ions. To reduce the momentum spread, a thin wedge momentum compensator was used at a momentum dispersive focussing point. Resultant energy spread at the final stopping point of

the ^{39}Ca was reduced to 3 MeV/nucleon (HWHM). Such a narrow energy spread is essential for proper utilization of the tilted foil technique.

Polarization of ^{39}Ca produced by passing through tilted foils was detected by β-ray asymmetry change using polarization destruction method in NMR technique.[3]

The resultant asymmetry change was R = 2ηAP = +(0.72± 0.24) % as sbown in the figure, where the asymmetry parameter A is predicted to be A ≈ +0.8, P is the polarization, and the correction factor for the large solid angle of the b counters is $\eta > 0.5$. A null calibration measurement gave R = -(0.11±0.24)%.

Footnotes and References

*Condensed from Proceedings of the Int. Conf. on Nucl. Struc. through Static and Dynamic Moments, Melbourne, Australia, Aug. 25-28, 98 (1987).

†Osaka University, Toyonaka, Osaka 560, Japan

‡Institute for Nuclear Study (INS), The University of Tokyo, Tanashi, Tokyo 188, Japan

§RIKEN, Wako, Saitama 351-01, Japan

**National Laboratory for High Energy Physics, Tsukuba, Ibaragi 305, Japan

††The University of Tokyo, Tokyo 113, Japan

‡‡Kyoto University, Kyoto 606, Japan

1. Y. Nojiri *et al.*, J. Phys. Soc. Japan **55 suppl.**, 391 (1986).

2. T. Minamisono *et al.*, Phys. Lett. **61B**, 155 (1976).

3. T. Minamisono, J. Phys. Soc. Japan **34 suppl.**, 324 (1973); K. Sugimoto *et al.*, Phys. lett. **18**, 38 (1965).

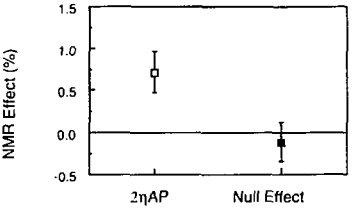

Fig. 1. NMR Effect for ^{39}Ca in CaF_2.

XBL 8712-5429

Probing the Direct Step of Relativistic Heavy Ion Fragmentation – (^{12}C,^{11}B+p) at 2.1 GeV/Nucleon with C and CH_2 targets.*

M.L. Webb,† H.J. Crawford,‡ J. Engelage,‡ M.E. Baumgartner,§
*D.E. Greiner, P.J. Lindstrom, D.L. Olson,** R. Wada††*

We have measured the momentum distributions and the excitation energy of the p,^{11}B pair in the (^{12}C,^{11}B+p) reaction at 2.1 GeV/nucleon with C and CH_2 targets. The cross section separates into three regions, (1) nucleon-nucleon quasi-elastic scattering, (2) nucleon-nucleon inelastic scattering, and (3) a low excitation energy and momentum transfer peak. The cross sections, by region, are (1) 8.8 ± 2.5 mb, (2) 10.1 ± 2.2 mb, and (3) 0.81 ± 0.45 mb for H(^{12}C,^{11}B+p)X and (1) 11.1 ± 2.4 mb, (2) 24.1 ± 3.7 mb, and (3) 4.50 ± 0.67 mb for C(^{12}C,^{11}B+p)X.

The shapes of the first two regions can be fit with a nucleon-nucleon cascade model[1] including π production. However, the cascade model prediction for the quasi-elastic component is too large by a factor of three. The low momentum transfer peak is consistent with two mechanisms, (1) an excitation and decay via proton emission of the carbon projectile and (2) a projectile proton scattering diffractively[2,3] off the C target.

Fig. 1 shows the cross section versus $-t$ for (a) C and (b) H targets. Here t is a modified Mandelstam $t = (\mathbf{p}_1 - \mathbf{p}_3)^2$, where $\mathbf{p}_1 = \mathbf{p}_{beam}/12$ before the reaction and $\mathbf{p}_3 = \mathbf{p}_{proton}$ after the reaction. The

reduced mass of a nucleon within a ^{12}C nucleus is accounted for by using $p_{beam}/12$. All p are four-vectors. The peak in Fig. 1a can be fit by e^{80t}. This is consistent with diffraction from an object with a radius of 3.66 fm, the C target. The peak in Fig. 1b is much smaller and is presumed to be due to excitation and decay of the C projectile by the H target.

Footnotes and References

*Condensed from Phys. Rev. C **36**, 193 (1987).

†Present address Lawrence Livermore National Laboratory

‡U.C. Space Science Laboratory

§Present address Hoffman-LaRoche, Basel, Switzerland

**Present address University of California at Riverside

††Present address Texas A&M University

1. J. Cugnon, Phys. Rev. C **22**, 1885 (1980).

2. K. Goulianos, Physics Reports **101**, 169 (1983).

3. W. Czyż, Advances in Nuclear Physics **4**, 61 (1971).

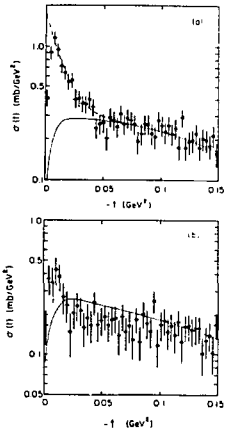

Fig. 1. Data cross section versus modified $-t$ (see text) for (a) C and (b) H targets. The solid lines are natural spline fits to the normalized Monte Carlo cascade model. The dashed line shows the effect of adding an e^{86t} component to the Monte Carlo cascade model results. XBL 8612-4815

Fragmentation of 1.65 GeV/nucleon ^{40}Ar at HISS

C. Tull,,† T. Kobayashi,† M. Baumgartner, F.P. Brady,† W. Christie,*,† H.J. Crawford,§ J.P. Dufor,** D.E. Greiner, P.J. Lindstrom, W.F.J. Müller, D.L. Olson,†† J. Romero,† T.J.M. Symons, I. Tanihata,‡‡ M. Webb,§§ and H. Wieman*

We have measured the fragmentation of three heavy beams (^{40}Ar, ^{56}Fe, and ^{93}Nb) at 1.65 GeV per nucleon and one beam (^{139}La) at 0.85 GeV/nucleon on targets of carbon, lead, and a target of the same size as the beam. Preliminary analysis of the ^{40}Ar data indicates that the data set provides an important extension of previous studies with medium-light ions.[1,2] Using the HISS facility at the Bevalac, we were able to accurately identify the isotope of each projectile rapidity fragment ($\Delta Z \approx 0.2$ e, and $\Delta A \approx 0.3$ u for Z=4–18), and measure its momentum in all three cartesian coordinates (Δ p / p $\approx 2 \times 10^{-3}$), as well as measure the multiplicity of mid-rapidity charged particles between theta $\approx 10° - 70°$ from the beam in the laboratory frame.

Fig. 1 shows the raw isotopic yields for the even charge fragments from 1.65 GeV/nucleon ^{40}Ar + C. Even without corrections for trigger bias or detector acceptances, one sees that they follow gaussian distributions similar to those seen at lower energy.[2]

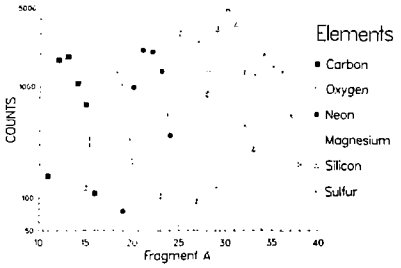

Fig. 1. The populations of isotopes of the even charged elements from carbon to sulfur shown here are gaussian in shape. Detector acceptance reduces the low A yields and trigger bias affects the high Z yields. XBL 8712-5162

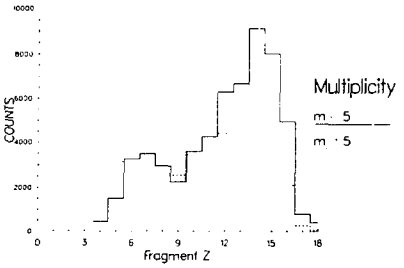

Fig. 2. The distribution of leading fragment charge for events with high multiplicity (m≥5), and with low multiplicity (m<5), as measured by the Multiplicity Array. XBL 8712-5163

Momentum distributions of the fragments are gaussian in shape in the longitudinal direction, and in each of the transverse directions. When analyzed in the context of Goldhaber's statistical model,[3] the average reduced momentum widths are consistent with a Fermi momentum of ≈240 MeV/c; comparable to the measured value of 251 ± 5 MeV/c for ^{40}Ca.[4]

Also addressed in the current experiment is the correlation between two "measures" of the collision impact parameter. Fig. 2 shows the distribution of leading fragment charge with different requirements on the multiplicity measured by our multiplicity array. The distribution for low multiplicity events (m<5) peaks at high charge, whereas the high multiplicity events (m≥5) are more strongly correlated with low fragment charge.

Preliminary results have been presented at the Oct. 1987 APS meeting in New Brunswick, and at the 8th High Energy Heavy Ion Study in Berkeley. Analysis is proceeding on the ^{40}Ar data and is commencing on the ^{93}Nb data. Final results should be available in Craig Tull's Ph.D. dissertation in 1988.

Footnotes and References

*Associated Western University Graduate Fellow

†Crocker Nuclear Laboratory, University of California, Davis, CA 94720.

‡National Laboratory for High Energy Physics (KEK), JAPAN.

§Space Science Laboratory University of California, Berkeley, CA 94720.

**Centre d'Etudes Nucléaires de Bordeaux-Gradignan, FRANCE.

††Heavy Ion Physics, University of California, Riverside, CA 92521.

‡‡Institute for Nuclear Study, University of Tokyo, Tokyo, JAPAN.

§§Lawrence Livermore Laboratory, Livermore, CA 94550.

1. D.E. Greiner, *et al.*, Phy. Rev. Lett. **35**, 152 (1975).

2. Y.P. Viyogi, *et al.*, Phys. Rev. Lett. **42**, 33 (1979).

3. A.S. Goldhaber, Phys. Lett. **53B**, 306 (1974).

4. E.J. Moniz, *et al.*, Phys. Rev. Lett. **26**, 445 (1971).

Bevalac Experiment E517H

D. Olson

The results of Bevalac experiment E517H, **Electromagnetic Dissociation of ^{16}O**, were presented at the APS meeting in Crystal City, Virginia in April, 1987. A paper describing these results is in process and should be completed soon. This is a coincidence experiment looking at the reaction T(^{16}O,^{15}N+p)X at 2.1 GeV/nucleon for the targets (T) U, Cu, and Be. Relative cross sections for the proton energy spectra (as measured in the ^{15}N+p rest frame) have been determined, see Fig. 1.

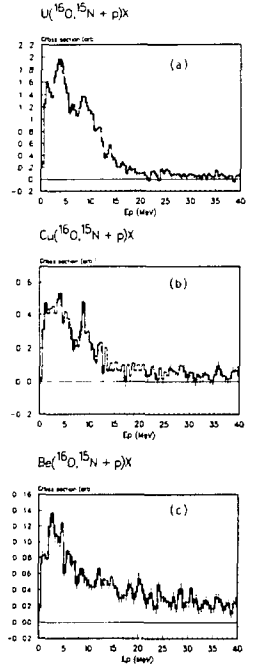

Fig. 1. Relative cross sections ($d\sigma/dE_p$) for the proton energy spectra for the reactions T(^{16}O,^{15}N+p) for U (a), Cu (b), and Be (c) targets.

XBL 8711-5028

By taking the difference between targets one can eliminate the component due to nucleon-nucleon diffractive scattering. The resulting spectrum is composed of both the electromagnetic dissociation contribution and a low energy peak which results from the difference in the nucleon-nucleus diffractive scattering between different targets.[1] See Fig. 2.

Footnotes and References

1. M.L. Webb, H.J. Crawford, J. Engelage, M.E. Baumgartner, D.E. Greiner, P.J. Lindstrom, D.L. Olson, R. Wada, Phys. Rev. **C36**, 193 (1987).

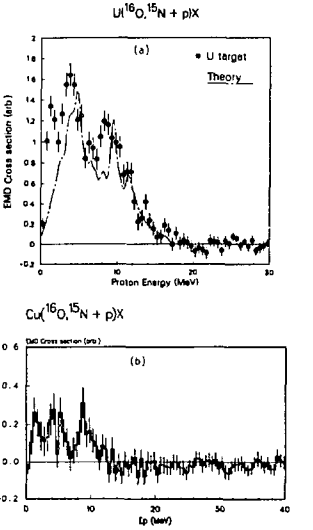

Fig. 2. Subtracted cross sections ($d\sigma(T)/dE_p - C \cdot d\sigma(Be)/dE_p$) where the normalization constant C is ratio (T/Be) of the integrated cross section for 50 MeV < E_p < 100 MeV, for U (a) and Cu (b) targets.

XBL 8711-5029

LAMPF 645: A Search for Neutrino Oscillations

S.J. Freedman, J. Napolitano,* B.K. Fujikawa,† R. McKeown,† K.T. Lesko, R.D. Carlini,‡ J.B. Donahue,‡ G.T. Garvey,‡ V.D. Sandberg,‡ W.C. Choi,§ A. Fazely,§ R.L. Imlay,§ W.J. Metcalf,§ L.S. Durkin,** R.W. Harper,** T.Y. Ling,** J.W. Mitchell,** T.A. Romanowski,** E.S. Smith,** and M. Timko***

The phenomenon of neutrino oscillations has been actively sought experimentally in recent years. Neutrinos of a given type may oscillate into another type if one or more of the neutrino types are massive and if the separate lepton-number-conservation rules are violated. For the past two years we have been searching for the appearance of $\bar{\nu}_e$ originating from the almost pure beam of $\bar{\nu}_\mu$, ν_μ, and ν_e obtained from Los Alamos Meson Physics Facility's beam dump. This reaction is detected by observing products from inverse beta decay, $\bar{\nu}_e + p \Rightarrow e^+ + n$. A 20 ton modular detector with both tracking and energy information was shielded from cosmic ray events with 4π passive and active shielding. Activity in both the shield and the detector is recorded for 53μs before and 107 μs after each trigger. With the completion of this year's run cycle we have succeeded in reducing our backgrounds to very close to our design specifications of 0.1 events/LAMPF-day. Analysis of the data is underway as well as plans for acquiring additional data. The preliminary analysis is very promising and we anticipate achieving a significant result this year.

Footnotes and References

*Argonne National Laboratory, Argonne IL 60439

†California Institute of Technology, Pasadena, CA 91124

‡Los Alamos National Laboratory, Los Alamos, NM 70803

§Lousiana State University, Baton Rouge, LA 70803

**Ohio State University, Columbus, OH 43210

Cross Sections and Multiplicities for Charged Particles in High Energy Nuclear Collisions

NA35 Collaboration

A. Bamberger, D. Bangert,† J. Bartke,‡ H. Bialkowska,§ R. Bock,** R. Brockmann,** S.I. Chase, C. De Marzo,†† M. De Palma,†† I. Derado,‡‡ V. Eckardt,‡‡ C. Favuzzi,†† J. Fendt,‡‡ D. Ferenc,§§ H. Fessler,†† P. Freund,‡‡ M. Gazdzicki,*** H.J. Gebauer,‡‡ K. Geissler,† E. Gladysz,‡ C. Guerra,** J.W. Harris,††† W. Heck,‡‡‡ T. Humanic,** K. Kadija,§§ A. Karabarbounis,§§§ R. Keidel,**** J. Kosiec,†††† M. Kowalski,‡ S. Margetis,*** E. Nappi,†† G. Odyniec, G. Paic,§§ A.D. Panagiotou,§§§,† A. Petridis,§§§ J. Pfennig,‡‡‡ F. Posa,†† K.P. Pretzl,‡‡ H.G. Pugh,‡‡‡‡ F. Pühlhofer,**** G. Rai, A. Ranieri,†† W. Rauch, R. Renfordt,‡‡‡ D. Röhrich,**** K. Runge,* A. Sandoval,** D. Schall,** N. Schmitz,‡‡ L.S. Schroeder, G. Selvaggi,†† P. Seyboth,‡‡ J. Seyerlein,‡‡ E. Skrzypczak,†††† P. Spinelli,†† R. Stock,†,‡‡‡ H. Ströbele,†,** A. Thomas,‡‡‡ M. Tincknell, L. Teitelbaum, G. Veszterqombi,‡‡,§§§§ D. Vranic,** and S. Wenig‡‡‡*

Charged particle production has been studied in collisions of 60 and 200 GeV/nucleon ^{16}O from the CERN SPS with nuclear targets. First results from this experiment have been published.[1] The experimental setup is described in ref. 2. The data presented here are based on the scanning and measuring of film from streamer chamber events. The streamer chamber was located in a 1.5 T magnetic field with Al, Cu, Ag and Au targets of 1 percent interaction thickness positioned 8 cm upstream from the chamber entrance. Most of the data reported here represent minimum bias samples with only an interaction trigger. The scanning efficiency, which is a function of the multiplicity, was determined on the basis of

double scanning part of the film in different laboratories and scanning of simulated events where true multiplicities were known. Corrections were made for the scanning efficiency, e^+e^- from gamma conversion in the target, secondary interactions and unresolved neutral particle decays. Due to the location of the target outside the chamber, all multiplicities pertain only to particles emitted in the $\Theta_{lab} < 60°$ forward cone. The experimental results can be summarized as follows: 1) The interaction cross sections are independent of the incident energy from 60 to 200 GeV/nucleon and follow a geometrical $A_p^{2/3} + A_t^{2/3}$ dependence on the nuclear radii. 2) The multiplicity of negative particles in oxygen-nucleus collisions, when normalized to that of pp collisions, does not depend upon the incident energy. 3) The dispersion of the negative particle multiplicity distributions for oxygen-nucleus collisions is proportional to the multiplicity and is larger in nucleus-nucleus collisions than in pp collisions. This can be seen in Fig. 1. The dispersion is also observed to decrease for central collisions, i.e., at small impact parameters. Furthermore it can be stated that the data are consistent with a simple superposition of independent nucleon-nucleus collisions, however the data are only qualitatively reproduced by existing theoretical models.

Footnotes and References

*Fakultät für Physik, Universität Freiburg, D-7800 Freiburg, Germany

†CERN, CH-1211 Geneva 23, Switzerland

‡Institute of Nuclear Physics, PL-30055 Cracow, Poland

§Institute of Nuclear Studies, PL-00681 Warszawa, Poland

**Gesellschaft für Schwerionenforschung, D-6100 Darmstadt 11, Germany

††Dipartimento di Fisica, Universita di Bari, and INFN, Bari Italy

‡‡Max-Planck-Institut für Physik und Astrophysik, D-8000 München, Germany

§§Rudjer Boskovic Institute, 41001 Zagreb, Yugoslavia

***Institut für Hochenergiephysik, Universität Heidelberg, D-6900 Heidelberg 1

†††A. v. Humboldt Foundation Fellow

‡‡‡Fachbereich Physik, Universität Frankfurt, D-6000 Frankfurt, Germany

§§§Physics Department, University of Athens, 157-71 Athens, Greece

****Fachbereich Physik, Universität Marburg, D-3550 Marburg, Germany

††††Institute of Experimental Physics, University of Warsaw, Warszawa, Poland

‡‡‡‡A. v. Humboldt Foundation U.S. Senior Scientist Award recipient

§§§§On leave of absence from Central Research Institute for Physics, Budapest, Hungary

1. A. Bamberger *et al.*, Phys. Lett. **B184**, 271 (1987).

2. A. Sandoval *et al.*, Nucl. Phys. **A461**, 465c (1987).

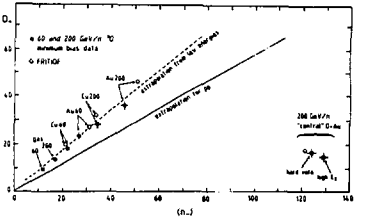

Fig. 1. Values of the dispersion vs average multiplicity of negative secondaries from inelastic collisions of ^{16}O with several target nuclei. The solid line represents the dependence of the dispersion on the mean negative multiplicity for pp collisions and the dashed line the same dependence for nucleus-nucleus collisions at Bevalac energies. Values obtained from the FRITIOF Lund Model simulation are also shown. XBL 8711-5031

Search for Free Quarks Produced by 14.5 GeV/nucleon Oxygen Ions*

*Howard S. Matis, George P. Alba,† Roger W. Bland,† Stephanie C. Dickson,† Christopher L. Hodges,† Robert T. Johnson,† Michael A. Lindgren,†,‡ Teresa L. Palmer,† Howel G. Pugh, Gordon L. Shaw,§ Richard Slansky,** David C. Stricker†*

Arguments have been given[1] that relativistic heavy ion collisions might be a much more favorable environment to produce free fractional charge than elementary particle interactions because the collision region could be much larger than one fermi. Fractional charge could be in the form of $\frac{1}{3}$e or $\frac{2}{3}$e charged particles or even in the form of charge $\frac{4}{3}$e diquarks.

An experiment was carried out to detect free quarks produced in collisions of 14.5 GeV/nucleon oxygen nuclei with a heavy target at BNL. The experiment was sensitive to any produced particle with fractional charge. Secondaries from the collisions were stopped in four liquid argon tanks, and charged atoms were collected electrostatically on gold coated electrodes. The gold coatings were dissolved in mercury. The Hg was then tested for quarks in the SFSU automated Millikan apparatus.

In Fig. 1, the distribution of residual charge (the non-integral part of the calculated charge) for the 29,971 drops that passed all tests is shown. All of the measurements except one lie in a Gaussian distribution of width 0.05e, representing integrally charged drops. The remaining measurement (shaded) is a test event used to measure the efficiency of the apparatus. Thus, there is no evidence for free fractional charge in this sample. The resulting upper limit is one quark produced per 1×10^9 incident oxygen ions at 90% Confidence Limit.

Footnotes and References

*Condensed from LBL-23034. To be published in Phys. Rev. D. December 1, 1987

†Physics and Astronomy Department, San Francisco State University, San Francisco, CA 94132

‡Present address: EP division, CERN, 1211 Geneva, Switzerland

§Physics Department, University of California, Irvine, CA 92717

**Los Alamos National Laboratory, Los Alamos, NM 87545

1. G.L. Shaw and R. Slansky, Phys. Rev. Lett. **50**, 1967 (1983)

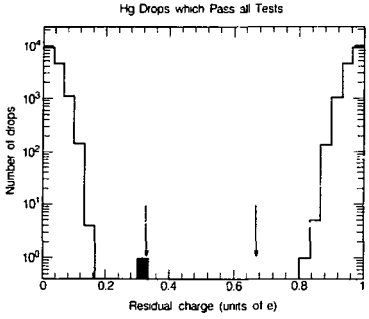

Fig. 1. Histogram of the residual (non-integral) charge for all mercury drops which passed the final cuts. The arrows point to where a charge $|\frac{1}{3}e|$ or $|\frac{2}{3}e|$ drop would lie. The crosshatched region represents a test event. There are no background events near the two arrows. XBL 873-8827

Forward and Transverse Energy Distributions in Oxygen-Induced Reactions at 60 GeV/nucleon and 200 GeV/nucleon*

WA80 Collaboration

*R. Albrecht,† T.C. Awes,‡ C. Baktash,† P. Beckmann,§ F. Berger,§ R. Bock,† G. Claesson,† L. Dragon,§ R.L. Ferguson,† A. Franz, S. Garpman,** R. Glasow,§ H.A. Gustafsson,** H.H. Gutbrod,† K.H. Kampert,§ B.W. Kolb,† P. Kristiansson, I.Y. Lee,‡ H. Löhner,§ I. Lund,† F. E. Obenshain,‡,9 A. Oskarsson,** I. Otterlund,** T. Peitzmann,§ S. Persson,** F. Plasil,‡ A.M. Poskanzer, M. Purschke,§ H.G. Ritter, R. Santo,§ H.R. Schmidt,† T. Siemiarczuk,† S.P. Sorensen,‡,11 E. Stenlund,** and G.R. Young‡*

Results are presented from reactions of 60 GeV per nucleon and 200 GeV per nucleon ^{16}O projectiles with C, Cu, Ag, and Au nuclei. Energy spectra at zero degrees and transverse energy distributions in the pseudorapidity range from 2.4 to 5.5 (Fig. 1) were measured. The importance of the collision geometry is stressed. Average total participant numbers are extracted and used to show that the average transverse energy per participant is nearly independent of target mass at a given bombarding energy. Estimates of stopping and of energy densities have been made. It is concluded that conditions required for the formation of the quark-gluon plasma may have been achieved in some of the most central collisions of $^{16}O+^{197}Au$ at 200 GeV per nucleon.

Footnotes and References

*To be published in Phys. Lett. B.

†Gesellschaft für Schwerionenforschung (GSI), D-6100 Darmstadt, West Germany.

‡Oak Ridge National Laboratory, Oak Ridge, Tennessee 37831, USA.

§University of Münster, D-4400 Münster, West Germany.

**University of Lund, S-22362 Lund, Sweden.

††University of Tennessee, Knoxville, TN 37996, USA.

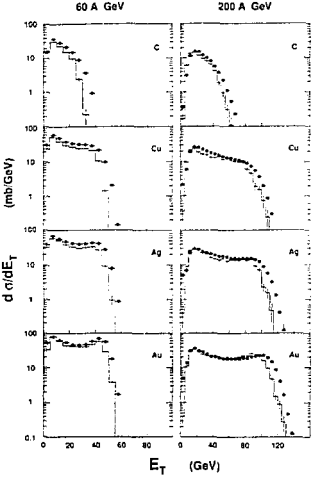

Fig. 1. Transverse energy distributions (filled circles) measured in the pseudorapidity range of $2.4 < \eta < 5.5$ for 60 GeV/nucleon and 200 GeV/nucleon ^{16}O projectiles incident on targets of C, Cu, Ag, and Au. Histograms give the results of the FRITIOF model.

XBL 8711-4679

Charged Particle Distributions in ^{16}O Induced Nuclear Reactions at 60 and 200 GeV/nucleon

WA80 Collaboration

R. Albrecht,† T.C. Awes,‡ C. Baktash,‡ P. Beckmann,§ F. Berger,§ R. Bock,† G. Claesson,†
*L. Dragon,§ R.L. Ferguson,‡ A. Franz, S. Garpman,**B.W. Kolb,† P. Kristiansson, R. Glasow,§*
*H.A. Gustafsson,** H.H. Gutbrod,† K.H. Kampert,§ I.Y. Lee,‡ H.Löhner,§ I. Lund,† F.E. Obenshain,‡*
*A. Oskarsson,** I. Otterlund,** T. Peitzmann,§ S. Persson,** F. Plasil,‡ A.M. Poskanzer, M. Purschke,§*
*H.G. Ritter, R. Santo,§ H.R. Schmidt,† T. Siemiarczuk,† S.P. Sorensen,‡,†† E. Stenlund,** and G.R. Young‡*

Results from ^{16}O induced nuclear interactions with C, Cu, Ag and Au at 60 and 200 GeV/nucleon are presented. Multiplicity and pseudo-rapidity density distributions of charged particles and their dependence on the target mass number are reported. Events with more than 450 charged particles have been observed. Particularly at 200 Gev/nucleon the Fritiof model underestimates the cross section for the highest multiplicities. The pseudo-rapidity value where the particle density reaches its maximum is observed to shift backwards as the target mass increases. This behavior is in qualitive agreement with the Fritiof model. We observe an excess in the particle yield in the central rapidity region which is emphasized at 200 GeV/nucleon and not explained by the model. The target dependence of the particle yield in central collisions is found to vary strongly between different angular regions. Although the particle yield increases as the energy increases, the influence of the target is the same at both energies. E_t/charged particle is essentially independent of energy, target mass and centrality of the interaction. Particle densities up to 160 charged particles per pseudo-rapidity unit are reached, which implies energy densities above 3 GeV/fm^3 are achieved.

Footnotes and References

†Gesellschaft für Schwerionenforschung (GSI), D-6100 Darmstadt, West Germany.

†Oak Ridge National Laboratory, Oak Ridge, Tennessee 37831.

§University of Münster, D-4400 Münster, West Germany.

**University of Lund, S-22362 Lund, Sweden.

††University of Tennessee, Knoxville, Tennessee 37996.

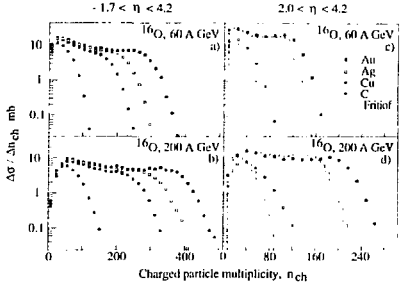

Fig. 1. Differential cross-sections for observing n_{ch} charged particles from ^{16}O induced interactions with various targets at a) 60 GeV/nucleon, b) 200 GeV/nucleon, c) 60 GeV/nucleon with $\eta > 2$, and d) 200 GeV/nucleon with $\eta > 2$. In c) and d) comparisons with the Fritiof model are made.

XBL 8711-4822

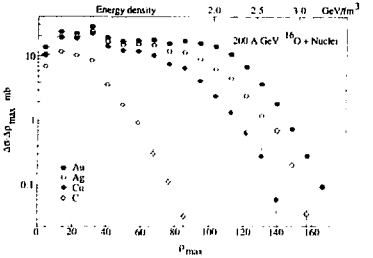

Fig. 2. Pseudo-rapidity density in various events for ^{16}O+Au reactions at 60 and 200 GeV/nucleon incoming energy. The upper axis shows the estimated energy density.

XBL 8711-4821

Photon and Neutral Pion Distributions in 200 GeV/nucleon ^{16}O + Nucleus and Proton + Nucleus Reactions*

WA80 Collaboration

*R. Albrecht,† T.C. Awes,‡ C. Baktash,‡ P. Beckmann,§ F. Berger,§ R. Bock,† G. Claesson,† L. Dragon,§ R.L. Ferguson,‡ A. Franz, S. Garpman,**B.W. Kolb,† P. Kristiansson, R. Glasow,§ H.A. Gustafsson,** H.H. Gutbrod,† K.H. Kampert,§ I.Y. Lee,‡ H.Löhner,§ I. Lund,† F.E. Obenshain,‡ A. Oskarsson,** I. Otterlund,** T. Peitzmann,§ S. Persson,** F. Plasil,‡ A.M. Poskanzer, M. Purschke,§ H.G. Ritter, R. Santo,§ H.R. Schmidt,† T. Siemiarczuk,† S.P. Sorensen,‡,†† E. Stenlund,** and G.R. Young‡*

The transverse momentum (p_T) distributions of inclusive photons at midrapidity are measured with a lead glass calorimeter in 60 and 200 GeV/nucleon ^{16}O + nucleus and proton + nucleus reactions. The variation of the average transverse momentum is investigated as a function of centrality, determined by measurements of transverse energy and charged particle multiplicity. For small values of the entropy, deduced from the multiplicity density, an increase in average p_T is observed which rises to a plateau for larger values of entropy for ^{16}O + Au at 200 GeV/nucleon. This deviation from a purely linear increase with entropy density has features expected in the presence of a phase transition. The π^0 p_T distributions show two components, a low p_T one with an inverse slope of about 150 MeV/c and a high p_T component with a flatter slope dependent slightly on target mass.

Footnotes and References

Condensed from Phys. Lett. **B201**, 390 (1988).

†Gesellschaft für Schwerionenforschung (GSI), D-6100 Darmstadt, West Germany.

‡Oak Ridge National Laboratory, Oak Ridge, Tennessee 37831, USA.

§University of Münster, D-4400 Münster, West Germany.

**University of Lund, S-22362 Lund, Sweden.

††University of Tennessee, Knoxville, Tennessee 37996.

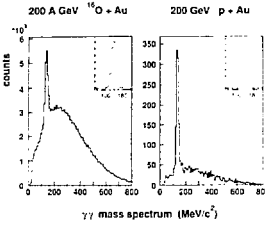

Fig. 1. Invariant mass spectra of $\gamma\gamma$ pairs for ^{16}O + Au and p + Au at 200 GeV/nucleon. Only photons with $E_\gamma > 500$ MeV and $p_{T_{\gamma\gamma}} > 1$ GeV/c are considered. The insets show the π^0 peak after background subtraction. XBL 8711-4691

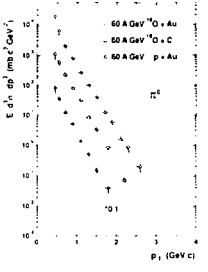

Fig. 2. Invariant cross sections for π^0 as a function of p_T from proton and oxygen induced reactions at 200 and 60 GeV/nucleon measured in $1.5 \leq \eta \leq 2.1$ for different target masses. XBL 8711-4690

Transverse Momentum Distributions from One-View Measurements of NA35 Streamer Chamber Pictures

NA35 Collaboration

A. Bamberger, D. Bangert,† J. Bartke,‡ H. Bialkowska,§ R. Bock,** R. Brockmann,** S.I. Chase, C. De Marzo,†† M. De Palma,†† I. Derado,‡‡ V. Eckardt,‡‡ C. Favuzzi,†† J. Fendt,‡‡ D. Ferenc,§§ H. Fessler,‡‡ P. Freund,‡‡ M. Gazdzicki,*** H.J. Gebauer,‡‡ K. Geissler,† E. Gladysz,‡ C. Guerra,** J.W. Harris,††† W. Heck,‡‡‡ T. Humanic,** K. Kadija,§§ A. Karabarbounis,§§§ R. Keidel,**** J. Kosiec,†††† M. Kowalski,‡ S. Margetis,*** E. Nappi,†† G. Odyniec, G. Paic,§§ A.D. Panagiotou,§§§,† A. Petridis,§§§ J. Pfennig,‡‡‡ F. Posa,†† K.P. Pretzl,†† H.G. Pugh,†††† F. Pühlhofer,**** G. Rai, A. Ranieri,†† W. Rauch, R. Renfordt,‡‡‡ D. Röhrich,**** K. Runge,* A. Sandoval,** D. Schall,** N. Schmitz,‡‡ L.S. Schroeder, G. Selvaggi,†† P. Seyboth,‡‡ J. Seyerlein,‡‡ E. Skrzypczak,†††† P. Spinelli,†† R. Stock,†,‡‡‡ H. Ströbele,†,** A. Thomas,‡‡‡ M. Tincknell, L. Teitelbaum, G. Vesztergombi,‡‡,§§§§ D. Vranic,** and S. Wenig‡‡‡*

Analysis of the NA35 streamer chamber data taken at CERN is in progress. A part of this effort was devoted towards extracting the transverse momentum (P_t) distribution of particles from a single view measurement of tracks and avoid the arduous steps of track recognition and matching in three views and the subsequent three dimensional space point reconstruction. This approach was motivated by the need to obtain a quick analysis of the data in order to reveal any unusual features of the data and potentially interesting physics. Such data runs may be identified at an early stage and later subject to careful scrutiny.

A typical central collision event is shown in Fig. 1. The beam direction is identified along the z-axis, whereas the x axis is orthogonal to the z-axis. The y-axis is along the magnetic field axis forming a right handed coordinate system. All tracks were measured and fitted. For each negatively charged particle, the component of its momentum along the x-axis is calculated and a histogram constructed. The procedure was applied to 87 central events from oxygen on gold collisions at 60 GeV/nucleon incident beam energy. The projected P_x distribution is shown in Fig. 1.

The P_t and P_x distributions are related by the matrix equation $Y = A \cdot X$ where X is a vector containing the elements of P_x and Y is the solution vector containing the unfolded P_t distribution. The coefficients of the transformation matrix A are easily calculated assuming azimuthal symmetry about the beam direction. The Matrix Inversion (MI) and Maximum Likelihood (ML) procedures[1] were investigated for obtaining the solution. The former simply involves inverting the matrix A using conventional techniques. The disadvantage of this method is that the solution is sensitive to 'noise', that is, the statistical fluctuations in P_x. Indeed, the solution vector (P_t) may contain negative counts. In short, the MI method does not guarantee 'positivity' and requires large statistics for a 'safe' reconstruction. The ML technique is an iterative solution to the problem and avoids all the shortcomings associated with MI. Positivity is guaranteed everywhere and the procedure converges rapidly to the solution. The unfolded P_t distribution is overlaid as crosses in Fig. 1. As a consistency check, the average value of P_x is 205 MeV/c and one expects a mean P_t value of $\pi * < P_x > /2 =$ 323 MeV/c. The actual value obtained from the unfolded P_t distribution is 332 MeV/c which is in good agreement and within the statistical uncertainty.

The P_t distribution is well represented by a two temperature thermal model. The preliminary temperatures listed in Fig. 1 were obtained by fitting the P_t spectrum with Hagedorn's expression:[2]

$$\frac{dN}{dP_t} = P_t \sqrt{P_t^2 + M_Z^2} \sum_{n=1}^{n=2} A_n \; \chi \sum_{M=1}^{\infty} (-1)^{M+1} K_1 \left(\frac{M\sqrt{P_t^2 + M_Z^2}}{T_n} \right)$$

where A1 and A2 are the low (T1) and high (T2) temperature normalization constants, respectively.

The K1 function is a modified Bessel function of the second kind.

Footnotes and References

*Fakultät für Physik, Universität Freiburg, D-7800 Freiburg, Germany

†CERN, CH-1211 Geneva 23, Switzerland

‡Institute of Nuclear Physics, PL-30055 Cracow, Poland

§Institute of Nuclear Studies, PL-00681 Warszawa, Poland

**Gesellschaft für Schwerionenforschung, D-6100 Darmstadt 11, Germany

††Dipartimento di Fisica, Universita di Bari, and INFN, Bari Italy

‡‡Max-Planck-Institut für Physik und Astrophysik, D-8000 München, Germany

§§Rudjer Boskovic Institute, 41001 Zagreb, Yugoslavia

***Institut für Hochenergiephysik, Universität Heidelberg, D-6900 Heidelberg 1

†††A. v. Humboldt Foundation Fellow

‡‡‡Fachbereich Physik, Universität Frankfurt, D-6000 Frankfurt, Germany

§§§Physics Department, University of Athens, 157-71 Athens, Greece

****Fachbereich Physik, Universität Marburg, D-3550 Marburg, Germany

††††Institute of Experimental Physics, University of Warsaw, Warszawa, Poland

‡‡‡‡A. v. Humboldt Foundation U.S. Senior Scientist Award recipient

§§§§On leave of absence from Central Research Institute for Physics, Budapest, Hungary

1. C.E. Floyd, R.J. Jaszcak, R.E. Coleman IEEE Transactions on Nuclear Science **NS-34**, 285 (1987).

2. R. Hagedorn Rivista Del Nuovo Cimento **6**, N10, 1 (1983).

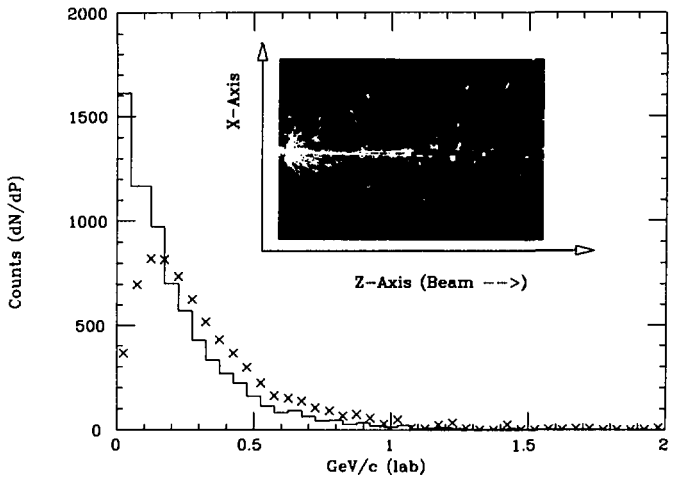

Fig. 1. Inset: A typical streamer chamber picture of a central collision. The Histogram shows the projected P_x momentum distribution. The symbols (crosses) describe the unfolded transverse P_t momentum spectrum which is fitted by a two component thermal model with temperatures T1 = 41 MeV, T2 = 139 MeV.

XBL 8711-5007

Probing the Space-Time Geometry of Ultrarelativistic Nucleus-Nucleus Collisions

NA35 Collaboration

A. Bamberger, D. Bangert,† J. Bartke,‡ H. Bialkowska,§ R. Bock,** R. Brockmann,** S.I. Chase, C. De Marzo,†† M. De Palma,†† I. Derado,‡‡ V. Eckardt,‡‡ C. Favuzzi,†† J. Fendt,‡‡ D. Ferenc,§§ H. Fessler,‡‡ P. Freund,‡‡ M. Gazdzicki,*** H.J. Gebauer,‡‡ K. Geissler,† E. Gladysz,‡ C. Guerra,** J.W. Harris,††† W. Heck,‡‡‡ T. Humanic,** K. Kadija,§§ A. Karabarbounis,§§§ R. Keidel,**** J. Kosiec,†††† M. Kowalski,‡ S. Margetis,*** E. Nappi,†† G. Odyniec, G. Paic,§§ A.D. Panagiotou,§§§,† A. Petridis,§§§ J. Pfennig,‡‡‡ F. Posa,†† K.P. Pretzl,‡‡ H.G. Pugh,†††† F. Pühlhofer,**** G. Rai, A. Ranieri,†† W. Rauch, R. Renfordt,‡‡‡ D. Röhrich,**** K. Runge,* A. Sandoval,** D. Schall,** N. Schmitz,‡‡ L.S. Schroeder, G. Selvaggi,†† P. Seyboth,‡‡ J. Seyerlein,‡‡ E. Skrzypczak,†††† P. Spinelli,†† R. Stock,†,‡‡‡ H. Ströbele,†,** A. Thomas,‡‡‡ M. Tincknell, L. Teitelbaum, G. Vesztergombi,††,§§§§ D. Vranic,** and S. Wenig‡‡‡*

Due to the macroscopic nature of ultrarelativistic heavy-ion collisions, it is important to study the spacetime evolution of the system to be able to understand the dynamics of the collision process at high energies and to determine whether conditions are favorable for the formation of a quark-gluon plasma.[1] Since the hadron momenta are coupled to the spacetime geometry of the source via time dilation,[2] the geometry should provide relevant information on the hadronization process as well as the underlying physics of the interactions. To study this spacetime geometry, the pion interferometry technique[3] has been employed. Since pions are bosons, the probability to measure two or more pions simultaneously is enbanced for pions in the same state due to the symmetry requirement of their wavefunctions. Using a particular model to characterize the spacetime geometry and dynamics of the pion source, information about the source can be extracted from the pion interferometry data.

In this work we report results from the first experimental study of two-pion interferometry applied to ultrarelativistic nucleus-nucleus collisions. 200 GeV/nucleon ^{16}O + Au interactions were studied at the CERN SPS in the NA35 Streamer Chamber. The $2 \times 1.2 \times 0.72$ m^3 chamber was located in the 1.5 T magnetic field of a superconducting vertex magnet for particle momentum analysis with a system of downstream calorimeters for triggering and energy flow measurements. For the present study 105 "central collision" events, with less than 300 GeV from the incident 3.2 TeV projectile remaining in the fragmentation region, were analyzed.

A summary of the results is provided in Table I. Two models which parameterize the spacetime geometry of the collision were used to fit to the experimental correlation function and extract pion source parameters. A model[4] assuming a source fixed in spacetime, where space and time are separable and described by Gaussians, is shown on the left for four rapidity intervals of the observed pions. R_T (R_L) is the transverse (longitudinal) radius parameter of the source relative to the beam axis and Λ the chaoticity parameter (where Λ=1 implies totally chaotic emission and Λ=0 implies totally coherent emission). The second model[5] includes more realistic dynamics including Lorentz covariance. The R_T and Λ are as defined in the first model. The τ_0 parameter describes the proper time for pion freezeout. The results exhibit a strong dependence upon the rapidity interval. Near the effective c.m. of the ^{16}O + Au system (rapidity y = 2.5), a large source is observed which exhibits a high degree of chaoticity and a relatively long lifetime. Farther away from $y_{cm} = 2.5$, R_T shrinks to the radius of the projectile and R_L diminishes to spatial dimensions which can be interpreted in terms of a correlation length[6] corresponding to $\Delta y \simeq 1$. Here the degree of chaoticity is observed to decrease for all rapidities away from y_{cm}.

Footnotes and References

*Fakultät für Physik, Universität Freiburg, D-7800 Freiburg, Germany

†CERN, CH-1211 Geneva 23, Switzerland

‡Institute of Nuclear Physics, PL-30055 Cracow, Poland

§Institute of Nuclear Studies, PL-00681 Warszawa, Poland

**Gesellschaft für Schwerionenforschung, D-6100 Darmstadt 11, Germany

††Dipartimento di Fisica, Universita di Bari, and INFN, Bari Italy

‡‡Max-Planck-Institut für Physik und Astrophysik, D-8000 München, Germany

§§Rudjer Boskovic Institute, 41001 Zagreb, Yugoslavia

***Institut für Hochenergiephysik, Universität Heidelberg,
D-6900 Heidelberg 1

†††A. v. Humboldt Foundation Fellow

‡‡‡Fachbereich Physik, Universität Frankfurt, D-6000 Frankfurt, Germany

§§§Physics Department, University of Athens, 157-71 Athens, Greece

****Fachbereich Physik, Universität Marburg, D-3550 Marburg, Germany

††††Institute of Experimental Physics, University of Warsaw, Warszawa, Poland

‡‡‡‡A. v. Humboldt Foundation U.S. Senior Scientist Award recipient

§§§§On leave of absence from Central Research Institute for Physics, Budapest, Hungary

1. S. Pratt, Phys. Rev. **D33**, 1314 (1986).

2. J.D. Bjorken, Phys. Rev. **D27**, 140 (1983).

3. G. Goldhaber et al., Phys. Rev. **120**, 300 (1960).

4. F.B. Yano and S.E. Koonin, Phys. Lett. **78B**, 556 (1978).

5. K. Kolehmainen and M. Gyulassy, Phys. Lett. **B180**, 203 (1986).

6. B. Andersson and W. Hofmann, Phys. Lett. **169B**, 364 (1986).

Table I

Summary of pion source parameters extracted for different rapidity slices

	Accepted	Gaussian			Kolehmainen-Gyulassy		
y-slice	Pairs	R_T (fm)	R_L (fm)	λ	R_T (fm)	τ_o (fm/c)	λ
1<y<4	203,612	4.1±0.4	$3.1^{+0.7}_{-0.4}$	$0.31^{+0.07}_{-0.03}$	3.6±0.3	2.9±0.7	0.29±0.05
1<y<2	24,633	4.3±0.6	2.6±0.6	$0.34^{+0.09}_{-0.06}$	4.0±0.7	2.5±1.0	0.30±0.12
2<y<3	39,310	8.1±1.6	$5.6^{+1.2}_{-0.8}$	0.77±0.19	7.3±1.6	6.4±1.0	0.84±0.15
3<y	20,282	$4.3^{+1.2}_{-0.8}$	5.8±2.2	0.55±0.20	—	—	—

Backward Going Tracks in the O – Pb Reaction at 200 GeV/nucleon

NA35 Collaboration

A. Bamberger, D. Bangert,† J. Bartke,‡ H. Bialkowska,§ R. Bock,** R. Brockmann,** S.I. Chase, C. De Marzo,†† M. De Palma,†† I. Derado,‡‡ V. Eckardt,‡‡ C. Favuzzi,†† J. Fendt,‡‡ D. Ferenc,§§ H. Fessler,‡‡ P. Freund,‡‡ M. Gazdzicki,*** H.J. Gebauer,‡‡ K. Geissler,† E. Gladysz,‡ C. Guerra,** J.W. Harris,††† W. Heck,‡‡‡ T. Humanic,** K. Kadija,§§ A. Karabarbounis,§§§ R. Keidel,**** J. Kosiec,†††† M. Kowalski,‡ S. Margetis,*** E. Nappi,†† G. Odyniec, G. Paic,§§ A.D. Panagiotou,§§§,† A. Petridis,§§§ J. Pfennig,‡‡‡ F. Posa,†† K.P. Pretzl,‡‡ H.G. Pugh,†††† F. Pühlhofer,**** G. Rai, A. Ranieri,†† W. Rauch, R. Renfordt,‡‡‡ D. Röhrich,**** K. Runge,* A. Sandoval,** D. Schall,** N. Schmitz,‡‡ L.S. Schroeder, G. Selvaggi,†† P. Seyboth,‡‡ J. Seyerlein,‡‡ E. Skrzypczak,†††† P. Spinelli,†† R. Stock,†,‡‡‡ H. Ströbele,†,** A. Thomas,‡‡‡ M. Tincknell, L. Teitelbaum, G. Vesztergombi,‡‡,§§§§ D. Vranic,** and S. Wenig‡‡‡*

Early studies have shown[1,2] that particles emitted in the backward laboratory direction in high-energy deuteron-nucleus collisions can acquire kinetic energies T much higher than the maximum values T allowed in collisions with free stationary nucleons. The effect was termed "cumulative". This effect has subsequently been investigated at accelerator energies from a few GeV up to 400 GeV and with cosmic rays above 1 TeV (for reviews see ref. 3 and references there). It was observed[3,4] that backward particles obey:

$$E\frac{d^3\sigma}{dp^3} = \text{const.} * \exp(-T/T_0)$$

with T_0 almost independent of projectile and target type and beam momentum. This behavior was called "nuclear scaling."[4] However some high-T points, with large error bars were observed to fall above the exponential.[5] It should be noted that all backward baryons cannot be understood in terms of nucleon-nucleon kinematics while a majority of all backward pions can. This phenomena was investigated during the heavy ion run at CERN. Interactions of O with Pb target located downstream from the 2m NA-35 Streamer Chamber were recorded. In this configuration Streamer Chamber pictures contained only the backward hemisphere of such a collisions in the LAB. We measured 101 events with 1129 backward emitted tracks: 267 negative and 862 positive. Fig. 1 top shows a PRELIMINARY P_t distribution of negative tracks (pions) and a two component thermal fit with T_1=57 MeV (97%), T_2=6 MeV (3%), χ^2=1.7; which does not differ significantly from that obtained from a one component fit: T = 54 MeV, χ^2=2.4. The "proton" (i.e., the difference between positive and negative tracks) PRELIMINARY P_t spectrum is shown in Fig.1 bottom (crosses) together with a single component thermal fit corresponding to T = 68 MeV. Attempts to fit the distribution with two components failed—the parameters always converged to the one component values.

This analysis is continuing. Qualitatively, our first results are in agreement with those of previous experiments.

Footnotes and References

*Fakultät für Physik, Universität Freiburg, D-7800 Freiburg, Germany

†CERN, CH-1211 Geneva 23, Switzerland

‡Institute of Nuclear Physics, PL-30055 Cracow, Poland

§Institute of Nuclear Studies, PL-00681 Warszawa, Poland

**Gesellschaft für Schwerionenforschung, D-6100 Darmstadt 11, Germany

††Dipartimento di Fisica, Universita di Bari, and INFN, Bari Italy

‡‡Max-Planck-Institut für Physik und Astrophysik, D-8000 München, Germany

§§Rudjer Boskovic Institute, 41001 Zagreb, Yugoslavia

***Institut für Hochenergiephysik, Universität Heidelberg, D-6900 Heidelberg 1

†††A. v. Humboldt Foundation Fellow

‡‡‡Fachbereich Physik, Universität Frankfurt, D-6000 Frankfurt, Germany

§§§Physics Department, University of Athens, 157-71 Athens, Greece

****Fachbereich Physik, Universität Marburg, D-3550 Marburg, Germany

††††Institute of Experimental Physics, University of Warsaw, Warszawa, Poland

‡‡‡‡A. v. Humboldt Foundation U.S. Senior Scientist Award recipient

§§§§On leave of absence from Central Research Institute for Physics, Budapest, Hungary

1. A. M. Baldin *et al.*, JINR Report P1-5819 (1971).

2. A. M. Baldin *et al.*, Proc. Rochester APS Meeting (1971).

3. S. Fredriksson *et al.*, Phys. Rep. **144**, N4&5, 187–320 (1987).

4. G. A. Leksin, Moscow Report (1985)

5. Yu. D. Bayukov *et al.*, Univ. of Pennsylvania Report UPR-0058E 11/78 (1978); S. Frankel *et al.*, Phys. Rev. **C20**, 2257 (1979); D. Ghosh *et al.*, Can. J. Phys. **58**, 969 (1980).

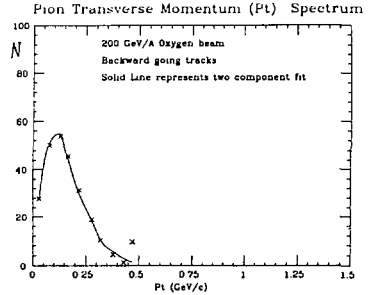

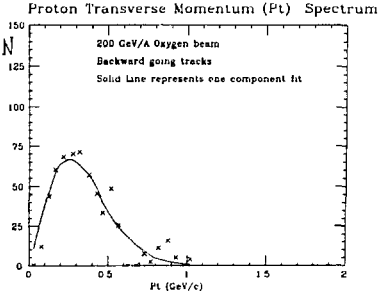

Fig. 1. See text.

Strangeness Production in the CERN NA35 Experiment

NA35 Collaboration

A. Bamberger, D. Bangert,† J. Bartke,‡ H. Bialkowska,§ R. Bock,** R. Brockmann,** S.I. Chase, C. De Marzo,†† M. De Palma,†† I. Derado,†† V. Eckardt,‡‡ C. Favuzzi,†† J. Fendt,‡‡ D. Ferenc,§§ H. Fessler,‡‡ P. Freund,‡‡ M. Gazdzicki,*** H.J. Gebauer,‡‡ K. Geissler,† E. Gladysz,‡ C. Guerra,** J.W. Harris,††† W. Heck,‡‡‡ T. Humanic,** K. Kadija,§§ A. Karabarbounis,§§§ R. Keidel,**** J. Kosiec,†††† M. Kowalski,‡ S. Margetis,*** E. Nappi,†† G. Odyniec, G. Paic,§§ A.D. Panagiotou,§§§,† A. Petridis,§§§ J. Pfennig,‡‡‡ F. Posa,†† K.P. Pretzl,‡‡ H.G. Pugh,‡‡‡‡ F. Pühlhofer,**** G. Rai, A. Ranieri,†† W. Rauch, R. Renfordt,‡‡‡ D. Röhrich,**** K. Runge,* A. Sandoval,** D. Schall,** N. Schmitz,‡‡ L.S. Schroeder, G. Selvaggi,†† P. Seyboth,‡‡ J. Seyerlein,†† E. Skrzypczak,†††† P. Spinelli,†† R. Stock,†,‡‡‡ H. Ströbele,†,** A. Thomas,‡‡‡ M. Tincknell, L. Teitelbaum, G. Vesztergombi,‡‡,§§§§ D. Vranic,** and S. Wenig‡‡‡*

The existence of extended quark matter at SPS beam energies is expected to influence both the energy spectra and the composition of particle production. Specifically, the ratio of yields such as particles/antiparticles and strange/nonstrange particles are expected to change[1,2] during the phase transition of hadronic matter into the quark gluon plasma. The yields of long-lived strange particles such as the kaon and the lambda are therefore ideal candidates to measure and this is, in fact, one of the principle goals of the NA35 experiment at CERN. Production of Λ^0, $\bar{\Lambda}^0$ and K^0_s were studied in nuclear collisions of oxygen with gold at 60 and 200 GeV/nucleon and in proton wit gold at 200 GeV/nucleon in the NA35 Streamer Chamber. The Streamer Chamber and experimental set-up are described elsewere.[3,4] Fig. 1 top shows a typical reconstructed mass spectrum for the Lambda mass hypothesis. Fig. 1 bottom shows a scatter plot of Λ^0 versus $\bar{\Lambda}^0$ reconstructed mass. Using standard procedure, the kaons were separated from the lambdas [5] and the results are presently being compared with the LUND-FRITIOF Model. Details of our preliminary findings were presented at the Quark Matter'87 Conference.[6]

Footnotes and References

*Fakultät für Physik, Universität Freiburg, D-7800 Freiburg, Germany

†CERN, CH-1211 Geneva 23, Switzerland

‡Institute of Nuclear Physics, PL-30055 Cracow, Poland

§Institute of Nuclear Studies, PL-00681 Warszawa, Poland

**Gesellschaft für Schwerionenforschung, D-6100 Darmstadt 11, Germany

††Dipartimento di Fisica, Universita di Bari, and INFN, Bari Italy

‡‡Max-Planck-Institut für Physik und Astrophysik, D-8000 München, Germany

§§Rudjer Boskovic Institute, 41001 Zagreb, Yugoslavia

***Institut für Hochenergiephysik, Universität Heidelberg, D-6900 Heidelberg 1

†††A. v. Humboldt Foundation Fellow

‡‡‡Fachbereich Physik, Universität Frankfurt, D-6000 Frankfurt, Germany

§§§Physics Department, University of Athens, 157-71 Athens, Greece

****Fachbereich Physik, Universität Marburg, D-3550 Marburg, Germany

††††Institute of Experimental Physics, University of Warsaw, Warszawa, Poland

‡‡‡‡A. v.Humboldt Foundation U.S. Senior Scientist Award recipient

§§§§On leave of absence from Central Research Institute for Physics, Budapest, Hungary

1. R. Anishetty, P. Koehler, L. McLerran Phys. Rev. **D22**, 2793(1980).

2. J. Rafelski Proc. Workshop Heavy Ion Exp.; GSI, Darmstadt Rep. 81-6, p. 282(81)

3. A. Sandoval *et al.*, Proc. 5 Quark Matter Conf.,

Asilomar 1986.

4. A. Bamberger *et al.*, Phys. Lett. B.

5. M. Anikina *et al.*, JINR, E1-83-524, Dubna, 1983.

6. G. Vestergombi *et al.*, Proceedings of the Quark Matter'87 Conference, Nordkirchen, West Germany.

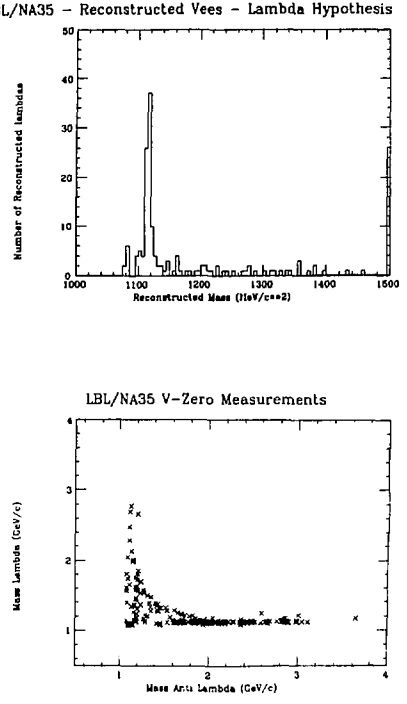

Fig. 1. Λ spectra

XBL 8711-5001

Charges and Angular Distributions of Fast Fragments Produced in 3.2 TeV ^{16}O Collisions with Pb*

G. Gerbier,† W.T. Williams,† P.B. Price,† and G-X. Ren,‡,† and G.-R. Vanderhaeghe§

Out of 30,000 interactions of 3.2 TeV ^{16}O nuclei in Pb, we found that no fast fragments had a charge $Z > 8$, none with $Z \gtrsim 5.5$ had a charge that differed from an integer by as much as 1.3, and none with $Z \gtrsim 5.5$ bad an angle to the beam >0.8 mrad. The cross section for production of a fast fragment with $Z > 8$ or a stable particle with charge 19e/3, 20e/3, 22e/3 or 23e/3 is less than 240 μb at 90% C.L. Fig. 1 shows the distribution of measured charges with $Z \gtrsim 5.5$. Using a measurement technique with a position resolution of 30 μrad, we found the transverse momentum distributions for C, N, and O to be gaussians with widths similar to those measured in projectile fragmentation of ^{16}O at a factor 100 lower energy. Fig. 2 shows the measured angular distributions of high-energy particles with Z = 6, 7, and 8. The widths of the gaussians in transverse momentum are ~120 MeV/c for Z=7 and ~170 MeV/c for Z=8.

Footnotes and References

*Condensed from a paper submitted to Phys. Rev. Lett., 1987.

†Also at Space Sciences Laboratory and Department of Physics, University of California at Berkeley.

‡Also at Institute of High-Energy Physics, Academia Sinica, Beijing, China.

§Formerly at CERN, Geneva, Switzerland; now retired.

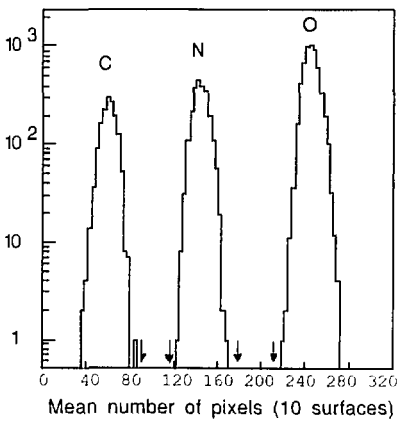

Fig. 1. See text. XBL 8710-4464

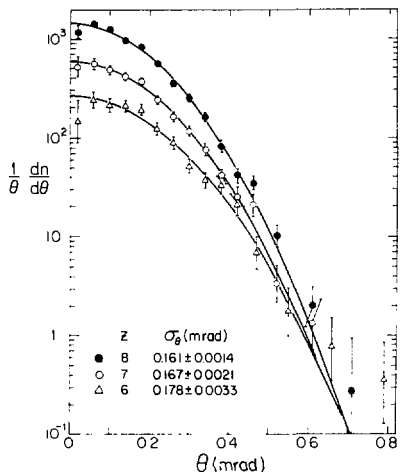

Fig. 2. See text. XBL 8710-4465

PART III: THEORY

QCD Transport Theory

H.-Th. Elze, M. Gyulassy, and D. Vasak

In a series of studies[1,2,3] we derived the exact gauge covariant equation of motion for the SU(N) quantum chromodynamic Wigner operators for quarks and gluons. The purpose of those studies was to establish a rigorous theoretical foundation for application to the evolution of quark gluon plasmas. Up to now most scenarios of ultra-relativistic nuclear collisions have assumed the validity of simple Abelian transport theories. Our aim was to derive necessary conditions under which the complex non-abelian QCD transport equations reduce to the much simpler Abelian ones.

Our starting point was the natural gauge covariant generalizations of the Wigner phase space functions to quarks and gluons. For quarks[1]

$$\hat{W}(x,p) \equiv \int \left\{ \frac{d^4y}{(2\pi)^4} e^{-ip\cdot y} \bar{\psi}(x) e^{\frac{1}{2}y\cdot D_x^{\rightarrow}} \otimes e^{-\frac{1}{2}y\cdot D_x^{\leftarrow}} \psi(x) \right\} \qquad (1)$$

where $D_x = \partial_x + gA(x)$ is the covariant derivative matrix. For gluons,[2] gauge covariance forces us to define the Wigner operator as

$$\hat{\Gamma}_{\mu\nu}(x,p) \equiv \int \left\{ \frac{d^4y}{(2\pi)^4} e^{-ip\cdot y} [e^{\frac{1}{2}y\cdot\mathcal{D}(x)} F_\mu^{\ \lambda}(x)] \otimes [e^{-\frac{1}{2}y\cdot\mathcal{D}(x)} F_{\lambda\nu}(x)] \right\} \qquad (2)$$

where the covariant derivative of a second-rank tensor $\mathcal{T}$ is defined by

$$\mathcal{D}(x)\mathcal{T}(x) \equiv \partial_x \mathcal{T}(x) + ig[A(x), \mathcal{T}(x)] \ .$$

Under local gauge transformations F, $\mathcal{D}F$, and so $\hat{\Gamma}$ transform covariantly. $\hat{\Gamma}$ is closely related to the energy-momentum tensor of the gluon field.

The equation of motion for the quark Wigner operator is found to be[1]

$$\left(\gamma^\mu p_\mu - m + \tfrac{1}{2}i\hbar\gamma^\mu \mathcal{D}_\mu(x)\right) \hat{W}(x,p) = \tfrac{1}{4}\hbar g \gamma_\mu \left(\{Q_1(\tfrac{1}{2}\hbar\Delta) F^{\mu\nu}(x), \partial_v^p W(x,p)\} + [Q_2(\tfrac{1}{2}\hbar\Delta) F^{\mu\nu}(x), \partial_v^p W(x,p)] \right) \ , \qquad (3)$$

where the "quantum" operators are

$$Q_1(x) = i\frac{\sin x}{x} + \frac{\sin x - x\cos x}{x^2} \ ,$$

$$Q_2(x) = i\frac{x\sin x + \cos x - 1}{x^2} + \frac{1-\cos x}{x} \ . \qquad (4)$$

and the *triangle operator*, Δ, is given by

$$\Delta = \partial_p \cdot \mathcal{D} = \partial_p \cdot \partial_x + \frac{1}{\hbar} ig \partial_p \cdot [A(x), \ ] \ . \qquad (5)$$

Because $\mathcal{D}_\mu$, $F_{\mu\nu}$, Δ and $\hat{W}(x,p)$ transform covariantly under a gauge transformation, eq.(3) is the sought after *gauge covariant operator equation* of motion.

From the above we see that the only sensible semi-classical limit of a non-Abelian theory is one where the *covariant* derivative of $F^{\mu\nu}$ is small. Only for covariantly slowly varying fields, in the sense that

$$(F\hat{W}) \gg (\mathcal{D}F\, \partial_p \hat{W}) \ , \qquad (6)$$

is it possible to carry out an expansion in powers of the Δ operator. In particular for covariant constant fields, the linear operator equation for $\hat{W}$ reduces to

$$\left(\gamma_\mu (p^\mu + \tfrac{1}{2}i\hbar(\mathcal{D}^\mu - \tfrac{1}{2}g\{F^{\mu\nu}, \ \}\partial_v^p - \tfrac{1}{4}g[F^{\mu\nu}, \ ]\partial_v^p) - m \right) \hat{W}(x,p) = 0 \qquad (7)$$

In the general case for strong or rapidly varying fields the full quantum equation, eq. 3, must be solved. This would be equivalent to solving the original field equations, i.e., hopeless at this time. Only under the rather restrictive conditions, (6), can we expect that the transport theory for quarks reduces to a simpler, more manageable form. Proceeding as in the Abelian case,[3] we can isolate the transport equation for (7) by converting it into a quadratic equation and isolating the anti-Hermitian part.

To reduce the quark-gluon transport equations to an effective Abelian one requires an even more drastic assumption. If and only if the ensemble average of $\langle \hat{W} \rangle$ is diagonal in the *same* gauge where $\langle F_{\mu\nu}(x) \rangle$ is diagonal does the transport equation reduce to

$$(p \cdot \partial_x + g\vec{\epsilon}_j \cdot \vec{F}_{\mu\nu} p^\nu \partial_p^\mu)\, f_j(x,p) = -\frac{1}{4} i g \vec{\epsilon}_j \cdot \vec{F}_{\mu\nu} [\, \sigma^{\mu\nu}, f_j(x,p) \,] \qquad (8)$$

where the "charges" $\vec{\epsilon}_j$ are just the root vectors of SU(N) in the fundamental representation and where f_j are the phase space densities of quarks of charge $\vec{\epsilon}_j$. Similarly, in ref. 2 we showed that the complex equations satisfied by the gluon Wigner operator reduce to effective Abelian ones as above but with ϵ_i and f_i replaced by the root vectors $\vec{\eta}_{ij}$ in the adjoint representations and the $N(N-1)$ "charged" gluon densities f_{ij} under the same brutal assumptions. Once in the Abelian form, then the spinor decomposition as derived in ref. 3 becomes possible and a complete intuitive set of equations for quark-gluon transport emerge. We refer to the approximations required to reduce the QCD equations to Abelian form as the Abelian Dominance Approximation (*ADM*). The central important question remaining unresolved at this point is whether ADM applies to nuclear collisions. Our work shows that only if Nature is kind in that sense, is it possible to follow the evolution of quark gluon plasmas with a practical, simple transport theory.

Footnotes and References

1. H.-Th. Elze, M. Gyulassy, D. Vasak, Nucl. Phys. **B276**, 706 (1986).

2. H.-Th. Elze, M. Gyulassy, D. Vasak, Phys. Lett. **B177**, 402 (1986).

3. D. Vasak, M. Gyulassy, H.-Th. Elze, Ann. Phys. **173**, 462 (1987).

Toward a Relativistic Selfconsistent Quantum Transport Theory of Nuclear Matter

H.-Th. Elze, M. Gyulassy, D. Vasak, H. Heinz, H. Stöcker, and W. Greiner

We derived[1] the relativistic quantum transport and constraint equations for relativistic field theories (QHD) of nucleons coupled to scalar and vector fields. We extracted a self consistent momentum dependent Vlasov term and the structure of quantum corrections for the Vlasov-Uehling-Uhlenbeck approach. Ambiguities in the extension of this transport theory to include pions and deltas are pointed out.

The investigation of nuclear matter properties at extreme densities and temperatures is one of the prominent motivations for studying high energy heavy ion collisions. A central problem is to find a link between the observed fragment distributions and the underlying nuclear equation of state. Quantum hadrodynamic model (QHD) provides such a link. In QHD the model parameters are constrained by static nuclear matter properties. Unfortunately, this does not completely determine all of them, and much freedom remains in the form of the equation of state at high energy densities. The hope is that nuclear collisions will provide further constraints on those parameters and hence on the sought-after equation of state. To extract information on those parameters from collisions of finite nuclei it is necessary to employ a transport theory consistent with QHD.

We showed that the transport theory based on QHD connects a number of features which are important in the analysis of nuclear collisions. In particular that theory naturally leads to momentum dependent forces that were expected to significantly influence the collective flow properties and the pion yields. Furthermore, this theory allows us to estimate the importance of quantum corrections that may arise in the presence of large momentum and spatial gradients occurring in nuclear collisions.

We derived the following quantum equation of mo-

tion for the nucleon Wigner function:

$$[\gamma\cdot K - M(x)]\, W(x,p) = 0 \ , \qquad (1)$$

$$K^\mu \equiv \Pi^\mu + \frac{1}{2}i\hbar\nabla^\mu = \left\{ [p^\mu - \cos(\frac{1}{2}\hbar\Delta)u^\mu] + \frac{1}{2}i\hbar[\partial_x^\mu + \frac{2}{\hbar}\sin(\frac{1}{2}\hbar\Delta)u^\mu(x)] \right\} \qquad (2)$$

$$M \equiv m_R - i\hbar m_I = \cos(\frac{1}{2}\hbar\Delta)m - i\sin(\frac{1}{2}\hbar\Delta)m \ , \quad (3)$$

and where $\Delta = \partial_x\cdot\partial_p$, $u^\mu(x) = g_v\omega^\mu(x) + g_\rho\frac{1}{2}\vec{\tau}\cdot\vec{\rho}^\mu(x)$ is the effective vector field, and $m(x) = m_N + g_s\sigma(x)$ is the dynamical mass.

In a spin-isospin saturated system, the scalar Wigner density, $F = \frac{1}{4}\langle tr\hat{W}\rangle$, obeys in the classical limit the following momentum dependent Vlasov equation:

$$[k_\mu(\partial_x^\mu - w^{\mu\nu}\partial_\nu^k) + m\Delta m]\, \tilde{F}(x,k) = 0 \ , \quad (4)$$

where $\tilde{F}(x,k) \equiv m_N/m(x)F(x,k+w(x))$.

Footnotes and References

1. H.T. Elze, *et al.*, Mod. Phys. Lett. **A2**, 451 (1987).

2. H.T. Elze, *et al.*, Nucl. Phys. **B276**, 706 (1986); Phys. Lett. **B177**, 402 (1986).

String/Rope Model Approach to Ultrarelativistic Nuclear Collisions

M. Gyulassy

To evaluate the significance of new CERN and AGS data ou nuclear collisions at energies in the range 10 - 200 GeV/nucleon, an independent Lund Monte Carlo program, ATTILA,[1] was developed along the lines of the FRITIOF code.[2] We study (1) how uncertainties in *pp* dynamics amplify in calculations of nuclear collisions; (2) to what extent present data on multiplicity, transverse energy, and veto energy distributions deviate from a *linear* extrapolation of *pp* dynamics; and (3) how novel non-equilibrium color rope effects could simulate quark gluon plasma signatures. Some of the important advantages of the specific Monte Carlo formulation of the color neutralization model provided by ATTILA are as follows:

(1) Four momentum and quantum numbers are exactly conserved.

(2) Glauber multiple collisions probabilities are calculated precisely.

(3) Exclusive events involving the physical hadronic resonance spectrum and decay chains are generated.

(4) Novel dynamical scenarios involving the extension of multi-strings to color rope fragmentation can be investigated quantitatively.

(5) The space-time evolution of the reaction can be followed and secondary cascading can eventually be incorporated.

First we derive the symmetric Lund fragmentation function and show how the fragmentation function would differ if multi-strings would merge into a color rope. We then calculate observables in *pp* collisions and study the sensitivity of the results to variations of the fragmentation parameters. We point out shortcomings of the Lund algorithm in connection with the leading particle spectra. Next, we show that the code can satisfactoraly reproduce *pA* data, and nuclear stopping power is investigated in this model. We compare calculations based on ATTILA using several options with available data on 200 GeV/nucleon O+A from the CERN-SPS and show that data on transverse energy, multiplicity, and veto calorimeter distributions are only reproduced qualitatively and that there are indications of systematic deviations from this linear extrapolation model at the 10–20% level. We find though that small model errors at the *pp* level amplify tremendously when extrapolated to O+A and thus current discrepancies may only reflect an inadequacy of present parameterizations of *pp* dynamics. We show furthermore that string models which assume that multiple interactions do not excite strings to invariant masses larger than in *pp* collisions fail to reproduce even the

gross features of the data. Two alternative implications of this observation are discussed. Finally, we study how color rope fragmentation could forge the higher mean $p_\perp$ and higher hyperon abundance signatures of quark-gluon plasma formation. We find that color ropes fragmentation could also be a novel source of charmed hadrons in the final state.

Footnotes and References

1. M. Gyulassy, CERN-TH.4794,4795 (1987) preprints.

2. B. Andersson, G. Gustafson, and B. Nilsson-Almqvist, Nucl. Phys. **B281**, 289 (1987).

Lund Model and an Outside-Inside Aspect of the Inside-Outside Cascade

A. Bialas and M. Gyulassy

We calculated[1] the hadronic formation length distribution, $D(x,z)$, i.e., the probability that a particle carrying a light cone fraction, x, of the total light cone momentum, $E+P_z$, is produced a distance z from the interaction point. We employed the Lund string model for multiparticle fragmentation which connects momentum space quantities to coordinate space through the string tension, $\kappa \approx 1$ GeV/fm. In that model pairs quarks-antiquarks are produced at space-time points distributed according to the inside-outside cascade picture nature of ultrarelativistic processes. In that picture the average formation length of a particle with momentum fraction x is

$$z(x) = xL \ , \qquad (1)$$

where $L = (E+P_z)/\kappa$ is the total "length" of the hadronization region that grows linearly with increasing energy. However, the above law is only correct for point-like particles. In the case of composite hadrons we showed that there is a basic ambiguity about the definition of the formation length since different constituents of a final hadrons could be produced at different times and distances. This is exactly what happens in the Lund model, where a hadron is considered to be a bound state of a quark and antiquark formed in two *separate* pair production points. To illustrate the ambiguity, we proposed two extreme definitions of the formation length. The first we call the constituent length, $z_c(z)$, is the distance at which the *first* of the two $q\bar{q}$ constituents is produced. The second we call the "yo-yo" length, $z_y(x)$, is the distance at which the world lines of the $q\bar{q}$ constituents cross for the first time. We note that the world lines of the q and $\bar{q}$ in the Lund model weave back and forth in a yo-yo motion. From the analytic distribution functions we computed for these two extreme definitions of the formation length, we found that

$$z_c(x) = xL\ln(1/x^2)/(1-x^2)]$$

$$z_y(x) = xL(\ln(1/x^2) - 1 + x^2)/(1-x^2) \ .$$

Note that the difference of $z_y(x) - z_c(x) = xL$ becomes maximal at $x=1$, implying a very large uncertainty in the production length of hadrons carrying a large fraction of the light cone momentum.

By analyzing the reaction $\pi^- + A \rightarrow \bar{p} + X$ we found that the A dependence of the data favored the constituent length, z_c as the relevant formation length beyond which the final hadron, $\bar{p}$, begins to rescatter in the nuclear medium. The novel point about this result is that unlike ref. 1 the constituent formation length actually *decreases* with increasing energy for $x > 0.5$ as $z_c(x) \approx (1-x)L$. Hence, we have uncovered the opposite of the inside-outside cascade picture for high x hadrons due to there composite nature!

Footnotes and References

1. A. Bialas, M. Gyulassy, Nucl. Phys. **B291**, 793 (1987).

Confinement of Heavy Quarks in a Color-Dielectric Soliton Model

G. Fái and L. Wilets†*

The description of hadrons in terms of quark-soliton type models[1,2,3,4] will continue to play an important role in our understanding of hadronic properties, at least until these properties can be calculated in QCD with great accuracy.

A general starting point for nontopological solitons is the covariant, gauge-invariant Lagrangian density

$$\mathcal{L} = \bar{\psi}[i\gamma_\mu\partial^\mu - m - g(\sigma)]\psi + \frac{1}{2}\partial_\mu\sigma\partial^\mu\sigma - U(\sigma) + \mathcal{L}_\mathcal{G}$$

where ψ is the Dirac field, $U(\sigma)$ is a fourth order polynomial in the chiral singlet scalar field σ and $\mathcal{L}_\mathcal{G}$ is the Lagrangian density of the gluon sector:

$$\mathcal{L}_\mathcal{G} = -\frac{1}{4}\kappa(\sigma)F_{\mu\nu}F^{\mu\nu} - g_s\bar{\psi}\gamma_\mu\frac{\lambda}{2}A^\mu\psi\ ,$$

where $\kappa(\sigma)$ is the color-dielectric function, $F_{\mu\nu}$ is the gauge field tensor and the color indices have been suppressed for simplicity. The underlying principle of such models is the color dielectric function $\kappa(\sigma)$: vanishing of κ in the vacuum assures absolute color confinement. The function $g(\sigma)$ represents the coupling between the σ and quark fields. In the original Friedberg-Lee model[1] this term is linear in the σ field: $g(\sigma) = g_0\sigma$, with g_0 a constant. Nielsen and Patkós[5] postulate the forms $\kappa(\sigma) = (1-\sigma/\sigma_v)^4$ and $g(\sigma) = g_0\kappa^{-1/4}$, where σ_v is the vacuum value of the σ field. Bayer, Forkel and Weise[4] assume $g(\sigma) = g_0\sigma\kappa^{-1/2}$.

We begin with a Lagrangian with $g(\sigma) = 0$ and $m = 0$, and hence chirally invariant. We then derive that, subject to short range regularization, the effective coupling for spatially fixed quarks is

$$g_{eff}(\sigma) = g_0\sigma_v\left(\frac{1}{\kappa(\sigma)} - 1\right)$$

and investigate the properties of the model with this coupling. Although the approximation of localized quarks is valid only for massive quarks, there is reason to believe that it provides a useful starting point for light quarks as well. The form (3) leads to absolute confinement and appears to generate only a small, positive effective quark mass in the interior of the region of confinement.

We want to examine further the role of chiral invariance in this model. Chiral invariance is destroyed in the mean field approximation, but we anticipate that the invariance is restored through the emergence of a massless boson by the Nambu–Goldstone mechanism.[4]

Footnotes and References

*Kent State University

†University of Washington

1. R. Friedberg and T.D. Lee, Phys. Rev. **D15**, 1694 (1977), **D16**, 1096 (1977).

2. R. Goldflam and L. Wilets, Phys. Rev. **D25**, 1951 (1982).

3. A.G. Williams and A.W. Thomas, Phys. Rev. **C33**, 1070 (1986).

4. L. Bayer, H. Forkel and W. Weise, Z. Phys. **A324**, 365 (1986).

5. H.B. Nielsen and A. Patkos, Nucl. Phys. **B195**, 137 (1982).

Interaction Energy in Infinite Nuclear Matter in the Hybrid Soliton Model*

D. Hahn and N. K. Glendenning

We describe nucleons as consisting of quarks and classical sigma and pion fields, where the form of the meson fields is given by the Hedgehog ansatz. Nuclear matter is modeled as a three-dimensional crystal with the nucleons at the center of each primitive cell. The quarks move in a potential generated by the meson fields and may occupy different bands according to the excitation energy of the nucleons. For each nucleus, the ground state band admits three quarks, which have to have different colors.

We calculate the properties of the nucleons in the crystal, e.g., the soliton mass and the quark energies in the various bands as functions of the cell separation R, or the nuclear density. In our model, a transition of the nuclear matter from a color insulator to a color conductor happens at the crossing point of the ground state band with a higher-lying band.

It turns out that the soliton mass is monotonically rising with increasing density, i.e., we have no attractive part in the nuclear interaction. This is due mainly to an increase in the quark kinetic energy, typically 300 MeV from zero density to ground state nuclear matter density. Despite the introduction of various higher order terms in the meson fields into the Lagrangian, we have not been able to produce a minimum in the soliton-soliton interaction energy. We may have to get rid of the Hedgehog ansatz to reach a satisfying behaviour of the soliton matter.

Footnotes and References

*Condensed from Phys. Rev. **C35**, 1297 (1987)

Hot Metastable State of Abnormal Matter in Relativistic Nuclear Field Theory*

N.K. Glendenning

Because of their non-linearity, the field equations of relativistic nuclear field theory admit of additional solutions besides the normal state of matter. One of these is a finite-temperature abnormal phase. Over a narrow range in temperature, matter can exist in the abnormal phase at zero pressure. This is a hot metastable state, for which there is a barrier against decay, because the field configuration is different than in the normal state, the baryon masses are far removed from their vacuum masses, there is an abundance of pairs also far removed from their vacuum masses, and a correspondingly high entropy. The abundance of baryon-antibaryon pairs is the glue that holds this matter together. The signals associated with this novel state are quite unusual. A fragment of such matter will cool by emitting a spectrum of black-body radiation, consisting principally of photons, lepton pairs and pions, rather than by baryon emission, because the latter are far removed from their vacuum masses. If produced at the upper end of its temperature range, a large fraction of the original energy, more than half in the examples studied here, is radiated in this way. The baryons and light elements produced in the eventual decay, after the abnormal matter has cooled to a domain where its pressure becomes positive, will account for only a fraction of the original energy. The energy domain of this state depends sensitively on the coupling constants, and within a reasonable range as determined by nuclear matter properties, can lie in the range of GeV to tens of GeV per nucleon.

Footnotes and References

*Condensed from Nucl. Phys. A **469**, 600 (1987).

Vacuum Renormalization of the Chiral-sigma Model and the Structure of Neutron Stars*

N.K. Glendenning

Vacuum renormalization corrections are calculated for normal nuclear matter and neutron star matter in the chiral-sigma model. The theory is generalized to include hyperons in equilibrium with nucleons and leptons. The equations of state corresponding to two compression moduli, a 'stiff' and 'soft' one for nuclear matter, are studied. It is shown that fully one half the mass of a neutron star at the limiting mass is composed of matter at less than twice nuclear density. Neutron star masses are therefore moderately sensitive to the properties of matter near saturation and to the domain of the hyperons, but dominated by neither. The predictions for the two equations of state are compared with observed neutron star masses, and only the stiffer is compatible.

Footnotes and References

*Condensed from LBL-23818

Evidence on Nuclear Equation of State from Nuclear Masses, Relativistic Collisions, Supernova Explosions and Neutron Star Masses*

N.K. Glendenning

Data on the nuclear equation of state from a number of different sources, from nuclear masses, high energy nuclear collisions, supernova and and neutron stars is analyzed. The current situation concerning supernova simulations is studied and it is concluded that supernova explosions of the prompt kind do not provide a constraint on the nuclear EOS, and that explosions due to the late-time neutrino heating mechanism of Wilson may do so. Fig. 1 shows the limiting mass of a neutron star as a function of K for several values of nucleon effective mass at saturation. The horizontal line is at the mass of the most massive known neutron star, which places therefore a lower bound on the limiting mass. The indicated value of K is around 300 MeV. Our conclusions are:

- Nuclear masses: K $\approx 310 \pm 100$MeV.
- High energy nuclear collisions: Equation of state not well determined by the methods used here
- Supernova: determination not possible for prompt bounce mechanism, but constraint may he possible from late-time mechanism.
- Neutron star masses: $K \geq 335 \pm 60 MeV$, stiff EOS.

*Condensed from LBL-23081

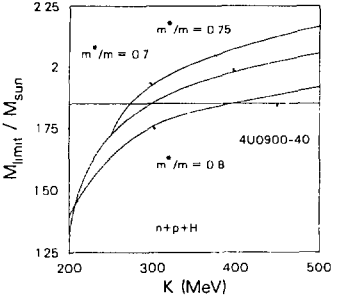

Fig. 1. See text. XBL 873-1451

Optimizing Heavy Ion Experiments to Probe Dense Nuclear Matter

G. Fái, W.-M. Zhang, and M. Gyulassy

We calculated[1] the dispersion of the azimuthal angle of the reaction plane in nuclear collisions as obtained using four different estimators (1) kinetic flow analysis (2) transverse velocity analysis (3) transverse projectile fragment analysis and (4) pseudorapidity analysis. For event simulations we employed the FREESCO generator[2] with parameters adjusted to fit the flow analysis of the Plastic Ball data. Our studies concentrated on Nb+Nb at 400 MeV/nucleon and mid impact parameters, where strong indications for collective flow have been observed. Our goal was to determine which of the above methods could be used to optimize future detailed triple differential cross section measurements.

We found a time of flight wall employing method (2) gave comparable dispersions to the more extensive method (1). In particular, rms dispersions of 30 deg in the azimuth could be achieved. That allows 20–30 MeV resolution of in-plane transverse momenta, quite adequate to study details of collective flow that involves on the average 100 MeV/c momenta at these energies. We found further that for not too central collisions, method (3) could be superior to all others as long as a few $Z > 2$ projectile fragments were left on the average. These results allow optimized planning of future experiments to focus on the triple differential cross sections needed in the program to extract the equation of state of nuclear matter from nuclear collisions.

Footnotes and References

1. G. Fái, *et al.*, Phys. Rev. **C36**, 597 (1987).
2. G. Fái, J. Randrup, Nucl. Phys. **A381**, 557 (1982).

Pion Spectra in Equilibrium Models of Nuclear Collisions*

D. Hahn and N. K. Glendenning

Recently, multiplicity selected pion data from relativistic heavy ion collisions have been published[1] which show two different slopes or temperatures in the spectra instead of one. Measurements by a Japanese group[2] have confirmed these experiments and indicate not only an energy, but also a mass dependence of this effect.

We have calculated pion spectra within three simple models of pion production in relativistic heavy ion collisions and compared them to the new data. All three models are based on particle freeze out from thermal and chemical equilibrium. In the first one nucleons, pions and Δ resonances freeze-out at a fixed temperature and density. The spectra are a superposition of thermal pions and pions from the decay of the Δ resonance. They show a peak at the Δ resonance energy which does not exist in the experimental data. In the second model we assume that pions are radiated from a hot, spherical source of nuclear matter, which cools due to this radiation. However, this proves to be a rather small effect. In the last calculation we employ a hydrodynamic model of the expansion process to determine the pion spectra produced by a sequential freeze-out at fixed density and different times and temperatures. Only this last description gives a shape of the pion distribution similar to the experimental one. It is found that three different effects contribute to the concave shape of the spectra in this model, namely the boost of the pion spectra caused by the hydrodynamic flow, the effect of the Bose versus the Boltzmann distribution and the superposition of contributions from areas with different temperatures.

Footnotes and References

*Condensed from LBL-23864.

1. J.W. Harris *et al*, Phys. Rev. Lett. **58**, 463 (1987).
2. S. Nagamiya, private communication.

Pion Production in a Field Theoretic Description of a Nuclear Fireball*

N.K. Glendenning

Pion yields are computed from the pion and delta populations found in a field theoretic description of hot dense matter. Two different prescriptions for the initial conditions are considered and the results of a quasi-hydrodynamic expansion are also studied. Fig. 1 illustrates the total pion yield in the latter case for three very different values of compression modulus. We note three points. The first is that the yields corresponding to vastly different values of K are not much different from each other. Second, although the isentropic expansion scenario can account for the observed yields, the freeze-out density is not measured in the experiment, and is consequently an undetermined parameter. If a freeze-out density closer to the initial density were chosen, then of course the computed yield would be closer to those shown in Fig. 1, whereas if a smaller value were chosen, the yields would shift to smaller values. Third, the coupling of the delta to the meson fields was here assumed to be the same as for the nucleon. Uncertainty in these couplings introduces additional uncertainty in the yields.

It may be that a more complete set of experiments including accurate spectra at a number of energies may serve to further define the evolution and final conditions, along the lines discussed in a separate publication. The premise of that work is that the concavity of the pion spectra and its energy and mass dependance carry information on the evolution of the system. In any case, the conclusion of the present work is that this more accurate rendering of the suggestion of Stock *et al.*, and hence their suggestion, are not capable of yielding unambiguous information on the equation of state. The dependence on the compression modulus is too weak, and the pion yield is too sensitive to assumptions about the initial conditions, the final freezeout, and the relative strength of delta and nucleon coupling to the mesons.

Footnotes and References

*Condensed from LBL-23912

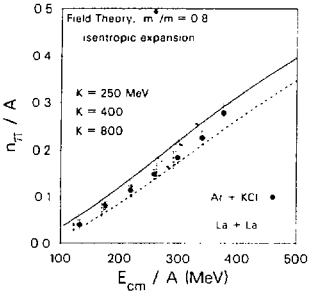

Fig. 1. See text. XBL 878-3622

Quantitative Analysis of the Relation between Entropy and Nucleosynthesis in Central Ca + Ca and Nb + Nb Collisions*

*L.P. Csernai,[†,‡] G. Fái,[§,**] D. Hahn, J.I. Kapusta,[†] J. Randrup, and H. Stöcker[††]*

In experiments performed by the GSI-LBL Plastic Ball Group,[1] the relative abundances of p, d, t, ^{3}He and α were measured as a function of the charged-particle multiplicity (roughly equivalent to impact parameter) for Ca + Ca collisions at 400 and 1050 MeV per nucleon and for Nb + Nb collisions at 400 and 650 MeV per nucleon. In an effort to infer the entropy in the final state of the exploding nuclear matter two different statistical models[2,3] were applied, which gave significantly different an-

swers. We have reanalyzed the situation with several independently developed statistical descriptions of nuclear disassembly,[4] and the quantum-statistical grand-canonical model (QSM),[3] and we obtain a consistent and unambiguous interpretation of the data. Furthermore, we demonstrate that there is an essentially one-to-one relationship between the observed relative adundancies of the light fragment species and the entropy per nucleon, for break-up temperatures greater than 30 MeV.

As an illustration of the results, we show in the figure $x = d$-like/p-like versus the entropy per baryon for the charge symmetric systems formed by central collisions of ^{40}Ca nuclei. The final fragment ratios d/p, t/p, ^{3}He/p and α/p were determined after the decay of all particle unstable nuclei. For temperatures between 30 and 90 MeV there is essentially a unique relationship between x and S: the difference amounts to roughly the width of the line. The lower temperature isotherms, with $T < 30$ MeV, begin to deviate at low entropy. For example, the $T = 10$ MeV isotherm is shown for illustration. However, even the low-temperature isotherms eventually converge at high entropy. Despite their physical and technical differences, the two models produce results in remarkable agreement with each other. Also shown is the simple formula $s = 3.945 - \ln x$ derived in ref. 2. While this formula provides a satisfactory reproduction of the results of the detailed statistical codes when the phase space density is low, it overestimates the entropy for larger x.

From our calculations we can determine the entropy corresponding to each x_{max}, assuming that $T > 30$ MeV. These values are intermediate between those obtained in ref. 1. This discrepancy came about and is resolved as follows: 1) The simple formula of ref. 2 is not very accurate unless $x < 0.2$ and since the data under consideration have considerably more deuteron-like correlations present, it should not be applied. 2) In ref. 1 the experimentally determined curve of x versus charged particle multiplicity was parameterized and extrapolated to infinite charged particle multiplicity. The extrapolated values differ significantly from the x_{max} values. Using the extrapolated values, from either QSM or *FREESCO*, one arrives at the low entropies quoted in ref. 1. However, there are arguments against analytically extrapolating the observed x distribution to infinite charged-particle multiplicity, so it is preferable to compare the observed x values at the maximum charged-particle multiplicity to the results of *FREESCO* or QSM and the results should be interpreted as the entropies actually achieved in central Ca + Ca and Nb + Nb collisions at those energies.

Footnotes and References

*Condensed from Phys. Rev. C35, 1297 (1987).

†School of Physics and Astronomy, University of Minnesota, Minneapolis, Minnesota 55455

‡On leave from the Central Research Institute for Physics, Budapest, Hungary. Present address: NSCL, Michigan State University, East Lansing, MI 48824

§Department of Physics, Kent State University, Kent, Ohio 44242

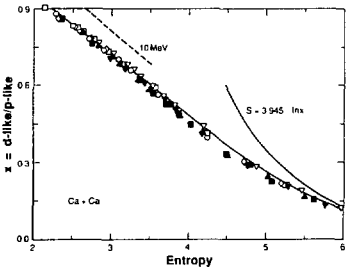

Fig. 1. Plot of $x = d$-like/p-like versus entropy per nucleon. The dashed curve has been calculated with the QSM at $T = 10$ MeV, and the solid curve with the QSM at $T = 30$ - 90 MeV. The symbols indicate the results of *FREESCO* as follows: $\nabla : T = 30$ MeV, $\theta : T = 45$ MeV, $\diamond : T = 60$ MeV, $\bigcirc : T = 75$ MeV, N: T = 90 MeV, $H : T = 105$ MeV, $\blacksquare : T = 120$ MeV.

XBL 8711-4988

**On leave from Roland Eötvös University, Budapest, Hungary

††Permanent address: Institut für Theoretische Physik, Johann Wolfgang Goethe Universität, Frankfurt am Main, West Germany

1. K.G.R. Doss, H.-Å. Gustafsson, H.H. Gutbrod, B. Kolb, H. Löhner, B. Ludewigt, A.M. Poskanzer, T. Renner, H. Riedesel, H.G. Ritter, A. Warwick and H. Wieman, Phys. Rev. **C32**, 116 (1985).

2. J.I. Kapusta, Phys. Rev. **C29**, 1735 (1983).

3. H. Stöcker, G. Buchwald, G. Gräbner, P. Subramanian, J.A. Maruhn, W. Greiner, B.V. Jacak and G.D. Westfall, Nucl. Phys. **A400**, 63c (1983).

4. G. Fái and J. Randrup, Nucl. Phys. **A404**, 551 (1983).

Effects of the Coulomb Energy on Fragment Yields in Medium Energy Nuclear Collisions

A.R. Deangelis, G. Fái,† and A.Z. Mekjian**

Conclusions reached by statistical fragmentation models about the equation of state of nuclear matter and about the fragment yields may critically depend on the fragment-fragment interactions included in these models. An earlier mean field type calculation[1] found in the framework of a microcanonical model that the mutual Coulomb interaction of the fragments plays an important role in shaping the fragment yield distributions. This appears to be in contrast with grand canonical expectations[2] and provides one of the motivations of the recent interest in incorporating the fragment-fragment interactions in statistical models.[3,4] The liquid-vapor phase transition in nuclear matter serves as another motivation to study these interactions on a more fundamental level than has been done to date. Specifically, the effects of hard-sphere nuclear repulsion and those of the Coulomb energy are investigated in ref. 4, based on a new microcanonical model of nuclear disassembly.[5] The present research[0] also addresses the Coulomb interaction, but focuses on the fragment yields. We attempt to simplify the treatment as much as possible while preserving the properties of the yield distributions.

We outline a simple procedure for calculating fragment yields from a gas of thermally equilibrated nucleons produced in intermediate energy nuclear collisions. The method can be viewed as an application of general statistical principles, or, equivalently,[7] as an application of the principle of minimum information subject to conservation of energy, charge and baryon number. Our main interest lies in the effect of the Coulomb energy on the fragment yield distribution. We therefore explore different approximations developed to include the Coulomb energy.

Preliminary calculations suggest the limited importance of the Coulomb interaction energies, but also seem to indicate that Coulomb interactions are not solely responsible for the minimum in certain fragment yield distributions. It appears that there are combinations of nucleon gas densities and temperatures for which the fragment yields show a 'U-shaped' distribution, even without the inclusion of the Coulomb energy.

Footnotes and References

*Rutgers University

†Kent State University

1. D.H.E. Gross, Phys. Lett. **161B**, 47 (1985).

2. G. Fái and J. Randrup, Nucl. Phys. **A381**, 557 (1982).

3. S. Pratt, P. Siemens and Q.N. Usmani, Phys. Lett. **189B**, 1 (1987).

4. J. Randrup, M.M. Robinson and K. Sneppen, Phys. Lett. B (in press).

5. S.E. Koonin and J. Randrup, Nucl. Phys. **A474**, 173 (1987).

6. A.R. Deangelis, A.Z. Mekjian and G. Fái, in preparation.

7. G. Fái and A.Z. Mekjian, Phys. Lett. **196B**, 281 (1987).

Multifragmentation and Nuclear Comminution

L.G. Moretto and M. Ashworth

A variety of mechanisms for the production of several complex fragments in the exit channel of intermediate-energy heavy-ion reactions has been proposed. These mechanisms assume the *simultaneous* production of these fragments either in statistical processes like liquid vapor equilibrium near the critical temperature, or in dynamical processes like shattering.[1]

A more conventional mechanism involving the sequential emission of several complex fragments by a very hot compound nucleus appears to be possible. It has been shown that complex fragments can be emitted by compound nuclei at low energies.[2,3] This process has been followed up to remarkably high bombarding energies, such as 50 MeV/nucleon.[4–6] It has been observed that the complex fragment emission probability increases quite rapidly with excitation energy as predicted by compound nucleus theory. Consequently, it is possible that, at sufficiently high energies, the residue after the emission of one complex fragment is sufficiently excited to emit another, and so on.

This process of sequential statistical production of several large fragments we call nuclear comminution. Its occurrence is practically certain if sufficiently excited compound nuclei can be produced, and it will constitute a background to more exotic processes if they exist – hence, the importance of studying the properties of comminution such as the mass distribution and its excitation energy or temperature dependence.

We have simulated the process by assuming a potential energy curve vs mass asymmetry V(A) (ridge line) with a maximum of 40 MeV at symmetry and a value of 8 MeV at the extreme asymmetries. The primary yield curve is of the form:

$$Y(A) = Kexp[-V(A)/T(A)] \qquad (1)$$

where T(A) is the temperature at a given asymmetry. Each of the resulting fragments is assumed to have a similar ridge line and a suitably scaled temperature and is allowed to decay accordingly until all the excitation energy is exhausted. The resulting mass distributions for a series of initial temperatures are shown in Fig. 1. The log-log plots show an exquisite power law dependence for the small masses with exponents around 2.3 – 2.4 which, incidentally are very close to the exponent expected for the liquid-vapor phase transition at the critical temperature.

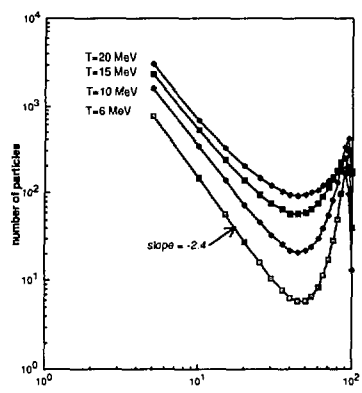

Fig. 1. Theoretical mass distributions from comminution calculations of the deexitation of a mass 100 compound nucleus at several temperatures. Notice the beautiful power law behavior at small masses.

XBL 8712-5082

This result shows that the power law dependence is not a specific or diagnostic feature of liquid vapor equilibrium, but, rather, it appears to be a "generic" property arising even from sequential binary decay or comminution.

Footnotes and References

1. For more information see L.G. Moretto and G.J. Wozniak, LBL - 24558.

2. L.G. Sobotka *et al.*, Phys. Rev. Lett. **51**, 2187 (1983).

3. M.A. McMahan *et al.*, Phys. Rev. Lett. **54**, 1995 (1985).

4. R.J. Charity *et al.*, Nucl. Phys. A, in press, LBL-22447.

5. R.J. Charity *et al.*, submitted to Nucl. Phys. A, LBL-22448.

6. D.R. Bowman *et al.*, Phys. Lett. **B189**, 282 (1987).

Microcanonical Simulation of Nuclear Multifragmentation*

J. Randrup and S. E. Koonin†

The properties of hot nuclear matter at subsaturation densities are of general physical interest, especially within the context of the "Equation of State" of matter at high energy densities. The topic is of direct relevance to astrophysics (e.g., supernova processes) and is intertwined with energetic nuclear collisions: a good understanding of the nuclear equation of state over a wide range of energies and densities is a prerequisite for making reliable predictions about the outcome of nuclear collisions and, conversely, nuclear collisions present a unique tool for probing the properties of nuclear matter away from its normal state. Because of its strong link to nuclear collision dynamics, the study of subsaturation matter is often performed in the guise of multifragmentation, in the sense that one considers an assembly of interacting nuclear fragments within a finite ("freeze-out") volume Ω.

We have formulated a practical and well-founded method for an exact description of the statistical mechanics of the type of finite, interacting system of nucleons and nuclei likely to be formed in an energetic nuclear collision. Its numerical implementation is accomplished by employing the method of Metropolis simulation, which provides a sample multifragment configurations picked according to their respective statistical weights. The microcanonical, canonical, and grand-canonical approximations can all be treated in a unified manner. A particular advantage of the developed model is the ease with which interfragment forces can be included; this feature has so far been lacking in statistical treatments of nuclear multifragmentation.

While we have demonstrated the quantitative significance of interfragment forces and unbound fragment states, both of these aspects are the topics of current studies. We have also made a tentative extension to incorporate a nucleon vapor, in order to facilitate studies of liquid-gas phase transition phenomena; this aspect is also being further developed.

Footnotes and References

*Condensed from Nucl. Phys. **A471**, 355c (1987) and Nucl. Phys. **A424**, 173 (1987).

†W.K. Kellogg Radiation Laboratory, California Institute of Technology, Pasadena, California 91125

Fragment Interactions in Nuclear Disassembly*

J. Randrup, M.M. Robinson, and K. Sneppen†

We have studied the role of interfragment forces in multifragment systems and devised improved one-body approximations for an assembly of hard spheres.

1.) The most important feature of the nuclear part of the interfragment potential arises from the high nuclear incompressibility which acts to prevent fragments from overlapping. To a rough approximation, this effect can be taken into account by representing the nuclear fragments as hard spheres. Although somewhat simplistic, the hard-sphere approximation is still quite demanding in terms of computation, since it requires knowledge of all the relative fragment positions. Most models developed so far do not contain this degree of detail and so it has been common to adopt some form of a one-body approximation. In intuitive terms, the presence of the other fragments limits the volume available for a given fragment. It is therefore natural to attempt to approximate the mutual fragment repulsion in terms of a reduced "effective" volume, $\Omega_{\rm eff}$, within which the fragments can be considered as independent. We have examined such approximations in order to ascertain their quality and we have devised more accurate approximations. A common feature of the usual excluded-volume approximations is that they are independent of the fragment multiplicity, a shortcoming which limits their accuracy greatly. We have developed a quite useful approximation which we denote the Jastrow approximation, because is based on the assumption of *independent pairwise correlations* between the fragments. This approximation is amenable to a one-body treatment and can therefore be turned into a powerful practical approximation for interacting fragments.

2.) The exact Coulomb energy of N non-overlapping uniformly charged spherical fragments has also been studied and we have tested several commonly employed simple approximations, namely the mean-field (a fragment interacts with the field generated by the smeared-out total system), the refined mean-field (a fragment interacts with the field generated by the smeared-out residual system), and the Wigner-Seitz approximations. Although the latter one usually is the most accurate, it is far from satisfactory, so we have sought to devise improved approximations. A simple but generally superior approximation consists in replacing the denominator R in the refined mean-field approximation by $\frac{5}{6}R + R_n$. (The first term is the mean separation between two random points within a sharp sphere and the second term is the minimum separation between the fragment n and another fragment.) Without being more complicated, this approximation maintains its accuracy up to higher fragment densities than any of the commonly used ones.

Footnotes and References

*Condensed from Phys. Lett. B (in press).

†On leave from Niels Bohr Institute, DK-2100 Copenhagen Ø, Denmark

Hot Nuclei in a Nucleon Vapor*

G. Fái† *and J. Randrup*

Experimental evidence[1,2] indicates the creation of metastable fragments in nuclear collisions at medium energies. This information can be used to distinguish between different models of nuclear multifragmentation.[3] It also indicates the quantitative importance of the treatment of unstable excited states in statistical models for nuclear disassembly. Arguments based on a comparison of the life-time of metastable states to the collision time have been used in the past[4] to decide whether a particular unstable

state should be included in the phase space.

Although intuitively appealing, such life-time arguments are inadequate for the treatment of static problems, e.g., excited infinite nuclear matter at subsaturation densities. We therefore find it desirable to seek a more solid theoretical foundation for the description of highly excited nuclear states applicable both for the static nuclear-matter case and for scenarios relevant to nuclear disassembly.

A consistent treatment of the metastable states can only be achieved if a nucleon vapor surrounding the fragments is included in the calculation.[5,6] Therefore, we discuss a hot nucleus embedded in a vapor of nucleons. By Levinson's theorem, the total intrinsic partition function of the entire system is invariant to the partitioning of the levels between the nucleus and the vapor, in the independent-particle idealizatiou. However, it is important in practice to calculate the yields of different fragment types, and the final species distribution is sensitive to how this separation is made. We show that the fragment yields are sensitive to the prescription used to define (and separate from the vapor) the hot nuclei. The separation is also relevant to the frequently discussed question of the liquid-vapor phase coexistence in nuclear matter.

In our study, we first consider independent nucleons moving in an idealized single-particle mean field consisting of a region with (constant, negative) potential energy V_0 (the interior of the nucleus) surrounded by space where the potential energy is zero and the nucleons move freely (vapor). Starting from the Fermi-gas single-particle level density, we calculate the mean excitation energy (and its dispersion) of nuclei embedded in the vapor, as a function of the temperature. A given excited level is assumed to belong to the nucleus with a probability equal to the angular-momentum averaged reflection coefficient at the given single particle energy. From this 'parameter-free' description, an effective nuclear temperature can be obtained in order to facibtate comparisons with various previously employed prescriptions.

On the basis of this idealized study, the complications of the nuclear many-body problem can be incorporated in an approximate manner which seeks to give a consistent treatment of the vapor and its interaction with the hot nuclei.

Footnotes and References

*Condensed from LBL-24845.

†Kent State University

1. J. Pochodzalla *et al.*, Phys. Rev. Lett. **55**, 177 (1985).

2. Z. Chen *et al.*, preprint, MSUCL-624 (1987).

3. G. Fái and A.Z. Mekjian, Phys. Lett. **196B**, 281 (1987).

4. G. Fái and J. Randrup, Nucl. Phys. **A404**, 551 (1983).

5. S.E. Koonin aud J. Randrup, Nucl. Phys. A **474**, 173 (1987).

6. D.L. Tubbs and S.E. Koonin, Astrophys. Journal **232**, L59, (1979).

Quasi-Classical Treatment of the Nucleon Gas*

C. Dorso, S. Duarte, and J. Randrup

This contribution reports on recent progress[1] toward developing a quasi-classical simulation model for nuclear dynamical processes, such as can be generated in nuclear collisions at intermediate energies. The ultimate goal of such efforts is to develop a dynamical model for nuclear systems within the framework of classical mechanics. We here report a tentative first step consisting of simulating the noninteracting nucleon gas by means of a momentum-dependent repulsive two-body interaction potential to simulate the Pauli exclusion principle. Such an approach was first taken by Wilets *et al.*[2] In that work, a repulsive momentum-dependent Pauli potential was postulated and the parameters of an ordi-

nary two-body potential were adjusted to fit certain gross nuclear properties. Although the model met with some success, it was never demonstrated that the phase-space distribution of the nucleons is actually well approximated. Since this property is expected to be important for the dynamical behavior of a colliding system, there is a need for scrutinizing the problem. Therefore, we have reconsidered the problem of determining an appropriate Pauli potential, and we have found that it is in fact possible to obtain a reasonably good reproduction of the important features of the Fermi gas, with a suitable choice of potential. Our Pauli potential is of Gaussian form and thus differs from that employed in ref. 2. We see our result as a possible first step in a program, of which the next step is the inclusion of a real two-body interaction for the purpose of describing both nuclear matter and finite nuclei.[3] If this proves possible, the foundation is laid for an interesting dynamical model for the evolution of a highly excited nuclear system far from equilibrium, including its disassembly into multi-fragment final states.

In dynamical simulation studies of nuclear collisions it is of interest to determine the effective temperature in the system (which may depend on position if the system is not translationally invariant). In the present context, this problem can be stated as follows: Imagine that we are presented with a configuration (or several configurations) sampled from a thermal ensemble with a definite but unknown temperature τ. Our task is then to estimate the temperature characterizing the ensemble from which the given configuration is picked. More generally, one would like to calculate that temperature that would characterize the statistical equilibrium of the system at the given energy density, also when the actual system under scrutiny is far from equilibrium. In a standard classical gas with only momentum-independent forces, that problem can be trivially solved by employing the (local) kinetic energy per particle, which is uniquely defined, but when momentum-dependent interactions are present, the situation is more obscure and a more careful approach is called for. After having studied the situation for our present model system, we have found a method which may prove to be of general utility. Our prescription for extracting the effective temperature, $\tau_{\rm eff} = \langle(\mathbf{p}\cdot\hat{\mathbf{n}}\,\dot{\mathbf{q}}\cdot\hat{\mathbf{n}})\rangle$, suggests itself when the standard thermodynamic relation $P = \rho\tau$ is invoked in conjunction with the relation for the pressure. This expression provides a general method for extracting a useful effective temperature $\tau_{\rm eff}$ for the system, applicable to any quasi-classical assembly of point particles.

Footnotes and References

*Condensed from Phys. Rev. Lett. **B188**, 287 (1987) and J. Physique **48**, C2-143 (1987).

1. C. Dorso, S. Duarte, and J. Randrup, Phys. Lett. **B188**, 287 (1987); J. Randrup, C. Dorso, and S. Duarte, J. Physique **48**, C2-143 (1987).

2. L. Wilets, E.M. Henley, M. Kraft, and A.D. Mackellar, Nucl. Phys. **A282**, 341 (1977); L. Wilets, Y. Yariv, and R. Chestnut, Nucl. Phys. **A301**, 359 (1978).

3. Such efforts are presently underway by D. Boal *et al.*, 8th High-Energy Heavy-Ion Study, Berkeley (1987).

Pre-Equilibrium Neutron Emission in the Nucleon Exchange Transport Model*

J. Randrup and R. Vandenbosch†

We have extended the Nucleon Exchange Transport model to include the emission of pre-equilibrium neutrons as a result of nucleon transfer to unbound states. The treatment takes account of the heating of the two nuclei caused by the energy dissipation and the cooling due to the pre-equilibrium emission. Furthermore, the transferred nucleons may induce cascading in the receptor nucleus by means of direct

two-body scattering with the resident nucleons. This is calculated using a reduced, Pauli-blocked, energy-dependent free NN cross section. Qualitative agreement with experimental data is achieved and the dependence of multiplicity on bombarding energy is reproduced. The energy spectra and their variation with angle are generally reproduced, although the yield is sometimes underestimated at the highest energies.

We are currently extending the model to incorporate the production of photons in the direct neutron-proton collisions during the cascade process.

Footnotes and References

*Condensed from Nucl. Phys. A **424**, 219 (1987).

†Departments of Physics and Chemistry, University of Washington, Seattle, Washington 98195

Analysis of the Window Dissipation Formula on the Basis of Linear Response Theory*

T. Døssing† and J. Randrup

The long nucleonic mean free path has profound consequences for the character of large-scale nuclear dynamics. The first comprehensive study of this "new dynamics", often referred to as *one-body nuclear dynamics* (since the motion of the nucleons is governed by the changing one-body mean field), was carried out about ten years ago within the framework of classical kinetic theory.[1] It led to two remarkably simple formulas for the rate of energy dissipation: the *wall formula* pertaining to a slowly deforming mononucleus, and the *window formula* pertaining to a dinucleus whose two parts are in slow relative motion. The wall and window dissipation formulas have been employed extensively, with a considerable degree of success, to low-energy nuclear dynamical processes such as occur in fusion, fission, and damped reactions. We have sought to clarify the conditions for the validity of the standard window formula and to develop a formal framework for systematic improvement.

Toward this end, we have adapted the linear response theory developed for one-body dissipation (and employed for studies of the wall formula in mononuclei)[2] to analyze the rate of energy dissipation in a binary one-body potential well whose two parts are connected by a small "window" and are in slow relative motion. We have shown that suitable randomization assumptions lead to the "completed wall-and-window formula", including the contribution from the change in the mass asymmetry.[3] The developed general formal framework provides a well-founded basis for systematic calculation of corrections in cases that are less than ideal, such as those encountered in quasi-fission reactions.

Footnotes and References

*Condensed from Nucl. Phys. **A475**, 557 (1987).

†Niels Bohr Institute, University of Copenhagen Blegdamsvej 17, DK-2100 Copenhagen Ø, Denmark

1. J. Błocki, Y. Boneh, J.R. Nix, J. Randrup, M. Robel, A.J. Sierk and W.J. Świątecki, Annals of Physics **113**, 330 (1978).

2. S.E. Koonin and J. Randrup, Nucl. Phys. **A289**, 475 (1977).

3. J. Randrup and W.J. Świątecki, Nucl. Phys. **A429**, 105 (1984).

Order, Chaos and Nuclear Dynamics

J. Blocki, Y.-J. Shi,† and W.J. Świątecki*

In the past few years it has become apparent that the character of collective nuclear dynamics is intimately related to the nature of nucleonic motions inside the nuclear mean-field potential well. If the nucleonic motions are ordered, the nucleus as a whole is expected to behave like an elastic solid, whereas for chaotic nucleonic motions the nucleus should behave like a very viscous fluid. The present paper describes a systematic study of this phenomenon in the case of a gas of non-interacting point particles bouncing about in a static or oscillating container in the form of a distorted sphere, representing an idealized nucleus in the mean-field approximation. Fig. 1 illustrates the increase in the relative energy of the gas caused by five cycles of a harmonic oscillation of the container. When the deformation is relatively regular (as described by a Legendre polynomial P_2) the gas responds as a nearly elastic solid, absorbing and then releasing most of the energy in a reversible manner, in phase with the oscillation. When the deformation is more irregular (curves labeled P_3, P_4, P_5, P_6) the gas acts as a very viscous fluid, absorbing energy irreversibly (in close correspondence with the one-body dissipation wall formula). In Fig. 2 this behavior is brought into correspondence with the transition from ordered to chaotic nucleonic motions. This figure shows the behavior of ten representative gas particles as they cross and recross (150 times each) the equational plane of a (static) container. The container is either a spheroid with a major axis stretched by 5% or a sphere with a Legendre polynomial ripple of similar magnitude. The angular momentum about the axis of symmetry of the ten particles varies from zero in the first column of Fig. 2 to a high value in the last. Each of the 24 plots records (as a dot) the radial position ρ and the radial velocity v_ρ of the crossings of the equatorial plane. In the case of regular shapes (or high angular momenta) the dots lie along regular curves, defining the Poincaré sections of 'invariant tori' in phase space. With increasing irregularity of the shapes the tori disintegrate into chaotic swarms, exhibiting in the process the generic resonance properties familiar from the general theory of non-linear dynamics.

These studies have been carried out for a variety of shapes and amplitudes and represent a first step in relating quantitatively the order-to-chaos transition in nucleonic motions to the properties of collective nuclear dynamics.

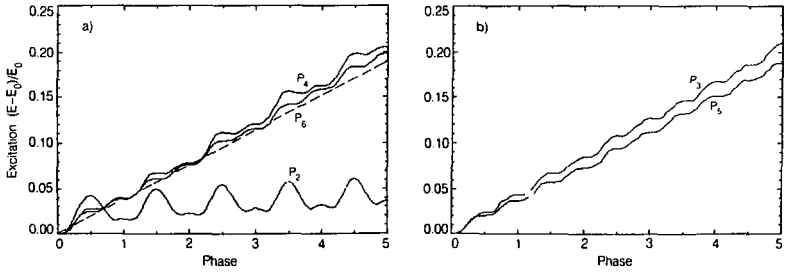

Fig. 1. The increase in the relative energy of a gas caused by the oscillation of a container undergoing Legendre polynomial deformations from P_2 to P_6. XBL 877-9298

*Institute for Nuclear Studies, Swierk, Poland

†Institute of Atomic Energy, P.O. Box 275 (18), Beijing, China

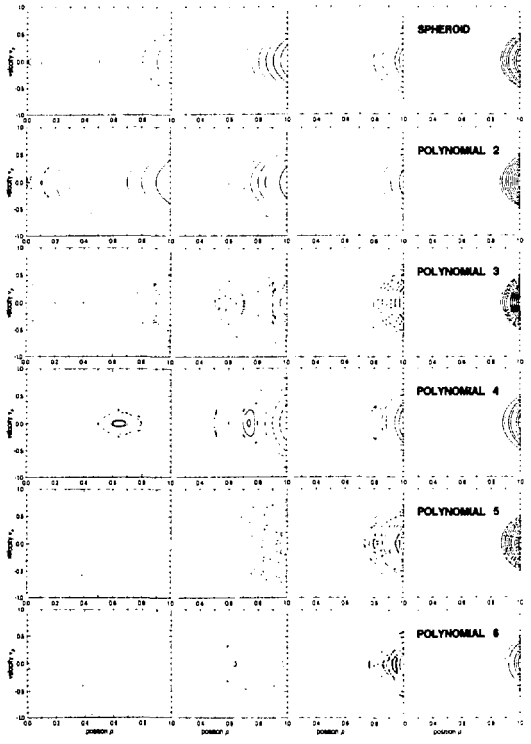

Fig. 2. Equatorial Poincaré sections for the motions of particles in variously deformed containers. XBL 877-3324

Semiclassical Quantization Using Adiabatic Invariance of Classical Actions Variables: Application to the Three-Dimensional Elliptical Boxes

*Francois Brut**

For multi-dimensional systems, semiclassical energies are obtained when the corresponding classical trajectories satisfy the so-called Einstein-Brillouin-Keller (EBK) quantization conditions:[1]

$$J_i = n_i + 1/2, i = 1, N, \tag{1}$$

where the J_i are the classical action variables in units of $\hbar = 1$, n_i are integer quantum numbers and N is the number of degrees of freedom.

To find among the classical trajectories those which satisfy the above conditions is not easy. An alternative method was proposed by Solov'ev.[2] This method utilizes the principle of adiabatic invariance of actions. The classical Hamiltonian of the system is divided into two parts.: $H = H_0 + H_1$ where H_0 is separable (i.e. integrable) and H_1 is the remaining part. We then construct a new time-dependent Hamiltonian function:

$$H(q,p,t) = H_0(q,p) + \alpha(t)H_1(q,p) \tag{2}$$

where $\alpha(t)$ is the adiabatic switching function which changes slowly over the time interval $0 \leq t \leq T$, from $\alpha(0) = 0$ to $\alpha(T) = 1$. An initial condition $q(0)$ and $p(0)$ is chosen on the semiclassical torus of H_0, and the equations of motion are integrated over the time interval $0 \leq t \leq T$. By the principle of adiabatic invariance, the actions will not change and therefore the same quantization conditions remain during the integration. In general, the energy is not conserved and, at the end of the integration interval it will be equal to the semiclassical bound state of the Hamiltonian H_0. More details on the method can be found in the works of R.T. Skodje, F. Borondo and P. Reinhardt[3] on the one hand and by B.R. Johnson[4] on the other hand.

This method is applied to the ellipsoidal cavity in three dimensions. The contour of the axially symmetrical cavity is defined by:

$$\frac{x^2 + y^2}{R_\perp^2} + \frac{z^2}{R_z^2} = 1 \tag{3}$$

where the deformation μ is defined by:

$$\mu = \frac{R_>}{R_<} = \begin{cases} \frac{R_z}{R_\perp} & \text{for a prolate deformation} \\ \frac{R_\perp}{R_z} & \text{for an oblate deformation.} \end{cases} \tag{4}$$

The volume conservation is written:

$$R_z R_\perp^2 = R_0^3 \tag{5}$$

where R_0 is the nuclear radius with $R_0 = r_0 A^{1/3}$.

Here the deformation μ is the adiabatic switching parameter which varies from 1 to 2, i.e., from the spherical billiard to a prolate or an oblate shape for which the ratio of the ellipsoid axes is 2:

$$\mu(t) = 1 + \alpha(t) \tag{6}$$

In this particular case, the motion of the particle is free between two successive collisions with the boundaries. The energy changes for the particle are calculated at each collision using the reflection conditions in the moving system boundary. At each step, the projection L_z of the angular momentum of the particle is calculated and conserved.

There is only one topology for classical trajectories in the prolate case ($L_z \neq 0$).[5] Thus there is no separatrix and we can obtain the single particle energies as a function of the deformation μ. Those functions are plotted in Fig 1 for the first 49 states of the axially symmetrical cavity, namely for the 1s,1p,1d,2s,1f,2p,1g,2d,1h,3s,2f,1i,3p,1i spherical multiplets. The adiabatic switching method reproduces the general behavior of the quantum mechanical calculations and is very close to the result of the uniform semiclassical quantization.

In the oblate case the classical trajectories can be classified in two topologies with a separatrix which corresponds to the top of a potential barrier, in a

spheroidal oblate system of coordinates.[5] A "uniform" semiclassical approximation must be used in this case which is related to a 'slipping of the actions cells'. Indeed, when the deformation increases, the semiclassical energy can cross the top of the potential barrier. The adiabatic switching method fails in the oblate case since it is unable to describe barrier tunneling, a fully quantal phenomenon. This effect needs the use of the uniform approximation[5] and corresponds to the slipping of the action cells. Some alternatives to this method are being investigated.

Footnotes and References

*On leave from Institut des Sciences Nucléaires, Université de Grenoble

1. A. Einstein, Verh. Dtsch. Phys. Ges. (Berlin) **19**, 82 (1917); L. Brillouin, J. Phys. Radium **7**, 353 (1926); J.B. Keller, Ann. Phys. **4**, 180 (1958); see also I.E. Percival, Adv. Chem. Phys. **36**, 1 (1977).

2. E.A. Solov'ev, Sov. Phys. JETP **48**, 635 (1978).

3. R.T. Skodje, F. Borondo, W.P. Reinhardt, J. Chem. Phys. **82**, 4611 (1985).

4. B.R. Johnson, J. Chem. Phys. **83**, 1204 (1985).

5. R. Arvieu, F. Brut, J. Carbonell, J. Touchard, Phys. Rev. **A35**, 2389 (1987).

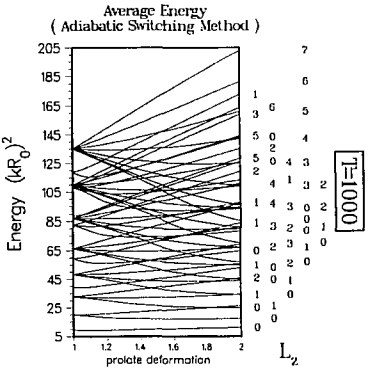

Fig. 1. See text. XBL 8711-4997

Calculated Fission Properties of Odd and Even Heavy Elements

P. Möller, J.R. Nix,† and W.J. Świątecki*

In ref. 1, to which we refer for definitions and notation used here, we undertook a theoretical study of the fission properties of heavy elements with even values of the proton number Z and the neutron number N, with the particular aims of exploring the existence of two distinct symmetric fission valleys and of understanding the rapidly changing fission properties of elements around fermium. Important aspects of the calculation were (1) the possibility of generating exactly the configuration of two touching spheres within the model and (2) the use of a finite-range model for the surface energy in the macroscopic part. The results obtained clearly showed two fission valleys, one leading to compact and the other to more elongated scission shapes. Calculated fission half-lives agreed well with experimental data for elements with $N \geq 152$ from Cf to $Z = 108$. The study was the first to calculate fission half-lives for paths leading into the new, compact valley.

To allow studies of the fission properties of odd nuclei we have here added the possibility of calculating the specialization energies associated with the odd particles. We have also studied the effect of mass-asymmetric shape distortions in a calculation that independently varies an elongation coordinate, a neck coordinate and a mass asymmetry coordinate in a full three-dimensional grid. We also study some shortcomings of the model used in ref. 1, that stood out particularly clearly when the behavior of the model for shapes evolving from a single nucleus to two different nuclei was considered. This has led us to include the following model modifications.

We have increased the smoothing range in the Strutinsky method from $1.0 \times \hbar\omega$ to $1.4 \times \hbar\omega$. In

the Strutinsky method the range in the smoothing procedure depends on the size of the system. As a fermium system evolves from a ground-state configuration to that of two touching spheres, the appropriate A value for determining the magnitude of the range parameter changes from about 260 to 130. To account for this change a shape dependence of the range should, in principle, be derived. However, by choosing the smoothing range γ in the shell correction calculation to have the value

$$\gamma = 1.4 \times \hbar\omega_0 \tag{1}$$

we can ensure that we will be on the "shell correction plateau," both at the ground-state and at the two-touching-sphere configuration of ^{264}Fm. In this way we avoid the complicated problem of deriving a shape dependence for the Strutinsky smoothing range.

The Wigner term, proportional to $|I|$, was first discussed by Wigner, and it accounts for a V-shaped trough or kink in the nuclear mass surface. A discussion in ref. 2 shows how a term of this unusual structure can arise from the increased overlap of particles in identical orbits. We refer to ref. 2 and original work referred to there, for a discussion on the Wigner term.

To derive an approximate shape dependence for the Wigner term we note that in ref. 2 it was pointed out that if a system is broken up into n identical pieces, then the Wigner term must be evaluated separately for each piece, with the result that it simply jumps to n times its original value. For symmetric fission into two identical fragments this simple argument would imply a shape dependence corresponding to a step function at scission. In reality one would expect that the step function is washed out over some range of shapes in the scission region. As a simple ansatz we assume for symmetric shapes the following shape dependence of the Wigner energy E_W

$$E_W = W|I| \left[\left(1 - \frac{S_3}{S_1} \right)^2 a_d + 1 \right] \tag{2}$$

Here S_3 is the area of a cross-section through the neck region and S_1 the area of maximum cross section of the end bodies. For cases where there is full communication between the two fragments, that is when there is a bulge at the middle instead of a neck, we use the conventional shape-independent expression for the Wigner energy. The *damping* coefficient a_d has been chosen $a_d = 0.9$. This parameter value accounts for the fact that for zero neck radius there is still some communication between fragments. For the A^0 term we choose an identical shape dependence.

The effect of including new shape dependences and a new range in the Strutinsky procedure are large, up to about 10 MeV close to scission. However, since the effect of the changes are of different sign, the results obtained in our previous study[1] are approximately retained.

To see the significance of the changes in the model we show some deformation energy contour maps in Fig. 1. The upper left part of the figure shows the shapes on which the contour maps are based and the upper right part shows the potential energy obtained without the improvements, as found in ref. 1 for ^{258}Fm. To the lower left we show the results obtained for ^{258}Fm with the new range $\gamma = 1.4 \times \hbar\omega_0$ in the Strutinsky method, but *without* the new shape dependence for the Wigner and A^0 terms included. For ^{258}Fm there is now no second barrier in the new valley, which would imply correctly a short half-life for this nucleus. However, the ridge between the old and new valley is much too high to allow any branching into the old valley as is indicated by experiment. This also holds true when mass-asymmetric shapes are considered. This contour map is very similar to the results recently obtained by refs. 3 and 4. This calculation uses a Woods-Saxon single-particle potential, the Yukawa-plus-exponential macroscopic model and a shape parameterization capable of generating shapes close to two touching spheres. As in our lower left contour map, their Wigner and A^0 terms are shape-independent. Other studies of the new fission valley may be found in refs. 5–10.

The last contour map, to the lower right, is calculated with the shape-dependences of the Wigner

and A^0 terms included. Here the structure of the surface is such that it provides an excellent interpretation of the experimental results. Most of the fission events will follow the path leading into the old valley. Just as in the calculation with the old version of the model in ref. 1 there is a *switchback* path leading from a point along the new path across a saddle at about $r = 1.50$ and $\sigma_2 = 0.85$ back to the old valley. This switchback path according to our interpretation is responsible for the few low-kinetic-energy events that are observed for this nucleus.

At this stage we calculate fission half lives for the old and new paths with the two semi-empirical models for the inertia that were proposed in ref. 1. A more extensive survey is planned. Here we give results for a few representative cases in Table I. For fermium isotopes we have also plotted the results in Fig. 2. Some half-lives along the old path are much longer in this calculation than in ref. 1 since we have here also calculated the effect of ϵ_6 deformations on the ground-state energy. This additional degree of freedom lowers the ground state by up to about 1 MeV around ^{252}Fm which explains the 6 orders of magnitude increase in half-lives we obtain for this nucleus. It is our view that consideration of half-lives along the switchback path would remove some of the discrepancies between calculated and experimental fission half-lives around the ^{252}Fm region. However, considering the sensitivity of fission half-life calculations to small changes in the barrier energies the deviations between calculated and experimental half-lives in Fig. 2 are of reasonable magnitude.

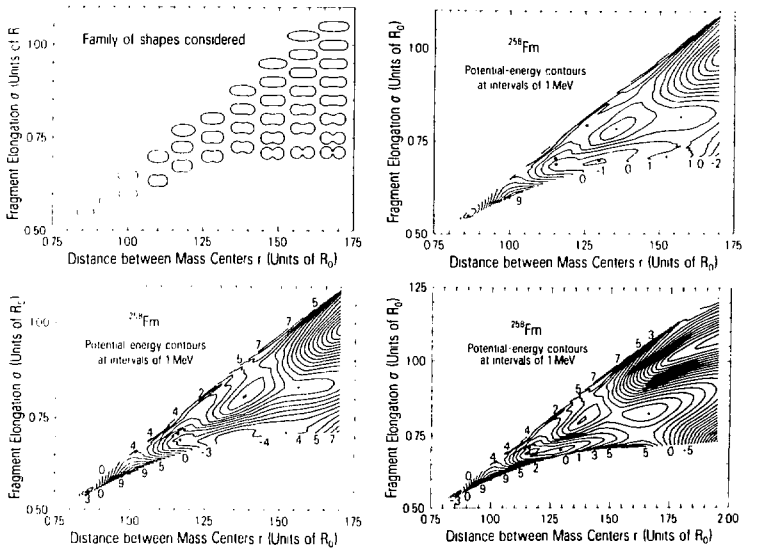

Fig. 1. Nuclear shapes and corresponding potential-energy surfaces. The three surfaces have been calculated under the different assumptions discussed in the text. The potential-energy surface in the lower right corner is based on our current model.

XBL 8711-4979

The overall agreement between calculated and experimental half-lives Table I is good despite a few large deviations. For $^{264}108$ the calculated half-life is very short compared to the limit set by experiments. However, as we move away from magic fragment particle numbers, we expect the inertia to increase, both because the particle number changes and because the position of the new valley changes. Thus we expect our calculated value to be an underestimate of the fission half-life. However, we still expect that fission half-lives on the "rock" of stability around $^{272}110$ are strongly affected by the presence of the magic-fragment neutron number 82. Calculations that consider only the old valley would tend to overestimate the fission half-lives of these elements.

One can make the further observation that in the new valley we usually obtain calculated values for even nuclei that are somewhat too long, but the half-lives for odd nuclei are usually too short. The reason may be that for odd nuclei there is an effect of the odd particle not just on the barrier but also on the inertia. We have also performed a three-dimensional calculation by including the effect of mass asymmetry in a region of deformations around the saddle leading to compact scission shapes and the switchback saddle. Asymmetry lowers the height of the switchback saddle somewhat but does not affect the height of the saddle leading to compact scission shapes. However, the basic structure of the potential-energy surface remains unchanged.

Table I
FISSION HALF-LIVES

Z	N	A	Calc., old path		Calc., new path		Exp.	
100	142	242	6.0	μs			800	μs
100	144	244	2.2	ms			3.7	ms
100	146	246	2.3	m			14	s
100	148	248	93	y			0.0046	y
100	150	250	$10^{5.0}$	y			6.9	y
100	152	252	$10^{0.7}$	y			150	y
100	154	254	11000	y			0.61	y
100	156	256	13	y	1.2	h	2.86	h
100	157	257			13	d	50000	d
100	158	258	130	d	158	ms	0.38	ms
100	159	259			0.17	s	1.5	s
100	160	260	704	y	50	μs	–	
101	159	260			0.3	d	30	d
102	152	254	21	y			0.0027	y
102	154	256	31	d			0.016	d
102	156	258	13	h	318	ms	1.2	ms
103	158	261			0.07	m	40	m
103	159	262			0.7	m	216	m
105	157	262			42	s	35	s
108	156	264			0.003	μs	≥100	μs
108	162	270			1.8	μs	–	
109	161	270			2.1	h	–	
109	163	272			$10^{7.7}$	y	–	

Our most important results are

- There are often three paths in the calculated potential-energy surfaces, namely the old path, the new path to compact scission shapes and a switchback path from the new path to the old path.
- There is a much lower inertia associated with fission in the new valley than in the old valley.
- The new valley is present at least up to $Z = 110$ for N values close to $N = 2 \times 82$. Its existence lowers the fission half-lives of some of these elements relative to earlier predictions.
- Odd-particle specialization effects bring substantial increases to the calculated fission half-lives also in the new valley.
- Calculated and experimental half-lives agree well with each other. Some remaining deviations sug-

gest that fission along the switchback path has to be considered and also that a model for how the inertia changes as one moves away from magic fragment neutron and proton numbers should be developed.

Peter Möller would like to thank the Los Alamos National Laboratory, the Lawrence Livermore National Laboratory and the Lawrence Berkeley Laboratory for the their hospitality and support during the course of this investigation.

Footnotes and References

*Lawrence Livermore National Laboratory, Livermore, CA 94550, USA

†Theoretical Division, Los Alamos National Laboratory Los Alamos, New Mexico 87545, USA

1. P. Möller, J.R. Nix and W.J. Świątecki, Nucl. Phys. **A469** (1987).

2. W.D. Myers, Droplet Model of Atomic Nuclei, (IFI/Plenum Data Co., New York, N. Y., 1977).

3. A. Sobiczewski, Proc. 22nd School on Nuclear Physics, Zakopane 1987.

4. S. Ćwiok, P. Rozmej, and A. Sobiczewski, Proc. 5th Int. Conf. on Nuclei far from Stability, Sept. 14-19, 1987, Rosseau Lake, Ontario, Canada, to be published.

5. M.G. Mustafa, U. Mosel and H.W. Schmitt, Phys. Rev. Lett. **28**, 1536 (1972).

6. M.G. Mustafa, U. Mosel and H.W. Schmitt, Phys. Rev. **C7**, 1519 (1973).

7. M.G. Mustafa, Phys. Rev. **C11**, 1059 (1975).

8. U. Mosel and H.W. Schmitt, Phys. Rev. **C4**, 2185 (1971).

9. U. Brosa, S. Großmann and A. Müller, Z. Phys. **A325**, 241 (1986).

10. U. Brosa, S. Großmann and A. Müller, Z. Naturforsch. **41** a, 1341 (1986).

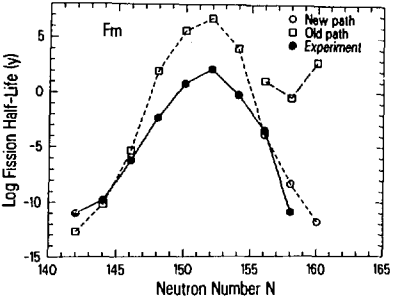

Fig. 2. Fission half-lives for Fm isotopes. We feel that the fairly large discrepancy present around ^{252}Fm is due to the fact that nuclei here do not fission along the old path but along the switchback path. If half-lives are calculated along the switchback path better agreement with experiment may result.

XBL 8711-4980

Nuclear mass Formulas with Finite-range Macroscopic Models and a Folded-Yukawa Single-particle Potential

P. Möller, W.D. Myers, J.R. Nix,* W.J. Świątecki, and J. Treiner†*

We calculate ground-state masses for 4678 nuclei ranging from ^{16}O to ^{318}122 by use of a macroscopic-microscopic model that incorporates several new features. Details of the calculations may be found in refs. 1–4. We study two different macroscopic models. One is the finite-range droplet model (FRDM) which was introduced in 1984. The other is the Yukawa-plus-exponential model (YPEM) developed in Los Alamos.[5] The FRDM is actually a combination of the Droplet model[6,7] and the YPEM. The microscopic contribution is in both models taken from a calculation described in refs. 1,3 based on a folded-Yukawa single-particle potential. To estimate the parameters of the macroscopic model we use an approach that starts by defining the *error* of a mass formula in a rigorous way, which leads naturally to the use of the *maximum-likelihood* method to derive a set of equations for estimating the parameters and error of the theoretical model. By considering 1593 experimental masses from ^{16}O to ^{263}106 we es-

timate the error of the theoretical models to be 0.769 MeV (FRDM) and 0.832 (YPEM). The models retain their accuracy far from stability and the values of the model parameters are very insensitive to details of the adjustment procedure. The major difference between the YPEM and the FRDM is that the latter accounts for compressibility effects. In Fig. 1 we show, for the FRDM case, experimental and calculated microscopic corrections, and at the bottom of the figure their difference, which is also the difference between experimental and calculated masses. We note that there are larger fluctuations in the error in the lighter region than in the heaviest region. This may be due to poorly determined spin-orbit and diffuseness parameters or to a gradual deterioration of the model for light nuclei. The single-particle parameters were determined from adjustments to experimental levels in the rare-earth and actinide regions. For lighter elements these parameters were determined by linear extrapolation through the known values in the rare-earth and actinide regions. We have some preliminary results that indicate that it is *not* possible to find a new set of single-particle spin-orbit strength and diffuseness parameters below the rare earth region that will substantially improve the agreement between both calculated masses and calculated single-particle level structures and their experimental counterparts. Since the deviations seem to be very systematically correlated with spherical magic numbers, some of the deviations in the light region may be removed by including some previously neglected residual interaction in the single particle model.

Footnotes and References

*Theoretical Division, Los Alamos National Laboratory, Los Alamos, NM 87545

†IPN, Bp no 1, 97406 ORSAY Cedex, France

1. P. Möller and J. R. Nix, Preprint LA-UR-86-3983, Los Alamos National Laboratory (1986).

2. P. Möller, W. D. Myers, W. J. Świątecki, and J. Treiner, Preprint LA-UR-86-4149 Los Alamos National Laboratory, Preprint LBL-22686, Lawrence Berkeley Laboratory, (1986).

3. P. Möller and J. R. Nix, At. Data Nucl. Data Tables, to be published.

4. P. Möller, W. D. Myers, W. J. Świątecki, and J. Treiner, At. Data Nucl. Data Tables, to be published.

5. H. J. Krappe, J. R. Nix and A. J. Sierk, Phys. Rev. C**20** (1979) 992.

6. W. D. Myers and W. J. Świątecki, Ann. Phys. (N. Y.) **55** (1969) 395.

7. W. D. Myers, Droplet Model of Atomic Nuclei, (IFI/Plenum Data Co., New York, N. Y., 1977).

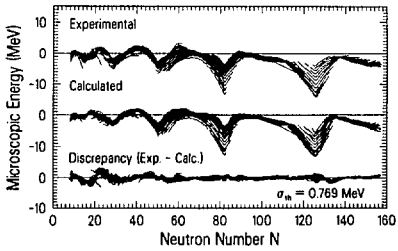

Fig. 1. Comparision of experimental and calculated ground-state microscopic energies for 1593 nuclei. Isotopes are connected by lines, even though some mass measurements are missing within certain isotopic chains. The macroscopic part of the energy was calculated with the FRDM. XBL 8711-4981

The Contribution of Collective Zero-Point Motion to Mean-Square Charge Radii*

W.D. Myers and P. Rozmej†

The average trend of the changes in mean square charge radii along an isotopic sequence predicted by the Liquid Drop Model is too steep by about a factor of two. The Droplet Model, because of the proper treatment of neutron skin effects, gives this average trend correctly. When this model is supplemented with information on the static deformations of the nuclei being considered, measured values can be predicted quite accurately. However, transition nuclei around magic neutron numbers show large deviations as can be seen in the upper part of Fig. 1, where the Droplet Model contribution has already been subtracted. Fig. 2 shows the results of zero-point motion calculations for these transition nuclei based on microscopically determined potentials and inertial parameters. The values of $\langle\epsilon^2\rangle$ deduced from these calculations are plotted as diamonds in the lower part of Fig. 1. These results do *not* agree with the measured values.

Additional calculations were performed to show that the results were not sensitive to the choice of inertial parameters.

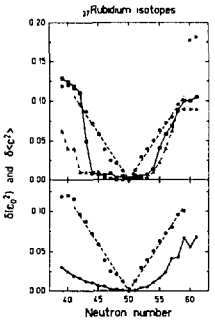

Fig. 1. Various values of the change in the mean-square deformation $\delta(\epsilon_0^2)$ or $\delta(\epsilon^2)$ that have been calculated or inferred from measurement are plotted against the neutron number. The round filled points are deduced from the measured values. The dashed line is meant to guide the eye and it represents the measured behaviour of the transition nuclei. The square symbols and the triangles represent static deformation calculations. The diamonds connected by a solid line in the lower part of the figure represent the results of the dynamical calculation.

XBL 8710-4011

Footnotes and References

*Condensed from GSI-87-14, to be published in Nuclear Physics.

†On leave from the Department of Theoretical Physics, University MCS, Lublin, Poland

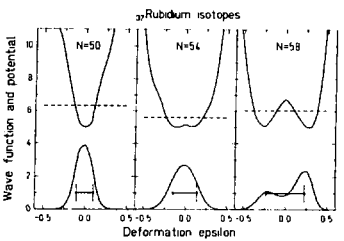

Fig. 2. Three examples of the potentials used in the zero-point motion calculations are shown. The horizontal dashed line represents the value of the energy and the probability distribution is shown at the bottom. The bars connected with a horizontal line are located at $\pm\langle\epsilon^2\rangle^{1/2}$.

XBL 8710-4012

Zero-point Fluctuations and the Diffuseness of the Nuclear Surface*

M.W. Guidry,† R. Donangelo,‡ J.O. Rasmussen, M.S. Hussein§

For heavy ion reactions such as deep inelastic scattering or subbarrier fusion, the motion of nuclei of various static shapes on classical trajectories often provides a convenient starting point for the understanding of the reaction. However, such a picture ignores the zero-point fluctuation which must be associated with such ions in their ground states. For processes such as subbarrier fusion or deep-inelastic scattering the distance between nuclear surfaces in the collision plays a crucial role, and surface fluctuations near the point of closest approach may have a significant effect on the reaction.[1]

The time scale of the reaction provides an important method for classifying such modes. Very high frequency fluctuations for which the period is much shorter than the heavy ion reaction time respond adiabatically and contribute only real polarization terms to the effective ion-ion potential.[2,3] Very low frequency fluctuations respond as if the shape is essentially frozen in the time of interaction. Thus the effective inertia associated with such modes is large, and strong net excitation may result from the collision. For beam energies <10 MeV/nucleon, giant resonances are expected to fall approximately into the former category, although fast components in the nuclear interaction may cause even these modes to make some contribution to deposition of energy and angular momentum in heavy ion reactions. Low-energy vibrations, such as those responsible for the first 2^+ states in many spherical nuclei, are expected to lie nearer the second category. In this paper we primarily are concerned with the effect of low-frequency, large-amplitude zero-point modes on heavy-ion scattering, and we ignore the effect of high-frequency small-amplitude motion connected with giant resonances. We also restrict attention to spherical vibrators, even though similar arguments may apply to vibrations about deformed equilibrium shapes.

The experimental procedure to determine the bare optical potential could be as follows. Very heavy ions would be used at energies in the Coulomb-nuclear interference region to excite multiphonon vibrational states. A detailed coupled-channel fit to the corresponding angular distributions (or excitation functions) would be used to find an ion-ion potential which simultaneously fits all the inelastic scattering data (state by state). By the preceding arguments such a potential should have most of the diffuseness due to zero-point fluctuation of the explicitly coupled modes removed. Conversely, a nuclear potential determined to fit only the total quasielastic cross section in this experiment will include an average over all phase angles and should exhibit a larger diffuseness. The implementation of such a study is is possible with present technology using γ coincidence spectroscopy.

Footnotes and References

*Condensed from Phys. Rev. C **36**, 609 (1987)

†Department of Physics, University of Tennessee, Knoxville, TN 37996 and Oak Ridge National Laboratory, Oak Ridge, TN 37830

‡Instituto de Fisica, Universidade Federal do Rio de Janeiro, 21944 Rio de Janeiro, Brazil

§Instituto de Fisica Universidade de Sao Paulo, 01498 Sao Paulo, Brazil

1. H. Esbensen, A. Winther, R.A. Broglia, and C.H. Dasso, Phys. Rev. Lett. **41**, 296 (1978).

2. J.O. Rasmussen, P. Möller, M.W. Guidry, and R.E. Neese, Nucl. Phys. **A341**, 149 (1980).

3. M.S. Hussein, A.J. Baltz, and B.V. Carlson, Phys. Rep. **113**, 134 (1984).

Geometrical Relationships of Macroscopic Nuclear Physics*

R.W. Hasse† *and W.D. Myers*

The purpose of this book was to provide a single reference source for the wealth of geometrical formulae and relationships that have proven useful in the description of atomic nuclei and nuclear processes. Fig. 1 serves to illustrate the explosive growth of new ideas in this field during the 70's. Currently, the rate at which new material is appearing is considerably slower. This provides us with the opportunity to bring the formulae together in a meaningful way.

Eleven different chapters (with appropriate references and illustrations) deal with such subjects as Folded Distributions, Spheriodal Deformations, Saddle Point Properties and Exotic Shapes.

One example of new material developed in the course of this work is shown in Fig. 2. In this figure the deformation energy is shown for y-family shapes. (the actual LDM fission saddle point shapes) for different choices of the parameter x (which is determined from the ratio of the Coulomb energy to the surface energy).

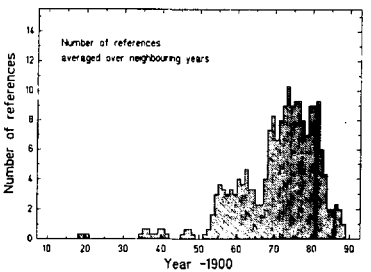

Fig. 1. A histogram showing the distribution of the publication date's of the references cited in this work.

XBL 8710-4013

Footnotes and References

*Condensed from the manuscript of a book to be published by Springer-Verlag, Heidelberg.

†Gesellschaft für Schwerionenforschung GSI, D-6100 Darmstadt 11, Germany

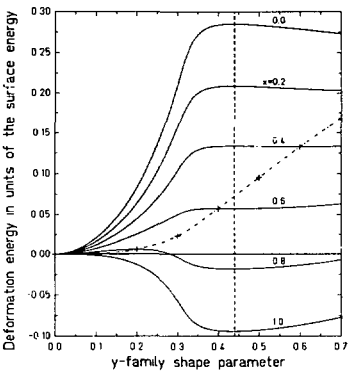

Fig. 2. The quantity $B_{Def}(x,y)$, which is the deformation energy in units of the surface energy of the sphere, is plotted versus y for various values of x. The vertical dashed line locates the extremum at y = 0.437 and the dot-dashed line is the locus of the extrema corresponding to the fission saddle point shapes. For each x it lies at y = 1 − x.

XBL 8710-4014

The Nuclear Deformation Parameters at High Excitation Energies*

J.L. Egido,† C. Dorso,‡ J.O. Rasmussen, and P. Ring§

The behavior of the deformation parameters with increasing excitation energy is analyzed in different theories. Realistic calculations are done for the nucleus ^{158}Er.

The full probability distribution $P_M(a_0, a_2)$, i.e., including the mass dependence, is shown in Fig. 1. For T=0.2 MeV the exponential dependence is too strong to be changed by the mass dependence on a_0, a_2. At temperature 1 MeV a second maximum appears at the oblate edge with equal probability to the prolate one. At T=1.2 and 1.4 MeV the probability maximum appears at the oblate edge with equal probability to the prolate one. At T=1.2 and 1.4 MeV the maximum appears for the oblate shape only. For T= 2 MeV the maximum extends around the spherical shape.

Other examples are given in the full paper.

Footnotes and References

*Condensed from Phys. Lett. **B178**, 139 (1986).

†Departamento de Física Teórica, Universidad Autónoma, Madrid, Spain

‡Facultad de Ciencias Exactas, Universidad de Buenos Aires, Argentina

§Physik-Department der Technischen Universität München, Garching, West Germany

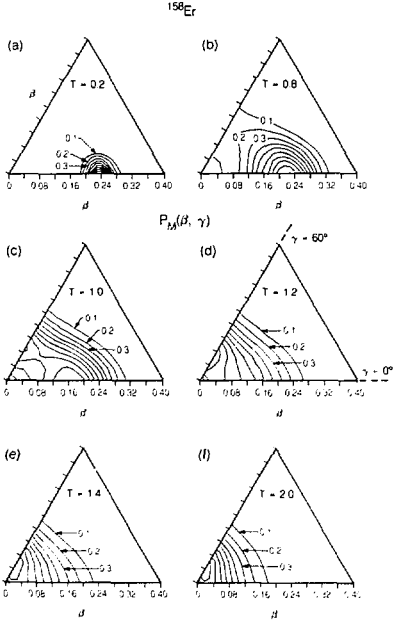

Fig. 1. The probability distribution $P_M(a_0, a_2)$, with mass dependence for different temperatures for the nucleus ^{158}Er. The outer contour corresponds to 0.1; the stepsize is 0.1; the maximum value is 1.0.

XBL 864-10752

Pair Transfer at High Angular Momenta*

J.L. Egido† and J.O. Rasmussen

Realistic calculations of nucleon pair transfer strength functions were performed for the nuclei ^{162}Dy and ^{164}Dy as a function of the angular momentum (to I=44) and excitation energy (to 10 MeV) in the frame of the self-consistent, cranked Hartree-Fock Bogolyubov (HFB) and random phase approximation (RPA) theories. At low angular momenta most of the strength is concentrated in the ground-to-ground transition.

At all spins the strength to excited states fluctuates under a flat envelope with no evident concentration attributable to pairing-vibrational excitation. The only systematic appearance of extra strength to excited states occurs in the first band-crossing region, where special strength goes to the crossing level just above the yrast level.

Footnotes and References

*Condensed from Phys. Rev. C 36, 316 (1987).

†Permanent address: Departmento de Física Teórica, Universidad Autónoma de Madrid, 28049 Madrid, Spain

A Scenario for Estimating the Charge on the Electron in Terms of Planck's Constant and the Speed of Light*

W.J. Świątecki

The conjecture that the electron might be a soliton of a non-linearly generalized, charge-free electromagnetic field, together with an estimate of the strength of the hypothetical non-linearity (based on the standard QED calculation of the scattering of light by light) leads to an estimate of the soliton's charge e such that hc/e^2 turns out to be equal to 45π multiplied by a number of order one, whose precise value depends on the details of the soliton's radial form factor.

Footnotes and References

*Condensed from LBL-23435 (1987).

Superstring Amplitudes and Contact Interactions*

J. Greensite† and F.R. Klinkhamer

Superstring field theory was originally constructed in light-cone gauge by Green and Schwarz,[1] who argued that the theory of closed superstrings is cubic *with only three-string vertices, while the only four-string vertex of open superstrings is of the Kaku-Kikkawa form. In two previous articles*[2,3] we took issue with the claim, and showed that supersymmetry (i.e., the closure of the super-Poincaré algebra) required the existence of new, local contact interactions, of quartic order in the stringfields. In other words, the string theory constructed by Green and Schwarz is incomplete, and not supersymmetric as it stands.

This leads to a puzzle. If the Green-Schwarz field theory is not supersymmetric, then scattering amplitudes constructed from that theory should not be supersymmetric either, even at tree level. But tree level amplitudes for arbitrary numbers of incoming and outgoing massless superstrings have been computed, and these amplitudes are manifestly supersymmetric. There would seem to be no need (and indeed no room) for any additional interaction terms.

The purpose of our study is therefore to closely re-examine the superstring tree amplitude calculation,

concentrating on the open and closed 2 string → 2 string process. We have shown that, contrary to common belief, a careful calculation based entirely on the existing theory does not yield a dual, relativistic, supersymmetric amplitude. In fact, the resulting amplitude is not even finite! A finite amplitude can be obtained by performing certain partial integrations[4] in the Koba-Nielsen variables, which leaves a finite supersymmetric Koba-Nielsen integral, plus divergent and unwelcome boundary terms. In existing calculations of tree amplitudes, these divergent surface terms have simply been dropped by hand. It is clear that the only-systematic way of dropping contributions to scattering amplitudes is to introduce counter terms in the Hamiltonian to cancel them. Our main result is to construct the required quartic counter terms of open and closed superstrings in detail. We show that these terms are local contact interactions of the form[2] shown pictorially in Fig. 1.

The existence of superstring contact interactions had been previously deduced from the following. Consider, for example, the type IIB theory. The super-Poincaré algebra contains, in the notation of ref. 1, the following relations.

$$\{Q_I^{-\dot{A}}, Q_I^{-\dot{B}}\} = 2\delta^{\dot{A}\dot{B}} H \qquad (1a)$$

$$\{Q_I^{-\dot{A}}, Q_I^{-\dot{B}}\} = \{Q_I^{-A}, Q_I^{-B}\} = 0 \qquad (1b)$$

where Q_I^- is one of the (N = 2) supercharges and similar relations hold for Q_{II}^-. The supercharges and the Hamiltonian were constructed in ref. 1 to $O(\lambda)$

$$Q_I^- = Q_{2,I}^- + \lambda Q_{3,I}^- \qquad (2a)$$

$$H = H_2 + \lambda H_3 \ , \qquad (2b)$$

(where suffixes 2,3 indicate that the operator is quadratic or cubic in the string fields; λ is the coupling) and shown to satisfy (1) also to $O(\lambda)$. Green and Schwarz in ref. 1 argued that contributions to the matrix element of the lhs of (1) cancel at $O(\lambda^2)$; however the main point of our previous papers[2,3] was that this cancellation is not complete. As a result there must he a further term in the supercharge $\lambda^2 Q_{4,I}^-$ and also a quartic term in the hamiltonian $\lambda^2 H_4$ given by

$$2\delta^{A\dot{B}} H_4 = \{Q_{3,I}^{-\dot{A}}, Q_{3,I}^{-\dot{B}}\}$$

$$+\{Q_{2,I}^{-A}, Q_{4,I}^{-\dot{B}}\} + \{Q_{4,I}^{-A}, Q_{2,I}^{-\dot{B}}\} \ . \qquad (3)$$

For details we refer the reader to our previous work. One point that should be noted, however, is that the cubic part of the supercharge Q_3^- has the form of a 3-string vertex, and the non-vanishing piece of Q_3^-, Q_3^- comes from contributions where the string join/split points of each vertex coincide. This is why H_4 has the form of a local contact interaction.

From Eq. (3) we see that the computation of H_4 requires knowledge of Q_4^-, which in principle could be constructed from the super-Poincaré algebra, but is at present unknown. In this paper our approach is, instead, to construct H_4 from the requirement that tree amplitudes be finite and supersymmetric. This approach has the great advantage that we are able to construct H_4 explicitly, without detailed knowledge of higher order terms in the supercharge Q^-.

Our motivation for finding the counter terms of the light-cone superstring is not simply to redo tree amplitudes, but rather to understand the structure of the interaction terms in the superstring Hamiltonian. If, for example, we uncover a Higgs-like structure in the light-cone Hamiltonian, then it may be possible to address non-perturbative questions of vacuum structure in superstring field theory. We have given some preliminary discussion of this issue.

Our results were for a fixed gauge, i.e. light-cone, but we suspected that invariant formulations might also "suffer" from extra contact interactions. Recently this has been shown[6] to be the case for Witten's superstring field theory. Our discovery of new contact interactions is thus quite general.

Footnotes and References

*Condensed from LBL-23830.

†San Francisco State University, San Francisco, CA 94132

1. M. Green and J. Schwarz, Nucl. Phys. **B243**, 475 (1984).

2. J. Greensite and F.R. Klinkhamer, Nucl. Phys. **B281**, 269 (1987).

3. J. Greensite and F.R. Klinkhamer, Nucl. Phys. **B291**, 557 (1987).

4. S. Mandelstam, Nucl. Phys. **B69**, 77 (1974).

5. M. Kaku and K. Kikkawa, Phys. Rev. **D10**, 1110 (1974). E. Cremmer and J. Gervais, Nucl. Phys. **B90**, 410 (1975).

6. C. Wendt, SLAC preprint.

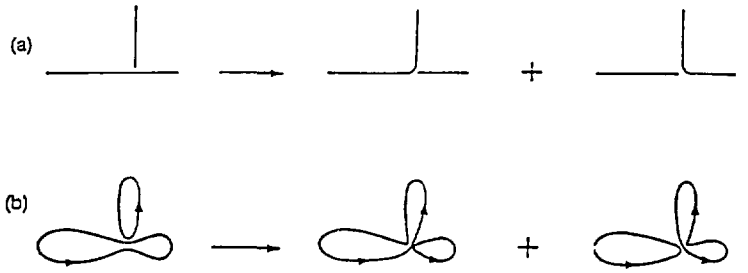

Fig.1. Quartic superstring contact interactions in the light-cone gauge: (a) non-planar contact interactions for open superstrings (b) contact interactions for closed type II superstrings (and also for heterotic strings).

XBL 881-300

PART IV: INSTRUMENTATION AND METHODS

A New Low-Energy Proton Telescope

J.D. Robertson, D. Moltz, J. Reiff, T. Lang, and J. Cerny

In order to search for ground state (g.s.) one- and two-proton emission from light proton rich nuclei, we have developed a detector capable of measuring very low energy protons in the presence of a high β^+ background. The ability to identify protons in a high background (β^+ rates of ~105 cps) is necessary because the nuclei which are predicted to decay by g.s. one- and two-proton emission are expected to have half-lives well below 10 ms and be produced in reactions with very small cross sections. As a result, mass separation of the multiple reaction products for the proton measurements is almost impossible. The detector must be able to measure protons with an energy range of 100 keV to 1 MeV because any proton-rich nucleus with more than 1 MeV of energy available to these g.s. proton decay channels will not live long enough to be observed.

The particle identification telescope which we have designed to search for g.s. one- and two-proton emission consists of a gas ΔE counter and a silicon E counter. The window of the gas counter is 30 μg/cm^2 stretched polypropylene. The active volume of the gas ΔE is defined by two wire grids 2.5 mm on either side of a 70 μg/cm^2 nickel foil. The wire grids are grounded and the nickel foil is maintained at a potential of 500 to 540 volts. This high electric field (~2000 V/cm) places the gas detector just below the avalanche region and provides the gas amplification necessary for particle identification. Isobutane, Freon-14, propane, and an argon methane mixture were tested as gases for the counter, and it was found that Freon-14 gave the best gas amplification for protons and the best shaped signal.

In this telescope, the signals from the ΔE counter are used for particle identification, but the final energy signal is taken solely from the silicon E counter. It was tested offline with 500 keV and 1 MeV protons from a Van de Graaff generator and was recently tested online by measuring the protons from the β-delayed proton decay of ^{25}Si. From a comparison of the two spectra shown in Fig. 1, it can be seen that the telescope can readily separate the 389 V proton group from a high β^+ background. The β^+ rate during the experiment was 9×10^4 cps. And finally, although the telescope was originally designed to measure low energy protons, it is clear from the ^{25}Si data that it also works well for measuring high-energy protons. This approach has the advantage over the solid state particle identification telescopes used in our previous proton measurements[1,2] in that the resolution of the detector telescope is only limited by the resolution of the silicon E counter and the entrance window thickness because the protons lose only a few keV of energy in the gas ΔE counter.

Footnotes and References

1. D.J. Vieira, R.A. Gough, and J. Cerny, Phys. Rev. **C19**, 177 (1979).

2. J. Äystö *et al.*, Phys. Rev. **C32**, 1700 (1985).

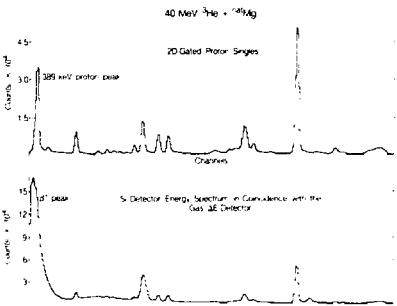

Fig. 1. The singles and 2-dimensional gated proton spectra from the measurement of ^{25}Si decay.

XBL 8712-8202

A New Shielded Detector Station for the Mass Separator RAMA

T.F. Lang, J.D. Robertson, D.M. Moltz, J.E. Reiff, and J. Cerny

The helium-jet coupled on-line mass separator RAMA achieved initial success in the late seventies with the discoveries via their beta-delayed proton decays of the $T_z = -2$ nuclides ^{20}Mg, ^{24}Si and ^{36}Ca.[1] Other early experiments involved β-γ studies of the neutron deficient isotopes ^{105}In.[2] Proposed β-γ studies of neutron deficient light nuclei, however, require the use of intense light ion beams. The large neutron flux associated with such beams produces an unacceptably high background for the detectors located at the RAMA focal plane. We have addressed this problem by constructing a beam transport line from the RAMA focal plane to a highly shielded area 22.2 ft downstream (see Fig. 1). The shielding platform, measuring 10 ft × 10 ft, is lined on the bottom and two sides with cans of saturated sodium tetraborate solution. The transport line consists of an electrostatic quadrupole triplet followed by an Einzel lens, which compresses the beam to the 1 cm diameter necessary for convenient collection. We can collect the radioactivity using a conventional tape transport system or with a fast pulsing system. The latter setup employs deflector plates which pulse the beam between the two collector boxes located at the ends of the small beam pipes. Utilizing this system will eliminate the delay times associated with tape transport methods. The fast (ns) rise time of the pulse, combined with standard multiscaling techniques, will permit precise half-life determinations.

The first use of the shielded detector station will involve β-γ and γ-γ studies of the $T_z = -3/2$ nuclei ^{23}Al and ^{27}P to complement their initial characterizations via their weak beta-delayed proton branches.[3,4]

Footnotes and References

1. J.Äystö, M.D. Cable, R.F. Parry, J.M. Wouters, D.M. Moltz and J. Cerny, Phys. Rev. **C23**, 879 (1981).

2. J.M. Wouters, H.M. Thierens, J.Äystö, M.D. Cable, P.E. Haustein, R.F. Parry and Joseph Cerny, Phys. Rev. **C27**, 1745 (1983).

3. R.A. Gough, R.G. Sextro and J. Cerny, Phys. Rev. Lett. **28**, 510 (1972).

4. J.Äystö, X.J. Xu, D.M. Moltz, J.E. Reiff, J. Cerny and B.H. Wildenthal, Phys. Rev **C32**, 1700 (1985).

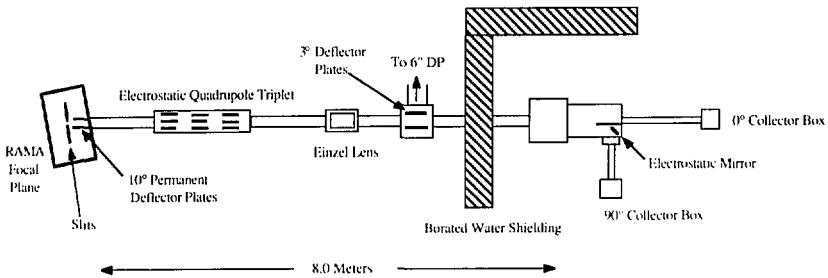

Fig. 1. *Beam transport line.* XBL 885-1778

Performance of a Phoswich Detector Array for Light Particles and Heavy Ions*

J.Pouliot, Y.Chan, A.Dacal,† A.Harmon, R.Knop,‡ M.E.Ortiz,† E.Plagnol,§ and R.G.Stokstad.

The average number of particles produced in a heavy ion collision increases rapidly with the bombarding energy in the intermediate energy region (20–100 MeV/nucleon). A large particle multiplicity can result from multifragmentation of the projectile induced by a peripheral interaction with the target. In most cases, the energetic fragments are kinematically focused in the forward direction, making it possible to measure such quantities as the total longitudinal momentum and total charge of all the emitted fragments.

In order to detect most of these fragments, a phoswich array consisting of 48 ΔE-E elements with sufficient granularity ($\Delta\Theta = \pm 2.5°$) to handle high multiplicity events has been built. The full angular coverage is a 35°× 35°square cross section of the 4π sphere (Fig. 1). Unit charge resolution for Z ≤ 10 and mass resolution for Z=1 particles has been achieved with a ± 5% energy resolution. To simplify and speed up the analysis procedure, one detector is chosen as a reference and the responses of the other phoswich detectors are then mapped onto that detector's response using a second order polynomial procedure. Fig. 2 shows the superimposed ΔE-E scatter plot of all the detectors mapped together. It can be seen that good charge resolution is maintained.

The first experiment performed with the array was to determine the multifragmentation of the projectiles (^{16}O,^{14}N,^{12}C). The array was then used in conjunction with two position sensitive multiwire proportional/parallel plate counters (for fission fragments) to investigate particle correlations as a function of momentum transfer for the ^{16}O+^{238}U reaction. Data analyses of both experiments are in progress.

Footnotes and References

*Condensed from LBL-24396

†Permanent address: Instituto De Física, UNAM, México D.F. 01000, México.

‡Summer research participant from Harvey Mudd College.

§Permanent address: Institut de Physique Nucléaire, B.P. No 1, 91406 Orsay, France.

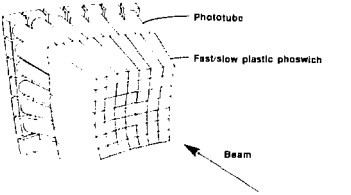

Fig. 1. Perspective view of the array. The fast scintillator (NE-102) is used for the 1 mm thick ΔE and the slow component (NE-115) is 10.2 cm long. Each detector faces the target at a distance of 19 cm. The frontal area of a detector is 1.68 x 1.68 cm^2, ($\Delta\Theta = \pm 2.5°$). The energy thresholds, due to the 1 mm thick ΔE layer, range from 9.0 MeV for protons to 19.0 MeV/nucleon for ^{16}O. XBL-8711-4685

Fig. 2. Mapped ΔE-E Spectrum. This spectrum is the superposition of all the phoswich detectors after each one has been mapped to a reference detector. Separate maps are used for the light Z=1 region and for the heavy ion region (Z≥2). Only one set of gates needs to be applied for the particle identification of any detector. The spectrum is for the ^{16}O + ^{12}C reaction at 32.5 MeV/nucleon. XBL 8711-4687

The Application of Position-Sensitive Phoswich Detectors for Low-Mass Fragment Detection in an Array Environment*

Y. Chan, E. Chavez, A. Dacal, S. Gazes, B.A. Harmon, M.E. Ortiz, E. Plagnol, J. Pouliot, and R.G. Stokstad

Large solid angle position-sensitive phoswich detectors have been constructed to replace smaller units in an array for detecting light mass fragments in nuclear experiments. There are three major advantages in using position-sensitive phoswich detectors: (i) the large available geometrical coverage (for the present example, a single module covers 5°×60°) (ii) the low electronics overhead cost as compared with a segmented configuration, and (iii) the possibility of obtaining *continuous* position information, which in some cases is very desirable as, for instance, in the study of sequential-breakup processes.

The detector is composed of four major parts: the scintillator section, the photo-tube assembly, the LED light pulser, and a mechanical fixture (Fig. 1). The dimension of the plastic scintillator section is 30cm×2.5cm×2.5cm (composed of a fast component made up of 0.5–1.0mm thick NE102A sheet and and a slow, 2.5cm thick, NE115 counterpart). For some later versions, the slow part is 10cm thick and is tapered towards the front surface (Fig. 1b).

To examine the position response and particle identification capability of the detector, we have measured reaction products emerging from the $^{16}O+^{12}C$ reaction at 32.5 MeV/nucleon. A slotted mask was positioned in front of the detector for position resolution study and calibration purposes. The overall performance of the detector can be summarized as a triad in a plot of the independent I_{short}, I_{long}, and TAC_{pos} parameters (lower part of Fig. 1). This plot has made use of the fact that the position dependence of the raw signals could be eliminated to first order by simply taking the geometrical mean of the corresponding top and bottom signals, $I_{Short(long)} = [I^{top}_{s(l)} \times I^{bot}_{s(l)}]^{1/2}$. It can be seen that the detector could resolve charged particles with Z≤10. The position information was derived from a time difference approach based on the intrinsic amplitude dependence of the leading edge discrimination method. The position resolution was found to be ~6 mm.

A problem with these rectangular detector geometries is that particles impinging at different angles to the detector surface will encounter ΔE elements of different geometrical thicknesses. This effect in principle could be totally corrected for by software procedures from the known position information. It was found that by setting narrow gates on the position, one can actually resolve p, d, and t particles within the Z=1 group. We plan to improve the performance of the detector by altering the geometry to a tapered semi-circular concentric configuration (Fig. 1c). This has the advantage that all particles will impinge *normally* on the detector surface and traverse identical ΔE thicknesses.

*Condensed from LBL-24529

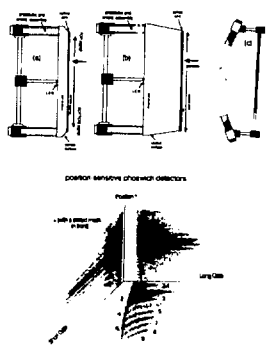

Fig. 1. Schematics of position-sensitive phoswich detectors corresponding to three different geometries (a)–(c). The lower part shows the particle identification capability and position response of the detector.

XBL-8712-5136

Improvements to OASIS

P. Wilmarth, L. Archambault, A. Wydler, and J.M. Nitschke

A number of improvements have been made to the SuperHILAC's online mass separator, OASIS (Fig. 1), since ref. 1 was published. The ion source (bottom inset, Fig. 1) now uses a slit extraction geometry which has improved the yield by at least 50%. The ion sources used to have a tungsten liner to increase the surface ionization yield compared to tantalum but mechanical problems at the high operating temperatures caused little increase in yield. The ion source is now 100% Ta in the high temperature regions. A bundle of capillary tubes inside the ion source prevents the stopped recoils from migrating back toward the target after they have diffused out of the anode/catcher. The finite wall thickness (75 to 100 micron) of the capillary tubes stopped a significant fraction of the recoils so the use of very thin-walled capillary tubes (35 to 50 micron wall thickness) has improved the transmission from the target to the catcher by about 25%. In an effort to protect fragile targets, the beam intensity is continuously monitored and the SuperHILAC beam interrupted if the intensity exceeds a preset limit. Also, a change in the ion source electrode configuration eliminated a potential gradient between the anode and target which gave rise to arc discharges that could damage the target.

Many improvements have taken place in the low background spectroscopy laboratory, ref. 2. Modifications to the IBM 729 tape drive have improved the tape positioning accuracy at the fastest tape transport speeds and reduction gearing was added to allow for a variety of transport speeds. The detector chamber is now pumped directly by a 500 l/s turbomolecular pump and fully automated rewinding of the collection tape is now possible. The present detector configuration is shown in the top insert of Fig. 1. The large (52%) Ge detector, located in close counting geometry, has greatly improved gamma ray detection sensitivity. The complexity associated with large Q value decays in the neutron-deficient lanthanides requires absolute gamma and x ray intensity measurements along with half-life information to unravel the mixture of activities present in an isobaric chain. This is accomplished with two time-resolved spectroscopy systems recording singles data from the HPGe detector (8 by 512 channels maximum) and the 52% Ge detector (8 by 8192 channels maximum).

Footnotes and References

1. J.M. Nitschke, Nucl. Instr. and Meth. **200**, 341 (1983).

2. P.A. Wilmarth, *et al.*, Nuclear Science Division Annual Report 1982-1983, LBL-16870, p. 280 (1984).

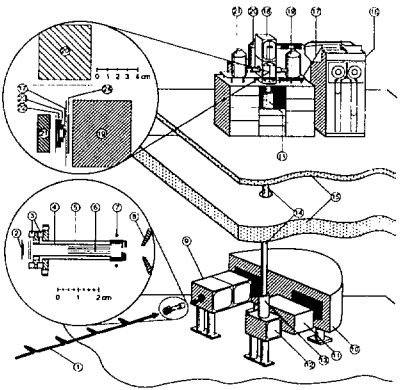

Fig. 1. A simplified representation of the OASIS mass separator online at the SuperHILAC. The separator and tape system are approximately to scale.

XBL 875-2308

An Offline Counting Facility for Rare-Decay Experiments

E.R. Norman, K.T. Lesko, R.M. Larimer, and E. Horch

In many of our experiments in nuclear astrophysics or tests of fundamental symmetries, we are "looking for a needle in a haystack"—that is, searching for a small number of events of interest hidden among a much larger background. Our experimental sensitivity is ultimately limited by background events caused by cosmic rays and/or other unwanted sources of radiation within the sample under study. To significantly enhance our sensitivity to small effects such as those sought in the experiments described elsewhere in this report and those we envision for the future, we have set up an offline counting facility in Building 88. The centerpiece of this system is a 4π NaI detector that can surround primary alpha, beta, or gamma detectors. For most applications, the NaI shield is operated in anti-coincidence with the main detector. This provides high rejection efficiency for cosmic-ray induced events, since a cosmic ray has to traverse a large amount of NaI to reach the central detector. In the case of gamma-ray counting, the NaI shield also significantly reduces the background observed in a central Ge detector caused by gamma rays which Compton scatter and deposit only a fraction of their total energy in the Ge detector.

The NaI system consists of a 30-cm long × 30-cm diameter annular detector and two 7.6-cm long × 7.6-cm diameter removable endcap detectors. The annulus is segmented into two halves to allow the possibility of using it in coincidence with the central detector for experiments such as electron-positron pair spectroscopy. Some of our experiments involve online and offline counting of samples bombarded with beams from LBL's 88-Inch Cyclotron. Others make use of samples activated at UC Berkeley's TRIGA reactor, and still others involve counting natural samples of various materials. Most of these experiments require long, uninterrupted counting periods. For this reason, we acquired a self-contained data acquisition and storage system consisting of an IBM PC/AT with 4 ORTEC plug-in multichannel analyzer cards, an HP plotter and an EPSON printer. This counting facility is now fully operational and has already been used in a number of experiments.

RAGS - A Real-time Acquisition and Graphics System

Richard G. Leres

A family of small, functionally comprehensive, CAMAC-based data acquisition systems has been developed to support LBL experimenters whose requirements are not always compatible with available acquisition systems.

Distinguishing features of these systems are their commercially built computer and CAMAC hardware, and the Fortran-77 programming language environment they provide the user. These RAGS (Realtime Acquisition and Graphics System) units are most appropriate when the user is not able to support the development of original or "one of a kind" hardware or software for data acquisition.

Alpha-Fission Spectroscopy System

R.A. Henderson, C.M. Gannett, D.M. Lee, and D.C. Hoffman

Fission spectroscopy in the heavy element region is very important in order to determine more about the fission process and the eventual limits that fission will place on nuclear stability. We have constructed a new alpha-fission spectroscopy system based on the EG&G ORTEC ADCAM. With this system we can

measure both alpha and fission spectra simultaneously from four separate detectors. The alpha energies measured are from 5.0 to 10.0 MeV. The lower cutoff on the fission spectra is about 30 MeV.

Signals from the preamplifiers of four Si(Au) surface barrier detectors are routed to both a high gain amplifier for alpha spectroscopy and a low gain amplifier for fission spectroscopy. Fission pulses will appear as saturation pulses from the alpha amplifier and are coincident in time with the fission pulses from the corresponding fission amplifier. Since these signals all go through an eight-way multiplexer, the pulses from the alpha amplifier are delayed by 20 μs to avoid rejection of the coincident fission signals. Signals from the multiplexer are then sent to the ADCAM unit, consisting of an ADC and a multichannel buffer. The spectrum for each individual segment is stored here until the end of the count interval, when it is stored on a disk by the host computer, in this case an IBM PC/AT.

In addition to recording the fission energy spectrum, the total number of fissions is also stored in channel zero of the corresponding alpha spectrum. This is done by using a discriminator pulse generated by the fission amplifier to trigger a gate module which allows the ADCAM data buffer to store the event in channel zero of the corresponding alpha spectrum. Thus, even when we do not measure the fission spectrum of a sample, we can still record the total number of fission counts.

Effect of Chemical Composition on Sensitivity of Phosphate Glass Track Detectors*

Wang Shicheng[†,‡] *and P.B. Price*[†]

If it were not for their generally lower sensitivity to radiation, glass track detectors would be superior to plastic detectors (e.g., response is independent of oxygen pressure). We are engaged in a detailed study of the dependence of radiation sensitivity on proportions of alkali, alkali-earth, transition metal, rare earth, and other elements relative to glass-forming oxides such as phosphates, arsenates, fluorides, borides, and silica. In a study of about 85 different compositions, we find that phosphates and arsenates containing cations of several different sizes are the most sensitive. The Bevalac is an essential tool in this research. Our leading candidate at this stage is a variant of VG-13, a glass that we have characterized thoroughly[1] and are using in nuclear reaction studies in an attempt to resolve isotopes of heavy elements in cosmic rays.

Footnotes and References

*Unpublished results.

†Also at Space Sciences Laboratory and University of California at Berkeley.

‡Also at Institute of High Energy Physics, Academia Sinica, Beijing, China.

1. P.B. Price, H.S. Park, G. Gerbier, J. Drach and M.H. Salamon, Nucl. Instr. Meth. **B21**, 60 (1987).

Development of ACCESS

H.L. Hall, C.E.A. Palmer, D.C. Hoffman, and P.A. Baisden**

In collaboration with the Inorganic Chemistry Group of the Nuclear Chemistry Division at the Lawrence Livermore National Laboratory, we have undertaken the development of the Automated Chromatographic Chemical Element Separator System, **ACCESS**. This is a computer-controlled ion chromatography system which is designed to provide a rapid and reproducible separation of actinides and lanthanides using well-known procedures such as α-hydroxyisobutyrate elutions from cation exchange

resins or bis(2-ethylhexyl)-orthophosphoric acid reverse phase extraction chromatography. The system is modular, and can be used in either an on-line or an off-line configuration. **ACCESS** is controlled by an IBM PC running a BASIC program. A Data Translation DT-2801 board in the PC provides 16 digital I/O ports, 8 ADC inputs, and 2 DAC outputs. With the digital outputs, we control two chemically inert pumps and the pneumatically actuated slider valves used to direct the flow of solution through the system. Radioactivity is injected into the system, either by the on-line KCl/He jet interface or the off-line injection loop. The PC then directs the flow of solution through the valves so that the activity is loaded onto the top of a column. At this point, the PC activates a second pump, sending the appropriate eluent through the column. The separated elements are then collected by a Gilson Scientific FC-203 fraction collector, which is controlled by the PC through an RS-232C serial interface. In the on-line configuration, **ACCESS** will be coupled to our target chamber at the 88-Inch Cyclotron via a KCl/He-jet aerosol. The recoiling products from heavy ion reactions will be transported to the chemistry area on the KCl aerosols, which will then be collected on a ceramic frit.

After a suitable collection period, the PC will direct solvent through the frit, dissolving the activity, and sorbing the activity onto the column. The activity will then be separated by elution and collected. The off-line configuration, shown in Fig. 1, is essentially the same except that activity is introduced via an injection loop rather than from a frit. We have currently completed off-line calibration of **ACCESS** at the tracer level. We have been able to achieve separation of lanthanide tracers quickly and reproducibly, usually in about 1-5 minutes. The system is now being moved to the Cave 0 chemistry area at the 88-Inch Cyclotron for on-line testing.

Footnotes and References

*Lawrence Livermore National Laboratory, Livermore, Ca.

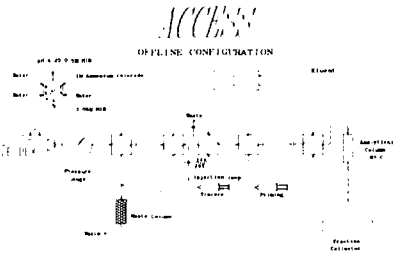

Fig. 1. Schematic representation of **ACCESS** in the off-line configuration. A mixture of actinides and lanthanides is injected at the injection loop. They are then separated by elution through the analytical column. XBL 8711-4579

A Novel Approach to the Measurement of the Neutron Multiplicity Associated With Reverse Kinematics Heavy Ion Reactions*

A. Pantaleo,† R.J. Charity, N. Colonna,† G. D'Erasmo,† E.M. Fiore,† L. Fiore,† G. Guarino,† L.G. Moretto, V. Paticchio,† and G.J. Wozniak

The knowledge of the neutron multiplicity associated with nuclear reactions has become increasingly important in intermediate energy heavy ion physics where it can provide a measure of the size of the participant region and the energy dissipation.

So far two main techniques of neutron multiplicity measurements have been developed, the first based on multidetector walls or balls, the second on the thermalization of the neutrons and the counting of the capture events wbich are dispersed in time (Gd-doped liquid balls). For high multiplicities of fast neutrons, these techniques suffer from a large cross talk between the detectors due to the increased path length of multiple scattered neutrons, or from the

difficulty of thermalizing high energy neutrons in a reasonable volume of scintillating liquid. In addition, the Gd balls are very slow because of the thermalization time of about 1005s.

A cost effective calorimetric neutron multiplicity technique is presented here, which is particularly well adapted to high energy neutrons and higher multiplicity.

The response function of a plastic scintillation detector to a neutron is very broad, extending up to the maximum light yield associated with the proton recoils. In Fig. 1 the response of a 100 cm × 50 cm cylindrical block of NE 110 plastic scintillator to 10 and 20 MeV neutrons is shown, as simulated by a Monte Carlo (MC) program.[1]

Even if this response were completely flat (and it is not, see Fig. 1), the integral response to a number ν_n of monoenergetic neutrons detected at the same time has a mean value equal to ν_n times the mean response to a single neutron, and a dispersion approximately $\sqrt{\nu_n}$ times the dispersion for a single neutron. If the neutron multiplicity ν_n is sufficiently high, a reasonably low relative dispersion can be obtained. Thus, high multiplicities of neutrons of approximately the same energy can be measured through the total light response of a plastic scintillator calorimeter to the neutrons. This calorimetric approach requires neutrons with approximately the same energy. This can be realized with reverse kinematics reactions where the source velocities can be made much greater than the mean neutron velocity in the source frame.

The MC program of ref. 1 has been modified to accumulate the response of many neutron histories and, in addition, to propagate the neutrons in inert materials, constituting the shielding. Calculations have been performed for $\nu_n = 30$ for the same geometrical configuration and neutron energies of Fig. 1; the resulting response functions, reported in Fig. 2, show dispersions respectively of ±14.5% and ±19%, an acceptable resolution for a multiplicity measurement of very fast neutrons.

Footnotes and References

*Condensed from LBL-24720, submitted to Nucl. Instr. and Meth.

†Istituto Nazionale di Fisica Nucleare - Sezione di Bari, and Dipartimento di Fisica dell'Università di Bari, Via Amendola, 173 - 70126 Bari, Italy.

1. M. Aghinolfi *et al.*, Nucl. Instr. and Meth. **165**, 217 (1979).

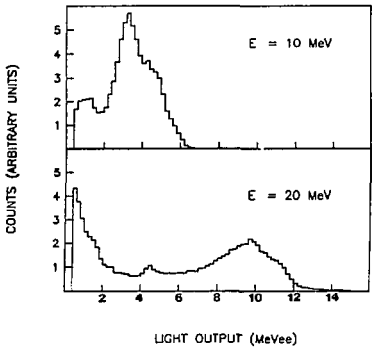

Fig. 1. Monte Carlo simulation for the response function of a cylindrical 100 cm × 50 cm plastic scintillator to 10 and 20 MeV neutrons uniformly impinging on the central part of the base (40 cm radius).

XBL 881-283

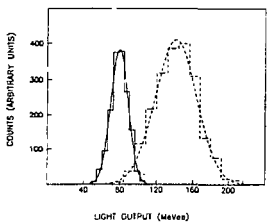

Fig. 2. Calculated response to a neutron multiplicity $\nu_n = 30$ at neutron energies of 10 MeV (full-line histogram) and 20 MeV (dashed-line histogram). The curves are gaussian fits with FWHM of 29% (full line) and 38% (dashed line). XBL 881-284

Status of the MUSIC II Detector

W.F.J. Müller, G. Bauer, H. Beeskow,* F. Bieser, W. Christie,†*
U. Lynen, H. Sann,* and C. Tull†*

A new tracking detector for LBL's Heavy Ion Spectrometer System (HISS) was designed, built and tested by a collaboration of GSI and LBL scientists. The new device is a second generation MUltiple Sampling Ionization Chamber[1] and employs concepts from classical ionization chambers and time projection chambers. MUSIC II will provide a unique charge identification and a precise determination of track position and angle for up to 10 particles in a wide range from carbon to uranium. The system is optimized for the detection of heavy projectile-rapidity fragments and complements the existing HISS drift chamber system which will be mainly used for lighter fragments and mid rapidity coverage.

MUSIC II consists of three field cages with an active area of 100 by 60 cm as sketched in Fig. 1. The first and last cage have a horizontal drift field and determine the bending plane coordinates, the middle cage has a vertical drift field and determines the non-bending plane coordinates. The electrons generated in the primary ionization of a track drift under the influence of the drift field and are collected without further gas amplification on 96 anodes (16 per cage side). Each anode signal is processed in a specially developed low noise charge sensitive amplifier and sampled and digitized every 60 ns. The time sampling permits the handling of multiple tracks in the active volume.

The system has been constructed and tested with a 20 MeV/nucleon bismuth beam at GSI and was shipped to LBL and installed at the Bevalac in February and March, 1987. First tests with N, Ne, Ar, Fe and Xe beams of about 1 GeV/nucleon were performed in May and November, 1987. A first analysis confirms the expectations for the position and charge resolution and shows that the large dynamic range is indeed obtainable. We achieved a charge resolution of better than 0.3 units FWHM around Z=26 (Fig. 2) and 0.36 units FWHM for Z=7 with only a *single* field cage. The position resolution for a *single* anode is 110 μm (sigma) for Z=54 and 1.4 mm for Z=7.

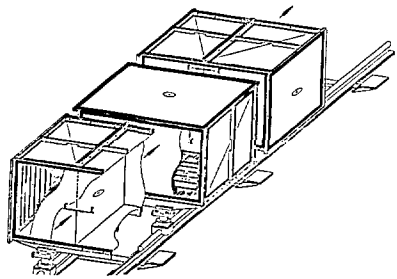

Fig. 1. MUSIC II field cage geometry
XBL 8711-5005

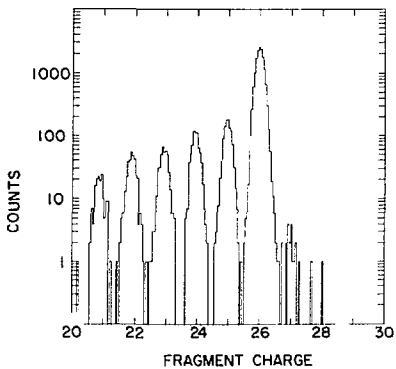

Fig. 2. Charge spectrum obtained from one field cage for a 1050 MeV/nucleon iron beam fragmented on a CH_2 target. XBL 8711-5006

A dedicated sampling ADC system is currently under construction at LBL and will be available in February, 1988. The whole system will be ready for experiments in April, 1988.

Footnotes and References

*GSI Darmstadt, West Germany

†Crocker Nuclear Laboratory, University of California, Davis, CA 95616 and LBL

1. W. Christie *et al.*, NIM A255, 466(1987)

Uncertainties of Particle Emission Probabilities*

E. Browne

Particle emission probabilities, i.e., the percentages of various particle groups (or electron capture transitions) emitted in a nuclear transformation, are basic quantities which are either directly measured or derived from decay schemes. Their importance for testing nuclear models and for calculating average radiation energies per disintegration is well recognized. Particle emission probabilities are expressed on an absolute scale per nuclear disintegration, and are usually determined from relative particle spectral intensities. For emission probabilities measured directly, the reported uncertainties should include both the uncertainties due to the normalization procedure, and those for the relative spectral intensities of the pertinent particle groups. The same applies to emission probabilities measured indirectly, i.e., those derived from γ-ray transition intensity balances and knowledge of the decay scheme. For these latter, the propagation of uncertainties is very complex and is related to that for the uncertainties of the absolute γ-ray intensities. Methods for calculating uncertainties of particle emission probabilities, measured both directly and indirectly, are presented in this paper.

Footnotes and References

*Condensed from a paper accepted for publication in Nuclear Instruments and Methods in Physics Research, 1987.

Operation of the CCD Supervision System at the Bevalac and NA35 Streamer Chambers

S.I. Chase, J.W. Harris, W. Rauch, L. Teitelbaum, and M.L. Tincknell

The CCD Supervision System[1] is an electronic camera and computer system built to acquire and analyze streamer chamber images. It has been under development at LBL since the summer of 1985. It was operated in the fall of 1986 in experiment NA35 at CERN, in May 1987 at the Bevalac, and again in the fall of 1987 at CERN. At least one more experiment at the Bevalac is planned, and future possibilities at CERN are under discussion.

The current configuration of the system includes three image intensified cameras, each containing a 1024×1024 pixel CCD. Each image intensifier assembly has two stages, the output of which is lens coupled to the CCD. This provides an effective optical gain of approximately 10000. The high gain allows the streamer chamber to be operated at a relatively low pulse voltage, which reduces the light output, but improves resolution and virtually eliminates flaring and sparking. In this regime, the track brightness and streamer distribution are more closely related to dE/dx, which may allow particle identification. The computer system is a VAXstation II, including a high speed integer coprocessor for data acquisition and image processing, and a high resolution color display with an interactive cursor. Since the addition of the third CCD camera in the summer of 1987, the VAX memory has been expanded to 16 Mbyte, and coprocessor memory to 8 Mbyte, and the disk

space to over 350 Mbyte, all to improve the handling of the three 1 Mbyte images acquired in every event. A high capacity (2.4 Gbyte) digital magnetic tape drive that uses standard VHS video cassettes has been added for data acquisition. Because the recording rate of this tape drive is only 120 Kbytes, the recording system must be upgraded further for future experiments. Digital optical disks (WORM) were determined to be unsuitable for this application because they are too slow, and the media cost is high.

The system has evolved from its initial application as a monitoring tool in the first run of NA35 to a full data acquisition system in the second run of NA35. In its monitoring capacity the system provided direct online displays of streamer chamber events, quantitative streamer chamber performance measures, and track multiplicities. Shown in the figure is the edge of a CCD streamer chamber picture and the light intensity profile taken along the straight contour that cuts across the tracks. A peak-finding algorithm finds and marks the positions where tracks cross the contour. In this way the overall track multiplicity was determined to an accuracy of 15%, and online correlations were made among track multiplicity, luminous intensity, and energy deposited in the downstream calorimetry of NA35. In the May 1987 run, the system was used to test the first low pulse voltage, low light output operation of the Bevalac streamer chamber. Some Ho+Ho events at 1.2 GeV/nucleon were recorded. In the second run of NA35, the data acquisition hardware and software matured into a stable and reliable system. During this run the system was largely dedicated to three-view data recording. Almost 7000 three-view events were taken.

The ultimate goal of this project is to boost the data production rate from the streamer chamber substantially by minimizing the time a human operator spends with each picture. In addition, the quantitative brightness of each track that is uniquely available with digitized images may allow particle identification by the combination of dE/dx and momentum, at least for some ranges of particle momenta. The success of this program would make the combination streamer chamber/CCD system the only detector at either the Bevalac or the CERN SPS with 4π tracking and particle identification.

Footnotes and References

1. M.L. Tincknell, S.I. Chase, T. Dinh, J.W. Harris. and L. Teitelbaum, Optical Eng. **26(10)**, 1067–1076 (1987).

Fig. 1. Picture from the streamer chamber (see text). XBB 874-3083

Studies of Plastic and Glass Track-Etch Detectors

J. Drach, Ren Guoxiao,*† M.H. Salamon,* M. Solarz,* and P.B. Price**

The above authors in various combinations have reported results of a number of new studies of properties of track-etch detectors:

1 In a study[1] of Cronar polyethylene terephtbalate film, we measured its response to Bevalac beams as a function of Z/β, its charge resolution, its track-fading behavior, and the dependence of its response on ambient temperature, with a view to long-duration space experiments.

2 Using beams of Bevalac Au and U ions, we found[2] that the sensitivity of CR-39, Rodyne polycarbonate, and Cronar polyester track detectors depends on the length of time for which the sample is exposed to oxygen before irradiation and to the partial pressure of oxygen before and during irradiation. In contrast, the sensitivity of phosphate glass detectors is independent of the presence or absence of oxygen before or during irradiation. These results favor the use of glass rather than plastic inside vacuum systems or in the vacuum of space.

3 We found that, in general, the response (track etch rate) of a plastic track detector to an energetic charged particle depends not only on ionization rate but also on the "aging" time between irradiation and chemical etching, on the ambient temperature during aging, and on the atmosphere during aging.[3] We presented data relevant to the use of plastic track detectors on long-duration space missions.

Footnotes and References

*Also at Space Sciences Laboratory and University of California at Berkeley.

†Also at Institute of High-Energy Physics, Beijing, China.

1. J. Drach, P.B. Price and M.H. Salamon, Nucl. Instr. Meth. **B28**, 49 (1987).

2. J. Drach, M. Solarz, Ren Guoxiao, and P.B. Price, Nucl. Instr. Meth. B, in press, 1987.

3. P.B. Price and J. Drach, Nucl. Instr. Meth. B, in press, 1987.

Magnetic Monopoles and Other Highly Ionizing Particles at the SSC*

P.B. Price†

The full version of this paper lists the properties of magnetic monopoles relevant to their identification; surveys previous searches for classical (point) monopoles at accelerators; shows that plastic and glass track-etch detectors are ideally suited for monopole searches in a very high background of radiation and particles created in an accelerator environment; discusses design considerations for a monopole detector at the proposed Supercollider; and concludes that glass track detectors with improved sensitivity but also capable of surviving within 10 cm of an interaction region at an integrated luminosity of 10^{40} could be developed for use at the SSC. A recent experiment carried out at the Fermilab collider at 1600 GeV by my colleagues and me[1] is cited as a prototype for a SSC experiment.

Footnotes and References

*Condensed from Proceedings of the SSC Detector Workshop, UC. Berkeley, July, 1987.

†Also at Space Sciences Laboratory and Department of Physics, University of California at Berkeley.

1. P.B. Price, Ren Guoxiao, and K. Kinoshita, Phys. Rev. Lett., in press, 1987.

Detector Simulations and Acceptance Calculations for the Di-lepton Spectrometer

P.A. Seidl, J. Bystricky, J. Carroll,† S. Christo,‡ J. Gordon,† T. Hallman,§ G. Igo,†*
*P.N. Kirk,‡ G. Krebs, E. Lallier, G. Landaud,** L. Madansky,§ H.S. Matis, D. Miller,††*
C. Naudet, G. Roche,‡‡ L. Schroeder, Z.F. Wang, A. Yegneswaran††

In order to determine the acceptance of the DLS spectrometer,[1] to study the background yields and to estimate yields of direct e^+e^- pairs based on theoretical models, a detailed Monte-Carlo simulation of the DLS spectrometer was carried out using the GEANT3[2] detector simulation package. The simulation code is installed on the VAX computers at LBL and on the Cray X-MP at the MFE Computer Center. The acceptance for $A + A \rightarrow \pi^{\pm} + X$ and $A + A \rightarrow p + X$, as a function of production angle θ, and momentum P have been calculated. This calculation was necessary to compare our inclusive pion and proton production data to other reported measurements. The results show that the acceptance varies slowly for P>0.3 GeV/c and $27° < \theta < 59°$. The acceptance of the detector to electron-positron pairs, $A + A \rightarrow e^+e^- + X$, as a function of pair rapidity y, pair transverse momentum P_t, and invariant mass M has been calculated. The generation of Čerenkov photons, the reflection of photons by the mirrors and the acceptance of the Winston cones have been introduced, as well as the photo-cathode efficiencies of the associated photomultiplier tubes. Cuts equivalent to those performed on our Čerenkov ADC data, and to a test of the hodoscope hit pattern were performed on the simulated data.

Fig. 1 shows that the pair acceptance (integrated over y) drops rapidly as a function of P_t, and increases with M. Before applying these results to the raw data, the acceptance is fit to an analytic function of y, P_t and M which smooths the statistical fluctuations of the Monte Carlo data. Examples of background processes under study are the pair yields arising from $\pi^0 \rightarrow e^+e^-\gamma$, the Dalitz decay of heavier mesons, and the external conversion of photons.

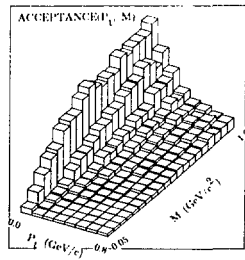

Fig. 1. Acceptance of the DLS spectrometer vs. P_t and M, resulting from an input e^+e^- distribution that is flat in M, y, and P_t. The vertical axis represents the number of accepted pairs. The acceptance shown is for one lepton per arm. XBL 8711-5030

These calculations are necessary for the subtraction of the contributions of Dalitz and Bethe-Heitler pairs to the measured yield of e^+e^- pairs, and the calculation of the Čerenkov detector efficiencies.

Footnotes and References

*On leave from Institut National de Physique Nucléaire et de Physique des Particules, France.

†Department of Physics, University of California at Los Angeles, Los Angeles, CA 90024.

‡Department of Physics, Louisiana State University, Baton Rouge, LA 70803-4001.

§Department of Physics, The Johns Hopkins University, Baltimore, MD 21218.

**Université de Clermont II-Institut National de Physique Nucléaire et de Physique des Particules, 63170 Aubière, France.

††Department of Physics, Northwestern University, Evanston IL 60201.

‡‡On leave from the Université de Clermont II, Aubière, France.

1. G. Roche *et al.*, Bevalac Proposal #780H, (1984).

2. R. Brun, F. Bruyant, M. Maire, A.C. McPherson, P. Zanarini, CERN DD/EE/84-1 (1986).

Development of a User-Friendly Version of LISA Software

J. Liu and H. Matis

LISA,[1] a software package available on computer nodes: DLS, BEVAX, 88VAX and CSA, has been used for both on-line and off-line data analysis. This software package, designed to use the VAX VMS operating system, provides research groups with histogramming capability, live scatterplots, event analysis, and other important functions. However, use of the LISA software previously required much user knowledge of LISA protocol, and thus made LISA difficult to learn and use.

Through use of the VAX screen management facilities and other recently available run-time library routines,[2] LISA has been upgraded to be more user-friendly. Changes included error-checking (i.e., making the program "smart"), providing more options so users can configure LISA to their particular experiment, making functions available through single keystrokes, and finally making commands more tutorial in nature. Some new features which have been added to LISA include:

- new updated status screen providing LISA system information such as elapsed time, cpu time and performance, events processed, I/O status, data file status, etc.;
- editor for data entry of histogram definitions which improves speed and ease of data entry;
- graphics screen configuration subroutine, which allows users to configure the graphics screen to accommodate up to 30 simultaneous plots on the same screen and also to load histogram data and plot the data within the subroutine;
- multiple live plot capability, which allows users to interactively obtain up to thirty simultaneous live scatterplots all on one screen;
- LISA to HBOOK[3] converter, which translates LISA graphics data into HBOOK-compatible format, thus making LISA exportable to users of the HBOOK plotting package.

In addition, numerous other utility and graphics subroutines were modified or rewritten to include screen management and run-time library compatibility. Fig. 1 shows an example of a multiple plot made with LISA. Upgrading of LISA is ongoing. Current modifications underway include multiple terminal access during the same analysis session in a compatable manner, and improvement of the documentation.

Footnotes and References

1. This version of LISA was provided to us by B. Kolb of GSI.

2. See VAX/VMS V4 manual for Run-Time Library routines. Volume 5c.

3. HBOOK is a histogram package originally from CERN, written in Fortran 77.

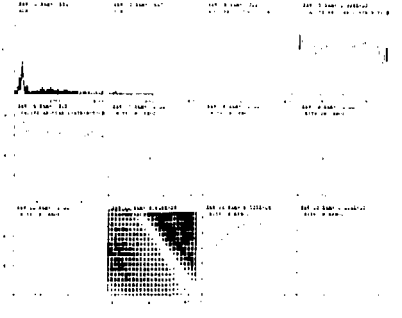

Fig. 1. See text. XBL 8711-4630

A New VME-Based, Multi-Processor Data Acquisition Station for the Bevalac

Charles McParland

We have developed a VME-based multi-processor data acquisition station for use at Bevalac experimental areas. Our aim has been to provide a high performance, inexpensive replacement for our aging base of DEC PDP and VAX data acquisition machines. Each station has been implemented as a set of 68000-based processors, interfaces and memory arrays connected to CAMAC instrumentation crates through a VME/VMX-CAMAC interface of our design. This system receives control information and issues data packets over an accelerator-wide Ethernet using the TCP/IP protocol. Control information is issued and data is received by a central VAX cluster where data taping is performed.

We have long believed that, although a general purpose computer (e.g., VAX 11/780) represents a cost-effective solution to problems of data analysis and manipulation, it is a particularly costly environment in which to perform simple data formatting and bit manipulation tasks. Our design capitalizes on a functional division of data acquisition tasks between dedicated, single purpose VME-based processors and a commercial general-purpose computer system.

We have split up the data acquisition process into several tasks. These tasks are distributed among several processors located within a single VME system crate. Some of these tasks require operating system services such as scheduling and memory allocation. They execute within a processor that has a simple multi-tasking operating system. Others require none of these services and perform better when in complete control of all of a processor's resources. These tasks execute in processors that have no operating system. Data structures and control mechanisms have been designed to allow both control and data passing between these two very different computing environments.

This multi-processor design allows parallel access to multiple CAMAC crates. If properly configured, the system can read out several detector subsystems simultaneously. Data packets are formatted by each processor and placed into a common data queue for transmission to the host system. An additional processor de-queues data packets and controls their transmission over an accelerator-wide Ethernet. The host system, currently the BEVAX cluster of VAX 11/780's, receives these packets and logs them on magnetic tape. Data is also made available to on-line analysis programs. A menu-driven control program can he executed on the VAX to start and stop data taking. In addition, several diagnostic programs are available for testing and monitoring CAMAC crates, interfaces and associated cabling.

Two systems have been installed at the Bevalac. These systems have been used in several experiments at the LEBL, Beam 44 and Beam 40 areas. System throughput has been measured and is substantially higher than that of the old PDP-MBD systems. The use of standard Ethernet hardware and software has improved system flexibility dramatically. These acquisition systems are easily moved and can be used at most LBL experimental sites. Two additional systems are under construction for use at the Beam 44 and HISS experimental facilities.

A VME/VMX - CAMAC Interface and Crate Controller

C. McParland and F. Bieser

In conjunction with the design of the VME-based data acquisition station, we have designed and built a VME/VMX - CAMAC interface. In order to achieve a degree of parallel processing, system design required simultaneous readout of multiple CAMAC crates. This could be accomplished by dedicating a single VME-based 68000 processor to each CAMAC crate. Since multiple processors accessing multiple CAMAC crates over a single VME bus would yield unacceptable acquisition performance, we decided on the use of a local bus which would carry all bus activity between a CAMAC crate and its processor. Therefore, we designed an interface using the VMX bus, which can be used to connect VME-based processors to one or more physically adjacent interface boards via a "private" bus. In addition, the data acquisition system required global access to each individual CAMAC crate by a single processor–one that could not physically appear on each of the "private" VMX buses found in the VME system. This consideration yielded a dual-ported VME/VMX to CAMAC interface.

The interface can he accessed by either a VME or VMX bus master. The interface is fully transparent to accesses on both buses and will, if necessary, arhitrate to give preference to the VMX port. Addresses that fall within the appropriate range will he mapped onto CAMAC functions and be transmitted to the crate controller for execution. Base addresses on hoth the VME and VMX bus are individually selectable from a set of predetermined addresses. The specification of the actual CAMAC command to be performed is contained within the address used in accessing the interface. The format of the F, N, and A fields within the address have been selected to provide fast and efficient block transfers of CAMAC data by a 68000 processor. The auto-increment addressing mode used in conjunction with a move word instruction loop yields transfers in the 2 microsecond per word range.

The VME/VMX board is connected to its companion crate controller through a bi-directional differential cable bus. Cable lengths in excess of three hundred meters are possible. Since previous CAMAC systems have suffered from an inability to diagnose crate controller and branch highway problems, this controller has been designed to allow simple effective diagnostics to be performed. The controller retains the last F, N, and A performed and will return it on an appropriate request. It also contains a full 24 bit test register that can be used to test the integrity of both the VME/VMX interface data paths and the differential cable that connects it to the crate controller. A crate controller status register is readable and will indicate the status of CAMAC crate power supplies and temperature.

Four interface-crate controller pairs have been built and an additional ten pairs are now under construction. These units and the data acquisition system they are part of have been used in several Bevalac experiments, primarily at the LEBL and Beam 44 facilities.

PART V: APPENDICES

Publications

Berkeley High Energy Resolution Array

R.M. Diamond

ACS Symposium Series 324/52,January 1987; LBL-20241

Pion Production in Nucleus-Nucleus Collisions

J.W. Harris, J. Bartke, G. Odyniec, H.G. Pugh, L.S. Schroeder, M.L. Tincknell, W. Rauche, R. Stock, R. Bock, R. Bockmann, A. Sandoval, H. Strobele, R.E. Renfordt, D. Schall, D. Bangert, J.p. Sullivan, K.L. Wolf, A. Dacal, C. Guerra, and M.E. Ortiz

Physical Review Letters; LBL-20373

Excitation Energy Division in the First 160 MeV of Total Kinetic Energy Loss for the Reaction: 684 MeV $^{80}Kr + ^{174}Yb$

L.G. Sobotka, G.J. Wozniak, R.J. McDonald, M.A. McMahan, R.J. Charity, L.G. Moretto, Z.H. Liu, F.S. Stephens, R.M. Diamond, M.A. Deleplanque, and A.J. Pacheco

LBL-21059

K-Shell Ionization in 7.5- and 8.6/a.m.u. U + U Collisions at Very Small Impact Parameters

J.D. Molitoris, Ch. Stoller, R. Anholt, W.E. Meyerhof, D.W. Spooner, R.J. McDonald, L.G. Sobotka, G.J. Wozniak, L.G. Moretto, M.A. McMahan, E. Morenzoni, M. Nessi, and W. Wolfli

LBL-21031

Operation of the LBL ECR Source Injection System

D.J. Clark and C.M. Lyneis

Proceedings of the 11th International Conference on Cyclotrons and their Applications, Tokyo (Oct. 1986) and LBL-21738.

Synchrotrons in Cyclotron Territory

D.J. Clark, and R.A. Gough

Presented at the 11th International Conference on Cyclotrons and their Applications, Tokyo, Japan, October 13-17, 1986; LBL-21739

Operational Performance of the LBL 88-Inch Cyclotron with an ECR Source

C.M. Lyneis

Proceedings of the 11th International Conference on Cyclotrons and their Applications, Tokyo (Oct 1986) and LBL-21860. (Invited talk)

Improvements to the Helium-Jet Coupled On-Line Mass Separator RAMA

F.B. Blonnigen, D.M. Moltz, T.F. Lang, W.F. Knoll, X. Xu, M.A.C. Hotchkis, J.E. Reiff, and J. Cerny

To be published in the Proceedings of the Electromagnetic Isotope Separators-11 Conference, Los Alamos, NM, August 18-22, 1986 to appear in Nuclear Instruments and Methods; LBL-22188

EOS: A Time Projection Chamber for the Study of Nucleus-Nucleus Collisions at the Bevalac
H.G. Pugh, G. Odyniec, G. Rai, and P. Seidl
December 1986; LBL-22314

On-line Isotope Separation of Projectile Fragments Produced in Relativistic Heavy-ion Reactions
Y. Nojiri, K. Matsuta, T. Minamisono, K. Sugimoto, K. Takeyama, H. Hamagaki, S. Nagamiya, K. Omata, Y. Shida, I. Tanihata, T. Kobayashi, S. Matsuki, S. Shimoura, J.R. Alonso, G. Krebs, and T.J.M. Symons
Presented at the 7th International Conference on Hyperfine Interactions, Bangalore, India, September 8-12, 1986; LBL-22406.

Complex Fragment Emission in Intermediate Energy Reactions
R.J. Charity
Invited talk at the symposium on Central Collisions and Fragmentation Processes at the ACS spring meeting, Denver, Colorado, April 5-10, 1987; LBL-22426.

Systematics of Complex Fragment Emission in Niobium Induced Reactions
R.J. Charity, M.A. McMahan, G.J. Wozniak, R.J. McDonald, L.G. Moretto, D.G. Sarantites, L.G. Sobotka, G. Guarino, A. Pantaleo, L. Fiore, A. Gobbi and K.D. Hildenbrand
submitted to Nuclear Physics A; LBL-22448

ECR Ion Sources for Cyclotrons
C.M. Lyneis
Presented at RCNP-Kikuchi Summer School on Accelerator Technology, Osaka, Japan, October 20-23, 1986; LBL-22450.

Gamma-Ray Energy Correlations from Nuclei at Very High Spins
F.S. Stephens, J.E. Draper, J.C. Bacelar, E.M. Beck, M.A. Deleplanque, and R.M. Diamond
submitted to Phys. Lett. B; LBL-22537

Nuclear Mass Formula with a Finite-Range Droplet Model and a Folded-Yukawa Single-Particle Potential
P. Moller, W.D. Myers, W.J. Swiatecki, and J. Treiner
Atomic Data and Nuclear Data Tables, December 1986; LBL-22686

The Reconstruction of the Deformation Energy of ^{152}Dy from the Properties of Its Superdeformed Band
W. Swiatecki
December 1986; LBL-22666

The LBL 88-Inch Cyclotron Operating with an ECR Source
D.J. Clark
Presented at the 10th National Conference on Particle Accelerators, Dubna, U.S.S.R., October 21-23, 1986; LBL-22715

Contact Interactions in Closed Superstring Field Theory
F.R. Klinkhamer, and J. Greensite
submitted to Nuc. Phys. B, January 1987; LBL-22759

Quad Fourfold (4x4) Logic Unit (LBL 21x6421 P-1) *R.J. McDonald, D.A. Landis, M.R. Maier, B.S. Rude and G.J. Wozniak*
January 1987; LBL-22832

Beta-Delayed Two-Proton Emission D. Moltz and J. Cerny
LBL-22998

Superdeformed Bands in Nd Nuclei
E.M. Beck, R.J. Mcdonald, A.O. Macchiavelli, J.C. Bacelar, M.A. Deleplanque, R.M. Diamond, J.E. Draper, and F.S. Stephens
submitted to Physics Letters B., July 1987; LBL-23029

Influences of the Astrophysical Environment on Nuclear Decay Rates
E.B. Norman
194th National Meeting of the American Chemical Society, New Orleans, Louisiana, Aug 30-Sep 4, 1987; LBL-23037

High Spin Spectroscopy of ^{168}Hf
E.M. Beck, M.A. Deleplanque, R.M. Diamond, R.J. McDonald, F.S. Stephens, J.C. Bacelar, and J.E. Draper
Phys. Rev. Lett.; LBL-23068

Evidence on Nuclear Equation of State from Nuclear Masses, Relativistic Collisions, Supernova Explosions and Neutron Star Masses
N.K. Glendenning
Submitted to Phys. Rev. C, April 1987; LBL-23081.

Angular Distribution for ^{56}Fe(pi+,pi-)^{56}Ni(DIAS)
P.A. Seidl, G. Rai, R. Gilman, C.L. Morris, G.R. Burleson, K.S. Dhuga, M. Burlein, H.T. Fortune, J.D. Zumbro, M.A. Machuca, C.F. Moore, S. Mordechai, and D.L. Watson
submitted to Phys. Rev. Lett.; LBL-23141

Status of ECR Souce Technology
C.M. Lyneis
Presented at the IEEE 1987 Particle Accelerator Conference, Washington, D.C., March 16-19, 1987; LBL-23160

Weak Skyrmions and Sphalerons
J. Boguta and F.R. Klinkhamer
Submitted to Phys. Rev. Lett., March 1987; LBL-23197

Decay of Neutron Deficient Eu, Sm and Pm Isotopes Near the Proton Drip Line
K.S Vierinen, J.M. Nitschke, P.A. Wilmarth, R.B. Firestone and J. Gilat
submitted to Nucl. Phys. A; LBL-23221

Particle Evaporation Spectra with Inclusion of Thermal Shape Fluctuations
L.G. Moretto and D.R. Bowman
Presented at the 25th International Winter Meeting on Nuclear Physics, Bormio, Italy, January 19-23, 1987; LBL-23228

Advanced Accelerator Methods: The Cyclotrino
J.J. Welch, K.J. Bertsche, P.G. Friedman, D.E. Morris, and R.A. Muller
Presented at the University of California-California Institute of Technology Accelerator Mass Spectrometry Conference, Irvine, CA, February 15, 1987; LBL-23323

Status of the Berkeley Small Cyclotron AMS Project
K.J. Bertsche, P.G. Friedman, D.E. Morris, R.A. Muller and J.J. Welch
Presented at the 4th International Symposium on Accelerator Mass Spectrometry, Ontario, Canada, April 27-30, 1987, and to be published in the Proceedings; LBL-23324

Formation of Large Target Residues in Intermediate Energy Nuclear Collisions
W. Loveland, K. Aleklett, L. Shiver, Z. Xu, C. Casey, and G.T. Seaborg
American Chemical Society Symposium on Central Collision and Fragmentation Processes, Denver, Colorado, April 7, 1987; LBL-23365

Recoil Spectrometer for the Detection of Single Atoms
Albert Ghiorso
International Conference on Methods and Applications of Radioanalytical Chemistry, Kona, Hawaii, April 5-10, 1987; LBL-23366.

Role of Pions and Hyperons in Neutron Stars and Supernovae
N. K. Glendenning
PANIC 1987, Kyoto, Japan; LBL-23373

Energetic Particle Emission and Linear Momentum Transfer in Central Collisions Induced by 32.5 MeV/nucleon $^{16}O + {}^{238}U$ ^{197}Au
Y. Chan, E. Chavez, A. Dacal, S.B. Gazes, A. Harmon, M.E. Ortiz, E. Plagnol, J. Pouliot, R.G. Stokstad
Xth Oaxtepec Nuclear Physics Symposium, Oaxtepec, Mexico, January 5-8, 1987; LBL-23381

Delayed P.. ..on Emission of N=81 Odd-Odd Precursors: ^{148}Ho, ^{150}Tm and ^{152}Lu
J.M. Nitschke, P.A. Wilmarth, J. Gilat, K.S. Toth, F.T. Avignone, III
submitted to Phys. Rev. C, June 1987; LBL-23408

Preparation of Accelerator Targets by the Evaporation of Acetate-Organic Solutions in the Presence of NH3 Gas
S.Y. Cai, A. Ghiorso, and D.C. Hoffman
March 1987; LBL-23409

Quasi-Classical Treatment of the Nucleon Gas
J. Randrup, C. Dorso, and S. Duarte
Workshop on Semiclassical and Phase Space Approaches to the Dynamics of the Nucleus, Aussois, France, March 15-20, 1987; to be published in Les Editions de Physiques (France); LBL-23414

High-Spin Research with HERA
R.M. Diamond
Presented at the Winter School on Physics, Zakopane, Poland, May 1-8, 1987; LBL-23551 June 1987

Probing the Direct Step of Relativistic Heavy Ion Fragmentation–(^{12}C,^{11}B+p) at 2.1 GeV/Nucleon with C and CH2 Targets *M.L. Webb*
thesis (June 1987); LBL-23570

A Measurement of the Magnetic Dipole Moment of the delta++(1232) from the Bremsstrahlung Process pi p yields pi p gamma
C.A. Meyer
thesis (June 1987); LBL-23688

Origin of Complex Fragments in Intermediate Energy Heavy Ion Reactions
L. Moretto
Invited talk at the 6th Adriatic International Conference on Nuclear Physics "Frontiers of Heavy Ion Physics," Dubrovnik, Croatia, Yugoslavia, June 15-18, 1987; LBL-23699.

Production of Radioactive-Ion Beams at the 88-Inch Cyclotron
T. Lesko, D.J. Clark, and E.B. Norman
presented at American Physical Society, New Brunswick, NJ, Oct 15-17, 198787; LBL-23713A

Charged Particle Multiplicities Associated with Slow and Intermediate Rapidity Fragments in the Reactions ^{250}MeV/u ^{20}Ne + Ag, Au
D.R. Bowman, R.J. Charity, M.A. McMahan, H. Han, K. Jing. G.J. Wozniak, L.G. Moretto, W.L. Kehoe, B. Libby, and A. Mignerey
presented at American Physical Society, New Brunswick, NJ, Oct 15-17, 1987; LBL-23732A

Superstring Amplitudes and Contact Interactions
J. Greensite and F.R. Klinkhamer
submitted to Nucl. Phys., August 1987; LBL-23830

Neutron Stars in the Renormalized Chiral-Sigma Model
N.K. Glendenning
submitted to J. Astrophys., July 1987; LBL-23832

The Role of Basic Research in Society
G.T. Seaborg
Media Conference concerning the Superconducting Super Collider, Lawrence Berkeley Laboratory, July 30, 1987; LBL-23833

Aqueous Chemistry of Element 105
K.E. Gregorich, R.a. Henderson, D.M. Lee, M.J. Nurmia, R.M. Chasteler, H.L. Hall, D.A. Bennett, C.M. Gannett, R.B. Chadwick, J.D. Leyba, D.C. Hoffman and G. Herrmann
Radiochemica ACTA, August 1987; LBL-23834

Emittance Measurements on the LBL ECR Source
D. Clark
presented at the International Conference on ECR Ion Sources and their Applications, E. Lansing, MI, Nov 16-18, 1987; LBL-23866A

Dynamics and Clusterization in Nuclear Collisions
K. Sneppen and L. Vinet
submitted to Nucl. Phys. A, August 1987; LBL-23871

Electromagnetic Radiation and Electrons Produced by ^{238}U Beams at Inertial Fusion Energies
Z.Z. Xu, H.R. Bowman, J.O. Rasmussen, T. Humanic, S. Folkman, and R. Anholt
August 1987; LBL-23874 **Beta-Delayed Proton Decay in the Lanthanide Region**
J.M. Nitschke, P.A. Wilmarth, J. Gilat, P. Moller and K.S. Toth
5th International Conference on Nuclei Far from Stability (Invited Talk), Rosseau Lake, Ontario, Canada, Sept. 14-19; LBL-23929

The Case Studies of Neutron Deficient Rare Earth Isotopes with OASIS
J. Gilat, J.M. Nitschke, P.A. Wolmarth, K. Vierinen, and R.B. Firestone
5th International Conference on Nuclei Far from Stability, Rosseau Lake, Ontario, Canada, Sept. 14-19, 1987; LBL-23991

Upper Limit on the Charge of Electron Anti-Neutrons from SN ^{1987}A
Shawn Carlson
Nature, September 1987; LBL-23933

Beta-Delayed Two-Proton Emission as a Nuclear Probe
D.M. Moltz, J.E. Reiff, J.D. Robertson, T.F. Lang and J. Cer.
5th International Conference on Nuclei Far from Stability, Rosseau Lake, Ontario, Canada, Sept. 14-19, 1987; LBL-24035

Vacuumlike State of Matter and Inflationary Scenarios in Cosmology
E.B. Gliner
Submitted to Phys. Rev. D, September 1987; LBL-24036

Measurements of Cross Sections Relevant to gamma-ray Line Astronomy
K.T. Lesko, E.B. Norman, R.-M. Larimer, S. Kuhn, D.M. Meekhof, S.G. Crane, and H.G. Bussell
submitted to Phys. Rev. C; LBL-24051

An Introduction to Nuclear Astrophysics
E.B. Norman
Lectures presented at the Latin American School of Physics, La Planta University, La Planta, Argentina July 6-24, 1987; LBL-24067

Uncertainties of Particle Emission Probabilities
E. Browne-Moreno
Nucl. Inst. & Methods A, May 1987; LBL-23481

Heavy Ion Physics Challenges at Bevalac/SIS Energies
M. Gyulassy
8th High Energy Heavy Ion Study, Berkeley, CA Nov 16-20, 1987; LBL-24398

Complex Fragments from Excited Actinide Nuclei: A New Test of the Finite Range Model
D.G. Sarantites, D.R. Bowman, G.J. Wozniak, R.J. Charity, Z.H. Liu, R.J. McDonald, M.A. McMahan and L.G. Moretto
submitted to Phys. Lett. B; LBL-24495

Nuclear Breakup and Particle Densities in 200 A GeV–^{16}O Interactions with Emulsion Nuclei
M.I. Adamovich, Y.A. Alexandrov, S.A. Asimov, S.K. Badyal, E. Basova, K.B. Bhalla, A. Bhasin, R.A. Bondarenkov, T.H. Burnett, X. Cai, L.P. Chernova, M.M. Chernyavsky, B. Dressel, E.M. Friedlander, S.I. Gadzhieva, E.R. Gassauge, S. Garpman, S.G. Gerassimov, A. Gill, J. Grote, K.G. Gulamov, V.G. Gulyamov, V.K. Gupta, S. Hackel, H.H. Heckman, B. Jakobsson, B. Judek, F.G. Kadyrov, H. Kallies, Y.J. Karant, S.P. Karlamov, S. Kitroo, J. Kohli, G.L. Koul, V. Kumar, P. Lal, V.G. Larinova, P.J. Lindstrom, L.S. Liu, S. Lokanathan, J. Lord, N.S. Lukicheva, L.K. Mangotra, N.V. Maslennikova, E. Monnand, S. Mookerjee, C. Mueller, S.H. Nasyrov, W.S. Nawotny, G.I. Orlova, I. Otterlund, N.G. Peresadko, S. Persson, N.V. Petrov, R. Raniwala, S. Raniwala, N.K. Rao, J.T. Rhee, N.G. Salmanova, W. Schulz, F. Schussler, V.S. Shukla, D. Skelding, K. Soderstrom, E. Stenlund, R.S. Storey, J.F. Sun, M.I. Tretyakova, T.P. Trofimova, Z.O. Weng, R.J. Wilkes, G.F. Xu, and P.Y. Zheng
Presented at the XVIII International Symposium on Multiparticle Dynamics, Tashkent, USSR, Sept 8-12, 1987; LBL-24596

Quark Matter '87: Concluding Remarks
M. Gyulassy
Quark Matter '87, Nordkirchen, West Germany, Aug 24-28, 1987; LBL-24768

Microscopic Model of Nucleus-Nucleus Collisions
B.G. Harvey
Presented at the Heavy Ion Conference in the Fermi Energy Domain, Caen, France, May 12-16, 1986; LBL-21452 published in Journal de Physique, Colloque **C4**, supplement to No. 8, 47, 29 (1986)

Spontaneous Fission
D.C. Hoffman and L.P. Somerville
In Charged Particle Emission from Nuclei, Vol. II, CRC Press, Inc., (Boca Raton, FL) 1987.

The Nuclear Deformation Parameters at High Excitation Energies
J.L. Egido, C. Dorso, J.O. Rasmussen, and P. Ring
Phys. Lett. **B178**, 139 (1986).

Transport Equations for The QCD Quark Wigner Operator
H.-Th. Elze, M. Gyulassy and D. Vasak
Nucl. Phys. **B276**, 706 (1986)

Angular Correlations Between Projectile and Target Fragments Emitted from Nuclear Collisions of ^{238}U at 0.85 A GeV
H.H. Heckman, Y.J. Karant, and E.M. Friedlander
Phys. Rev. **C34**, 1333 (1986).

Partition of Excitation Energy in Peripheral Heavy-Ion Reactions
H.R. Schmidt, S.B. Gazes, Y. Chan, R. Kamermans, and R.G. Stokstad
Phys. Lett. **B180** 9 (1986).

Pion Interferometry of Ultra-Relativistic Hadronic Collisions
K. Kolehmainen, and M. Gyulassy
Phys. Lett. **B180**, 3, 203 (1986).

Trends in The Study of Light Proton Rich Nuclei
D. Moltz, et al.
ACS Symposium Series 324/67

Finite Size Effects for Quark-Gluon Plasma Droplets
H.-T. Elze and W. Greiner
Phys. Lett. **B179**, 385 (1986).

Isomeric Levels in ^{180}Lu and the Nucleosynthesis of 180mTa
K.T. Lesko, E.B. Norman, D.M. Moltz, R.M. Larimer, S.G. Crane, and S.E. Kellogg
Phy. Rev. **C34**, 2256 (1986)

^{12}C Decay of ^{24}Mg Following Nuclear Inelastic Scattering J. Wilczynski, K. Siwek-Wilczynska, Y. Chan, E. Chavez, S.B. Gazes, and R.G. Stokstad
Phys. Rev. Lett. **B181**, 229 (1986).

Damping of Rotational Motion at Modest Temperatures
F.S. Stephens, J.E. Draper, J.L. Egido, J.C. Bacelar, E.M. Beck, M.A. Deleplanque, and R.M. Diamond
Phys. Rev. Letts. 57, 2912 (1986).

Dependence of Actinide Production on the Mass Number of the Projectile: Xe + ^{248}Cm *R.B. Welch, K.J. Moody, K.E. Gregorich, D. Lee, and G.T. Seaborg*
Phys. Rev. **C35**, 204 (1987).

FREESCO: Statistical Event Generator for Nuclear Collisions
G. Fai and Jorgen Randrup
Computer Physics Communications 42, 385 (1986).

Beta-Delayed Emission in the Lanthanide Region
P.A. Wilmarth, J.M. Nitschke, R.B. Firestone, and J. Gilat
Zeitschrift fur Physik **A325**, 485 (1986)

Hyperons in Neutron Stars
N.K. Glendenning
Invited paper presented at the Workshop on the Equation of State, Berkeley, CA, April 21-23, 1986 Z. Phys. **A326**, 57 (1987).

Introductory Remarks on the Beauty and the Beast
F.R. Klinkhamer
Nucl. Phys. **A461**, 289c (1987).

Role of Tracking in Future Relativistic Heavy Ion Experiments
C.R. Gruhn
Nucl. Phys. **A461**, 391 (1987).

Pion Interferometry of Ultra-Relativistic Hadronic Collisions
K. Kolehmainen
Proceedings of the Quark Matter 1986, Fifth International Conference *on Ultra-Relativistic Nucleus-Nucleus Collisions, Pacific Grove, CA April 13-14, 1986; and Nucl. Phys.* **A461**, *239c (1987).*

Superheavy Elements
G.T. Seaborg and W. Loveland
Contemp. Phys. 28, 33 (1987)

Lifetime Measurements of High Spin States in ^{160}Yb
J.C. Bacelar, A. Holm, R.M. Diamond, E.M. Beck, M.A. Deleplanque, J. Draper, B. Herskind, and F.S. Stephens
Phys. Rev. Lett. 57, 3019 (1986).

Quantum Transport Theory for Abelian Plasmas
D. Vasak, M. Gyulassy, and H.-Th. Elze
Annals of Physics 173, 462 (1987)

Reaction Mechanisms in the Raiolysis of Peptides, Polypeptides, and Proteins
W.M. Garrison
Chem. Rev. 87, 381 (1987).

Estimates of the Influence of Nuclear Deformations and Shell Effects on the Lifetimes of Exotic Radioactivities
Y.S. Shi, and W.J. Swiatecki
Nucl. Phys. **A464**, 205 (1986)

Muon Catalyzed D-T Fusion at Low Temperature
W.H. Breunlich, M. Cargnelli, P. Kammel, J. Marton, N. Naegele, P. Pawlek, A. Scrinzi, J. Werner, J. Zmeskal, J. Bistirlich, K.M. Crowe, M. Justice, J. Kurck, C. Petitjean, R.H. Sherman, H. Bossy, F.J. Hartmann, W. Neumann, and G. Schmidt
Phys. Rev. Lett. 58, 329 (1987).

Finite Temperature Metastable Matter
N.K. Glendenning
Phys. Lett. **B185**, 275 (1987).

The Beta-Delayed Proton Decay of ^{61}Ge
M.A.C. Hotchkis, J.E. Reiff, D.J. Vieira, F. Blonnigen, T.F. Lang, D.M. Moltz, X. Xu, and J. Cerny
Physical Review **C35**, 315 (1987).

Search for the Beta-Decay of ^{180}Lu to ^{180}Hfm
S.E. Kellogg, and E.B. Norman
Phys. Rev. **C34**, 2248 (1986).

Lineshape Analysis of High Spin States: Collectivity in ^{160}Yb
J.C. Bacelar, R.M. Diamond, E.M. Beck, M.A. Deleplanque, J. Draper and F.S. Stephens
(Rapid Communications) Phys. Rev. **C35**, 1170 (1987)

Masses of ^{77}Kr and ^{75}Kr
D.M. Moltz, A.C. Betker, J.P. Sullivan, R.H. Burch, C.A. Gagliardi, R.E. Tribble, K.S. Toth, and F.T. Avignone III
Phys. Rev. **C35**, 1275 (1987).

Projectile-breakup and transfer-reemission reactions in the ^{12}C+^{20}Ne system
K. Siwek-Wilczynska, J. Wilczynski, C.R. Albiston, Y. chan, E. Chavez, S.B. Gazes, H.R. Schmidt and R.G. Stokstad
Phys. Rev. **C35**, 1316 (1987).

Quantitative Analysis of the Relation between Entropy and Nucleosynthesis in Central Ca + Ca and Nb + Nb Collisions
L.P. Csernai, J.I. Kapusta, D. Hahn, J. Randrup, and H. Stocker
Phys. Rev. **C35**, 1297 (1987).

Pion Production in High Energy Nucleus-Nucleus Collisions
J.W. Harris, G. Odyniec, H.G. Pugh, L.S. Schroeder, M.L. Tincknell, W. Rauch, R. Stock, R. Bock, R. Brockmann, A. Sandoval, H. Strbele, R.E. Renfordt, D. Schall, D. Bangert, J.P. Sullivan, K.L. Wolf, A. Dacal, C. Guerra, and M.E. Ortiz
Phys. Rev. Lett. 58, 463 (1987).

Classical Simulation of the Fermi Gas
C. Dorso, S. Duarte, and J. Randrup
Phys. Lett. **B188**, 287 (1987).

Searches for Supermassive X- Particles in Iron
E.B. Norman, S.B. Gazes, and D.A. Bennett
Phys. Rev. Lett. 58, 1403 (1987).

The Superdeformed Band in ^{152}Dy as Evidence for the Centrifugal Solidification of a Rotating Nucleus *W.J. Swiatecki*
Phys. Rev. Lett. 58, 1184 (1987).

Complex Fragment Emission at 50 MeV/u: Compound Nuclei Forever?
D.R Bowman, R.J. Charity, R.J. McDonald, M.A. McMahan, G.J. Wozniak, L.G. Moretto, W.L. Kehoe, S. Bradley, A.C. Mignerey, A. Moroni, A. Bracco, I. Iori, and M.N. Namboodiri.
Phys. Lett. **B189**, 282 (1987).

Three-Photon Correlations in Rotational Nuclei
F.S. Stephens, J.C. Bacelar, E.M. Beck, M.A. Deleplanque, R.M. Diamond, and J.E. Draper
Phys. Rev. Lett. 58, 2186 (1987).

Projectile-breakup and transfer-reemission reactions in the $^{12}C+^{20}Ne$ system
K. Siwek-Wilczynska, J. Wilczynski, C.R. Albiston, Y. chan, E. Chavez, S.B. Gazes, H.R. Schmidt and R.G. Stokstad
Phys. Rev. **C35**, 1316 (1987).

Fission Mechanisms of 0.2 TeV Uranium Beams
L.F. Canto, R. Donangelo, L.F. Oliveira, and J. Rasmussen
Phys. Rev. **C35**, 2175 (1987).

Actinide Production in ^{136}Xe Bombardments of ^{249}Cf
K.E. Gregorich, K.J. Moody, D. Lee, W.K. Kot, R.B. Welch, P.A. Wilmarth, and G.T. Seaborg
Phys. Rev. **C35**, 2117 (1987).

Subthreshold Pion Production with Associtated Multiplicity Selection in the Reaction $^{139}La+^{139}La$ yields pi+ + X
J. Miller, J. Bercovitz, G. Claesson, G. Krebs, G. Roche, L.S. Schroeder, W. Benenson, J. van der Plicht, J.S. Winfiled, G. Landaud, J.-F. Gilot
Phys. Rev. Lett. 58, 2408 (1987).

Superdeformed Band in ^{135}Nd
E.M. Beck, F.S. Stephens, J.C. Bacelar, M.A. Deleplanque, R.M. Diamond, J.E. Draper, C. Duyar, and R.J. McDonald
Phys. Rev. Lett. 58, 2182 (1987).

Probing the Direct Step of Relativistic Heavy Ion Fragmentation–(^{12}C,^{11}B+p) at 2.1 GeV/Nucleon with C and CH2 Targets *M.L. Webb, H.J. Crawford, J. Engelage, M.E. Baumgartner, D.E. Greiner, P.J. Lindstrom, D.L. Olson, and R. Wada*
Phys. Rev. **C36**, 193 (1987).

Pair Transfer at High Angular Momenta
J.L. Egido, and J.O. Rasmussen
Phys. Rev. **C36**, 316 (1987).

New Structures at High Spin in ^{150}Er
M.A. Deleplanque, J.C. Bacelar, E.M. Beck, R.M. Diamond, J.E. Draper, R.J. McDonald, and F. Stephens
Phys. Lett. **B193**, 422 (1987).

Tangential Friction in Nuclear Reactions Studied with the Time-Dependent Hartree-Fock Model
F.H. Jorgensen, T. Dossing, B.S. Nilsson, and J. Randrup
Phys. Lett. **B191**, 323 (1987).

Superdeformed Bands at High Spin in Z=66 and 68 Isotopes
M.J.A. de Voigt, J.C. Bacelar, E.M. Beck, M.A. Deleplanque, R.M. Diamond, J.E. Draper, H.J. Riezebos and F.S. Stephens
Phys. Rev. Lett. 59, 270 (1987).

Hot Metastable State of Abnormal Matter in Relativistic Nuclear Field Theory
N.K. Glendenning
Nuclear Physics **A469**, 600 (1987).

New Limits on the Double Beta Decay Half-Lives of ^{94}Zr, ^{116}Cd, and ^{124}Sn
E.B. Norman and D.M. Meekhof
BAPS 31, 1211 (1986); Phys. Lett **B195**, 126 (1987).

Microcanonical Simulation of Nuclear Multifragmentation
J. Randrup and S.E. Koonin
Proceedings for the Symposium on Central Collisions and Fragmentation Processes, Denver, CO, 5-10 April 1987; **A471**, 355c (1987).

Superdeformed Bands in Nd Nuclei
E.M. Beck, R.J. Mcdonald, A.O. Macchiavelli, J.C. Bacelar, M.A. Deleplanque, R.M. Diamond, J.E. Draper, and F.S. Stephens
Submitted to Phys. Lett. **B195**, 531 (1987).

Role of Hyperons and Pions in Neutron Stars and Supernovae
N.K. Glendenning
Z. Phys. **A327**, 295 (1987).

Complex Fragment Emission at Intermediate Energies
Robert Charity
Nuclear Physics **A471**, 225c (1987)

Multifragmentation and Flow in Central Collisions of Heavy Systems
J.W. Harris, B.V. Jacak, K.-H. Kampert, G. Claesson, K.G.R. Doss, R. Ferguson, A.I. Gavron, H.-A. Gustafsson, H. Gutbrod, B. Kolb, F. Lefebvres, A.M. Poskunzer, H.-G. Ritter, H.R. Schmidt, L. Teitelbaum, M. Tincknell, S. Weiss, H. Wieman and J. Wilhelmy
Proceedings of the Symposium on Central Collisions and Fragmentation Processes, Denver, CO, April 5-10, 1987 Nucl. Phys. **A471**, 241c (1987).

A Fast Megapixel Charge-Coupled-Device Image Acquisition and Analysis System for High Energy Nuclear Physics *M.L. Tincknell, S.I. Chase, T. Dinh, J.W. Harris and L Teitelbaum*
Optical Engineering 26(10), 1067 (1987).

Particle-Hole States at High Spin in ^{150}Dy

M.A. Deleplanque, J.C. Bacelar, E.M. Beck, R.M. Diamond, F.S. Stephens, J.E. Draper, Th. Dossing, and K. Neergard

Phys. Lett. **B195**, 17 (1987).

Improvements to the Helium-Jet Coupled Mass-Separator RAMA

F. Blonnigen, D. Moltz, T. Lang, M. Hotchkis, J. Reiff, X. Xu, and J. Cerny

Nucl. Instru. and Meth. **B26**, 328 (1987); Proceedings Eleventh International Conference on Electromagnetic Isotopr Separators and Techniques Related to their Applications, Los Alamos, NM, August 18-22, 1986.

Interaction Energy in Infinite Nuclear Matter in the Hybrid Soliton Model

D. Hahn, and N.K. Glendenning

Phys. Rev. **C36**, 1181 (1987).

Range-Energy Relation for Au Ions E/A [less than or equal to] 150 MeV

H.H. Heckman, H.R. Bowman, Y.J. Karant, J.O. Rasmussen, A.I. Warwick, and Z.Z. Xu

Phys. Rev. **A36**, 3654 (1987).

The Contribution of Collective Zero-Point Motion to Mean-Square Charge Radii

W.D. Myers, and P. Rozmej

Nucl. Phys. **A470** (1987).

Nuclear Science Division Seminars

October 6, 1986	Howard Hall, GSRA	Search for Beta-Delayed Fission in ^{256m}Es
	Michael Webb, GSRA	Probing the Direct Step of Relativistic Heavy Ion Fragmentation: (^{12}C,p+^{11}B) at 2.1 GeV/Nucleon with ^{12}C and CHO_2 Targets
October 27, 1986	Dr. H. Crawford SSl/LBL	Nuclear Structure Studies at HISS
November 3, 1986	Dr. David Lissauer Brookhaven National Laboratory	Study of Extreme Peripheral and Central Collisions Induced by Relativistic Heavy Ions
November 10, 1986	Dr. John Schiffer Argonne National Laboratory	Will the Cooled Beams of Storage Rings Condense in a Crystalline Array?
November 24, 1986	Dr. Eric Norman LBL	Searches for Exotic Relics of the Big Bang
December 1, 1986	Armit Yegneswaran, GSRA	The Dilepton Spectrometer
	Marvin Justice, GSRA	Muon Catalyzed Fusion Experiment at SIN
December 8, 1986	Dr. Gerald Garvey LAMPF	Strong Interaction Physics with a KAON Factory
December 15, 1986	Dr. H. Pugh LBL	Multiplicity and Transverse Energy Flux in ^{16}O + Pb at V Per Nucleon
January 5, 1987	Thomas Lang, GSRA	A New Technique for Studying the Decay of Proton Rich Nuclei
	William Christie, GSRA	The Music Detector at HISS
January 12, 1987	Dr. Wladyslaw Swiątecki LBL	Order, Chaos, and Nuclear Dynamics
January 26, 1987	Dr. J. Michael Nitschke LBL	Proton Emission from Magic Nuclei
February 22, 1987	Dr. S. Jha University of Cincinnati	Prospect of x-ray Laser
February 9, 1987	Dr. Craig Sangster LLNL	Proton Induced Nuclear Fragmentation in the Threshold Region: 1< E_p <GeV
February 23, 1987	Dr. Charles Gale University of Minnesota	Dynamical Simulations of Heavy Ion Collisions
March 2, 1987	Roger Henderson, GSRA	The Radio Chemistry of Laurencium
	Larry Teitelbaum, GSRA	Backward Particle Production: Exclusive Event Analysis in the Streamer Chamber for 2.1 GeV Protons + Carbon

March 9, 1987	Gary Westfall Michigan State University	Two Particle Correlations in 40 MeV per Nucleon ^{12}C and ^{14}N Induced Reactions
March 23, 1987	Dr. John Stevenson Michigan State University	High Energy γ-ray Emission in Heavy-Ion Collisions
April 6, 1987	Carolyn Gannett, GSRA	Above Target Transfer Reaction Products of $^{18}C + {}^{249}Bk$
	Craig Tull, GSRA	Inclusive Measurement of 1.65 GeV/A Ar Fragmentation at HISS
April 13, 1987	C. Gregoire GANIL	Nuclear Landau-Vlasov Dynamics
April 27, 1987	Professor Gunter Hermann University of Mainz	Fallout in West Germany after the Chernobyl Reactor Accident
May 4, 1987	Professor V. Goldanskii Institute of Chemical Physics, Moscow, U.S.S.R.	Mossbauer Studies of Tunneling Phenomena in Chemical and Biological Physics
May 11, 1987	Dr. J. Wouters LANL	TOFI: Not Just Another Candy (Adventures in Nuclear Mass Measurements)
May 18, 1987	Dr. E. Gliner LBL	The General Relativistic Foundations of Inflationary Cosmology
June 1, 1987	Diane Bennett, GSRA	The Hydrolysis and Carbonate complexation of Dioxoplutonium(V)
	Mark Stoyer, GSRA	Neutron Transfer Reactions in the Actinide Region
June 8, 1987	Dr. John Harris LBL	Multifragmentation and Flow in Collisions of Heavy Systems
June 15, 1987	Dr. Richard Hoff LLNL	Constraints on Beta-delayed Fission in Neutron-rich Transuranic Nuclei and their Relationship to Astrophysical r-process Calculations
June 22, 1987	Prof. E. Adelberger University of Washington	A Search for the Fifth Force – Results of the Eotvos Experiment
June 29, 1987	Dr. W.D. Myers LBL	The Contribution of Zero-point Motion to Isotope Shifts
July 6, 1987	Dr. Ronald Mayle LLNL	Supernovae and SN1987A
July 20, 1987	W. Greiner University of Frankfurt	Clusters and Flow
July 27, 1987	Dr. Michael Hass Weizmann Institute	Tilted Foil Polarization Measurements with Separated Reaction Products

August 3, 1987	Dr. Itshak Tserruya Weizmann Institute	Incomplete Fusion Reactions Induced by ^{12}C
August 17, 1987	Prof. Hans Weidenmuller University of Heidelberg	Transients in Fission.
September 21, 1987	Dr. Claude Petitjean Swiss Institute for Nuclear Research	Muon Catalyzed Fusion - Where is the Limit?
September 28, 1987	Dr. U. Brosa Phillips-Universität Marburg	Fission of the Actinides

88-Inch Cyclotron Seminars

October 17, 1986	N.A. Greenhouse LBL	Accelerator Radiation Safety
November 14, 1986	Eric Plagnol Orsay/LBL	From Evaporation to Fission in a Light Excited Nucleus
November 17, 1986	J. Rama Rao Banaras Hindu University, India	Precompound Doorway States
November 21, 1986	Efrain R. Chavez-Lomeli LBL/I.F.U.N.A.M., Mexico	Peripheral Reactions Induced by 520-MeV ^{16}O
December 5, 1986	D. Clark and C. Lyneis LBL	Reports on Recent Accelerator Conferences in Japan and the Soviet Union
January 9, 1987	E.K. Hulet LLNL	Bimodal Fission in Trans-Fermium Nuclei
January 16, 1987	J. Pouliot LBL	Polarization and Analyzing Power Comparison in the $^{13}C(^3He,\vec{p})^{15}N$ Two-Nucleon Transfer Reaction
January 23, 1987	J. and R. Stokstad CPS and LBL	Impressions of China
February 6, 1987	David Robertson LBL	Intrinsic Reflection Asymmetry in Medium Mass Nuclei
February 20, 1987	E. Norman LBL	Report on Two Recent Astrophysics Conferences (SS433 Meeting and Texas Relativistic Astrophysics Meeting)
March 6, 1987	Karl Van Bibber LLNL	Deep Inelastic Electron Scattering and the EMC Effect
March 20, 1987	Horst Schmidt-Böcking University of Frankfurt	Kansas State University Time Measurements in the 10^{-20} Second Range Using Hydrogen-Like Projectiles
May 1, 1987	R. Jahn University of Bonn	Beethoven by the Bit
May 8, 1987	E. Norman LBL	Report on the Crystal City APS Meeting
May 15, 1987	R. Roy University of Laval	Beam Fragmentation at 40 MeV/nucleon
May 29, 1987	G. Peaslee S.U.N.Y. at Stony Brook	Recent Results from 8.5 MeV/nucleon ^{56}Fe + ^{nat}Ag

June 26, 1987	A. Harmon LBL	Momentum Correlations in ^{16}O + Au, U Collisions at 32.5 MeV/nucleon
July 10, 1987	J. Jastrezebski Warsaw University	Linear Momentum Deposition Deduced from the Investigation of Radioactive Reaction Products
August 7, 1987	Yves Jongen Catholic University	Louvain-la-Neuve Initial Results from a New Very High Intensity 30 MeV Proton Cyclotron
August 21, 1987	Mark Stoyer LBL	Neutron Transfer Reactions in the Actinide Region
September 25, 1987	Eric B. Norman LBL	Report on the Nuclear Science Symposia at the New Orleans Meeting of the ACS

Author Index

A

B

C

D

E

F

G

H

I

J

K

L

M

N

O

P

R

S

T

V

W

X

Y

Z